UNIVERSITY OF SOUTHAMPTON

CHARACTERISATION OF THE *Solute carrier family member 11a1 (Slc11a1)* PROMOTER: REGULATION BY c-Myc AND Miz-1

HOLLY BOWEN

SUBMITTED FOR AWARD OF DOCTOR OF PHILOSOPHY

BIOCHEMISTRY AND MOLECULAR BIOLOGY DEPARTMENT

FEBRUARY 2003

UNIVERSITY OF SOUTHAMPTON

ABSTRACT

FACULTY OF SCIENCE

BIOCHEMISTRY AND MOLECULAR BIOLOGY

Doctor of Philosophy

CHARACTERISATION OF THE Solute carrier family member 11a1 (Slc11a1) PROMOTER: REGULATION BY c-Myc AND Miz-1

by Holly Bowen

In mice, natural resistance to infection with several antigenically unrelated intracellular pathogens including Salmonella typhimurium, Leishmania donovani and Mycobacterium bovis, is mediated by a single gene on chromosome 1 termed Slc11a1 (Solute carrier family 11a member1, formerly Nramp1). Slc11a1 encodes a 548 amino acid integral membrane protein that localises to the late endocytic compartments of resting macrophages. Infection of the macrophage with intracellular pathogens leads to targeting of Slc11a1 from endocytic vesicles to the phagosomal membrane where it alters the microenvironment of the vesicle, thereby controlling replication of the pathogen. How Slc11a1 performs this task is the centre of much controversy. High sequence similarity (77% protein identity) to Nramp2, a ubiquitous divalent cation symporter, and the presence of a highly conserved transport motif has led to the suggestion that Slc11a1 may also function as a divalent cation transporter, leading to a decrease in cytoplasmic iron levels.

Wu and colleagues showed reciprocal control of iron regulatory protein expression H-ferritin and IRP2 by c-Myc and suggest a role for c-Myc in the regulation of cytoplasmic iron. As both c-Myc and Slc11a1 modulate cytoplasmic iron, but in opposite directions, a role for c-Myc in the regulation of Slc11a1 was evaluated. c-Myc co-transfection into both Cos1 and RAW264.7 macrophage lineage cells repressed expression of Slc11a1 promoter driven reporter constructs. An initiator (Inr) element flanking the transcriptional start site is a candidate site for the inhibition as c-Myc repression was observed on a 34bp region of 5' flanking sequence containing only 2 Inr elements and a consensus Sp1 binding site. Down regulation of the Slc11a1 promoter by c-Myc is thought to involve the Inr binding protein Miz-1 (Myc interacting zinc finger protein-1). Miz-1 recruits coactivators p300/CBP to the site of transcriptional initiation, thereby promoting gene expression, binding of c-Myc to Miz-1 interferes with coactivator recruitment, silencing the target gene. Co-transfection with both Miz-1 and p300 leads to transactivation of the Slc11a1 promoter driven reporter constructs. Miz-1 mediated transactivation is observed only in the absence of E-box c-Myc binding sites (EMS) but requires the presence of the consensus Sp1 binding site. p300 transactivation is independent of EMS but dependent upon the presence of the consensus Sp1 binding site. Data presented within this thesis provide a basis for the model of regulation of the Slc11a1 promoter.

ACKNOWLEDGEMENTS

I would like to acknowledge the following people for their help during my PhD.

CHB-you have the patience of a saint, how you put up with me and my nagging I don't know but I am glad you did. Thank you for everything you have done for me, I would never have got through it without your help and support. THELMA-the best postdoc I could have asked for, you always have the answers. Thank you not only for your help but also for being a good friend along the way. PROFESSOR VH PERRY & DR DA MANN-thank you both for your support and advice throughout my PhD. KAREN-thank you for all your advice over the years but more importantly for being Welsh! "MY ANDY"-thank you baby, I love you. SALLY-my ever-ready shopping partner, thank you for supplying the Chardonnay when things were going wrong, it may not have made things better but it certainly made me forget about them!

Mummy, Daddy, Steve, Cynthia, Dave, Seren and Pegi, you have all supported me in different ways and are unashamedly proud of me, thank you all for believing in me.

All the other students and postdocs who have had the misfortune to work with me, thanks for making it fun to be in the lab.

PUBLICATIONS

Some of the work presented in this study has been published or submitted for publication as listed below.

Bowen H, Biggs TE, Phillips E, Baker ST, Perry VH, Mann DA and Barton CH. (2002). c-Myc represses and Miz-1 activates the murine natural resistance-associated macrophage protein 1 promoter. *J.Biol.Chem.* 277, 4997-5006.

Bowen H, Biggs TE, Baker ST, Phillips E, Perry VH, Mann DA and Barton CH. (2002) c-Myc represses the murine Nramp1 promoter. *Biochem. Soc. Trans.* 30(4), 774-7.

Biggs TE, Bowen H, Phillips E, Perry VH, Mann DA and Barton CH. (2003) Divalent cation transport in macrophages: Role of *Nramp1* (*Natural resistance-associated protein*) Submitted as invited review to Research Signpost.

CONTENTS

FIGURE CONTENTS

CHAPTER 5

CHAPTER 6

CHAPTER 7

ABBREVIATIONS

ABCA1	ATP-binding cassette transporter A1
AP1	Activator Protein-1
bHLH/LZ	Basic helix-loop-helix leucine zipper
BMM	Primary bone marrow derived macrophages
BrdU	5-Bromo-2'-deoxyuridine
BTB/POZ	Broad-complex, Tramtrack, Brick-a-brac/ Poxvirus and zinc finger
BCG	Bacille Calmette-Guerin
CAT	Chloramphenical Acetyl Transferase
CBP	CREB binding protein
ChIP	Chromatin immunoprecipitation assays
CTM	Conserved transport motif
DNA	Deoxyribonucleic acid
EAE	Experimental autoimmune encephalomyelitis
EMS	E-box myc sites
EMSA	Electrophoretic mobility shift assays
Ets	E-twenty six specific
Fra1	Fos related antigen 1
G/M-CSF	Granulocyte/Macrophage-colony stimulating factor
IBS	Inflammatory bowel disease (Crohn's disease and ulcerative colitis)
IDD	Insulin dependent diabetes
IFNγ	Interferon-gamma
IL	Interleukin
Inr	Initiator
Ir	Immune response
IRE	Iron response element
IRP	Iron response protein
JAK	Janus Kinase
KLF	Krüppel-like factor
LDU	Leishman Donovan Units
LPS	Bacterial Lipopolysaccharide
MAP	Mitogen activated protein
Max	Myc-associated factor X
MB	Myc Box
Miz-1	Myc interacting zinc finger protein-1
MS	Multiple sclerosis
MTP	*Microtitre plate*
c-Myc	Cellular Myelocytomatosis
NCAM	Neural cell adhesion molecule
Nramp	Natural resistance-associated macrophage protein
NFκB	Nuclear factor kappa B
NLS	Nuclear localization signal
PBL	Peripheral blood leukocytes
PCR	Polymerase chain reaction
pdgf-βR	Platelet derived growth factor-β receptor
PG	Prostaglandin
Pu	Purine
PU Box	Purine rich region
Py	Pyrimidine
RA	Rheumatoid arthritis
RNA	Ribonucleic acid
ROS	Reactive oxygen species
RT	Room temperature
Slc11a1	Solute carrier family 11 member 1
Sp1	Stimulatory Protein 1
STAT	Signal transducer and activator of transcription
TAD	Transactivation domain
TF	Transcription factor

TGFβ	Transforming growth factor beta
TNF-α	Tumour necrosis factor-α
USF	Upstream factor
YAC	Yeast artificial chromosome

CHAPTER 1

Introduction

1.1 INTRODUCTION

1.1.1 Genetic Susceptibility to Intracellular Infections

In the early 1970s, it was recognised that murine susceptibility to several antigenically unrelated intracellular pathogens, including *Salmonella typhimurium, Leishmania donovani* and *Mycobacterium bovis*, was influenced by a host genetic factor. The first indication of this came from studies of *S. typhimurium* infection in inbred strains of mice (Plant and Glynn, 1974a). Subcutaneous infection of 6 inbred strains of mice, of differing ancestry, with increasing doses of *S. typhimurium* C5 enabled the distinct segregation of the mouse strains into those susceptible to less than 100 organisms, and those resistant to over 10^5 organisms. The distinct segregation between the two groups indicated that genetic factors may be involved in controlling infection. Furthermore, polarisation of the mouse strains into high and low resistance groups, with no intermediate groupings, suggested that only a very small number of genes, or even a single gene may control the resistance phenotype. The candidate gene, or group of genes, was provisionally termed *Ity* (immunity to typhimurium). It was proposed that *Ity* was involved in the acquired immune response and strains of mice were tested for the ability to raise antibodies to ovomucoid, ovalbumin and BPO-BGG. The pattern of antibody production, hence H2-haplotype, correlated with the pattern of resistance to *S. typhimurium* C5. Based on preliminary data it was suggested that a major factor in the resistance of mice to salmonella is the presence of an immune response (Ir) gene controlling the response to some unknown, but probably protein antigen, present within *S. typhimurium* C5.

In response to these observations, Bradley (1974) reported similar observations in inbred strains of mice infected with *L. donovani* L82, showing growth rates of the intracellular parasite within the first 2 weeks of infection varied greatly between the different strains of mice. 25 inbred strains of mice were intravenously infected with *L. donovani* L82, and parasite load measured in Leishman-Donovan Units (LDU) at day 15[1]. As seen with the *S. typhimurium* C5 infection (Plant and Glynn, 1974a), the

[1] To calculate LDU parasite numbers were estimated using Stauber's method, the ratio of parasites to liver cells was determined on liver imprints and multiplied by the liver weight in mg, giving a reproducible index of parasite load.

L. donovani L82 infected mice also fell into two distinct, non-overlapping categories. Twelve highly susceptible strains showed about a 100-fold multiplication of parasitic load, whereas the 13 remaining strains were resistant with less than 8-fold increase in parasitic load. Comparison of the two studies showed a correlation between resistance to *S. typhimurium* C5 and *L. donovani* L82 infection. In breeding experiments (Bradley, 1974), crossing the *L. donovani* L82 resistant mouse strain C3H/He, with the susceptible strain NMRI, generated an F_1 population that were subsequently self-, and back-crossed with each parental strain. Infection of the various inbred progeny with *L. donovani* L82 revealed a Mendelian pattern of inheritance of the resistance phenotype. These studies provided strong evidence for the control of *L. donovani* L82 growth in the mouse liver by a single gene or tight linkage group provisionally termed *Lsh* (leishmaniasis resistance). Unlike Plant and Glynn, Bradley reported no involvement of the H2 or Ir genes in the control of leishmania infection. Plant and Glynn quickly responded reporting that further breeding experiments showed no association between *S. typhimurium* resistance and a particular H2-haplotype (Plant and Glynn, 1974b).

In 1981 Gros *et al.* reported a third class of intracellular pathogen where natural resistance to infection is under genetic control, *M. bovis*. Intravenous infection of 13 inbred strains of mice with the Montreal strain of *M. bovis* (BCG), and recovery of the pathogen from the spleen from infected mice 3 weeks later enabled classification of the various strains of mice as either resistant, or susceptible to infection, as judged by the extent of bacilli recovery. Recovery of BCG bacilli was 100 fold higher in the susceptible mice compared to the resistant mice. A breeding experiment, similar to those performed by Bradley, showed that natural resistance to infection to BCG challenge was inherited with Mendelian genetics; the candidate gene responsible was provisionally named *Bcg* (Bacille Calmette-Guerin). Furthermore, following the time course of BCG infection in representative resistant and susceptible strains of mice, they established that the genetic advantage of the resistant strains is apparent early in the course of infection (0-3 weeks). These observations indicated *Bcg* is involved in the innate immune response, thereby discounting the involvement of the Ir genes, which are associated with the later (3-6 weeks) cell-mediated, or humoral, immune response. In support of this H2-haplotypes were examined in typed inbred mouse strains (Gros *et al.* 1981). Bcg^S B10.A congenic mice possess the $H2^a$-haplotype from

the Bcg^R A/JAX donor, confirming no linkage between H2-haplotype and BCG resistance.

Comparison of data from the 3 groups revealed precise correspondence between inbred strains of mice resistant and susceptible to infection with *Salmonella typhimurium, Leishmania donovani* and *Mycobacterium bovis* (see figure 1.1.3.1), suggesting a single gene, or group of genes, may control resistance to all 3 pathogens. The mapping of all 3 genes, *Ity* (Plant and Glynn, 1976; Plant *et al.* 1982), *Lsh* (Bradley, 1977) and *Bcg* (Skamene *et al.* 1982; Schurr *et al.* 1989), to the same region of the murine chromosome 1 reinforced this idea. It was concluded that *Ity/Lsh/Bcg* controls the capacity of inbred strains of mice to restrict the replication of several antigenically and taxonomically unrelated intracellular pathogens.

1.1.2 Cloning of a Candidate Gene for *Ity/Lsh/Bcg*

In order to isolate the candidate gene of the *Ity/Lsh/Bcg* locus the Gros group used positional cloning to identify the candidate gene. This monumental task took over 10 years and focused on *Bcg* infection. The *Ity/Lsh/Bcg* locus was assigned to the proximal portion of mouse chromosome 1 between *Idh-1* and *Pep-3* by linkage analysis in recombinant inbred strains, and backcross progeny derived from inbred strains, carrying either Bcg^R (resistant), or Bcg^S (susceptible) alleles (Skamene *et al.* 1982). Mapping of the *Ity/Lsh/Bcg* locus gave investigators a starting point for the arduous task of isolating and identifying the illusive candidate gene. Segregation analysis in recombinant inbred strains and inter-specific and intra-specific backcross mice were used to position a number of structural genes with respect to *Ity/Lsh/Bcg* (Vidal *et al.* 1992; Malo *et al.* 1993a; Malo *et al.* 1993b). These genetic mapping studies identified and mapped a group of polymorphic DNA markers closely linked to the *Ity/Lsh/Bcg* locus, enabling delineation of maximal genetic and physical intervals defining boundaries for the *Ity/Lsh/Bcg* candidate gene region as 0.3cM and 1.1Mbp, respectively. Yeast artificial chromosome (YAC) clones of this region were isolated from the Princeton mouse YAC library using the *Vil* and *λMm1C165* markers as entry probes (Vidal *et al.* 1993). *Vil* and *λMm1C165* markers were most tightly linked to the *Ity/Lsh/Bcg* gene, with no recombination being observed in the 1424 meiosis tested (Vidal *et al.* 1993). A cosmid and bacteriophage contig was constructed from the YAC clones that spanned 400Kbp of mouse chromosome 1 and contained both the *Vil* and *λMm1C165* entry probes. CpG island identification within the 400Kbp contig detected six potential coding sequences, which were subsequently isolated using the technique of exon amplification. This technique identified 22 putative exons, which were subjected to stringent analysis in order to distinguish genuine exons from false positives and to group these genuine exons into true transcriptional units. Complementary DNA clones corresponding to the 6 true transcriptional units were subsequently isolated from two cDNA libraries derived from the mouse precursor B-cell line 70/Z and rat brain RNA. The isolated cDNAs were used to determine the pattern of expression of each of the 6 candidate genes. *In vitro* and *in vivo* studies had previously indicated the macrophage displayed the genetic difference at *Bcg* (Gros *et al.* 1983; Goto *et al.* 1989), expression in these cells was therefore analysed. One of the 3 transcriptional units isolated from the pre-B cell library, termed candidate 5,

displayed the expected pattern of expression. Candidate 5, which mapped approximately 50kbp proximal to *Vil*, encoded a 2.5Kbp mRNA transcript restricted to the macrophage-enriched fraction of the spleen, with low level expression in the liver. Owing to the finding that the gene encoded by candidate 5 displayed tissue and cellular expression, consistent with those that show phenotypic differences at *Bcg*, and chromosomal location, made it a strong candidate for *Ity/Lsh/Bcg*. The candidate gene for *Ity/Lsh/Bcg* was subsequently termed the *Natural resistance-associated macrophage protein 1(Nramp1),* and has since been reassigned as *Solute carrier family 11a member1 (Slc11a1).*

1.1.3 Candidacy of *Slc11a1* as *Ity/Lsh/Bcg*

When *Slc11a1* was first isolated (Vidal *et al.* 1993), kinetic analysis of mRNA levels in control and infected macrophages revealed that the level of *Slc11a1* gene expression was similar for the resistant and susceptible phenotypes throughout the course of infection. It was therefore proposed that a mutation within the encoded protein may result in the phenotype observed, and the mRNA transcripts from BCG resistant and susceptible strains were analysed for the presence of sequence alterations within the coding portion of the *Slc11a1* gene. Analysis of 6 susceptible strains and 7 resistant strains identified a guanine to adenine transition within codon 169 that resulted in the non-conservative replacement of the small, neutral glycine residue at position 169 for the more bulky, negatively charged aspartate residue. cDNA cloning and nucleotide sequencing for a total of 20 BCG resistant, and 7 BCG susceptible inbred strains of mice (Malo *et al.* 1994), revealed an absolute association of this G169D allelic variation with BCG phenotype (see figure 1.1.3.1). Sequence analysis of this region from distantly related species indicated amino acid conservation of TMD 4, including this invariant glycine (Cellier *et al.* 1995). Haplotype mapping of the *Slc11a1* containing region of mouse chromosome 1 revealed that the BCG resistant strains display diverse allelic combinations within this region, whereas BCG susceptible strains share a conserved 2.2Mbp core, overlapping and including *Slc11a1*. It was concluded from these findings firstly that Gly^{169} is the wild type of *Slc11a1* and that the non-conservative substitution for Asp^{169} underlies the BCG susceptible phenotype, and secondly the alleles carrying Asp^{169} are identical by descent (Malo *et al.* 1994).

The first direct evidence to verify candidacy of *Slc11a1* as *Ity/Lsh/Bcg* was provided by *in vitro* gain-of-function gene transfer experiments in the $Ity^S/Lsh^S/Bcg^S$-derived macrophage RAW 264.7 cell line (Barton *et al.* 1995). Gene transfer of the $Slc11a1^R$ allele on to a susceptible background resulted in the appearance of a resistant phenotype within these previously susceptible cells. Functional analysis of RB activity, nitrite release and L-arginine uptake, macrophage activation phenotypes that are increased in bone marrow derived macrophages isolated from Lsh^R mice compared with those derived from Lsh^S mice (Blackwell *et al.* 1994), revealed that expression of $Slc11a1^R$ enhanced macrophage priming/activation (Barton *et al.* 1995). These data, and the allelic association between *Slc11a1* and resistance or

susceptibility to BCG infection provided good evidence that *Slc11a1* was *Ity/Lsh/Bcg*, however *in vivo* gene targeting (Govoni *et al.* 1996), and gene disruption (Vidal *et al.* 1995) were used to confirm that *Slc11a1* and *Ity/Lsh/Bcg* were allelic. Homologous recombination in embryonic stem cells (ESC) generated an *Slc11a1* null allele ($Slc11a1^{-/-}$) on the BCG resistant genetic background of the ESC J1 from the 129/sv inbred mouse strain (Vidal *et al.* 1995). Loss-of-function was confirmed by the absence of *Slc11a1* mRNA transcripts in the $Slc11a1^{-/-}$ mice. The $Slc11a1^{-/-}$ mice developed normally, were healthy, and the architecture of the liver and spleen, the organs where *Slc11a1* expressing macrophages reside, were normal, suggesting *Slc11a1* expression plays no-role in the development of these organs. Disruption of *Slc11a1* did however restrict the capacity of the mice to control the growth of *S. typhimurium*, *L. donovani* and *M. bovis*, when compared with littermates with the $Slc11a1^{G169}$ unmutated allele. Mice homozygous for the null allele $Slc11a1^{-/-}$ were unable to limit bacterial proliferation or initiate bacterial clearance in the late phase of infection, confirming *Slc11a1* exerts its effects during the early stage of infection, a finding that had been previously reported for *Ity* (Plant and Glynn, 1974a), *Lsh* (Bradley, 1974), and *Bcg* (Gros *et al.* 1981). Taken together the results of the gene disruption experiments provided definitive evidence *Slc11a1* and *Ity/Lsh/Bcg* were allelic. Control of bacterial proliferation, as judged by recovery of BGC bacilli from the spleen of infected animals, was indistinguishable between $Slc11a1^{D169/D169}$, $Slc11a1^{D169/-}$ and $Slc11a1^{-/-}$, suggesting that the $Slc11a1^{D169/D169}$ is functionally null (Vidal *et al.* 1995).

Although the gene disruption experiments did indicate that *Slc11a1* and *Ity/Lsh/Bcg* were allelic, the method used introduced a 4Kbp deletion into the *Slc11a1* gene. A 4Kbp deletion and the insertion of a *neo* cassette could potentially affect the overall structure of the targeted chromosomal region, possibly altering the regulation of neighbouring genes such as *il-8rb*, a gene involved in the inflammatory response. In order to discount such effects, the same group performed the complementary experiment; transfer of $Slc11a1^{G169}$ onto the BCG susceptible background of C57BL/6J inbred mouse strain (Govoni *et al.* 1996). A 23Kbp proximal portion of mouse chromosome 1 containing the entire *Slc11a1* structural gene, 5Kbp of 5' sequence, 6Kbp of 3' sequence and 200bp of the pCos4 cosmid vector, was injected into $Slc11a1^{G169/D169}$ heterozygote fertilised eggs before reimplantation into pseudo-

pregnant females. Southern blotting using the 200bp pCos4 fragment of the inserted DNA identified transgenic pups. The transgenic pups were subsequently backcrossed with C57BL/6J, and offspring analysed for the presence of the transgene. Haplotype analysis allowed the identification of offspring that were either heterozygous or homozygous for chromosome 1 markers, enabling the identification of pups containing the transgene on a homozygous *Slc11a1*$^{D169/D169}$ background. Finally C57BL/6J homozygotes containing the transgene were interbred to expand the transgenic line, this line was referred to as *Slc11a1*$^{G169*D169/D169}$. The presence of the transgene was confirmed using an anti-serum raised against the amino-terminal of Slc11a1. Control *M. bovis* infection in the *Slc11a1*$^{G169*D169/D169}$ transgenic mice was indistinguishable from that of the *Slc11a1*$^{G169/G169}$ mice. Furthermore unlike the *Slc11a1*$^{D169/D169}$ mice that all died on, or before day 5, the *Slc11a1*$^{G169*D169/D169}$ transgenic mice overcame the fatal effects of intravenous *S. typhimurium* infection. These experiments established that transfer of *Slc11a1*^{G169} onto an *Slc11a1*^{D169} susceptible background restored the capacity of mice to control pathogenic infection, confirming the findings of the gene knockout experiments, that *Slc11a1* and *Ity/Lsh/Bcg* were allelic.

The findings of the *in vivo* gain-of-function gene transfer experiments have been repeated and confirmed *in vitro* (Govoni *et al.* 1999). Stable transfection of the RAW 264.7 immortalised macrophage cell line with a *Slc11a1*^{G169} containing mammalian expression vector, introduces the resistant *Slc11a1*^{G169} allele into a cell line homozygous for the *Slc11a1*^{D169} susceptible allele. The RAW 264.7 cell line was transfected with the Slc11a1 family member Slc11a2 to provide a control for the experiments. The resultant cell line was found to express the mature, highly-glycosylated 90-100kDa form of the protein, furthermore the recombinant protein was observed to undergo recruitment to bacterial containing phagosomes in a manner similar to that observed in primary macrophages. The parental, *Slc11a1*^{G169} and *Slc11a2* expressing RAW 264.7 cell lines were challenged for 30 minutes with *S. typhimurium* SL1344 and pathogenic load determined, as CFU/μg protein, recovered from lysed cells. The *Slc11a1*^{G169} expressing cells displayed an approximate 20-fold reduction in pathogenic load compared with the parental and *Slc11a2* expressing cells. The results indicated that expression of the Slc11a1^{G169} protein in the RAW 264.7 cell

line confers upon these cells the ability to control replication of *S. typhimurium* SL1344. Interestingly unlike Slc11a1^{G169}, expression of the highly related protein Slc11a2 was unable to correct the susceptible phenotype. Much of the Slc11a1^{G169} protein functional data has been based on the assumption that it behaves in a similar fashion to Slc11a2; the results of these experiments however suggested the two proteins may be functioning via different mechanisms. The results of the *in vivo* and *in vitro* experiments verified the candidacy of *Slc11a1* as *Ity/Lsh/Bcg*.

FIGURE 1.1.3.1 Genetic Control of Natural Resistance to Infection in Inbred Strains of Laboratory mice. Table summarises codon and amino acid at position 169 in Slc11a1 and resistance (R) or susceptibility (S) to *Salmonella typhimurium (Ity), Leishmania donovani (Lsh)* and *Mycobacterium bovis (Bcg)* respectively, for 30 inbred strains of laboratory mice. This table has been adapted from Malo *et al.* 1994 using information provided by Plant and Glynn (1974), Bradley (1974) and Gros *et al.* (1981).

Strain	Codon 169 (Gly/Asp)	*Ity* (Plant & Glynn, 1974)	*Lsh* (Bradley, 1974)	*Bcg* (Malo *et al.* 1994)
LP/J	GGC (Gly)			R
L129/J	GGC (Gly)			R
C58/J	GGC (Gly)			R
AKR/J	GGC (Gly)			R
C57L/J	GGC (Gly)			R
C57BR/cdJ	GGC (Gly)			R
DBA2/J	GGC (Gly)	R	R	R
RIIIs/J	GGC (Gly)			R
P/J	GGC (Gly)			R
BUB/BnJ	GGC (Gly)			R
RF/J	GGC (Gly)			R
PL/J	GGC (Gly)			R
SJL/J	GGC (Gly)			R
C3H/HeJ	GGC (Gly)	R	R	R
NZB/BINJ	GGC (Gly)			R
CBA/J	GGC (Gly)	R	R	R
NOD/Lt	GGC (Gly)			R
Mus spretus	GGC (Gly)			R
SWR/J	GG**A** (Gly)			R
A/JAX	GGC (Gly)	R	R	R
BALB/cJ	G**A**C (Asp)	S	S	S
C57BL/6J	G**A**C (Asp)	S	S	S
C57BL/10J	G**A**C (Asp)			S
CE/J	G**A**C (Asp)			S
SWV	G**A**C (Asp)			S
DBA1/J	G**A**C (Asp)			S
NZW/LacJ	G**A**C (Asp)		S	S
B10.A				S
B10.D2		S	S	S
NMRI		S	S	

1.1.4 The Slc11a1 Protein

Since the original isolation of *Slc11a1* (Vidal *et al.* 1993; Barton *et al.* 1994), homologues have been identified in a large number of distantly related and unrelated species including humans, SLC11A1 (Cellier *et al.* 1994), *Drosophila melanogaster,* Malvolio (Rodrigues *et al.* 1995) and *Oryza sativa* (rice), OsNramp (Cellier *et al.* 1995). Computer assisted analysis of amino acid sequences from a diverse array of Slc11a1 related proteins (Cellier *et al.* 1995) has indicated a high degree of sequence conservation, a situation rare for membrane proteins separated by such large evolutionary distances, suggesting they may belong to a class of ancient membrane transporters.

Slc11a1 was initially reported to encode a 484 amino acid polypeptide with a predicted molecular weight of 53kDa (Vidal *et al.* 1993) however subsequent isolation of *Slc11a1* from an activated macrophage cDNA library (Barton *et al.* 1994), yielded *Slc11a1* clones that differed in the 5' region from the original clone. Primer extension analysis, using macrophage RNA as a template, and synthetic oligonucleotides corresponding to the 5' region of the Barton sequence and the putative 5' region of the published Vidal sequence, was used to confirm that the newly isolated clone was the correct candidate for *Ity/Lsh/Bcg.* The oligonucleotide corresponding to the Barton sequence yielded products from both the resistant and susceptible mice, whereas oligonucleotides corresponding to the Vidal sequence failed to yield products from either resting or activated macrophages. The findings of Barton *et al.* introduced a further 64 amino acids to the NH_2-terminal domain of the Slc11a1 protein. *Slc11a1* is now accepted to encode a 548 amino acid polypeptide with a predicted molecular weight of 56kDa (see figure 1.1.4.1).

Hydropathy profiles of the predicted amino acid sequence (Vidal *et al.* 1993; Cellier *et al.* 1995), has identified a series of strongly hydrophobic domains that are similar to the membrane-spanning regions of polytopic integral membrane proteins, and has enabled the positioning of 10-12 potential transmembrane domains (TMD). The authenticity of the first TMD does however need to be reviewed further to the observation by Searle *et al.* (1998) that in confocal microscopy studies, antibodies corresponding to amino acids 58-63 and 52-56, found within TMD 1, could detect membrane bound Scl11a1 protein.

Computer assisted analysis (Cellier *et al.* 1995) has also indicated a high degree of sequence conservation within the first 10 TMD of the various Slc11a1 orthologues, assigning this region the hydrophobic core. Sequence analysis of individual TMD within the hydrophobic core has revealed a remarkably high level of conservation for TMD 1, 4, 6 and 10. The high degree of conservation within TMD 4 is of particular interest, as it is the mutation of the glycine at position 169 to an aspartate within TMD 4 of the murine Slc11a1 protein that causes the complete loss of function (Vidal *et al.* 1995), resulting in susceptibility to infectious disease. Helical wheel representation of TM 4 revealed that the mutated residue maps to a strongly hydrophobic face of the proposed helix (Vidal *et al.* 1993). The non-conservative substitution of the small neutral glycine residue for the negatively charged bulky aspartate residue is expected to dramatically alter the physical properties of this proposed TMD. The possible results of this may affect the overall membrane associated structure and/or membrane insertion of the protein in the susceptible mouse strains. The absence of a mature (90-100kDa) immunoreactive Slc11a1 protein on a western blot (Baker *et al.* 2000) is supportive of this however, there are reports of membrane bound Slc11a1 protein in pathogen infected macrophages derived from susceptible mouse strains, albeit at much lower levels (Searle *et al.* 1998).

Sequence analysis of the intra- and extra-cytoplasmic loops within the hydrophobic core has revealed a high degree of sequence and size conservation between the Slc11a1 proteins. The short TMD 1-2, 2-3, 3-4 and 8-9 intervening loops displayed a high degree of sequence similarity, whereas the TMD 1-2, 2-3, 8-9 and 9-10 intervening loops showed size conservation. The intra-cytoplasmic loop between TMD 8-9 contained a precisely conserved transport motif (CTM) known as the "binding-protein-dependent transport system inner membrane component signature"[2] between amino acids 370-389 in Slc11a1 (Vidal *et al.* 1993). Such CTM, when located amino-terminal to the last two TMD (approximately 95-130 residues from the carboxy-terminus) on the cytoplasmic side of the membrane within a highly hydrophobic integral membrane protein, are believed to participate in substrate translocation across the membrane (reviewed Vidal *et al.* 1993).

[2] The CTM within the murine Slc11a1 protein; NH_2-(QSSTMTGTYAGQFVMEGFLK)-COOH

The intervening loops between TMD 4-5, 5-6, 6-7, 7-8, 10-11 and 11-12 showed no degree of sequence or size conservation (Cellier *et al.* 1995). This finding is surprising as murine Slc11a1 has been shown to contain a potential protein kinase C (PKC) phosphorylation site at Ser-274 within the TMD 6-7 intra-cytoplasmic loop, and two N-linked glycosylation sites at positions 321 and 335 clustered within the TMD 7-8 extra-cytoplasmic loop (Vidal *et al.* 1993). Despite a lack of sequence conservation the presence of a glycosylated loop between TMD 7-8 is maintained in all but the yeast Slc11a1 proteins (Smf1&2) (Cellier *et al.* 1995), implying glycosylation plays an important role in the correct targeting, stabilisation, or processing of the polypeptides. In agreement with this Barton and Atkinson (1998), showed glycosidase PNGase F treatment of the Slc11a1^{G169} expressing murine cell line N11 caused the disappearance of the 90-100kDa immunoreactive bands on a western blot. This disappearance was coupled with the strong appearance of the 45kDa immunoreactive band, a band that is also be observed in cell lines expressing the mutant Slc11a1^{D169} protein. These results suggested that failure of the mutant Slc11a1^{D169} protein to undergo essential post-translational modifications such as glycosylation may play an integral role in the loss of function of this protein.

The regions flanking the hydrophobic core include the TMD 11 and 12, and the amino- and carboxy-terminal tails; these sequences show a low degree of conservation between species, with the *Drosophila melanogaster Mvl* gene not even encoding these last two TMD. Analysis of the non-conserved domains within Slc11a1 identified four further putative PKC phosphorylation sites, Ser-3, Ser-37, Ser-52 (Barton *et al.* 1994) and Ser-530 (Vidal *et al.* 1993). The identification of putative phosphorylation sites, and the observation that the level of Slc11a1 phosphorylation in *in vitro* phosphorylation assays is decreased by cytokine treatment (Barton *et al.* 1999), suggested a role for phosphorylation in the induction of Slc11a1 function. Analysis of the non-conserved domains has also identified amino- and carboxy-terminal dileucine and tyrosine based motifs for endocytic targeting motifs (Atkinson *et al.* 1998), and a proline-serine-rich, putative carboxy-terminal SH3-binding motif (Barton *et al.* 1994).

Based on hydropathy profiles, and conserved sequence motifs, first identified in Slc11a1, a model for the membrane-associated organisation was predicted (Vidal *et al.* 1993) (see figure 1.1.4.2). This model was based on 2 assumptions, firstly that the

hydrophobic segments identified by the hydropathy profiles do correspond to TMD, the accuracy of which has been questioned following the finding that an antibody directed against an epitope that maps to TMD 1 can detect Slc11a1 in subcellular localisation studies (Searle *et al.* 1999), and secondly, that the CTM is located on the cytoplasmic side of the membrane. This arrangement places the amino- and carboxy-terminals and all 5 putative PKC phosphorylation sites within the cytoplasm, and the highly glycosylated loop on the extracellular/lumenal side of the membrane, this arrangement was found to be in agreement with the membrane organisation of a number of integral membrane proteins. The Vidal model is still proposed to depict the correct membrane associated organisation of Slc11a1. Based on this model, structural predictions have suggested an α-helical bundle within the membrane composed of a charged interior, owing to the presence of multiple charged residues in 6 out of the 10 TMD, and a semi-conserved hydrophobic core (Cellier *et al.* 1995). The presence of polar residues within the predicted TMD would impart an ampipathic character to the 6 TMD, such organisation has been found in TMD of several ion transporters/channel, confirming and expanding on the previous proposal (Vidal *et al.* 1993) that Slc11a1 may function as an ion transporter (Cellier *et al.* 1995).

FIGURE 1.1.4.1 Annotated Slc11a1 Amino Acid Sequence. The 548 Slc11a1amino acid sequence (EMBL accession number X75355). The 12 putative alpha helical membrane spanning domains are highlighted in pink, and the TMD number indicated beneath is accompanied by an arrow (←→) indicating direction with respect to membrane (arrow toward cytoplasm) (adapted Vidal et al. 1995). Putative PKC phosphorylation sites are underlined and indicated by **PKC** above. The N-Linked glycosylation sites are underlined and indicated by **N-Gly** above. The "binding-protein-dependent transport system inner membrane component signature" is underlined and indicated by |--**CTM**--| above. A black arrow (⬇) indicates position of the Gly169 that is mutated in susceptible strains.

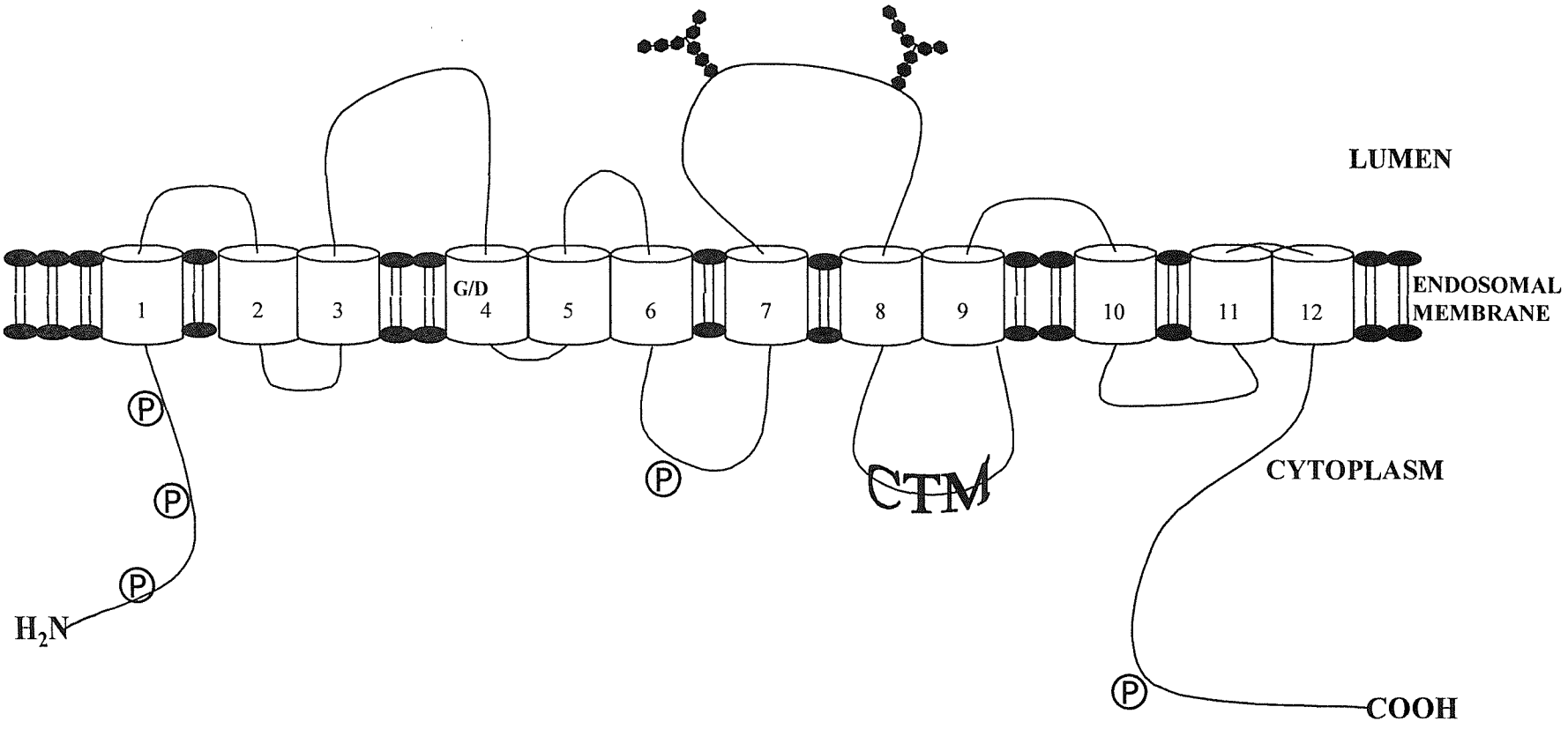

FIGURE 1.1.4.2 Schematic Representation of the Putative Structure of the murine Slc11a1 Protein and its Orientation in the Cell Membrane. The 12 putative TMD are depicted as open columns with the NH_2-termianl domain, COOH-terminal domain and loops regions as black lines. The potential N-Linked glycosylation sites are represented by the grey stars indicated by , the putative PKC phosphorylation sites are represented by the open stars labelled P Ⓟ , and the location of the Gly-169-Asp mutation indicated by G/D within TMD 4. The conserved transport motif is represented as the letters CTM. This figure has been adapted from Vidal *et al.* 1993.

1.1.5 Cellular and Sub-cellular Localisation of the Slc11a1 protein

In vivo studies analysing resistance and susceptibility *M. bovis* infection revealed the cell population responsible for the phenotypic expression of *Bcg* to be, bone marrow derived, radiation resistant, and sensitive to silica, a phagocytic poison (Gros *et al.* 1983). Furthermore, explanted macrophages from Bcg^R and Bcg^S inbred strains of mice displayed differential capacities to restrict growth of the intracellular pathogen *Mycobacterium intracellulare* (Goto *et al.* 1989). Together these results established that the macrophage was the cell type expressing the genetic difference at *Bcg,* hence *Slc11a1*, which was isolated on the basis of its macrophage-restricted expression. Vidal *et al.* (1993) showed *Slc11a1* mRNA expression was restricted to organs of the reticuloendothelial system (spleen and liver), and specifically to the macrophage enriched fractions of these organs. They went on to show *Slc11a1* mRNA expression in the J774A and RAW 264.7 macrophage cell lines, but not in cell lines of different lineages. In order to determine which bone marrow precursors and differentiated cell lines express *Slc11a1* the technique of global cDNA amplification (RT-PCR) was applied to pluripotent or committed progenitor cells (Govoni *et al.* 1997). This technique indicated that *Slc11a1* expression is specific to mature cells of the myeloid lineage's, granulocytes (eosionophil, neutrophil), and mononuclear phagocytes (monocytes/macrophages). Furthermore human SLC11A1 expression has been shown to occur late in neutrophil maturation (Cannone-Hergaux *et al.* 2002), suggesting that *Slc11a1* expression may not only prove to be a good marker of cells of the myeloid lineage, but more specifically mature cells of this lineage.

Computer assisted analysis of the Slc11a1 polypeptide suggested the protein is membrane bound (Vidal *et al.* 1993; Cellier *et al.* 1995). Immunofluorescence and confocal microscopy, using a series of markers corresponding to known membranous compartments within the cell, were used to elucidate the subcellular localisation of Slc11a1 within 129/sv derived peritoneal macrophages (Gruenheid *et al.* 1997). Production of a null mutation at *Slc11a1* ($Slc11a1^{-/-}$) within the 129/sv-mouse strain, which bears the wild-type *Slc11a1* allele $Slc11a1^{G169}$, provided an adequate control for these studies (Vidal *et al.* 1995). Indirect immunofluorescence of the Slc11a1 protein within the 129/sv derived peritoneal macrophages resulted in strong perinuclear staining patterns within the wild type ($Slc11a1^{G169}$) cells, that was absent from the mutant control ($Slc11a1^{-/-}$) cells, similar patterns of staining were

concomitantly observed by other researchers (Atkinson *et al.* 1997). Kishi *et al.* (1996) had previously reported localisation of the human SLC11A1 protein to the plasma membrane within the lymphoma pre-monocyte/macrophage cell line U937. Such distribution has not subsequently been observed for either the human SLC11A1 protein (Cannone-Hergaux *et al.* 2002) or the murine Slc11a1 protein (Atkinson *et al.* 1997; Gruenheid *et al.* 1997; Searle *et al.* 1998), however in transient transfection studies a eGFP-Nramp1 chimeric protein transient surface staining minutes after PMA treatment has been observed (Baker & Barton unpublished). Comparison of Slc11a1 staining patterns with markers specific to the golgi apparatus (MG160), endoplasmic reticulum (calnexin), early endosome (Rab5), late endosomes (Rab7), early lysosomes (Lamp1) and lysosomes (cathepsin B), indicated that the pattern of Slc11a1 staining showed similarity with that of Rab5, Rab7 and particularly Lamp1. Confocal microscopy showed a complete co-localisation of Slc11a1^{G169} and Lamp1 to the same subcellular structures, confirming Slc11a1^{G169} is expressed in the late endosomal/lysosomal compartments of resting macrophages. Upon phagocytosis of latex beads, wild-type Slc11a1^{G169} was seen to migrate to, and co-localise with Lamp1 at the surface of these maturing latex bead-containing vesicles, with the pattern of staining becoming less perinuclear and more diffuse within the cytoplasm. Slc11a1^{G169} remained associated with the phagosome throughout phagolysosome biogenesis (Greunheid *et al.* 1997). Identification of Slc11a1 on membranes of the endocytic pathway is consistent with the identification of tyrosine-based endocytic targeting motifs within the N- and C-terminals of the Slc11a1 polypeptide, YGSI and YGLP respectively (Atkinson *et al.* 1997). Confocal and Immunogold-electron microscopy analysis of Slc11a1^{G169} mostly confirmed the findings of previous localisation/ co-localisation studies (Searle *et al.* 1998). However, like Atkinson *et al.* (1997) they did observe staining of the mutant Slc11a1^{D169} protein in a pattern analogous to that of the wild-type protein Slc11a1^{G169}, albeit at 3-4 fold lower levels (Searle *et al.* 1998). These studies went on to show that activation of the bone marrow derived macrophage cells, by treatment with the pro-inflammatory cytokines interferon γ (IFNγ) and bacterial Lipopolysaccharide (LPS), increased the frequency of labelled late endosome and lysosomes, with a corresponding increased dispersion of Slc11a1 positive vesicles throughout the cells. Furthermore, it was shown that infection of macrophages with *Leishmania major* and *Mycobacterium avium* resulted

in the recruitment of Slc11a1 to the membranes of the bacterial containing vesicles. *M. avium* infection induced a greater degree of migration of the Slc11a1 protein compared with *L. major* infection, resulting in a striking pattern of vesicles located along the microtubule structures of the cell. This finding is compatible with observation that human SLC11A1 was associated with α and β-tubulin molecules within the microtubules (Kishi *et al.* 1996; Tokuraku *et al.* 1998), and the presence of a putative SH3 binding domain within Slc11a1 that shared identity to the microtubule-binding region of dynamin (Barton *et al,* 1994).

1.1.6 *Slc11a1* Function

In vivo and *in vitro* functional studies have shown that *Slc11a1* plays an important role early in the macrophage activation pathway. A possible role in the macrophage activation pathway, the presence of a CTM, and proposed secondary structure that was strikingly similar to that of the Asperigillus nidulans nitrate transporter protein CrnA, led to the suggestions Slc11a1 may function as either a nitric oxide (NO) transporter (Vidal *et al.* 1993), or an L-arginine transporter (Barton *et al.* 1994). NO and L-arginine are both intimately involved in the signal transduction pathway that regulates the antimicrobial activity of the cell. However, these proposed mechanisms of Slc11a1 function could not sufficiently explain many of the pleiotropic effects associated with Slc11a1 function (figure 1.1.6.1; reviewed Bellamy, 1999; Blackwell *et al.* 2000). A greater understanding of Slc11a1 function has come from research into, and similarities drawn with, other members of the Slc11a-protein family.

Slc11a1 belongs to a very large family of membrane proteins, the structure, characterised by the presence of a common hydrophobic core of 10 TMD, and function, divalent ion transport, of which have been conserved throughout evolution (reviewed Cellier *et al.* 1995; Bellamy, 1999; Blackwell *et al.* 2000; Forbes and Gros, 2001). *Slc11a1* orthologues have been identified in a broad range of organisms including, humans (SLC11A1 and SLC11A2), mouse (*Slc11a2)*, rat (*DCT1/DMT1)*, *Drosophila melanogaster (Mvl), Caenorhabditis elegans, Oryza sativa (OsNramp1), Saccharomyces cerevisiae (Smf1, Smf2 and Smf3), Arabidopsis thalania* and *Mycobacterium leprae* (reviewed Cellier *et al.* 1995). However, clues to *Slc11a1* function have come from studies into the *Drosophila melanogaster Slc11a1* orthologue *Malvolio (Mvl),* the mouse and rat orthologues, *Slc11a2* and *DMT1* respectively, and the *Saccharomyces cerevisiae* orthologues *Smf1* and *Smf2*. *Slc11a2* was identified using a positional cloning approach for the *mk* gene associated with microcytic anaemia, implying a role for the *Slc11a2* gene in iron uptake (Fleming *et al.* 1997). Functional cloning experiments, involving $^{55}Fe^{2+}$ uptake in *Xenopus* oöcytes, identified a rat mRNA that stimulated uptake more than 200 fold, the gene was termed divalent cation transporter 1/divalent metal transporter 1 (DCT1/DMT1) (Gunshin *et al.* 1997). Subsequent sequence analysis showed *DMT1* was the rat *Slc11a2* orthologue. *Slc11a2* and *DMT1* contained identical G185R mutations that are responsible for microcytic anaemia in the *mk* mouse (Fleming *et al.* 1997) and the

Belgrade rat (Gunshin *et al.* 1997). Studies on *Slc11a2* and *DMT1* revealed that they are ubiquitously expressed, upregulated by deprivation of dietary iron, and function as proton coupled divalent cation symporters (reviewed Blackwell *et al.* 2000; Forbes and Gros, 2001; Lieu *et al.* 2001). In line with this, both the sensory neurone taste discrimination defect, associated with the *Drosophila melanogaster Mvl* gene (Orgad *et al.* 1998), and the sensitivity to low Mn^{2+} concentrations in *Smf1*-null *Saccharomyces cerevisiae* (Supeck *et al.* 1996), could be suppressed by the addition of either Fe^{2+} or Mn^{2+}, to the diet/growth medium. Subsequently it has been shown that both *Mvl* and *Smf1* function as divalent cation transporters (reviewed Blackwell *et al.* 2000; Forbes and Gros, 2001). Together, the findings of *Slc11a2, DMT1, Mvl* and *Smf1* have led to the suggestion that like other members of its family, *Slc11a1* functions as a divalent metal transporter and that susceptibility to infection is a manifestation of impaired divalent cation transport.

Much of the earlier studies conducted on congenic resistant and susceptible mice, aimed to define the molecular defect underlying the $Slc11a1^{G169D}$ mutation, revealed a large number of differences between resistant and susceptible strains. In fact so many differences were identified it became clear that no obvious mechanism for the phenotype would come out from this type of analysis, however, macrophages from resistant mice appeared to mount a much more aggressive inflammatory response than those from susceptible mice and release quantitatively higher levels of pro-inflammatory cytokines. Differences in the pools of divalent cations by transport between the lumen of the phagolysosome and the cytoplasm was thought to explain the pleiotropic effects on macrophage function associated with *Slc11a1* expression. Such reported pleiotropic effects include, regulation of the CXC chemokine KC, inducible nitric oxide synthase (iNOS), major histocompatibility (MHC) class Ia, IAβ, II molecules, tumour necrosis factor-α (TNF-α), NO release, L-arginine flux and oxidative burst (figure 1.1.6.1; reviewed Bellamy, 1999; Blackwell *et al.* 2000). The direction of divalent cation transport by Slc11a1 is however the subject of much controversy, with data supporting both the transport of divalent cations into (Kuhn *et al.* 1999; Goswami *et al.* 2001) and out of (Jabado *et al.* 2001) the lumen of the phagolysosome. How does this putative transport function relate to the observed resistance to infection conferred by the expression of functional *Slc11a1*? Based on

the conflicting transport data, two models of *Slc11a1* mediated antimicrobial mechanisms have been proposed, the bacteriostatic mechanism and the bactericidal mechanism (see figure 1.1.6.2).

EFFECT	CHANGE	REFERENCE
Growth of intracellular pathogens	↓	Plant and Glynn, 1974 Bradley, 1977 Gros *et al.* 1974
Antigen presentation	↑	Denis *et al.* 1988a
Respiratory burst	↑	Denis *et al.* 1988c Channon *et al.* 1984 Barton *et al.* 1995
Mixed lymphocyte reactive	↑	Denis *et al.* 1988b
mRNA stabilisation	↑	Brown *et al.* 1997
I-A antigen expression	Continuous cf transient	Johnson *et al.* 1985 Zwilling *et al.* 1987 Barrera *et al.* 1997 Kaye *et al.* 1988 Lang *et al.* 1997
Nitric oxide production	↑	Barrera *et al.* 1994 Arias *et al.* 1997 Formica *et al.* 1994 Barton *et al.* 1995
STAT-1α phosphorylation	↑	Wojciechowski *et al.* 1999
Mn-SOD and BCL-2	↑	Kovarova *et al.* 1998
KC chemokine	↑	Roach *et al.* 1994
TNFα, IL-1β	↑	Formica *et al.* 1994 Kita *et al.* 1992
L-arginine transport	↑	Barton *et al.* 1995
Antigen processing/presentation	↑	Lang *et al.* 1997
T-Helper response	1 versus 2	Soo *et al.* 1998 Kramnik *et al.* 1994
Behavioural/stress response	More aggressive cf Less aggressive	Evans *et al.* 2001
PKC Activity	↑	Brown *et al.* 1994 Olivier *et al.* 1998
PKC-β1, cell growth	↓	Baker *et al.* 2000
IRP2	↑	Baker *et al.* 2000
Cathepsin D	↑	Biggs *et al.* 2003
Iron Export .	↑	Biggs *et al.* 2001 Mulero *et al.* 2002

FIGURE 1.1.6.1 Table summarising the many pleiotropic effects attributed to *Slc11a1* alleles. The pleiotropic effects attributed to *Slc11a1* alleles are listed in column one, column 2 indicates the change of the effect in resistant $Slc11a1^{G169}$-expressing mice with respect to the susceptible $Slc11a1^{G169}$-expressing mice, an increased effect is indicated by an upward pointing arrow (↑), and a decreased effect by a downward arrow (↓). Column three indicates the reference describing the effect. Figure adapted from Biggs *et al.* 2003.

THE BACTERIOSTATIC MECHANISM

Metabolic labelling of leishmania amastigotes *in vivo* showed that a difference in the rate of replication, as opposed to active elimination was associated with the genetic advantage seen in Lsh^R strains of mice (Bradley, 1979). Experiments with replication-defective strains (Benjamin *et al.* 1990) and temperature sensitive strains (Govoni *et al.* 1999) of *S. typhimurium* suggested that the resistance phenotype, associated with $Slc11a1^{G169}$ expression, is a consequence of enhanced bacteriostatic activity as opposed to enhanced bactericidal activity of the macrophages. More recently electron microscopy has shown that bacteria within phagosomes of macrophages isolated from $Slc11a1^{G169}$ mice showed signs of dormancy as opposed to death (Frehel *et al.* 2002). This is supported by the findings of Gomes and Appelberg (2002) in which macrophages, isolated from $p47^{Phox}$ knockout mice, which are defective in their ability to produce superoxide (Jackson *et al.* 1995), showed no change in their ability to suppress pathogen growth. These data suggested that the *Slc11a1*-dependent influence on pathogen growth is independent of superoxide production, supporting a bacteriostatic mechanism of resistance. The bacteriostatic mechanism is based on the premise that like Slc11a2, Slc11a1 transports divalent cations out of the lumen of the phagosome into the cytoplasm. The high sequence similarity between the Slc11a1 and Slc11a2 proteins (66% identity, 77% similarity (Cellier *et al.* 1995)), and almost identical secondary structures, and membrane topologies, supports that their mode of action will also be similar. Consequently it has been proposed that *Slc11a1* transports divalent cations out of the lumen of the phagolysosome into the cytoplasm, thereby depleting the pathogen containing vesicles of essential nutrients, such as iron and other divalent cations, required for growth. Iron is an essential nutrient for all living organisms, and is intricately involved in the regulation of gene expression, the synthesis of both DNA and RNA, cellular respiration, proliferation and differentiation (reviewed Lieu *et al.* 2001). The ability of microorganisms to acquire iron is proposed to be one determining factor as to whether they can establish infection within its host. Without iron they will be unable to protect themselves against the antimicrobial activity of the cell. Support for this observation has come from experiments where injection of iron compounds into animal hosts significantly enhanced the virulence of invading pathogens (reviewed Ratledge and Dover, 2000) and restricting iron levels by the addition of specific chelators severely impairs *M. avium* growth within the host animal (Gomes *et al.* 1999). In light of these data,

Gomes and Appelberg (1998) hypothesised that if Slc11a1 were functioning to deplete the phagolysosome of iron, iron overload should overcome any advantage conferred by a more efficient pumping system in the *Slc11a1*^{G169} expressing mice compared with the *Slc11a1*^{D169} expressing mice. By inference, if Slc11a1 were functioning to transport divalent cations into the phagosome, iron overload would enhance the antimicrobial activity of the cell. Infection of mice with *M. avium* 2447 after 20 days of iron loading resulted in increased bacterial loads in the lungs, liver and spleen of both the *Slc11a1*^{G169} (resistant) and *Slc11a1*^{D169} (susceptible) expressing mice 4 weeks post infection. Furthermore, the bacterial loads of the animals that received the highest iron dose (12mg) were not significantly different between the *Slc11a1* alleles, this was found to be independent of the acquired immune system. These findings do not take into account any deleterious effects excess iron maybe having on the animals. Excess iron is highly toxic due to its ability to generate reactive oxygen species via the Fenton reaction[3]; hydroxyl and superoxide radicals react rapidly with all living cells, severely impairing cellular integrity. Furthermore it is well documented that iron overload can directly interfere with the capacity of the body to mount an efficient immune response, altering the CD8:CD4 ratio towards the CD8 $T_{suppressor}$ cells, and decreasing antibody and mitogen mediated phagocytosis by macrophages (reviewed Walker and Walker, 2000). Iron can also downregulate transcription of the *inducible nitric oxide synthetase* (*iNOS*) gene (Dlaska and Weiss, 1999). Production of NO by macrophages constitutes a major effector mechanism against invading pathogens, inducing cytostatic effects by interfering with the catalytic iron centres of enzymes within the target cell. Together, immune interference and cellular damage, due to excess iron stores, has the potential to severely compromise the antimicrobial capacity of the host, and could explain the finding that bacterial load is increased in all 3 organs tested from both the resistant and susceptible mice. However, Gomes and Appelberg (1998) concluded that Slc11a1 transports divalent cations out of the lumen of the phagolysosome.

Jabado *et al.* (2000) provided further evidence for this proposal. Using a divalent cation sensitive flurophore COOH-FF6$(COOEt)_4$ covalently linked to particulate zymosan, they showed *Slc11a1*^{G169} expressing phagosomes extrude divalent cations to

[3] Fenton Oxidation-Reduction Reaction:
$Fe^{3+} + {}^{\bullet}O_2^- \rightarrow Fe^{2+} + 0_2$; $Fe^{2+} + H_2O_2 \rightarrow Fe^{3+} + {}^{\bullet}OH + OH^-$

a greater extent than *Slc11a1*$^{-/-}$ phagosomes. Therefore they concluded that Slc11a1 was functioning to pump divalent cations from the lumen of the phagolysosome into the cytoplasm. However divalent cation accumulation within the cytoplasm was not shown. Jabado *et al.* (2000) also performed the opposite experiment, measuring net influx of divalent cations, into the lumen of the phagolysosome, and showed *Slc11a1*$^{-/-}$ cells accumulated higher levels of divalent cations than *Slc11a1*^{G169} expressing cells. This difference was proposed to be due to increased efflux in the wild-type *Slc11a1*^{G169} expressing cells as opposed to increased influx in the mutant *Slc11a1*$^{-/-}$ cells. Furthermore this difference could be abrogated by the addition of concanamycin, a macrolide antibiotic that specifically targets the vacuolar H^+-ATPase. Inhibition of the vacuolar H^+-ATPase prevents phagosomal acidification thereby dissipating the proton gradient between the phagosome and the cytoplasm. These observations indicated divalent cation transport by Slc11a1 was proton coupled, a finding upheld by Goswami *et al.* (2001). Considering their finding that Slc11a1 transports divalent cations out of the phagosome, Jabado *et al.* (2000) proposed that like Slc11a2, Slc11a1 functions as a divalent cation symporter.

The high sequence similarity of Slc11a1 and Slc11a2 does however seem to be rather misleading. Stable expression of Slc11a1^{G169} but not Slc11a2 was able to correct the susceptible phenotype of the RAW 264.7 cell line, which is homozygous for the *Slc11a1*^{D169} allele (Govoni *et al.* 1999). The inability of Slc11a2 to confer resistance to *S. typhimurium* SL1344 challenge may have been due to differing patterns of expression of the two proteins unlike Slc11a1^{G169}, Slc11a2 may not come into close proximity to pathogen containing vesicles and is therefore unable to exert an effect. Slc11a1^{G169} is present within the membranes of the late endosomal/early lysosomal compartments, whereas Slc11a2 locates to the plasma membrane and early endosomal compartments within murine macrophages (Greunheid *et al.* 1999; Blackwell *et al.* 2003; Baker and Barton unpublished results). Early endosomes fuse with, and exchange membrane with, pathogen containing vesicles even in *M. avium* infected cells where phagosome maturation has been inhibited (Sturgill-Koszycki *et al.* 1996; Frehel *et al.* 2002), therefore like Slc11a1^{G169}, Slc11a2 comes into close proximity to the invading pathogen. Considering the high degree of sequence similarity between Slc11a1 and Slc11a2, and the proximity of Slc11a2 to the invading pathogen, if the two proteins were functioning with similar mechanisms a certain degree of

redundancy would be expected. Furthermore, expression of *Slc11a2* but not *Slc11a1*, was able to complement a yeast strain defective in its *Slc11a1* related *SMF* genes (Pinner *et al.* 1997). *SMF* is expressed on the yeast plasma membrane and is involved in high affinity Mn^{2+} uptake. The ability of Slc11a2 but not Slc11a1 to complement the yeast SMF proteins, and the inability of Slc11a2 to complement Slc11a1 in the $Slc11a1^{D169}$ allele containing RAW 264.7 cell line provides firm evidence that Slc11a1 and Slc11a2 are functionally different, suggesting Slc11a1 may be transporting divalent cations into the lumen of the phagolysosome.

THE BACTERICIDAL MECHANISM

Previous studies into *S. typhimurium* infection showed that macrophages derived from Ity^R inbred strains of mice displayed increased bactericidal activity compared to their Ity^S counterparts (Lissner *et al.* 1983). The bactericidal mechanism is based on the premise that Slc11a1 is transporting divalent cations, specifically iron, from the cytoplasm into the lumen of the phagolysosome. Within the enhanced acidic environment of the phagolysosome the iron is proposed to participate in an oxidation-reduction reaction known as the Fenton reaction[3], leading to the production of hydroxyl radicals and hydroxyl anions. These highly reactive radicals, and indeed free iron, can interact with, and severely impair the integrity of the invading pathogen, thereby preventing pathogen proliferation. Evidence for the bactericidal mechanism has come from two consecutive reports from the same group of researchers. Zwilling *et al.* (1999) reported that supplementation of $Slc11a1^{G169}$ expressing cells with iron induced an anti-microbial activity within these cells that was inhibited by the addition of hydroxyl radical scavengers. This observation was followed up by the demonstration that $Slc11a1^{G169}$, but not $Slc11a1^{D169}$ expressing cell lines, displayed a significant increase in hydroxyl radical production in response to *M. avium* infection (Kuhn *et al.* 1999). These data have been confirmed in primary bone marrow-derived macrophages isolated from the $Slc11a1^{G169}$ and $Slc11a1^{D169}$-expressing strains 129sv and C57Bl/6, respectively; superoxide production was higher in the 129sv-derived macrophages compared to the C57Bl/6-derived macrophages in response to IFNγ and tumour necrosis factor-α (TNF-α) (Gomes and Appelberg, 2002). The increased production of hydroxyl radicals in $Slc11a1^{G169}$-expressing cells has been assumed to be a result of enhanced acidification of *M. bovis* (Hackman *et al.* 1998) and *M. avium*

(Frehel *et al.* 2002) containing phagosomes within *Slc11a1*^{G169}-expressing cells when compared with *Slc11a1*$^{-/-}$/*Slc11a1*^{D169}-expressing cells. Furthermore, the increased acidity of phagosomes containing live bacteria is proposed to be a result of increased fusion with the vacuolar type ATPase-containing late endosomes/lysosomes within the *Slc11a1*^{G169}-expressing cells compared with the *Slc11a1*$^{-/-}$-expressing cells. The acidic environment is optimal for the production of both reactive oxygen and reactive nitrogen species, in addition to the activation of the microbicidal enzymes required for host defence (Hackman *et al.* 1998).

The first suggestions that Slc11a1 may be involved in Fe^{2+} transport into the lumen of the phagolysosomes came from a report by the Zwilling (1996) showing a 50%, IFNγ-mediated, reduction in cellular iron content in macrophages isolated from *Slc11a1*^{G169}-expressing mice compared with those isolated from *Slc11a1*^{D169}-expressing mice. This report was quickly followed up by two consecutive reports from Atkinson and Barton. They showed that ectopic expression of *Slc11a1*^{G169} into both the Cos-1 (1998) and RAW 264.7 (1999) cell lines was associated with lower net iron levels than their non-transfected counterparts, with the *Slc11a1*^{G169} expressing RAW 264.7 macrophage cells exhibiting a 1.2-2-fold decrease in chelatable iron pool levels. These experiments were followed up with the demonstration that the lower cytoplasmic iron levels seen in the *Slc11a1*^{G169} expressing cell line resulted in qualitative and quantitative differences in the expression and function of iron-regulated genes/proteins (Baker *et al.* 2000). Unstimulated *Slc11a1*^{G169}-expressing RAW 264.7 macrophage cells, displayed higher iron-regulatory protein (IRP)-2 binding activity than control *Slc11a1*^{D169}-expressing cells. IRP 1 & 2 are cellular iron sensors that bind to hairpin loop structures termed, iron-response elements (IRE), within the 5'-UTR and 3'-UTR of target mRNA, thereby regulating iron-dependent translational efficiency and mRNA stability, respectively. IRP1 is a stable, bifunctional protein that, in the presence of iron exhibits cytoplasmic aconitase activity, under iron deplete conditions however, the fourth iron ion is released from the iron-sulphur cluster enabling IRE binding activity. IRP2 is not bifunctional protein and under iron replete conditions is selectively degraded by the proteasome via an iron-dependent mechanism. This has been proposed to involve iron-dependent oxidation, which predisposes IRP2 to sequential ubiquitinylation and degradation

(Iwai *et al.* 1998). Increased IRP2-binding within the *Slc11a1*^{G169}-expressing cell line is consistent with these cells having lower cytoplasmic iron levels than the control cells. These results have been confirmed by the findings of Mulero *et al.* (2002) that *Slc11a1*^{G169}-expressing cells contain lower ferritin levels than their non-expressing counterparts. Ferritin mRNA contains an IRE within the 5'-UTR, binding of IRPs to this IRE regulates expression of ferritin by sterically blocking translation of the protein. Therefore, the increased IRP2 binding activity seen in the *Slc11a1*^{G169}-expressing cells may account for the decreased ferritin levels observed. Parallel experiments showed quantitative differences of a second iron-regulated protein, cellular protein kinase C-β1 (cPKCβ1), between cell lines (Baker *et al.* 2000). cPKCβ1 gene transcription is upregulated by iron (Alcantara *et al.* 1994). The *Slc11a1*^{G169}-expressing cell lines showed reduced cPKCβ1-immunoreactivity compared to the non-expressing cell lines. Serum starvation of the non-expressing cell lines, and ferric ammonium sulphate (FAS) treatment of the *Slc11a1*^{G169}-expressing cell lines to either decrease or increase iron levels respectively, resulted in the depletion or appearance of cPKCβ1 immunoreactivity respectively. These experiments showed that there is no defect in the cPKCβ1 response to iron in either cell line, confirming the difference seen in untreated cells reflect the differing cytoplasmic iron levels within the two cell lines.

It is proposed the lower cytoplasmic iron levels seen in the *Slc11a1*^{G169}-expressing cell lines may be due to increased iron flux from the cytoplasm into the lumen of the phagolysosome as has been reported by Kuhn *et al.* (1999). Transport of Iron-citrate into latex bead containing phagosomes (LBP) isolated from *Slc11a1*^{G169}-expressing cells was significantly more rapid and at significantly higher levels than in LBPs isolated from *Slc11a1*^{D169}-expressing cells. Furthermore, within the whole cell, the amount of radiolabelled iron within the LBP containing cellular fraction was 2.5 fold higher in the *Slc11a1*^{G169}-expressing cells compared with the non-expressing cells, with no significant difference being seen between the other 3 cellular fractions. These data were followed up by observations that iron transport from the cytoplasm into the lumen of the phagolysosome could be further increased by the addition of the macrophage activating, and *Slc11a1*-inducing (Brown *et al.* 1995; Govoni *et al.* 1995 & 1997; Atkinson *et al.* 1997; Baker *et al.* 2000), cytokines TNFα, IFNγ and GM-

CSF prior to *M. avium* infection (Kuhn *et al.* 2001). Subsequently Goswami *et al.* (2001), have shown that *Slc11a1* functions as a pH-dependent divalent cation antiporter. Expression of various *Slc11a1* constructs within *Xenopus* oöcytes provided a model to analyse Slc11a1 mediated divalent cation transport under differing internal and external conditions. These studies showed that the direction of divalent cation transport was pH dependent. At pH 9.0 there was a net influx of divalent cations into the oöcytes, at pH 7.5 there was no net movement, and at pH 5.5 (near physiological) there was a net movement of divalent cations out of the oöcytes. These results suggested Slc11a1 functions as a proton-coupled divalent cation antiporter. Addition of Zn^{2+} to pre-acidified (pH_i 6.5), *Slc11a1*^{G169}-expressing oöcytes resulted in a steady increase in pH_i, implying Zn^{2+} movement into the oöcytes is coupled with the outward movement of H^+ ions, confirming an antiport mechanism. Furthermore, dissipation of the electrochemical proton gradient across the membrane neutralised the Slc11a1 mediated divalent cation transport within the oöcytes, confirming a proton-coupled mechanism of action. Unlike Kuhn *et al.* (1999), who showed radiolabelled Fe^{2+} transport could only be competed by cold Fe^{2+} and Cu^{2+}, substrate specificity experiments confirmed transport of Fe^{2+}, Zn^{2+} and Mn^{2+} by Slc11a1 in the *Xenopus* oöcytes, showing Slc11a1 shares substrate specificity with Slc11a2.

The results of these data suggest Slc11a1 functions as broad-specificity, highly pH dependent divalent cation antiporter which, at a physiological pH, functions to transport divalent cations, specifically Fe^{2+}, from the cytoplasm into the lumen of the phagolysosome, thereby lowering cytoplasmic iron levels.

FIGURE 1.1.6.2 **Proposed Models of *Slc11a1* Function.** Based on the unresolved findings of the direction of Slc11a1 mediated divalet cation transport two models of Slc11a1 function have been proposed. (A) THE BACTERICIDAL MECHANISM: Slc11a1 ◯ transports divalent cations, specifically Fe^{2+} into the lumen of the phagolysosome where they can participate in the Fenton chemistry mediated production of hydroxyl radicals, thereby controlling pathogenic proliferation (●). (B) THE BACTERIOSTATIC MECHANISM: Slc11a1 transports divalent cations out of the lumen of the phagolysosome into the cytoplasm, thereby starving the bacterial of essential nutrients required for growth and proliferation.

Slc11a1 recruits to phagolysosomes
and alters the microenvironment

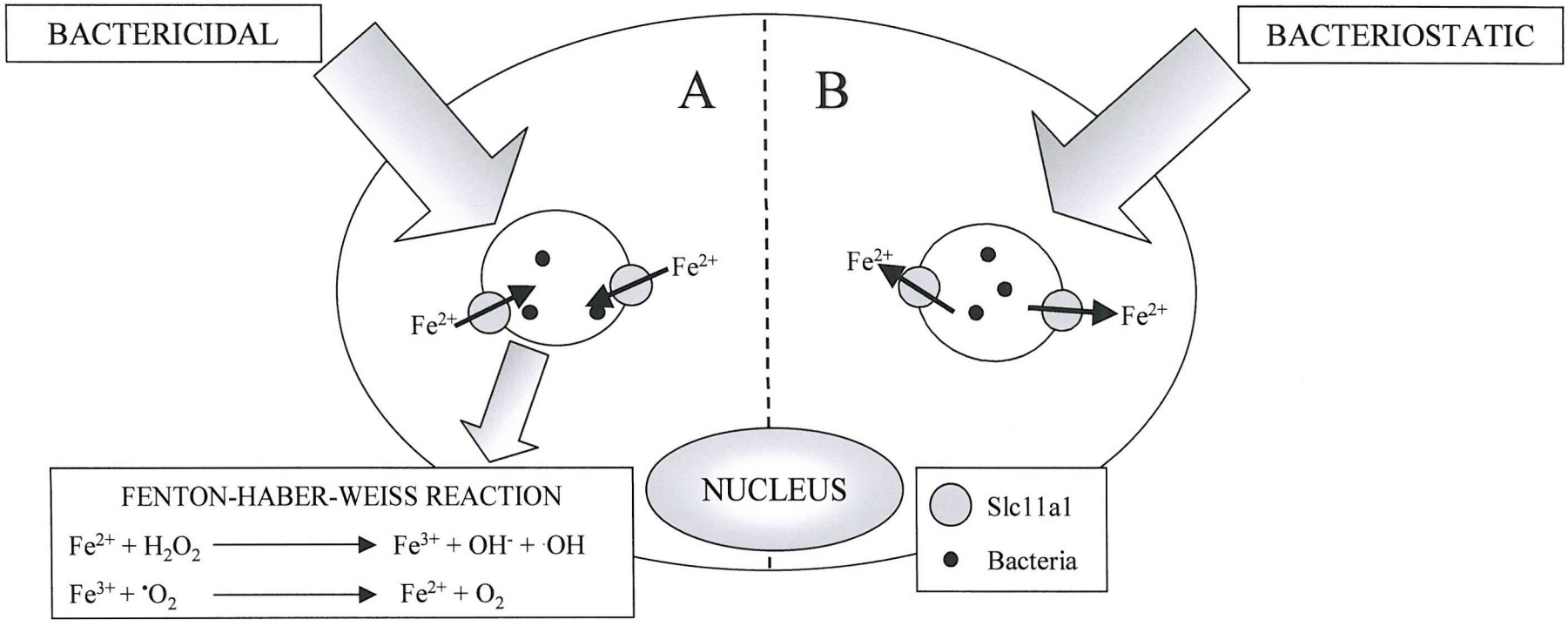

A ROLE IN IRON HOMOEOSTASIS?

The observation that Slc11a1 is constitutively expressed in macrophages within the erthrophagocytosing organs of the reticuloendothelial system, but retains the ability to be dramatically induced by IFNγ/LPS treatment, suggested a role for *Slc11a1* in both resting and activated macrophages (Govoni *et al.* 1997). Recent evidence has suggested that in the absence of such inflammatory stimuli, Slc11a1 plays an integral role in cellular iron homoeostasis, promoting the recycling of iron from senescent erythrocytes (RBC).

As discussed, $Slc11a1^{G169}$-expressing cells have been shown to display lower cytoplasmic iron levels than its non-expressing counterparts, these findings have been coupled with the observation that both *Slc11a1* mRNA and protein levels are upregulated by treatment of the cells with 100μM FAS (Baker *et al.* 2000). Regulation of *Slc11a1* expression by addition of exogenous iron has led to the suggestion that *Slc11a1* activity may control its own expression via a negative autoregulatory loop. An increased iron level induces expression of the Slc11a1 protein, Slc11a1 functions to transport iron out of the cytoplasm, thereby decreasing both cytoplasmic iron levels and its own expression. It was therefore proposed that Slc11a1 was involved in cellular iron homoeostasis, a proposal that was soon expanded to include a role for Slc11a1 in recycling iron from senescent RBCs. *In vitro*, *Slc11a1* expression in primary macrophage cells can be upregulated by the addition of both exogenous RBCs, and a synthetic haem analogue, hemin (Biggs *et al.* 2001). *In vivo* data has shown that *Slc11a1* expression is induced in a model of haemorrhagic trauma in the brain, involving the leakage of blood into the brain, and that this expression correlated with decreased iron levels around the lesion in the $Slc11a1^{G169}$ expressing, but not in the $Slc11a1^{DI69}$ expressing mice (Biggs *et al.* 2001). Furthermore, *Slc11a1* expression is restricted to a subset of resident tissue macrophages within organs of the reticuloendothelial system (RES), namely, the liver and the spleen, these cells are also the major site of erythrophagocytosis within the body (Biggs *et al.* 2001).

After their approximate 120-day life cycle, senescent RBCs are 'marked' for uptake by the resident tissue macrophages of the spleen and liver, the major site of

erythrophagocytosis within the body. The mechanism for this is unknown, however both CD47 (Oldenborg *et al.* 2000) and phosphatidylserine (PS) symmetry (McEvoy *et al.* 1986) have been proposed to be markers of age, defining cells for uptake by tissue macrophages. RBCs are unable to undergo apoptosis due to a lack of cytochrome c, mitochondria and nucleus however, they do show signs of membrane phospholipid redistribution, displaying PS on their outer leaflets (Mc Evoy *et al.* 1986). In apoptosis PS redistribution is essential for uptake of the apoptotic cell by macrophages (Bratton *et al.* 1999). Furthermore, it has been shown that PS on the cell surface of RBC directly correlated with their uptake by monocytes *in vitro* (Connor *et al.* 1994; Diaz *et al.* 1996), and clearance by the spleen *in vivo* (Allen *et al.* 1988). In apoptotic cells the exposed PS is recognised by the PS receptor (PSR) on the surface of the macrophage, triggering the uptake of the cells via receptor-mediated endocytosis. Once internalised the endosomes mature via fusion with other endocytic vesicles, such as recycling endosomes, early endosomes, late endosomes and lysosomes. During these fusion events the maturing vesicle acquires membrane proteins from other endocytic vesicles, Slc11a1 is one such protein with is recruited from late endosomes and lysosomes (Greunheid *et al.* 1997; Searle *et al.* 1998). In addition to acquiring membrane proteins, with each successive fusion event the pH within the vesicle is decreased, creating a highly acidic environment within the phagolysosome that is optimal to activate a series of proteases, leading to the degradation of RBC proteins. The complex multistep oxidative cleavage process that breaks down Haem releases iron, carbon monoxide and bilverdin Ixa. In man there are three enzymes that catalyse this reaction, however the haem oxygenase (HO) system constitutes the major degradative pathway (reviewed Morse and Choi, 2002), as HO-1 deficient mice models have illustrated (Poss and Tonegawa, 1997). During the iron salvage/recycling process $\approx 10^9$-iron ion are liberated from a single splenic macrophage from haem molecules in 24 hours, of which $\approx$ 50% are purged from cells as high molecular weight complexes (Kondo *et al.* 1988).

As discussed, a role for Slc11a1 in the process of erythrophagocytosis has been suggested, however the precise role is not yet clear. Kondo *et al.* (1988) reported increased ferritin levels after RBC uptake, suggesting the liberated iron passes through the cytosol and is sensed by IRP1/2, however treatment of macrophage cell

lines with iron via Tf-anti-Tf immune complexes resulted in no changes in ferritin protein levels (Mulero *et al.* 2002). Furthermore this group went on to show that *Slc11a1*^{G169}-expressing macrophages were more efficient at degrading the [^{59}Fe]Tf-anti-Tf immune complex within the late endosomal/lysosomal compartments than their *Slc11a1*^{D169}-expressing counterparts, an observation also made by members of our laboratory (Barton, unpublished results). These data suggested that Slc11a1 participates in erythrophagocytosis by promoting the liberation of iron from haem, and a potential mechanism for this is via the promotion of phagosomal acidification by Slc11a1. *M. bovis* (Hackman *et al.* 1998) and *M. avium* (Frehel *et al.* 2002) containing phagosomes are reported to be more acidic within *Slc11a1*^{G169}-expressing cells when compared with *Slc11a1*$^{-/-}$/*Slc11a1*^{D169}-expressing cells. The increased acidity of the lumen of the phagolysosome creates the optimal environment for the production of reactive oxygen and reactive nitrogen species, as well as the activation of many lysosomal proteolytic enzymes, all of which lead to the degradation of RBC proteins, making the haem iron more readily accessible for its liberation. In support of this Mulero *et al.* (2002) have shown that treatment of macrophage cell lines with IFNγ/LPS to induce phagocytosis of the [^{59}Fe]Tf-anti-Tf immune complex iron correlated with a nitric oxide dependent increase of iron release from the *Slc11a1*^{G169} expressing but not *Slc11a1*^{D169} expressing cells. Unpublished results (Barton) go on to propose that the liberated iron is secreted from the cell via packaging into small vesicular bodies termed exosomes. Furthermore Slc11a1 immunoreactivity was associated with these vesicular bodies, suggesting the Slc11a1 protein is also shed from the cell during iron recycling.

The results suggest that the Slc11a1 protein is intimately involved in the recycling of iron from senescent red cells by promoting the release of iron from haem, enabling its package into exosomes and subsequent release from the cell.

1.1.7 Regulation of *Slc11a1* Expression

The majority of the studies involving *Slc11a1* have involved functional studies into the role of *Slc11a1* within the body, and as discussed these results have led to conflicting results. It is hoped that analysis of the regulation of *Slc11a1* expression will provide crucial evidence towards the elucidation of *Slc11a1* function *in vivo*.

Regulation of *Slc11a1* by the proinflammatory cytokines IFNγ and LPS was proposed owing to the isolation of *Slc11a1* as the gene controlling resistance to intracellular infection (Vidal *et al.* 1993), and the identification of multiple IFNγ and LPS response elements within the proximal promoter region of *Slc11a1* (Govoni *et al.* 1995). Regulation of mRNA expression by IFNγ and LPS has subsequently been observed both *in vitro* and *in vivo* by a variety of researchers (Govoni *et al.* 1995 & 1997; Atkinson *et al.* 1997; Baker *et al.* 2000). This upregulation of mRNA levels correlated with an increase in the immature 45kDa protein in macrophages expressing both $Slc11a1^{G169}$ and $Slc11a1^{D169}$-alleles, and an increase in the 90-100kDa mature protein in macrophages expressing the $Slc11a1^{G169}$-allele (Baker *et al.* 2000; Biggs *et al.* 2001).

Activation of macrophages by either IFNγ/LPS or *M. avium* infection is associated with an increase in reactive oxygen and reactive nitrogen species, which can themselves lead to an increase in *Slc11a1* expression. It has been shown that in IFNγ/LPS-activated macrophages, *Slc11a1* mRNA derived from cells expressing the $Slc11a1^{G169}$-allele is 2-fold more stable than mRNA derived from cells expressing the $Slc11a1^{D169}$-allele (Brown *et al.* 1997). Stability of the $Slc11a1^{G169}$ mRNA was decreased to the level of the $Slc11a1^{D169}$ mRNA by the addition of antioxidants, and furthermore treatment of the $Slc11a1^{D169}$-expressing cells with menadione, an oxidant generator, increased mRNA stability to levels equivalent to the $Slc11a1^{G169}$ mRNA (Lafuse *et al.* 2000). In addition, $Slc11a1^{G169}$ mRNA and protein levels were induced by the addition of sodium nitroprusside (SNP), a nitric oxide donor (Baker *et al.* 2000). Together these data support a role for reactive oxygen and reactive nitrogen species in the positive regulation of *Slc11a1* expression.

Previous reports have shown that *Slc11a1*^{G169} expressing macrophages by IFNγ (Brown *et al.* 1994) or *M. bovis* (Olivier *et al.* 1998) have higher PKC activity than *Slc11a1*^{D169} expressing macrophages. Lafuse *et al.* (2000) have also shown that addition of PKC inhibitors decreased the *Slc11a1*^{G169} mRNA stability to the levels of the *Slc11a1*^{D169} mRNA. Furthermore, co-treatment of cells with the PKC inhibitor Go6976 and the oxidant generator menadione increased *Slc11a1*^{G169} mRNA stability in a PKC-dependent manner (Lafuse *et al.* 2000). Inhibitors of PKC activity have also been shown to interfere with Slc11a1 function, decreasing the Slc11a1-mediated iron transport into *M. avium* containing phagosomes (Kuhn *et al.* 2001). The involvement of the PKC pathway in regulating *Slc11a1* expression has been expanded to include the MAP kinases, ERK1, ERK2 and p38 (Lafuse *et al.* 2002). These data are supported by the findings that treatment of HL-60 cells with vitamin D alone, which is known to activate PKC and MAP kinases (Veenstra *et al.* 1997), and a combination of vitamin D and PMA, a pharmacological stimulator of PKC activity, led to the accumulation of *Slc11a1* mRNA (Roig *et al.* 2002). Regulation of *Slc11a1* by the PKC pathway may provide a link to the observed regulation of *Slc11a1* by both iron loading and iron deficiency, as iron is known to regulate expression of the PKCβ1 isoform (Alacantra *et al.* 1994). Iron loading macrophages using ferric ammonium sulphate (FAS) (Baker *et al.* 2000), RBC, or the synthetic haem analogue hemin (Biggs *et al.* 2001), led to the upregulation of *Slc11a1*^{G169} mRNA and protein levels. Conversely iron chelation using desferrioxamine (DES) decreased *Slc11a1*^{G169} mRNA stability (Lafuse *et al.* 2000), and *Slc11a1*^{G169} mRNA and protein expression (Baker *et al.* 2000). Taken together these data suggest as previously proposed by the Barton group (Baker *et al.* 2000), that *Slc11a1* is intimately involved in iron homoeostasis, controlling its own expression via a negative auto-regulatory loop.

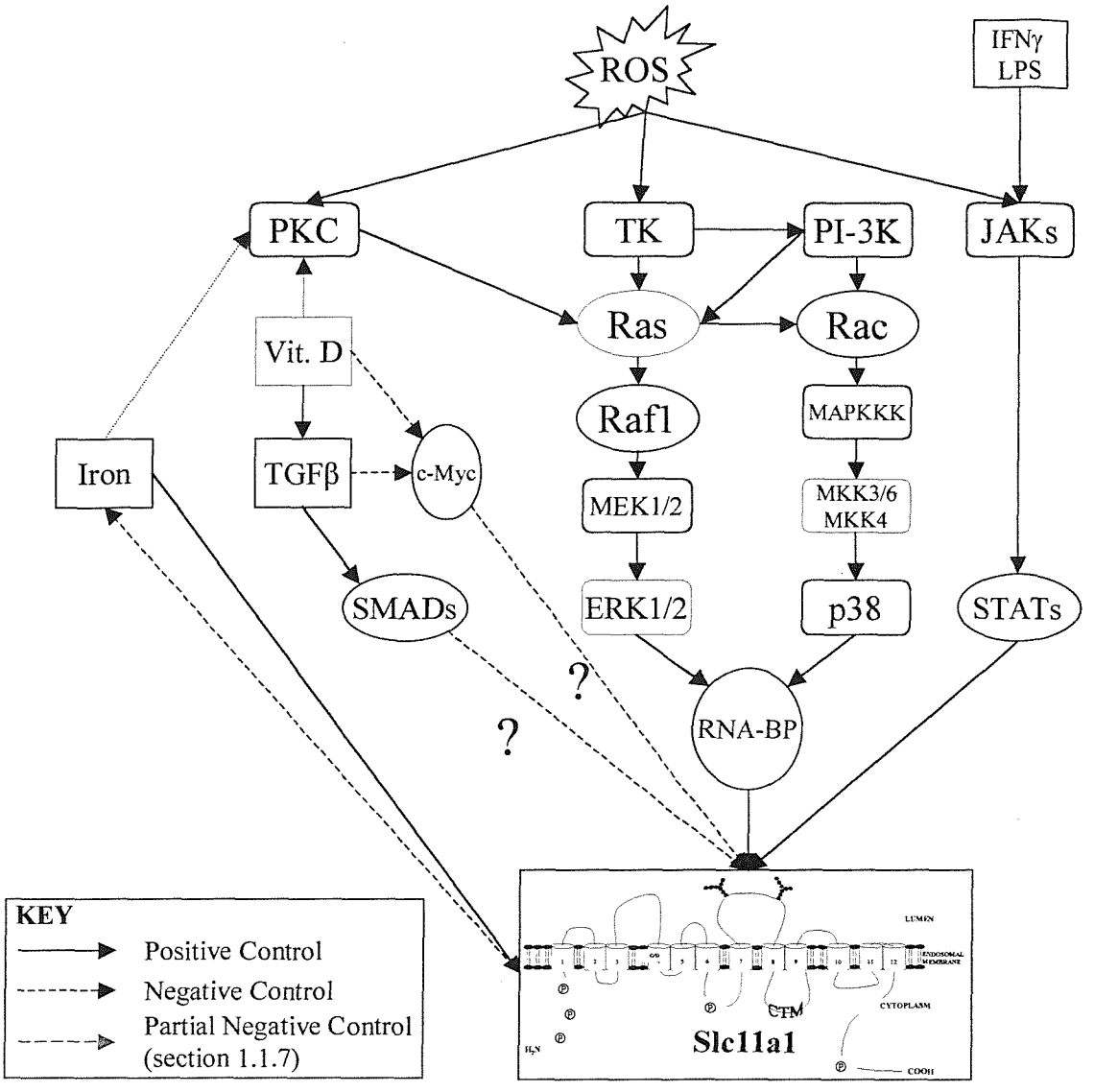

FIGURE 1.1.7.1 Pathways for Regulation of *Slc11a1* Expression. Diagram summarising proposed *Slc11a1* regulatory pathways, adapted Lafuse *et al.* 2002.

1.2 AIMS

Slc11a1/SLC11A1 plays an important role in controlling susceptibility to infection in mouse, likewise in human, as well as autoimmune disease susceptibility in human. In mouse a disease-causing mutation is found within the open reading frame, whereas in human a functional polymorphism associated with a microsatellite repeat element within the promoter contributes to disease susceptibility. However, little is known of the mechanisms controlling *Slc11a1*/SLC11A1 expression in mouse or in human.

The primary aim of this project was to prepare reagents to allow functional characterisation of the murine *Slc11a1* promoter, both as a model macrophage gene that could be used for subsequent macrophage-specific expression in potential transgenic mouse studies, and to understand how *Slc11a1* is controlled at the level of transcription. During the course of these studies a role for the proto-oncogene c-Myc in the control of genes that regulate cellular iron levels was identified. Furthermore, studies showed an antagonistic role for the c-Myc interacting zinc finger protein 1 (Miz-1), a protein isolated as a novel c-Myc binding protein. The second aim was therefore to elucidate if c-Myc and Miz-1 are important for Slc11a1 regulation and if so to examine the mechanistic basis for the regulation.

CHAPTER 2

Materials and Methods

2.1 MATERIALS

2.1.1 Chemicals

Chemicals were purchased from Sigma-Aldrich Chemical Company, Poole, UK, unless otherwise stated. Cell culture reagents, Penicillin, Streptomycin, Glutamine, Media etc. were obtained from Life Sciences Gibco BRL. Radioactive isotopes were obtained from ICN Biochemicals, Thane, UK. All materials and chemicals were stores and handled as per manufacturers instructions.

2.1.2 Water

Analar® high quality water (BDH Laboratory suppliers, Poole, UK.) was used during these experiments and will from this point be referred to as Deionised (DI) water.

2.1.3 Sterilization

Heat stable materials were sterilized by autoclaving at 15 psi for 15 minutes.
Heat labile solutions were sterilized by filtration through a 0.22mm filter (Millipore).

2.1.4 Bacterial Culture Media

Luria-Bertani (LB) Medium

LB broth is an all-purpose bacterial culture medium. 10g sodium chloride, 10g Bacto-tryptone and 5g Bacto-yeast were dissolved in 1 litre of DI water and then autoclaved. To produce solid medium (LB agar) 1.5% (w/v) purified agar was added prior to autoclaving.

SOB and SOC Medium

SOB and SOC are enriched mediums used for transformation of plasmid constructs into *E. coli* JM109 competent cells. An incomplete SOB medium consisting of 20g/l Bacto-tryptone, 5g/l Bacto-yeast and 0.5g/l sodium chloride was prepared in DI water and autoclaved. To the incomplete medium 10ml/l of both 1M magnesium chloride and 1M magnesium sulphate were added. The complete SOB medium was sterilized via filtration. SOC medium was produced immediately prior to use by adding 1ml 2M filter-sterilize glucose to 100ml complete SOB medium. SOC was sterilized via filtration.

Ampicillin

Ampicillin was added to culture medium to select for bacteria containing plasmids encoding Ampicillin resistance. Ampicillin was made as a stock solution at 50mg/ml in DI water, filter sterilized and stored in aliquots at -20^0C. Unless otherwise stated the final working concentration of Ampicillin was 100μg/ml.

Kanamycin

Kanamycin was added to culture medium to select for bacteria containing plasmids encoding Kanamycin resistance. Kanamycin was made as a stock solution at 15mg/ml in DI water, filter sterilized and stored in aliquots at -20^0C. Unless otherwise stated the final working concentration of Kanamycin was 30μg/ml.

2.1.5 Cell Culture Medium

RAW 267.4, N11 and Cos-1 cell lines were cultured in low-endotoxin Dulbecco's Modified Eagles Medium (DMEM) containing 10%(v/v) Myoclone foetal calf serum, 2mM L-Glutamine, 10 units/ml Penicillin with 100mg/ml Streptomycin and 20mM HEPES buffered saline (tissue culture grade). These cells were cultured on Nunc 75cm^2 flasks and centrifuged in polypropylene Falcon tubes to reduce adhesion of cells to the plastic. THP-1 human macrophage cell lines were cultured in RPMI 1640 containing 10%(v/v) Myoclone foetal calf serum, 2mM L-Glutamine, 10 units/ml Penicillin with 100mg/ml Streptomycin.

2.1.6 Plasmid Preparation

STE (Sodium-Tris-EDTA)

0.1M	NaCl
10mM	Tris-Cl (pH8.0)
1mM	EDTA (pH8.0)

Solution I (Tris-Glucose-EDTA)

50mM	Glucose
25mM	Tris-Cl (pH8.0)
10mM	EDTA (pH8.0)

Solution II (NaOH-SDS)

0.2M	NaOH
1.0%(w/v)	SDS

Solution III (KAC Working Solution)

3M	Potassium Acetate
5M	Glacial Acetic acid

Agarose Gel

1% (w/v)	Electrophoresis grade agarose
1x	TBE

5x TBE (Tris-Boric-EDTA) (1litre)

54.0g	Tris-base
27.5g	Boric acid
20ml	0.5M EDTA (pH8.0)

6x DNA Gel Loading Buffer

30%	Glycerol
0.25%	Bromophenol Blue
0.25%	Xylene Cyanol FF

2.1.7 Chloramphenicol Acetyl transferase (CAT) assay

Running Solvent

95% (v/v)	Chloroform
5% (v/v)	Methanol

2.1.8 Polyacrylamide Gel Electrophoresis (PAGE)

2x Resolving Gel Buffer (200ml)

14.52g	Tris (pH8.8)
4ml	10% SDS

Make to 200ml with Deionised water

2x Stacking Gel Buffer (200ml)

6.04g	Tris (pH6.8)
4ml	10% SDS

Make to 200ml with Deionised water

10% Resolving Gel Mix (10ml)

3.35ml	30% Acrylamide stock
5.00ml	2x Resolving gel buffer
1.65ml	Deionised water
100µl	10% APS (Ammonium persulphate)
10µl	TEMED (N,N,N'N'-tetra-methylenediamide)

4% Stacking Gel Mix (10ml)

700µl	30% Acrylamide stock
2.5ml	2x Stacking gel buffer
1.8ml	Deionised water
100µl	10% APS
10µl	TEMED

SDS-PAGE Running Buffer

25mM	Tris-base
190mM	Glycine
0.1%(w/v)	SDS

2.1.9 Sequencing

NaOH/EDTA

2M	NaOH
2mM	EDTA

155λ

100µl	100% Ethanol
5µl	3M Na Acetate (pH 5.7)

Denaturing Polyacrylamide Sequencing Gel

21g	Urea
5ml	5x TBE
7.5ml	40% Acrylamide
200µl	10% APS
20µl	TEMED

Running Buffer

1x	TBE

2.1.10 Western Blotting

Western Blotting Buffer

1:4 Methanol: SDS-PAGE running buffer

2.1.11 Antibody Detection

Phosphate Buffered Saline (PBS)

Prepared from tablets as per manufacturers' instructions.

PBS/Tween

0.10% (v/v) Tween 20 in PBS

Blocking Agent

10% (w/v) Milk powder in PBS/Tween

Antibody Diluent

5% (w/v) Milk powder in PBS/Tween

2.1.12 Proliferation Assays

Crystal Violet Stain

1g	Crystal Violet
4ml	Methanol

Once dissolved make up to 20ml DI and filter through 3MM Whatman paper.

2.1.13 Genomic DNA Isolation

Lysis Buffer

0.5M	EDTA (pH 8.0)
100µg/ml	Proteinase K
0.5%	Sarcosyl

Dialysis Solution

50mM	Tris-Cl (pH 8.0)
10mM	EDTA
10mM	NaCl

2.1.14 Preparation Nuclear Extracts

Dignam Buffer A

10mM	HEPES (pH 7.9)
1.5mM	$MgCl_2$
10mM	KCl
0.5mM	DTT
0.2%	NP40

Make up 10ml aliquot into 500µl aliquots and store at -20^0C. Prior to use add 1µl PMSF and 1µl Apoproteinin per aliquot.

Dignam Buffer C

20mM	HEPES (pH 7.9)
25%	Glycerol
0.42M	NaCl
1.5mM	$MgCl_2$
0.5mM	DTT
0.2mM	EDTA

Make up 10ml aliquot into 500µl aliquots and store at -20^0C. Prior to use add 1µl PMSF and 1µl Apoproteinin per aliquot.

2.1.15 Electrophoretic Mobility Shift Assay (EMSA)

5% EMSA Gel (50ml)

10ml	30% Acrylamide
1.25ml	10x TBE
38.75ml	Deionised water
500µl	10% APS
50µl	TEMED

EMSA Loading Dye

250mM	Tris-Cl (pH 7.5)
40%	Glycerol
0.2%	Bromophenol Blue
0.1%	Xylene Cyanol FF

EMSA Running Buffer

0.5x TBE

NAME	SEQUENCE
HB#1	5'-ATGCGGATCCTAATCAAGAGGACGCAGG-3'
HB#2	5'-TTTGCTTCTAGAATGTTG-3'
GT-AS	5'-TCCATAATAAGTCTGGCC-3'
MYC5-AS2	5'-CCAAACAAAAACCTCGAATTCATGTTTACAGCAATG-3'
MYC5-S	5'-CATTGCTGTAAACATGAATTC GAGGTTTTTGTTTGG-3'
MYC6M-AS	5'-AAAGGCAGAAGTGACGAATTCTGGCGGAAGGGGGTG-3'
MYC6M-S	5'-CACCCCCTTCCGCCAGAATTCGTCACTTCTGCCTTT-3'
NRP#1	5'-TCGACCCTCAGTGATGTGGAGATGAGGTCTGGAGGG-3'
NRP#2	5'-TCCCCTCCAGACCTCATCTCCACATCACTGAGGG-3'
NRP#3	5'-GATGGGAAGGGCGTGGGTTCCCACTCTTACTCACTCGGACC-3'
NRP#4	5'-CTGGTCCGAGTGAGTAAGAGTGGGAACCCACGCCCTTCCCA-3'
NRP#5	5'-AGCACCCACAGAAGGGGACAGATTGAG-3'
NRP#6	5'-GATCCTCAATCTGTCCCCTTCTGTGGGTG-3'
NRP #7	5'-GATTCCCACTCTTACTCACTCGGACC-3'
NRP #8	5'-CTGGTCCGAGTGAGTAAGAGTGGGAA-3'
REP#1	5'-GCTCTAGATTCACTAAGTTGTTTAGA-3'
REP#2	5'-GCTCTAGACCGTCATATGTATCCACT-3'
REP#3	5'-GCTCTAGAGGAGGTTTTTGTTTGGAC-3'
REP#4	5'-GCTCTAGAATCTGAGTGAGACCCTCA-3'
REP#5	5'-GCTCTAGACAGACTGAGATGAAAGAC-3'
Sp1M-AS	5'-AGAGTGGGAACCCATAGAATTCCCATCCCCTCCA-3'
Sp1M-S	5'-CACCCCCTTCCGCCAGAATTCGTCACTTCTGCCTTT-3'

FIGURE 2.1.1 **Table of Oligonucleotides used within these Studies.**

2.2 METHODS

2.2.1 Genomic Cloning of Murine *Slc11a1* Promoter

Genomic phage clones were isolated from a B6/CBAF1Jλ FixII library (Stratagene) by screening with a PCR-derived probe spanning the 5' end of the murine *Slc11a1* gene. The probe extended from –265bp of the major transcriptional initiation site to a BamHI site 43-48bp 3' of the last base of exon 2. From the screen two clones were isolated, λ1.4 and λ2.3 that were identical and these were plaque purified by routine methods. A SalI restriction fragment of ~ 9kb was sub-cloned into pBS and was analysed by sequencing (Oswel, Southampton). Plasmids produced designated **pS2** and **pS3** representing both orientations of the insert sequences respectively (see figure 2.2.1).

2.2.2 Preparation of Competent *E. coli*

The JM109 (e14$^-$(McrA$^-$) *recA1 endA1 gyrA96 thi-1 hsdR17* (r_K^- m_K^+) *supE44 relA1* Δ(*lac-proAB)* [F' *traD36 proAB* lacI^q*ZΔM15*]) strain of *E. coli* used during these studies were supplied already competent (Stratagene, UK), however cells can be made competent using the following method. Inoculate 10ml LB broth with stationary phase *E. coli* from a plate culture of *E. coli* and incubate overnight at 37^{0}C with agitation. Inoculate a fresh 10ml LB broth using 200μl of the overnight static culture. Incubate the inoculated culture at 37^{0}C with shaking until A_{550} reached ~0.5. Collect the cells using a refrigerated (4^{0}C) centrifuge at 3000rpm for 10mins. Remove the supernatant and resuspend the bacterial-pellet in 5ml ice cold sterile 0.1M $CaCl_2$, recentrifuge as above. Discard the supernatant and resuspend the bacterial pellet in 5ml. Store on ice for at lest 1hour before use.

2.2.3 Transformation of Competent *E. coli*

50μl of the competent *E. coli* were dispensed into pre-chilled 1.5ml microfuge tubes on ice. 0.4μl of β-mercaptoethanol (final concentration 25mM) was added to the competent cells and the mixture incubated on ice for 10 minutes, swirling gently

every 2 minutes. 2.5µl of the ligation mixture (0.1-50ng of DNA) was added to the competent cells, mixed gently, and incubated on ice for 30 minutes, allowing the DNA to precipitate around the competent cells. The cells were heat shocked by incubating at 42^{0}C for 45 seconds, enabling the uptake of DNA into the bacterial cells. The cells were allowed to recover by transferring back to ice for 2 minutes after the heat-pulse. 450µl of pre-warmed (42^{0}C) SOC medium was added to the cells and the cultures were incubated at 37^{0}C for 1 hour with shaking at 225-250 rpm. After recovery the cells were concentrated by centrifuging at 1000 rpm for 10 minutes, resuspended in 100µl of SOC medium and plated out onto LB agar plates containing the appropriate antibiotics for selection of positive colonies. The plates were incubated overnight at 37^{0}C.

2.2.4 Plasmid Preparation

Unless stated all plasmids were maintained in cultures of *E. coli* strain JM109 frozen in 25% glycerol in LB broth at –70^{0}C. Cultures from frozen stocks were streaked out onto LB plates containing the appropriate antibiotic and cultured overnight at 37^{0}C. 10ml LB-antibiotic liquid medium was inoculated with a single colony from the plated-out culture and incubated at 37^{0}C with agitation until A_{600} ~ 0.6. 250ml of pre-warmed (37^{0}C) LB media containing the appropriate antibiotic was inoculated with the 10ml culture and incubated for 18-24 hours at 37^{0}C with shaking at ~225-250 rpm. The cells were harvested by transferring to a clean sorval tube and centrifuged at 4500 rpm, 4^{0}C, for 20 minutes. Plasmid DNA was isolated using Quiagen endotoxin-free maxi-prep kits (Quiagen) following manufacturers protocol however, when kits were unavailable plasmid DNA was isolated using the following method. The supernatant was discarded and the pellet resuspended in 5-10ml ice-cold STE, transferred to Oakridge tubes and re-centrifuged at 4500 rpm (Hermle Z383K centrifuge; 220.80.V02 rotor), 4^{0}C for 10 minutes. The resulting pellet was resuspended in 2ml solution I, to this 4ml solution II was added, gently mixed by inversion, and incubated at room temperature for 5 minutes in order to lyse the cells. 3ml ice-cold solution III was added mixed by gentle shaking and a white precipitate allowed to form by incubation on ice for 10 minutes. The tubes were centrifuged at 10,000 rpm, 4^{0}C for 10 minutes. The supernatant was recovered, transferred to a

fresh tube and 0.6 volume of isopropanol added. The mixture was incubated at room temperature for 10 minutes, centrifuged at room temperature, 10,000 rpm for 15 minutes, the DNA pellet was washed with 80% ethanol and air dried after draining off excess ethanol. The pellet was resuspended in suitable volume (300µl) of sterile DI water and transferred to 1.5ml microfuge tube. An equal volume of 5M LiCl was added and the solution mixed and centrifuged at 12,000 rpm for 10 minutes at 4^0C. The supernatant was decanted and the pellet rinsed with 80% alcohol, centrifuged at 12,000rpm, drained and air-dried. The resultant pellet was resuspended in 50µl of sterile DI water and incubated at 37^0C with 20µl/ml DNase free RNase for 30 minutes. 500µl of 1.6M NaCl 13%(w/v) polyethylene glycol (PEG 8000) was added and mixed before centrifuging at 12,000 rpm for 5 minutes at 4^0C. After removing the supernatant the pellet was air-dried and resuspended in a suitable volume (400µl) of sterile DI water. The plasmid DNA was purified via extraction with phenol, phenol: chloroform and finally with chloroform. To the final extract an equal volume of isopropanol and 0.1 volume of sodium acetate were added, mixed and the resulting solution centrifuged at 12,000 rpm, 4^0C for 15 minutes in order to precipitate the plasmid DNA. The precipitated pellet was washed in 80% ethanol and re-centrifuged at 12,000 rpm, 4^0C for 2 minutes. After removing the ethanol, the pellet was left to air dry before addition of 200µl of sterile DI water. The optical density of the preparation was determined at 260nm and 280nm from a diluted sample allowing determination of DNA concentration. The plasmid was re-precipitated and resuspended to 1µg/µl using sterile DI water in cell culture condition then stored at – 20^0C prior to use.

Diagnostic digestions were used to test the origin, integrity and purity of the plasmid. A restriction digest reaction was made up using 1µl of the appropriate 10x enzyme buffer, 1µl of the appropriate restriction enzyme, 100ng plasmid DNA and made up to 10µl with sterile DI water. The reaction was incubated at 37^0C for 1 hour. 2µl 6x agarose gel loading dye was added to the reaction mixture and the reaction mixture was separated according to size by electrophoresis in a 0.8-1.0% agarose gel at 100V.

2.2.5 Cell Culture

RAW 264.7 & N11

RAW 264.7 murine leukaemic monocyte/macrophage cells (Raschke *et al,* 1978) and the N11 microglial cells (Righi *et al.* 1989) were cultured in complete DMEM. Approximately 10^6 cells were inoculated into a 75mm^2 flask in 12ml medium. When the cells reached confluence, the surface of the plastic was scraped, 11ml of medium was removed and replaced with 11ml fresh medium. Cultures of cell lines were maintained by plating to fresh flasks every four weeks or two days prior to use in experiments. Cells were harvested for experiments by removing from the plastic with a cell scraper, centrifuging at 1000 rpm for 5 minutes in polypropylene tubes, resuspended for counting and then diluted to the appropriate numbers for the experiment.

Cos-1

Cos-1 African green monkey kidney cells were cultured in complete DMEM. Approximately 10^6 cells were inoculated into a 75mm^2 flask in 12ml medium. When the cells reached confluence, the medium was removed, and the surfaces of the cells were rinsed with 5ml sterile PBS before addition of 2.5ml Trypsin-EDTA. The cells were incubated with Trypsin-EDTA at 37^{0}C for 5 minutes to detach the cells from the plastic surface, confirmed by visualisation under light microscope, an equal volume of complete medium was added back to neutralise the Trypsin-EDTA. 0.5ml of the cell-containing medium was inoculated into 11.5ml fresh medium in a fresh flask. Cells were harvested for experiments by removing from the plastic with trypsin as described, centrifuging at 1000 rpm for 5 minutes in polypropylene tubes, resuspended for counting and then diluted to the appropriate numbers for the experiment.

THP-1

Non-adhesive THP-1 human monocyte cells were cultured in complete RPMI1640. Approximately 10^6 cells were inoculated into a 75mm^2 flask in 12ml medium. When the cells reached confluence, 11ml medium was removed and replaced with 11ml fresh medium. Cultures of cell lines were maintained by plating to fresh flasks every four weeks or two days prior to use in experiments. Cells were harvested for experiments by centrifuging at 1000 rpm for 5 minutes in polypropylene tubes,

resuspended for counting and then diluted to the appropriate numbers for the experiment.

2.2.6 Isolation and Culture of Bone Marrow Derived Macrophages

Femurs were isolated from mice and the bone marrow flushed out using a 1ml syringe containing DMEM. Cells were pooled from multiple animals, resuspended and plated onto triple vent bacterial petri-dishes (Greiner) and grown in culture medium (2.1.5) in the presence of 10% L-cell conditioned media (the media from which L-929 cells have been grown) that contains granulocyte/macrophage colony stimulating factor (GM-CSF). After incubation for 5 days an additional 10% v/v of L-cell conditioned media was added. Precursor cells were allowed to mature and differentiate for a further 4 days at which point any cells left floating were washed off using pre-warmed serum free DMEM. Adherent cells were used as macrophages and shown to express macrophage antigens Slc11a1 and iNOS and were phagocytic. Cells were used in experiments after 2 days rest.

2.2.7 Transfection into Cell Lines

Electroporation

Cos-1

$5x10^6$ cells were added to 10μg of plasmid DNA in 0.5ml complete DMEM in an electroporation cuvette, 0.4cm distance between electrodes (Biorad). The cuvette containing plasmid DNA and Cos-1 cells were transferred into a pulse chamber the electroporated at the required voltage and capacitance (typically 450V/500μF). The cells were transferred to $60cm^2$ tissue culture grade Petri dish containing 6ml fresh complete DMEM and incubated at 37^0C in a 5% CO_2 humidified atmosphere for 48 hours.

RAW 264.7

$5x10^6$ cells were added to 10μg of plasmid DNA in 0.5ml complete DMEM in an electoporation cuvette, 0.4cm distance between electrodes (Biorad). The cuvette containing plasmid DNA and RAW 264.7 cells were transferred into a pulse chamber

the electroporated at the required voltage and capacitance (typically 350V/975μF). The cells were transferred to 60cm^2 tissue culture grade Petri dish containing 6ml fresh complete DMEM and incubated at 37^{0}C in a 5% CO_2 humidified atmosphere for 48 hours.

LipofectAMINE

Cos-1/RAW 264.7

1.5x10^5 cells (Cos-1) or 5x10^5 cells (RAW 264.7) were seeded onto a six-well tissue culture plate in 2ml complete tissue culture medium and incubated at 37^{0}C in a 5% CO_2 atmosphere for 18-24 hours (until 50-80% confluent). For each transfection two sterile microfuge tubes were labelled A and B. For each transfection, in tube A 2-3μg plasmid DNA was diluted into 100μl serum-free medium, no antibiotics. In tube B 5μl LipofectAMINE reagent (Life Sciences, GibcoBRL, UK) was diluted into 100μl serum-free medium. The tubes were incubated at room temperature for 10-15 minutes. After this time the two solutions were combined, mixed gently incubated at room temperature for 15-45 minutes to enable the formation of DNA-liposome complexes. During this incubation time the cells that had been seeded were washed in 2ml serum- free medium. For each transfection 0.8ml serum-free medium was added to the tubes containing the DNA-liposome complexes and mixed gently before being overlaid onto the rinsed cells. The DNA-liposome complex was left incubating on the cells for 5 hours (37^{0}C; 5% CO_2), after this time 1ml media containing 20% serum, no antibiotics was added back to the cells without removing the transfection mixture and incubated under the same conditions for a further 18 hours. After this 24 hour incubation the transfection mixture was replaced with fresh complete medium and further incubated for 24 hours.

2.2.8 Protein Estimation

Sample for SDS-PAGE

Unlysed eukaryotic cells, following washing to remove serum proteins, were resuspended in 200μl PBS. 20μl of the cell suspension was removed to a microfuge; the remaining 180μl was pelleted by pulse centrifugation to 12,000 rpm and stored at –20^{0}C. 2μl of the cell suspension was loaded in a well on a microtitre plate, to this

was added 100µl 0.1%(v/v) SDS-PBS and 100µl BCA protein detection reagents (Pierce). A standard curve was prepared using a range, (0µg-20µg) of BSA concentrations. The assay was incubated at 37^{0}C for 40 minutes and the absorbance determined at 570nm using plate reader. The standards were used to prepare a standard curve and the protein contents of the samples were estimated with reference to this curve.

Sample for CAT assay

Eukaryotic cells isolated as previously described were pelleted by centrifugation, washed in PBS and resuspended in 100µl 0.25M Tris-Cl (pH7.8). Cells were disrupted by 3 cycles of freezing in liquid nitrogen for 5 minutes, thawing at 37^{0}C for 5 minutes. The cell debris was pelleted by centrifugation at 12,000 rpm for 10 minutes and the supernatant removed to fresh tube. Protein concentrations of cell extracts were determined as above; samples can be stored at –20^{0}C.

Sample for Luciferase assay

The cells were harvested and centrifuged at 1000rpm. for 5 minutes, the resulting pellets were resuspended in 1ml cold PBS and transferred to microfuge tubes. The samples were centrifuged at 10000rpm for 10 seconds and the supernatant discarded. The pellets were resuspended in 100µl 1x reporter lysis buffer (Promega) by vortexing. Cells were disrupted by 1 cycle of freezing in liquid nitrogen for 5 minutes, and thawing at 37^{0}C for 5 minutes. The cell debris was pelleted by centrifugation at 12,000 rpm for 15 seconds at room temperature and the supernatant removed to fresh microfuge tube. Protein concentrations of cell extracts were determined as above; samples can be stored at –20^{0}C.

2.2.9 Chloramphenicol Acetyl Transfease (CAT) Assay

For each sample a set amount of protein (see individual experiments) was placed in a microfuge tube, and the volume made up to 90µl with 0.25M Tris-Cl (pH7.8). A master mix was made for all samples of; 20µl 4mM Acetyl CoA; 1µl [^{14}C]-Chloramphenicol; 35µl DI water, and 56µl of this master mix was added to each sample and incubated at 37^{0}C for 1-6 hours. The incubation time was determined

empirically, based on previous experiments and cell type used. After this incubation period the reaction was terminated by the extraction of the chloramphenicol, by the addition of 1ml ethyl acetate and vortexing for 30 seconds. Centrifugation at 12,000 rpm for 5 minutes allowed separation of the mixture into two phases. The top ethyl acetate layer containing the [^{14}C]-Chloramphenicol (ICN) and acetylated derivatives was removed to a fresh microfuge tube. The ethyl acetate was evaporated off in a Speed-vac on a low drying rate for 1 hour. Each sample was resuspended in 15µl ethyl acetate and spotted on to a Thin Layer Chromatography (TLC) plate (Whatman). After application the samples were allowed to dry and the TLC plate was placed in a TLC tank containing running solvent just sufficient to touch the bottom of the TLC plate. The samples were allowed to run until the solvent front had reached the top of the plate. The plate was then removed, air dried and exposed to film in an autoradiography cassette at room temperature. Calculation of % conversion was achieved by exposing a screen from a Phosphoimager (Molecular Dynamics) and calculating emissions as per manufacturers' instructions (figure 2.2.2).

2.2.10 SDS-PAGE

SDS-PAGE fractionates polypeptide-SDS complexes by electrophoretic molecular sieving in polyacrylamide gels according to molecular size assuming a linear non-structured conformation. The proteins are denatured by either by boiling in SDS and β-mercaptoethanol or if membrane bound, by passing through a syringe in SDS and β-mercaptoethanol. SDS and β-mercaptoethanol will disrupt secondary and tertiary structures and inter- and intra-chain disulphide bonds respectively. The resulting polypeptide chains have approximately equal charge to mass ratios and are separated solely on the basis of molecular size.

All glass plates and spacers (1.5mm) were cleaned and degreased with ethanol. The apparatus was assembled according to the manufacturers' instructions (Biorad). SDS-PAGE was performed using the discontinuous buffer system of Laemmli (1970), with 10% resolving and 4% stacking acrylamide gels, unless otherwise stated.

All buffers and solutions were prepared using DI water. Polymerisation of acrylamide to form gels was catalysed by free radicals from N,N,N'N'-tetra-methylenediamide (TEMED) generated by the action of initiator ammonium persulphate (APS). The 10% resolving and 4% stacking gel mixtures were prepared as described (2.1.8). The 10% resolving gel was poured and allowed to polymerise allowing enough room for the 4% stacking gel to be poured on top. The stacking gel was poured and the well forming comb carefully inserted and the gel allowed to polymerise.

The required volume of the SDS-PAGE running buffer was prepared immediately prior to use. Once the acrylamide within the 4% stacking gel had polymerised the comb was removed and the wells washed with DI water before being placed in the gel tank containing the SDS-PAGE running buffer. Air bubbles within the wells were removed before samples were loaded into the wells. Samples were in SDS-sample buffer at $\approx$ 2mg protein/ ml. 20μg protein/ track was loaded. Electrophoresis was carried out at 30mA constant current per gel.

The proteins within the gel were electrophoretically transferred to nitrocellulose membrane (Millipore) for immunodetection.

2.2.11 Western Blotting

After SDS-PAGE the glass plates were separated and the stacking gel cut away. The gel was soaked in blotting buffer until required. The nitrocellulose membrane (5 x 9.5cm) was pre-soaked in methanol before being soaked in the blotting buffer. 3 pieces of 3mm Whatman paper (Whatman) moistened in blotting buffer were stacked on dry graphite electrode of the semi-dry blotter (Biorad) and the membrane placed on top of the 3mm Whatman paper. The gel was placed on top of the membrane and 3 more moistened pieces of 3mm Whatman paper stacked on top. The assembled stack was rolled with a glass pipette to remove air bubbles and excess buffer. The assembled blot was run for 60 minutes at 100mA constant current per membrane.

2.2.12 Antibody Detection

Detection of specific proteins on Western blots was by immune detection using specific antibodies. Post transfer the blot was incubated in blocking agent at room temperature for 60 minutes with agitation. Antibody dilutions, previously calculated from titration experiments, were prepared in diluent buffer. The blot was incubated in primary antibody for 60 minutes, with agitation, at room temperature and then washed for 5 minutes x3 in PBS/ Tween. The blot was then incubated as for primary antibody in a horseradish peroxidase (HRP) conjugated secondary antibody raised against the animal used to produce the primary antibody. The blot was then washed twice with PBS/ Tween for 10 minutes and twice in DI water for 5 minutes prior to detection using enhanced chemiluminescence (ECL) reagent (Amersham) as per manufacturers' instructions.

2.2.13 Cellular Proliferation

Crystal Violet Estimation of Cell Number

Cells were counted using a haemocytometer (grid count x 10^4 x dilution factor = cell number /ml) and trypan blue exclusion as a measure of cell viability. The cells were added to a 96 well plate in 200µl of media, using $100x10^3$ cells in row 1, $50x10^3$ cells in row 2, 10 $x10^3$ in row 3, 5 $x10^3$ in row 4 and 1 $x10^3$ in row 5, row 6 contained 200µl of media only. This plate was used to produce a standard curve. $1x10^3$ cells in 200µl media were placed in the remaining wells for tests one plate was used per day of culture. Readings were made by emptying the plates of media, gently tapping onto paper towel and adding 200µl of crystal violet stain per well. The plates were incubated at room temperature for 10 minutes the stain decanted and washed in three changes of water and dried. The absorbed stain was resolubilised in 200µl methanol. The plates were agitated carefully, each plate was read on a MRX microtitre plate reader (Dynex) at 570nm. A standard curve was plotted from the known cell number against OD_{570nm}. Sample cell numbers were obtained by reference to this standard curve.

BrdU Incorporation

Cell proliferation was measured via 5-Bromo-2'deoxyuridine (BrdU) incorporation studies using a BrdU labelling kit (Amersham Biosciences) following manufacturers

instructions. Briefly, cells were cultured for 1-5 days in a sterile microtitre plate (MTP). Cells were labelled with BrdU for 2-24 hours, 37^{0}C. After this time labelling medium was removed by inversion of the MTP and the fixative solution added for 30 minutes at room temperature (RT). The fixative solution was removed and cells incubated with blocking reagent for 30 minutes at RT. The cells were incubated with the Anti-BrdU-HRP conjugated antibody for 30-120 minutes at RT and then washed 3 times for 15 minute at RT with washing buffer. Substrate was added 3 times for 5-30 minutes, stop reagent added, and absorbance measured at 450nm. All reagents used were supplied with the labelling kit.

2.2.14 Sanger Dideoxy Sequencing

Primer Annealing

2µl NaOH/EDTA and 100ng of a specific primer are added to 1µg DNA, volume was made up to 20µl with DI water. The solution was placed in a water bath at 95^{0}C and allowed to cool to room temperature to allow efficient annealing of the primer to the template DNA. After this time 100µl of the 155λ solution is added to neutralise NaOH/EDTA activity. The precipitated primer annealed DNA complex was retrieved by centrifugation at 12,000 rpm for 10 minutes at 4^{0}C. The supernatant was decanted and the pellet rinsed with 80% alcohol, centrifuged at 12,000rpm, drained and air-dried.

Sequencing Reaction

The sequencing reaction was performed using the Sequenase sequencing kit (Amersham Biosciences) following the manufacturers instructions. Briefly, the primer annealed DNA was resuspended in a solution containing 2µl sequenase buffer, 1µl dtt, 0.4µl label mix, 0.5µl α^{35}S-dATP, 0.25µl sequenase enzyme, reaction volume was made up to 15.5µl with DI water. 3.5µl of the sequencing solution premix was added to each of 4 tubes containing 2.5µl of either ddATP, ddTTP, ddCTP or ddGTP. The reactions were incubated at 37^{0}C for 5 minutes before the addition of 4µl of stop solution to quench the reaction. Samples may be stored at -20^{0}C at this point. All solutions for the sequencing reaction are provided with the Sequenase kit apart from the α^{35}S-dATP, which is supplied separately (Amersham Biosciences).

All glass plates and spacers (1.5mm) were cleaned and degreased with ethanol, one of the plates is then prepped with Acrylease (Stratagene) to prevent the gel sticking. All buffers and solutions were prepared using DI water. The denaturing polyacrylamide gel was prepared as described section 2.1.9. Polymerisation of acrylamide to form gels was catalysed by free radicals from N,N,N'N'-tetra-methylenediamide (TEMED) generated by the action of initiator ammonium persulphate (APS).

Sequencing reactions were heated to 85^0C for 3 minutes prior to loading. 2.5µl of reaction mix per sample was loaded onto the gel. The gel was run in 1x TBE at 1200V for 3 hours. Gels were dried onto 3mm Whatman paper and visualised via autoradiography.

2.2.15 Genomic DNA Isolation

Tissue was minced using either a scalpel or scissors, added to liquid nitrogen, and ground using a pestle and mortar. The liquid nitrogen was allowed to evaporate leaving a fine powder. 10 volumes of the lysis buffer (section 2.1.13) was added to the powder and the suspension left at 50^0C for 3-18 hours with periodical swirling. The DNA was gently extracted 3 times with an equal volume of phenol. After these extractions, the bottom DNA containing aqueous layer was dialysed against 4 litres of the dialysis solution (section 2.1.13) with several changes until the OD_{270nm} of the dialysate <0.05. The dialysed solution was treated with 100µg/ml of DNase-free RNase at 37^0C for 3 hours. The DNA was purified via extraction with phenol, phenol: chloroform and finally with chloroform. To the final extract an equal volume of isopropanol and 0.1 volume of sodium acetate were added, mixed and the precipitate transferred to a fresh microfuge tube. The DNA was washed in 80% ethanol, left to air dry and resuspended in approximately 1ml DI water.

2.2.16 Preparation of Nuclear Extracts

The cells were harvested and centrifuged at 1000rpm. for 5 minutes, the resulting pellets were resuspended in 500µl cold PBS and transferred to microfuge tubes. The samples were centrifuged at 7000rpm for 10 seconds and the supernatant discarded.

The cells were resuspended in Dignam Buffer A using 100µl/10^7 cells, and centrifuged for 10 seconds at 10000rpm, If cytoplasmic extracts were needed the supernatant was removed into a sterile microfuge tube and mixed 1:1 with Dignam Buffer C, samples stored at –70^{0}C. The pellet was resuspendend in 100µl/10^7 cells of Dignam Buffer C by vortexing and incubated on ice for 10 minutes with occasional vortexing. After this incubation cells were centrifuged at 10000rpm for 30 seconds. The 'nuclear extract' supernatant was stored at –70^{0}C in 5-10µl aliquots.

2.2.17 Electrophoretic Mobility Shift Assay (EMSA)

Double stranded oligos, or DNA fragments can be used to analyse binding affinity of recombinant proteins, or proteins within cell extracts, for specific DNA elements. Protein binding to DNA retards the mobility of DNA in an acrylamide gel causing an apparent 'shift' of the DNA band. 5-10µg protein from each sample were made up to 4µl using Dignam Buffer C, including a buffer only control. 1µl of the non-specific DNA competitor polydeoxyinosinic-deoxycytidylic acid (Poly dI-dC) was added to each sample and final reaction volumes made up to 10µl using DI water. After 15 minutes incubation on ice 2µl of the radiolabelled oligonucleotide probe (0.1ng/ml) was added and samples incubated on ice for a further 15minutes. 100-fold excess of unlabelled oligonucleotide was used for competition assays or for supershift assays 1µl of antibody (1µg/µl) was added to the relevant samples and incubated at 4^{0}C overnight. 3µl of 6 x EMSA loading dye was added to each sample prior to loading onto the EMSA gel.

Plates were scrubbed with decon, rinsed with deionised water and degreased with ethanol. The plates were assembled using 1.5mm spacers and the edges sealed with 2% agar. 50mls of 5% EMSA gel mix was prepared and poured between the plates. A well making comb was inserted carefully to prevent the formation of bubbles, and the gel left to polymerise. Once set the comb was removed, wells washed using deionised water and gel assembled in a tank containing an appropriate volume of 0.5x TBE running buffer. The gel was pre-run for 15 minutes on maximum voltage and a constant current of 10mA. After pre-running, the wells were rinsed with buffer and samples loaded under buffer to form tight bands at the base of the wells. The gel was

run at maximum voltage, a constant 10mA for approximately 3 hours, until the dye reaches the bottom of the gel. After removal from the tank the plates were separated, and the gel transferred to 3mm Whatman paper. The gel was dried for approximately 1 hour at 80^0C under vacuum. The dry gel was incubated with photographic film overnight at -70^0C.

2.2.18 Preparation of EMSA Probes Using the Klenow Reaction

Equimolar amounts (100ng/µl final concentration) of paired oligonucleotides were annealed by heating to 95^0C in a water bath and allowed to cool to room temperature. 1µl of the annealed double stranded oligonucleotides was combined with 1µl 10x EcoRI restriction endonuclease buffer (Promega, UK), 5µl α-^{32}P-dATP, 1µl Klenow fragment (Promega, UK) and volumes made up to 10µl with DI water, other dNTPs were added as required. The reaction was incubated at room temperature for 30 minutes and heating to 70^0C for a further 5 minutes stopped the reaction. Samples were purified by ethanol precipitation and resuspended in 100µl DI water.

2.2.19 Luciferase Assay

For each sample a set amount of protein (see individual experiments) was added to 100µl room temperature luciferase assay reagent (Promega) in a luminometer tube (Promega). Samples were placed in the luminometer and light emission measured 3 times per sample.

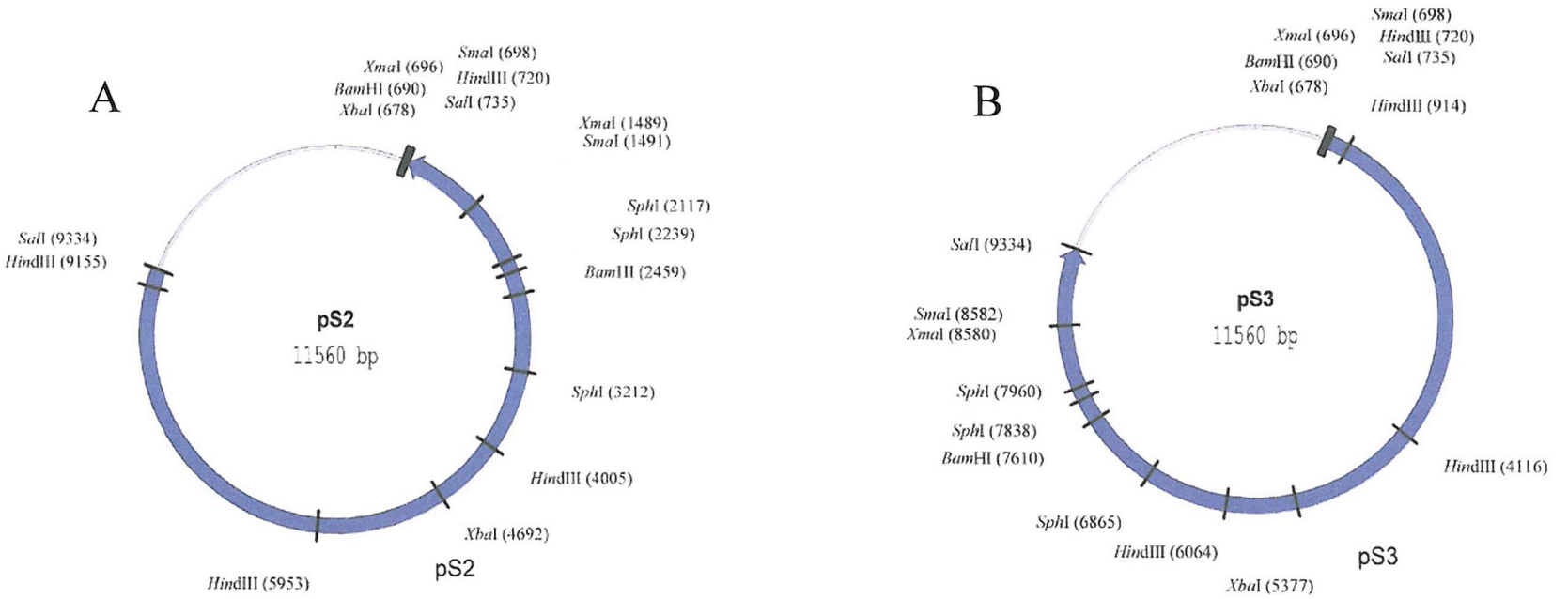

FIGURE 2.2.1 Plasmid Map of pS2 and pS3 Clones. (A) Plasmid map of pS2 indicating size (11.560Kbp) and restriction endonuclease recognition sites, unique sites are highlighted in red. (B) Plasmid map of pS3 indicating size (11.560Kbp) and restriction endonuclease recognition sites, unique sites are highlighted in red. pS2 and pS3 contain the same insert but are inserted in opposite orientations.

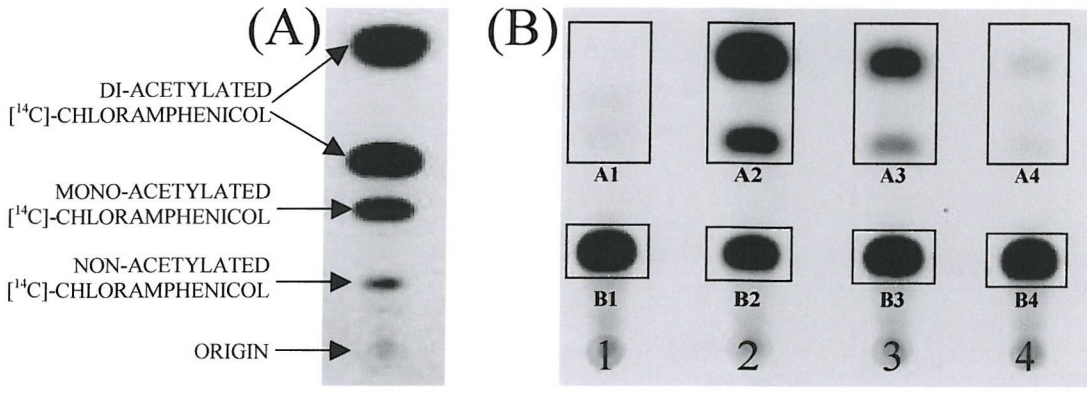

$$\text{(C) \% CAT Conversion} = \left[\frac{A}{(A+B)}\right] X\ 100$$

FIGURE 2.2.2 Calculation of % Chloramphenicol Acetyl Transferase (CAT) conversion. (A) Autoradiograph of a CAT assay indicating the origin and the different acetylated states of the [^{14}C]-Chloramphenicol. (B) Autoradiograph of a CAT assay, the areas used to quantitate % CAT conversion are outlined in black (1) Control; (2) Sample 1; (3) Sample 2; (4) Sample 3. (C) Equation used to calculate % CAT conversion; all samples were adjusted for background by subtracting % CAT conversion obtained for the control sample (lane 1).

CHAPTER 3

Analysis of the Murine *Slc11a1* Promoter

3.1 INTRODUCTION

Eukaryotic promoters are made up of a complex combination of basal promoter elements (TATA box, Initiator element), upstream transcription factor binding sites, enhancers and silencers. These unique combinations of binding sites enable different genes, in many different cell types, to share the same transcription factors, yet be modulated in both a cell specific and temporal fashion. Analysis of the proximal region of the murine *Slc11a1* promoter (Govoni *et al.* 1995) has revealed many features and transcription factor binding sites that are characteristic of macrophage-specific gene expression (reviewed Orkin, 1995; Clarke and Gordon, 1998). The sequence immediately upstream of the predicted transcriptional start site (Govoni *et al.* 1995) does not contain classical TATA or CAAT consensus elements (see Figure 3.1.1). However, two possible consensus sequence motifs for an Initiator (Inr) element have been found near the start site of transcription (Inr#1: $CACT_{+1}CGCT$ Inr#2: $TCCCACT_{+1}CTT$), which was identified by primer extension and S1 nuclease mapping (Govoni *et al.* 1995). Both of these potential sequences conform to the consensus sequence for Inr elements; Py Py A_{+1} N $^{T}/_{A}$ Py Py, with the core motif of both (CACT) being noted to promote good transcriptional activity (Javahery *et al.* 1994). Initially it was thought that in the absence of a TATA box an AT-rich region at –30bp would be preferable, and substitution of the GC-rich sequences with AT-rich sequences upstream of weak Inr elements did enhance the transcriptional activity of these Inr elements. Association of the TATA-box binding protein (TBP) subunit of transcription factor (TF)II-D with the TATA box is via relatively non-specific interactions with the minor groove of the DNA. An interaction between an upstream AT-rich region would therefore be predicted to stabilise the formation of the pre-initiation complex, thereby enhancing transcriptional activity (Javahery *et al.* 1994). However Javahery *et al.* also noted that a subset of Inr elements tested functioned with upstream GC rich regions and multiple consensus Sp1 enhancer sites (GGGCG), sequence analysis of the murine *Slc11a1* promoter (Govoni *et al.* 1995) identified one potential Sp1 binding site at -25bp. Analysis of the GC content of the -95 to +5 region reveals an even spread of base pairs (54 $^{G}/_{C}$ and 46 $^{A}/_{T}$). As well as ubiquitous transcription factor binding sites such as Activator proteins (AP) 1, 2 and 3, and Stimulatory protein (Sp1), *cis*-acting sequence motifs associated with expression in

the macrophage or associated with response to induction by differentiating agents specific to this lineage were found in the region between -265bp to +127bp. Govoni *et al.* (1995), identified a Purine rich region (PU box) at -173bp. The E-twenty six specific (Ets) transcription factor PU.1 binds to PU box sequences in myeloid-expressed genes where upon it regulates hematopoiesis. Finally, sequence motifs known to bind factors upregulated by proinflammatory agents such as Inferferon γ (IFNγ), bacterial Lipopolysaccharide (LPS) and Interleukin (IL)-1 have been identified. Furthermore Govoni *et al.* supported these latter findings, providing evidence to show murine *Slc11a1* mRNA is upregulated by IFNγ/LPS treatment in the RAW 264.7 cell line.

This chapter describes a more extended characterisation of the murine *Slc11a1* promoter region, identifying further transcription factor binding sites associated with macrophage specific expression, deletion mapping of the promoter identifying potential regulatory regions, and regulation of reporter constructs by the macrophage specific proinflammatory agents IFNγ and LPS.

FIGURE 3.1.1 Sequence of the 1.655Kbp *Slc11a1* Promoter Construct pHB4. Annotated sequence of the 1.655Kbp *Slc11a1* promoter sequence from the XbaI site at position -1556bp to the ATG translational initiation site at +95bp. Transcription factor binding sites on the sense-strand have been indicated above the sequence whereas those on the antisense-strand are indicated below the sequence. The initiator elements (Inr) at and around position +1 are highlighted in bold with the major transcriptional initiation site being indicated with a big arrow  and minor sites with smaller arrows,  the transcribed sequence is underlined. The translational initiation ATG codon at position +95 is indicated with an arrow  . The GT di-nucleotide repeat between -315pb and -368bp is highlighted in bold.

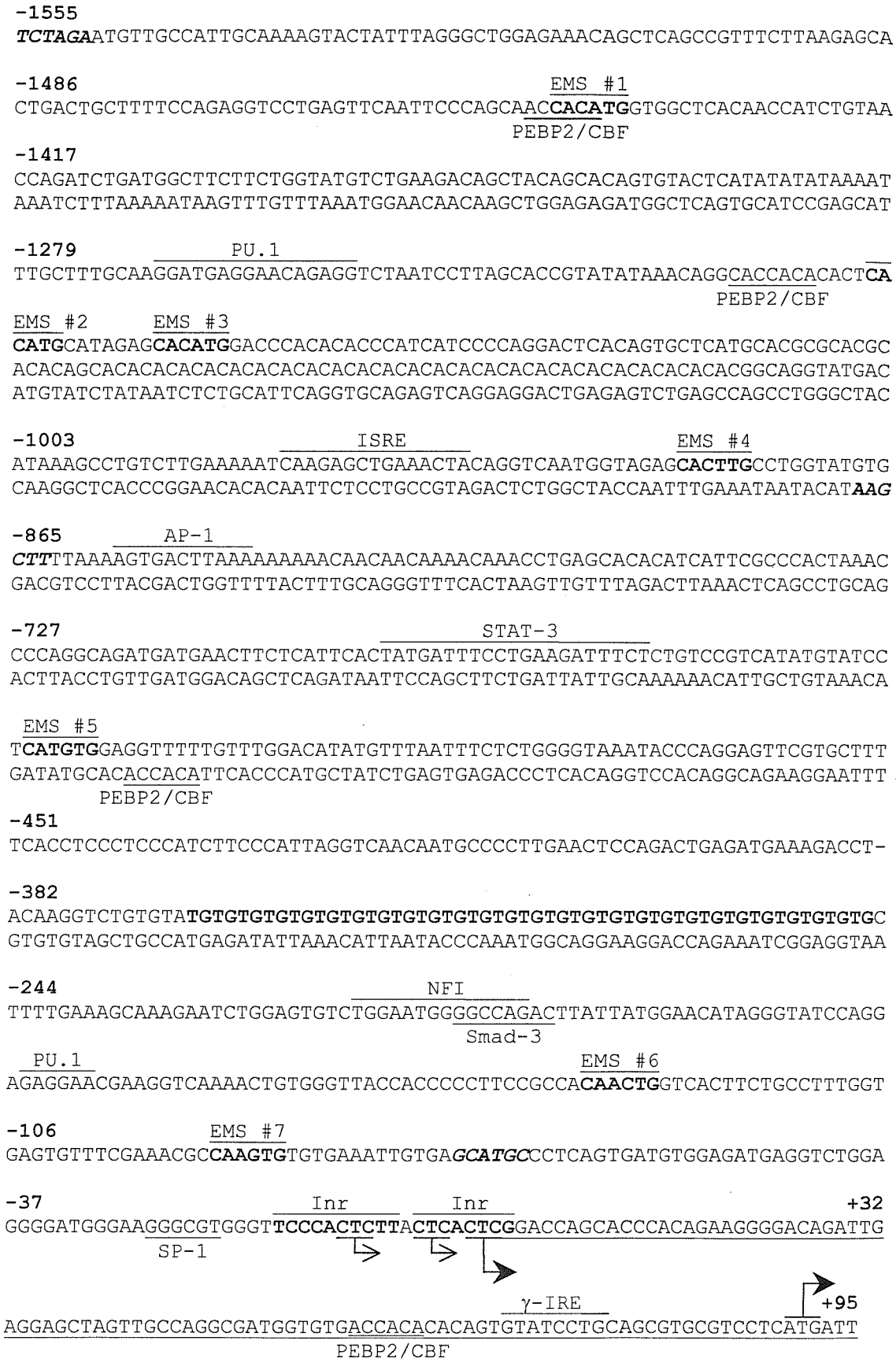
-1555
TCTAGAATGTTGCCATTGCAAAAGTACTATTTAGGGCTGGAGAAACAGCTCAGCCGTTTCTTAAGAGCA
-1486
EMS #1
CTGACTGCTTTTCCAGAGGTCCTGAGTTCAATTCCCAGCAACCACATGGTGGCTCACAACCATCTGTAA
PEBP2/CBF
-1417
CCAGATCTGATGGCTTCTTCTGGTATGTCTGAAGACAGCTACAGCACAGTGTACTCATATATATAAAAT
AAATCTTTAAAAATAAGTTTGTTTAAATGGAACAACAAGCTGGAGAGATGGCTCAGTGCATCCGAGCAT
-1279
PU.1
TTGCTTTGCAAGGATGAGGAACAGAGGTCTAATCCTTAGCACCGTATATAAACAGGCACCACACACTCA
PEBP2/CBF
EMS #2
EMS #3
CATGCATAGAGCACATGGACCCACACACCCATCATCCCCAGGACTCACAGTGCTCATGCACGCGCACGC
ACACAGCACACACACACACACACACACACACACACACACACACACACACACACACACACACACGGCAGGTATGAC
ATGTATCTATAATCTCTGCATTCAGGTGCAGAGTCAGGAGGACTGAGAGTCTGAGCCAGCCTGGGCTAC
-1003
ISRE
EMS #4
ATAAAGCCTGTCTTGAAAAATCAAGAGCTGAAACTACAGGTCAATGGTAGAGCACTTGCCTGGTATGTG
CAAGGCTCACCCGGAACACACAATTCTCCTGCCGTAGACTCTGGCTACCAATTTGAAATAATACATAAG
-865
AP-1
CTTTTAAAAGTGACTTAAAAAAAAACAACAACAAAACAAACCTGAGCACACATCATTCGCCCACTAAAC
GACGTCCTTACGACTGGTTTTACTTTGCAGGGTTTCACTAAGTTGTTTAGACTTAAACTCAGCCTGCAG
-727
STAT-3
CCCAGGCAGATGATGAACTTCTCATTCACTATGATTTCCTGAAGATTTCTCTGTCCGTCATATGTATCC
ACTTACCTGTTGATGGACAGCTCAGATAATTCCAGCTTCTGATTATTGCAAAAAACATTGCTGTAAACA
EMS #5
TCATGTGGAGGTTTTTGTTTGGACATATGTTTAATTTCTCTGGGGTAAATACCCAGGAGTTCGTGCTTT
GATATGCACACCACATTCACCCATGCTATCTGAGTGAGACCCTCACAGGTCCACAGGCAGAAGGAATTT
PEBP2/CBF
-451
TCACCTCCCTCCCATCTTCCCATTAGGTCAACAATGCCCCTTGAACTCCAGACTGAGATGAAAGACCT-
-382
ACAAGGTCTGTGTATGTGTGTGTGTGTGTGTGTGTGTGTGTGTGTGTGTGTGTGTGTGTGTGTGTGC
GTGTGTAGCTGCCATGAGATATTAAACATTAATACCCAAATGGCAGGAAGGACCAGAAATCGGAGGTAA
-244
NFI
TTTTGAAAGCAAAGAATCTGGAGTGTCTGGAATGGGGCCAGACTTATTATGGAACATAGGGTATCCAGG
Smad-3
PU.1
EMS #6
AGAGGAACGAAGGTCAAAACTGTGGGTTACCACCCCCTTCCGCCACAACTGGTCACTTCTGCCTTTGGT
-106
EMS #7
GAGTGTTTCGAAACGCCAAGTGTGTGAAATTGTGAGCATGCCCTCAGTGATGTGGAGATGAGGTCTGGA
-37
Inr
Inr
+32
GGGGATGGGAAGGGCGTGGGTTCCCACTCTTACTCACTCGGACCAGCACCCACAGAAGGGGACAGATTG
SP-1
γ-IRE
+95
AGGAGCTAGTTGCCAGGCGATGGTGTGACCACACACAGTGTATCCTGCAGCGTGCGTCCTCATGATT
PEBP2/CBF

3.2 RESULTS

3.2.1 Analysis of the *Slc11a1* Promoter

The *Slc11a1* promoter was isolated as described (see section 2.2.1) and sequenced (Oswel, Southampton, UK). The full sequence of 8.599Kbp 5'-promoter containing region of the murine *Slc11a1* gene can be seen in appendix 1, and its alignment with 6.1Kbp of the recently published sequence from the mouse genome-sequencing project can be seen in appendix 2. The pS3 sequence was analysed using the Genomatix MatInspector professional programme (http://geomatix.gsf.de). This computer assisted analysis detected 541 "patterns in DNA sequences" using a core similarity of "1.0" and "calculated optimised" matrix similarity in the matrix-search parameters, selected sites of interest are summarised in figure 3.2.1. As described by Govoni *et al.* the *Slc11a1* promoter contains binding sites for the ubiquitous transcription factors AP1 and Sp1. In addition to the previously described binding sites, (AP1, -1bp to -6bp (-ve strand); Sp1, -21bp to -26bp (-ve strand)), we have identified a further four potential AP1 binding sites, (-5664bp to -5875bp; -846bp to -857bp; +304bp to +313bp (-ve strand); +1184bp bp +1195bp), and a further two potential Sp1 binding sites (-4250bp to -4263bp; +1878bp to +1891bp (-ve strand)). Extended analysis of the murine *Slc11a1* promoter has identified promoter motifs recognised by Ikaros, Oct1, Oct2 and Nuclear factor Kappa B (NFκB; +1758bp to +1768bp), which are all involved in promoting lymphoid specific expression (reviewed Orkin, 1995). The *Slc11a1* promoter also contains multiple binding sites for transcription factors involved in macrophage specific gene expression (reviewed Orkin, 1995; Clarke and Gordon, 1998). In addition to the single PU.1 binding site, (-167bp to -173bp), identified by Govoni *et al.*(1995), we have identified a second PU.1 binding site, (-1252bp to -1268bp), as well as binding sites for the PU.1 family members Ets1 (-2498bp to -2513bp; -1764bp to -1779bp (-ve strand); -256bp to -271bp) and Ets2 (-2962bp to -2976bp; -684bp to -698bp (-ve strand)). Multiple PEBP2/CBF binding sites (-4693bp to -4699bp (-ve strand); -2989bp to -2995bp; -1690bp to -1696bp; -1412bp to -1418bp; -256 to -262 (-ve strand)). In addition to the involvement of specific transcription factors, myeloid specific expression relies on factors involved in the upregulation of the level of gene expression when macrophages are activated. These factors include IFNγ and LPS, binding sites for

their activation products have previously been reported (Govoni *et al.* 1995), and added to during this analysis (see figure 3.2.1). In addition to binding sites for the signalling of pro-inflammatory stimuli, the *Slc11a1* promoter contains sequence motifs associated with the signalling of anti-inflammatory factor Transforming growth factor β (TGFβ). Analysis also identified 6 non-canonical E-box motifs (EMS) involved in the binding of the proto-oncogene c-Myc and its cellular protein partner Max (Blackwell *et al.* 1993), and other related proteins such as the USFs.

3.2.2 *Slc11a1* Promoter Constructs

An 8.605Kb SalI *Slc11a1* promoter fragment in pBlueScript (pS2/S3), produced as described by C. H. Barton and E. Phillips, was used to prepare the murine *Slc11a1* promoter reporter constructs. Constructs are summarised in figure 3.2.2.

pHB1

A 6.881Kb restriction fragment from a SalI site at –6197bp to a BamHI site at +684bp was subcloned into the pBLCAT3 vector (see figure 3.2.3).

pBS-S2X

An XbaI restriction digest on pS2 removes the 4.895Kb region from the 5'-vector arm XbaI site, immediately upstream of the SalI site at –6197bp, to the XbaI site at –1555bp.

pHB2/ pHB3/ pHB4

A 1.654Kb region from an XbaI site at –1555bp to a synthetic BamHI introduced immediately downstream of exon 1 at position +99bp was amplified from pBS-S2X via the polymerase chain reaction (PCR), using a 5' vector arm primer, and the synthetic oligonucleotide HB#1 (5'-ATGCGGATCCTAATCAAGAGGACGCAGG-3'). The insertion of this synthetic BamHI site also converts the ATG translational initiation codon to TTG. The amplified region of the promoter was cloned via XbaI and BamHI into the plasmids pBS (pHB2) and pGEM (pHB3) for subcloning, and into the CAT reporter plasmid pBLCAT3 (pHB4, see figure 3.2.5).

pHB15

Digestion of the peGFPN3 control vector with AseI and BglII removed the CMV promoter region. Blunting and religation of the plasmid reconstitutes the BglII site but not the AseI site. A 1.645 Kbp fragment of the *Slc11a1* promoter, containing the region from an XbaI site at –1555bp to the synthetic BamHI at position +99bp, was purified from pHB2 and directionally cloned via the SacI and BamHI sites into the promoterless pEGFPN3 (pN3Δp) vector.

pHB4-M5M

A 1.655Kbp fragment was produced from pBS-S2X via a two-step PCR amplification process. A 5' 0.797Kbp fragment was amplified using a 5'vector arm primer, and the synthetic oligonucleotide MYC5-AS2 (5'-CCAAACAAAAACCTCGAATTCATGTTTACAGCAATG-3'). A 3' 0.688Kbp fragment was amplified using the synthetic oligonucleotides MYC5-S (5'-CATTGCTGTAAACATGAATTC GAGGTTTTTGTTTGG-3') and HB#1. MYC5-S and MYC5-AS2 are designed to disrupt the EMS #5 at –588bp with a synthetic EcoRI site. A 36bp sequence overlap allows the 5' and 3' fragments to anneal, and 10 PCR cycles in the absence of primers allows the complementary strands to form. The 1.655Kbp fragment from an XbaI site at –1555bp to a synthetic BamHI site at +100bp with a disrupted EMS at –588bp, was further amplified up using a 5' vector arm primer and the synthetic oligonucleotide HB#1. The fragment was cloned via XbaI and BamHI into the CAT reporter plasmid pBLCAT3 (see figure 3.2.6-A).

pHB4-M6M

A 1.655Kbp fragment was produced from pBS-S2X via a two-step PCR amplification process. A 5' 1.468Kbp fragment was amplified using a 5'vector arm primer, and the synthetic oligonucleotide MYC6M-AS (5'-AAAGGCAGAAGTGACGAATTCTGGCGGAAGGGGGTG-3'). A 3' 0.187Kbp fragment was amplified using the synthetic oligonucleotides MYC6M-S (5'-CACCCCCTTCCGCCAGAATTCGTCACTTCTGCCTTT-3') and HB#1. MYC6M-S and MYC6M-AS are designed to disrupt the EMS #6 at –87bp with a synthetic EcoRI site. A 36bp sequence overlap allows the 5' and 3' fragments to anneal, and 10 PCR cycles in the absence of primers allows the complementary strands to form. The

1.655Kbp fragment from an XbaI site at –1555bp to a synthetic BamHI site at +100bp with a disrupted EMS at –87bp, was further amplified up using a 5' vector arm primer and the synthetic oligonucleotide HB#1. The fragment was cloned via XbaI and BamHI into the CAT reporter plasmid pBLCAT3 (see figure 3.2.6-B).

pHB4-Sp1M

A 1.655Kb fragment was produced from pBS-S2X via a two-step PCR amplification process. A 5' 1.528Kbp fragment was amplified using a 5'vector arm primer, and the synthetic oligonucleotide Sp1M-AS (5'-AGAGTGGGAACCCATAGAATTCCCATCCCCTCCA-3'). A 3' 0.127Kbp fragment was amplified using the synthetic oligonucleotides Sp1M-S (5'-CACCCCCTTCCGCCAGAATTCGTCACTTCTGCCTTT-3') and HB#1. Sp1M-S and Sp1M-AS are designed to disrupt the consensus Sp1-binding site at –27bp with a synthetic EcoRI site. A 34bp sequence overlap allows the 5' and 3' fragments to anneal, and 10 PCR cycles in the absence of primers allows the complementary strands to form. The 1.655Kb fragment from an XbaI site at –1555bp to a synthetic BamHI site at +100bp with a disrupted consensus Sp1-binding site at -27bp, was further amplified up using a 5' vector arm primer and the synthetic oligonucleotide HB#1. The fragment was cloned via XbaI and BamHI into the CAT reporter plasmid pBLCAT3 (see figure 3.2.6-C).

pHB5

A 1.552Kb restriction fragment from a HindIII site at –868bp to a BamHI site at +684bp from pHB1 was replaced with a 0.967Kb pHB4 derived restriction fragment from the same HindIII site at –868bp to a synthetic BamHI at +99bp (see figure 3.2.4).

pHB6

A HindIII restriction digest on pHB4 removes the 0.687Kb region from the 5'-vector arm HindIII site, immediately upstream of the XbaI site at –1555bp, to the HindIII site at –868bp (see figure 3.2.7). This 5' truncation removes 4 of the 6-candidate EMS.

pHB6-M5M

A HindIII restriction digest on pHB4-M5M removes the 0.687Kb region from the 5'-vector arm HindIII site, immediately upstream of the XbaI site at –1555bp, to the HindIII site at –868bp (see figure 3.2.8-A).

pHB6-M6M

A HindIII restriction digest on pHB4-M6M removes the 0.687Kb region from the 5'-vector arm HindIII site, immediately upstream of the XbaI site at –1555bp, to the HindIII site at –868bp (see figure 3.2.8-B).

pHB6-Sp1M

A HindIII restriction digest on pHB4-Sp1M removes the 0.687Kb region from the 5'-vector arm HindIII site, immediately upstream of the XbaI site at –1555bp, to the HindIII site at –868bp (see figure 3.2.8-C).

pHB8

An SphI restriction digest on pHB4 removes the 1.484Kb region from the 5'-vector arm SphI site, immediately upstream of the XbaI site at -1555bp, to the SphI site at -71bp (see figure 3.2.9-A). This 5' truncation removes all 6-candidate E-box c-Myc-Max binding sites and the di-nucleotide GT-repeat.

pHB8-Sp1M

An SphI restriction digest on pHB4-Sp1M removes the 1.484Kb region from the 5'-vector arm SphI site, immediately upstream of the XbaI site at -1555bp, to the SphI site at -71bp (see figure 3.2.9-B)

pHB20, pHB21, pHB22 and pHB23

The *Slc11a1* promoter constructs pHB20, pHB21, pHB22 and pHB23 were produced using 4 pairs of specific synthetic oligonucleotides.

Pair 1

NRP#1 (5'-TCGACCCTCAGTGATGTGGAGATGAGGTCTGGAGGG-3')

NRP#2 (5'-TCCCCTCCAGACCTCATCTCCACATCACTGAGGG-3')

Pair 2

NRP#3 (5'-GATGGGAAGGGCGTGGGTTCCCACTCTTACTCACTCGGACC-3')

NRP#4 (5'-CTGGTCCGAGTGAGTAAGAGTGGGAACCCACGCCCTTCCCA-3')

Pair 3

NRP #7 (5'-GATTCCCACTCTTACTCACTCGGACC-3')

NRP #8 (5'-CTGGTCCGAGTGAGTAAGAGTGGGAA-3')

Pair 4

NRP#5 (5'-AGCACCCACAGAAGGGGACAGATTGAG-3')

NRP#6 (5'-GATCCTCAATCTGTCCCCTTCTGTGGGTG-3')

Combining equimolar amounts of constituent synthetic oligonucleotide, placing in a waterbath at 95°C, and allowing to cool to room temperature annealed pairs of oligonucleotides.

pHB20

Inserting oligonucleotide pairs 1, 2 & 4 into the SalI-BamHI digested pBLCAT3 produced a 0.105Kb *Slc11a1* promoter fragment corresponding to the region -71bp to +34bp (see figure 3.2.10).

pHB20E

EcoRI digestion of pHB20 removes a 1.407Kbp from and internal EcoRI site within the CAT gene to the EcoRI site within the MCS 3' of the SV40 promoter (see figure 3.2.10). This region was replaced with a corresponding EcoRI fragment from pCAT-Enhancer (Promega, UK), this EcoRI fragment however contains an enhancer sequence downstream of the CAT gene.

pHB21

pBLCAT3 was digested with both SalI and BamHI. The SalI overhang was partially filled in using dCTP and dTTP, leaving only a 2bp overhang (5'-CT-3'), this action had no effect on the BamHI overhang. Inserting oligonucleotide pairs 2 & 4 into the partially filled SalI-BamHI digested pBLCAT3 produced a 68bp *Slc11a1* promoter fragment corresponding to the region -34bp to +34bp (see figure 3.2.11).

pHB23

pBLCAT3 was digested with both SalI and BamHI. The SalI overhang was partially filled in using dCTP and dTTP, leaving only a 2bp overhang (5'-CT-3'), this action had no effect on the BamHI overhang. Inserting oligonucleotide pairs 3 & 4 into the partially filled SalI-BamHI digested pBLCAT3 produced a 53bp *Slc11a1* promoter fragment corresponding to the region -19bp to +34bp (see figure 3.2.12).

pHB22

pBLCAT3 was digested with both XbaI and BamHI. The XbaI overhang was partially filled in using dCTP and dTTP, leaving only a 2bp overhang (5'-CT-3'). Inserting the oligonucleotide pair 4 into the partially filled XbaI-BamHI digested pBLCAT3 produced a 27bp *Slc11a1* promoter fragment corresponding to the region +8bp to +34bp (see figure 3.2.13). The pHB22 sequence starts downstream of the potential Inr sequence and will therefore provide a negative control.

3.2.3 *Slc11a1* Promoter Constructs Display Comparable Expression Patterns in the Cos-1 and RAW 264.7 Cell lines.

Slc11a1 is a macrophage specific gene in mice and the human SLC11A1 promoter has been reported to drive differing patterns of expression in the cell lines tested (HL-60, Jurkat and 293-T) (Roig *et al.* 2002). In order to assess any such differences in expression of the murine *Slc11a1* promoter constructs between cell lines a constant amount (2μg) of the *Slc11a1* promoter constructs and 1μg of the pGL3-Control vector (Promega, UK.) were transfected into the Cos-1 African green monkey kidney cell line and the RAW 264.7 murine leukaemic monocyte/macrophage cell line using the LipofectAMINE (LA) reagent (see section 2.2.7). Promoter activities obtained via the CAT assay were normalised to the luciferase output from the co-transfected pGL3-Control vector. Although, due to low transfection efficiencies, levels of expression were lower in the RAW 264.7 cell line compared with the Cos-1 cell line, (figure 3.2.14-A) the pattern of expression of the deletion series is not significantly different ($P>0.3$ for all constructs). These data suggest that promoter activities obtained in the Cos-1 cell line are an accurate reflection of promoter activity within the RAW 264.7 cell line.

3.2.4 Normalisation to a Control Luciferase Vector does not Significantly Affect *Slc11a1* Promoter Activity in the Cos-1 Cell Line.

Comparison of the promoter activities within the Cos-1 cell line, before and after normalisation (figure 3.2.14-B), shows that there is no significant change in promoter activities as a result of this normalisation (as assessed by Student's T-test P>0.35 for all constructs). Therefore, for all subsequent studies a control plasmid has not been included.

3.2.5 *Slc11a1* Promoter Activity in the Cos-1 Cell Line.

A constant amount (2μg) of the *Slc11a1* promoter constructs were transfected into the Cos-1 African green monkey kidney cell line (see section 2.2.7). Figure 3.2.14-C shows the activity of the *Slc11a1* promoter constructs in the Cos-1. In the Cos-1 cell line the activities of *Slc11a1* promoter constructs pHB5 and pHB6 are not significantly different, as assessed by Student's T-test (P=0.9518), suggesting that the 5.329Kb region between -6197bp and -868bp exerts no significant effect on the activity of the promoter. The *Slc11a1* promoter constructs pHB6 and pHB8 show a significant difference in activity (P=0.000659). Deletion of the region between -868bp and -71bp results in a 3.96±2.14 fold increase in promoter activity, suggesting a repressor sequence lies within this 797bp region. The 66bp 3'-truncation between pHB8 and pHB20 results in a significant (P=0.007) 1.898±0.61-fold decrease in promoter activity, this suggests that the region between +34bp and +100bp contains a binding site for a positively acting factor. Further deletion of the *Slc11a1* promoter has no significant effects of activity (P=0.5478 between pHB21 and pHB23). pHB22 is inactive as would be expected based on its sequence content.

3.2.6 An E-box c-Myc-Max Binding Site at –127bp Acts as a Repressor within the *Slc11a1* Promoter.

Analysis of the *Slc11a1* promoter (section 3.2.5) showed that deletion of the region between –868bp and –71bp results in significant increase in promoter activity. In order to pin-point the region responsible for the repression activity observed, fine mapping was performed, and a series of *Slc11a1* promoter fragments were produced

that decreased the candidate region in ~90bp decrements between pHB6 and pHB8. These fragments were subsequently cloned into the pBLCAT3 vector and termed the REP series[4] (see figure 3.2.15-B). A constant amount (2μg) of the *Slc11a1* promoter REP constructs were transfected into the Cos-1 African green monkey kidney cell line and assayed for promoter activity as described (see sections 2.2.7&9). Figure 3.2.15-C shows that there was no change in promoter activity until the deletion from REP#5 to pHB8, corresponding to the deletion from –403 to –71bp, suggesting that any potential repressor lies within this region. Sequence analysis of this region identified a non-canonical EMS (termed EMS#6). It has previously been reported that the mitogen-induced expression of the fibroblast growth factor-binding protein (FGF-BP) is transcriptionally repressed via a non-canonical EMS element (5'-AACGTG-3'). Deletion of the EMS, which has been shown to bind c-Myc, resulted in enhanced responsiveness to TPA treatment (Harris *et al.* 2000). In order to establish whether the identified EMS#6 was responsible for the repression observed, both EMS#5 and EMS#6 were mutated separately in the context of both pHB4 and pHB6 (see section 3.2.2). Mutation of EMS#6, but not EMS#5 increases activity of the pHB4M6M promoter to a level significantly different from the pHB4 (P=0.0079), but not-significantly different from the pHB8 that does not contain any canonical or non-canonical EMS (P=0.15274) (Figure 3.2.16-A). Similar results were observed for the pHB6 mutants (see figure 3.2.16-B).

3.2.7 The Consensus Sp1-Binding Site at –27bp Influences Macrophage Specific Expression of the *Slc11a1* Promoter Constructs

Murine *Slc11a1* demonstrates tissue- and cell-specific expression, and is restricted to mature macrophages present in reticuloendothelial organs (Govoni *et al,* 1995; Biggs *et al*, 2001). Macrophage-specific expression of the *Slc11a1* promoter constructs was assayed using Cos-1 and RAW 264.7 cell lines. Activity of the *Slc11a1* promoter driven reporter constructs and the *β-actin* promoter driven reporter construct, LKCAT2, were calculated as CAT Conversion/μg protein/hour. Activity of *Slc11a1* promoter driven reporter constructs were then calculated as a percentage of the positive control LKCAT2. The LKCAT2 plasmid contains the CAT reporter gene

[4] Emma Siân Phillips produced the REP series.

driven by the strong *β-actin* promoter, and is expressed well in both cell lines used, although lower activities are seen in RAW264.7 cells, probably due to lower transfection efficiencies. The *Slc11a1* promoter activities were calculated, as a percentage of *β-actin* promoter activity (LKCAT2) for each cell line, to enable comparison of *Slc11a1* promoter activities, with the assumption that the *β-actin* promoter is expressed equivalently in both cell types. The *Slc11a1* promoter construct, pHB4, displays a relatively higher activity in the RAW 264.7 macrophage lineage cell line (10.49±9.79%) compared to the Cos-1 cell line (0.68±0.4%), this difference is not statistically significant (P=0.088) (Figure 3.2.17). It has been reported that the human SLC11A1 promoter drives differing patterns of expression in the cell lines tested (HL-60, Jurkat and 293-T) (Roig *et al.* 2002). The myeloid-specific elements of the human SLC11A1 promoter were reported to be located within the region spanning 558 and 262bp upstream of the ATG translational start codon. Deletion analysis of the murine *Slc11a1* promoter (see section 3.2.3 & figure 3.2.14-A) showed that the pattern of expression of the deletion series is similar between the Cos-1 and RAW 264.7 cell lines. Activity of the *Slc11a1* promoter constructs in the Cos-1 cells, relative to the activity in the RAW 264.7 cells, remained constant at 4.56±1.1% throughout the deletion from pHB5 to pHB8, -6197bp to –71bp, suggesting that the myeloid-specific elements are within the pHB8 sequence (figure 3.2.17-B). The Sp1 transcription factor is important in driving macrophage specific expression (reviewed Clarke and Gordon, 1998; Black *et al.* 2001). Mutation of the consensus Sp1-binding site at –27bp had little effect on promoter activity, a slight increase in Cos-1 cell activity and a slight decrease in RAW 264.7 cell activity (figure 3.2.18). These slight changes in activity did however affect macrophage specificity of the *Slc11a1* promoter constructs. The data in figure 3.2.19 show that mutation of the consensus Sp1-binding site at –27bp increases *Slc11a1* promoter activity, relative to LKCAT2 activity, within the Cos-1 cell line, with a concomitant decrease in *Slc11a1* promoter activity, relative to LKCAT2 activity within the RAW 264.7 cell line. The result of this mutation is an *Slc11a1* promoter construct that no longer directs macrophage specific expression.

3.2.8 Expression of a 64bp Fragment of the *Slc11a1* Promoter is Upregulated by the Proinflammatory Agents

The proinflammatory agents Interferon γ (IFNγ) and bacterial Lipopolysaccharide (LPS) influence the maturation/differentiation of macrophages toward activation for bactericidal activity, and upregulate both *Slc11a1* mRNA (Govoni *et al.* 1995) and protein (Baker *et al.* 2000) levels. RAW 264.7 cells were transfected (see section 2.2.7) with the *Slc11a1* promoter construct pHB20-E for 24hours, then treated with IFNγ (50U/ml), LPS (100ng/ml), or IFNγ/LPS and then assayed for CAT activity after a further 24 hours (see section 2.2.9). Treatment with IFNγ alone induces a small, but non-significant increase in promoter activity (Figure 3.2.20). Treatment with LPS alone induces a 2.085±0.06 fold increase in promoter activity (P=0.0015). Treatment of the cells with both IFNγ and LPS induces a 2.428±0.35 fold increase in promoter activity, which is significantly different from the untreated cells (P=0.011), but not statistically different from the effects of LPS alone.

FIGURE 3.2.1 Summary of Putative Transcription Factor Binding Sites within the *Slc11a1* Promoter. Table summarises a selection of putative transcription factor binding sites in the *Slc11a1* promoter identified using the Genomatix MatInsepctor professional programme (http://genomatix.gsf.de). Putative binding sites for identified transcription factors, or families of transcription factors, are indicated along with a summary of their function or pattern of expression. Position of binding sites highlighted in bold are those previously identified by Govoni *et al.* 1995.

TRANSCRIPTION FACTOR	FUNCTION/ EXPRESSION	POSITION RELATIVE TO TRANSCRIPTIONAL START SITE
Activator Protein 1 (API)	Ubiquitous	-5664 to -5875 -846 to -857 **-1 to -6 (-ve strand)** +304 to +313 (-ve strand) +1184 to +1195
Stimulating Protein 1 (Sp1)	Ubiquitous	-4250 to -4263 **-21 to -26 (-ve strand)** +1878 to +1891 (-ve strand)
NFκB	Lymphoid expressed genes	+1758 to +1768
Runt/PEBP2/CBF family -PEBP2/CBF	Myeloid-restricted factors	-4693 to -4699 (-ve strand) -2989 to -2995 -1690 to -1696 -1412 to -1418 -256 to -262 (-ve strand)
E-Twenty six specific (ETS) family -Ets1 -Ets2 -PU.1	Myeloid-restricted factors	-2498 to -2513 -1764 to -1779 (-ve strand) -256 to -271 -2962 to -2976 -684 to -698 (-ve strand) -1252 to -1268 **-167 to -173**
Interferon Regulatory Elements -IRE1 -IRE2 -IRSE -IFNγ	Activated by IFNγ	-4544 to -4557 -4408 to -4421 -2918 to -2931 -2139 to -2152 (-ve strand) +929 to +942 (-ve strand) -671 to -684 (-ve strand) -5979 to -5994 (-ve strand) -4506 tp -4521 (-ve strand) -967 to -982 **-176 to -183 (-ve strand)** **+68 to +75 (-ve strand)** **+107 to +114 (-ve strand)** **+117 to +124 (-ve strand)** **+126 to +133 (-ve strand)**
STAT PROTEINS -STAT1 -STAT3 -STAT	Activated by IFNγ	-3237 to -3258 -677 to -698 -4878 to -4887 (-ve strand) -4241 to -4250 -3379 to -3388 -2533 to -2542 +358 to +367
CCAAT/enhancer binding protein (C/EBP) family -NF-IL6	Rapidly induced by tissue injury, infection, IL-1 & LPS	-1529 to -1543 (-ve strand) -602 to -616 (-ve strand) **-235 to -243** **-136 to -144 (-ve strand)** +1125 to +1139 (-ve strand)
SMAD PROTEINS -Smad3 -Smad4	Involved in TGFβ signalling	-200 to -209 (-ve strand) +1319 to +1327 (-ve strand) +1707 to +1715 +2237 to +2245 (-ve strand) -4927 to -4935 -4667 to -4675 -3954 to -3962 (-ve)
NFI	Involved in TGFβ signalling	**-202 to -216**
E-Box	c-Myc-Max binding sites	#1 -1542 #2 -1377 #3 -1366 #4 -1049 #5 -588 #6 -127

FIGURE 3.2.2 The *Slc11a1* Promoter Construct Deletion Series. (A) A schematic of the 1.656Kbp 'pHB4' region of the *Slc11a1* promoter region indicating restriction endonuclease recognition sites and approximate sizes. (B) Schematic of the *Slc11a1* promoter construct deletion series indicating sequences of interest and the Initiator driven start site of transcription (see key). The sizes of the constructs are relative to each other and correlate with the sizing indicated in (A).

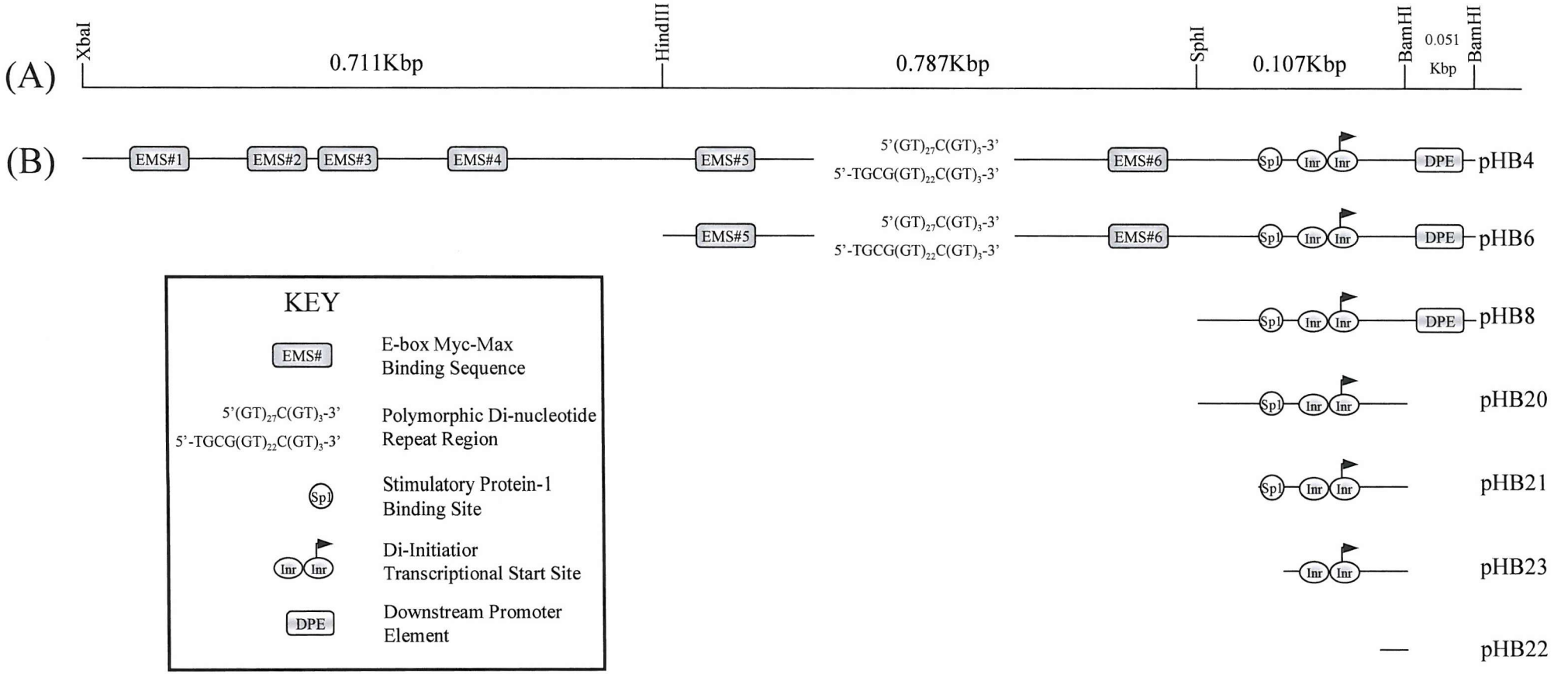
(A)
XbaI
0.711Kbp
HindIII
0.787Kbp
SphI
0.107Kbp
BamHI
0.051 Kbp
BamHI
(B)
EMS#1
EMS#2
EMS#3
EMS#4
EMS#5
5'(GT)27C(GT)3-3'
5'-TGCG(GT)22C(GT)3-3'
EMS#6
Sp1
Inr
Inr
DPE
pHB4
pHB6
pHB8
pHB20
pHB21
pHB23
pHB22
KEY
EMS#
E-box Myc-Max Binding Sequence
5'(GT)27C(GT)3-3'
5'-TGCG(GT)22C(GT)3-3'
Polymorphic Di-nucleotide Repeat Region
Sp1
Stimulatory Protein-1 Binding Site
Inr Inr
Di-Initiatior Transcriptional Start Site
DPE
Downstream Promoter Element

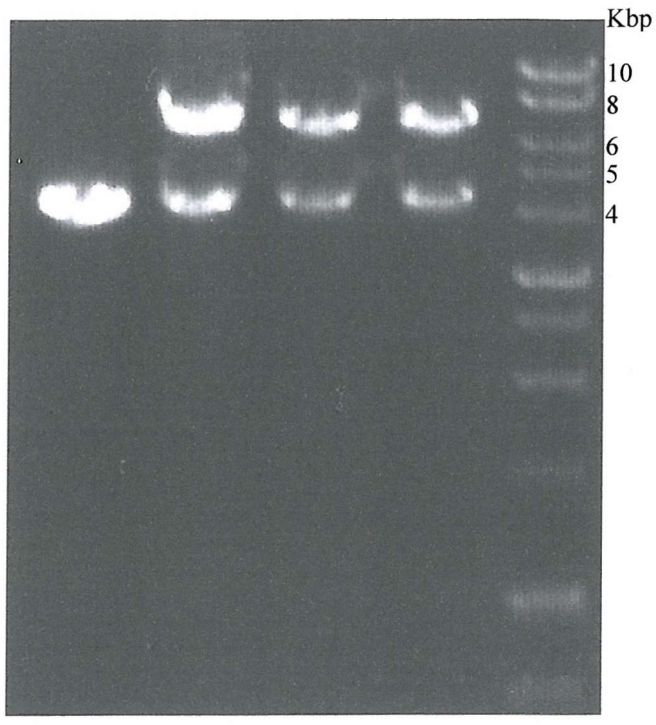

FIGURE 3.2.3 Restriction Digests Confirming pHB1 Clones. 1μl of DNA mini-preparations were incubated at 37°C for 1 hour with 10U of the BamHI restriction endonuclease (Promega, UK). Digests were loaded on a 1% Agarose-TBE gel containing 0.01% Ethidium Bromide, and run at 100V for 30-60 minutes. (1), pBLCAT3-BamHI; (2) pHB1 clone 1-BamHI; (3) pHB1 clone 2-BamHI; (4) pHB1 clone 3-BamHI; (5) 1Kbp DNA ladder (Promega, UK).

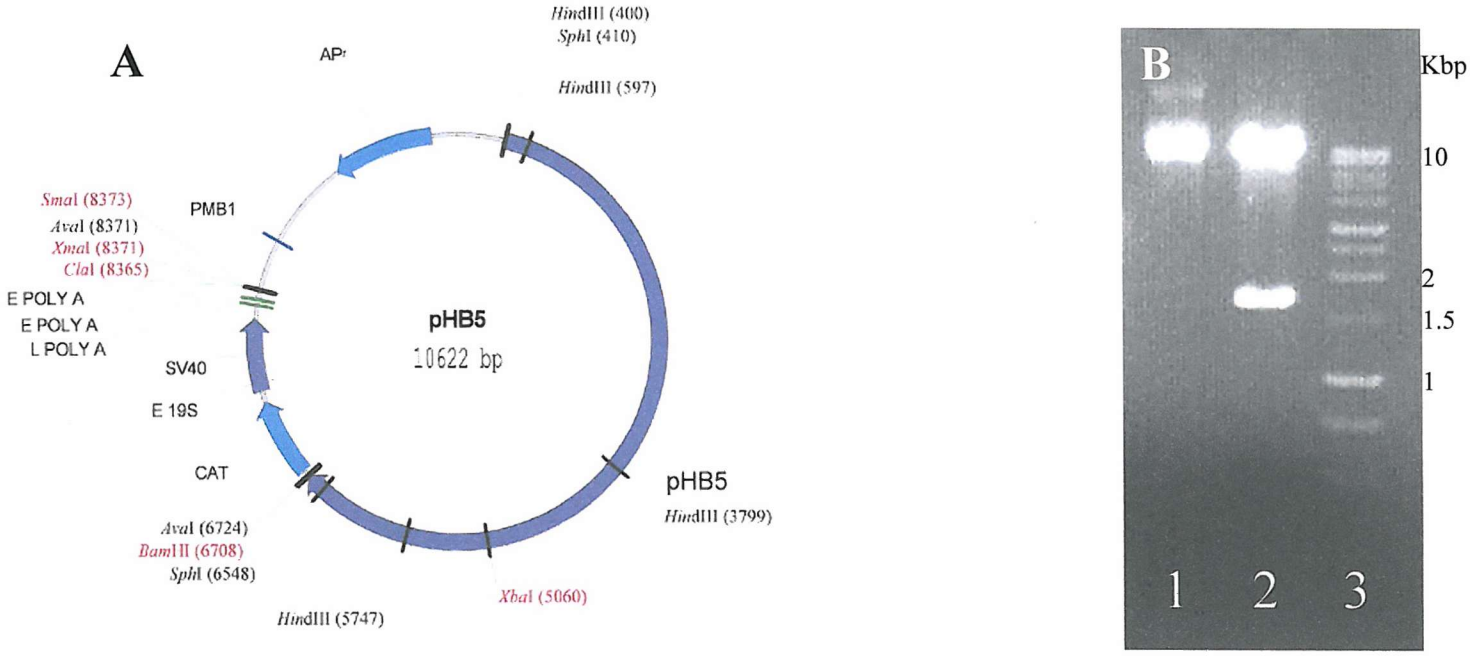

FIGURE 3.2.4 Plasmid Map and Restriction Digests Confirming pHB5 Clones. (A) Plasmid map of pHB5 indicating size (10.622Kbp) and restriction endonuclease recognition sites, unique sites are highlighted in red. (B) 2µl of DNA mini-preparations were incubated at 37°C for 1 hour with 10U of BamHI and 8-12U of XbaI restriction endonucleases (Promega, UK), if correct this digests should drop out a 1.648Kbp fragment corresponding to the XbaI site within the *Slc11a1* promoter region and the BamHI site within the multiple cloning site (MCS). Digests were loaded on a 1% Agarose-TBE gel containing 0.01% Ethidium Bromide, and run at 100V for 30-60 minutes. (1), pHB5-Uncut; (2) pHB5-BamHI/XbaI; (3) 1Kbp DNA ladder (Promega, UK).

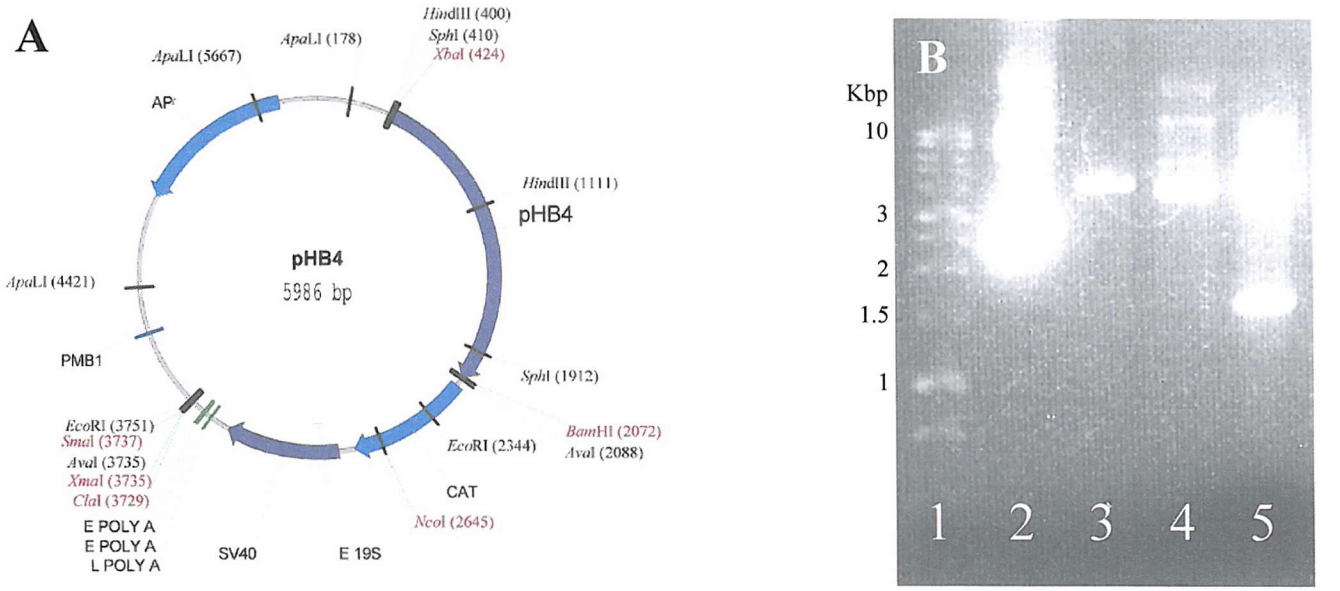

FIGURE 3.2.5 Plasmid Map and Restriction Digests Confirming pHB4 Clones. (A) Plasmid map of pHB4 indicating size (5.986Kbp) and restriction endonuclease recognition sites, unique sites are highlighted in red. (B) 2µl of DNA mini-preparations were incubated at 37°C for 1 hour with 10U of BamHI and 8-12U of XbaI restriction endonucleases (Promega, UK), if correct this digests should drop out a 1.648Kbp fragment corresponding to the XbaI site at the 5' end of the *Slc11a1* promoter and the BamHI site within the multiple cloning site (MCS). Digests were loaded on a 1% Agarose-TBE gel containing 0.01% Ethidium Bromide, and run at 100V for 30-60 minutes. (1), 1Kbp DNA ladder (Promega, UK); (2), pBLCAT3-Uncut; (3), pHB4 clone 1-BamHI/XbaI; (4), pHB4 clone 2-BamHI/XbaI; (5), pHB4 clone 3-BamHI/XbaI.

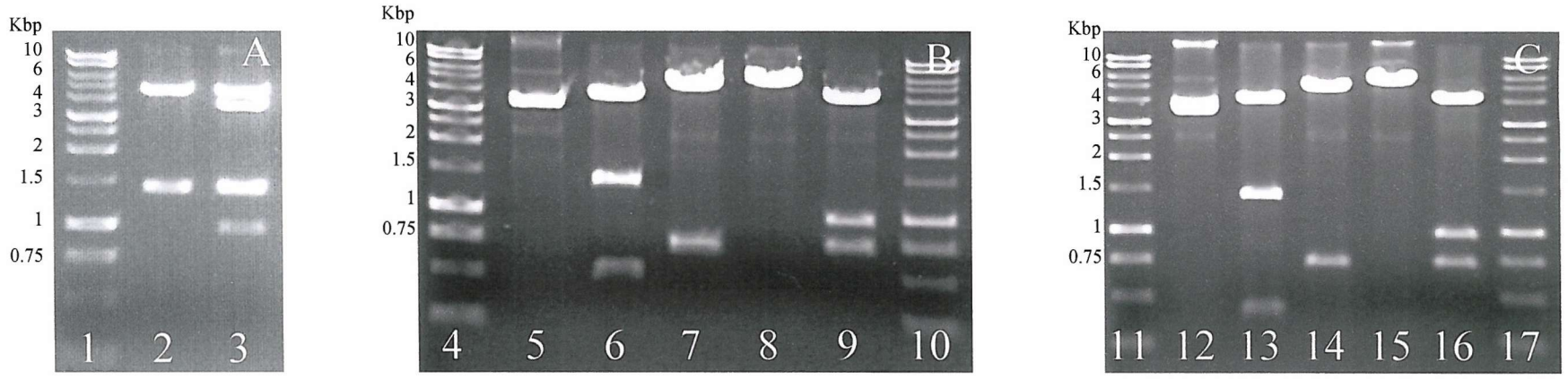

FIGURE 3.2.6 Restriction Digests Confirming pHB4M5M pHB4M6M and pHB4Sp1M Clones. (A) pHB4M5M: 1µl of DNA was incubated at 37°C for 1 hour with 12U of the EcoRI restriction endonuclease (Promega, UK). Mutation of EMS #5 at position –588bp inserts an EcoRI site in replacement of EMS enabling identification of clones via the pattern of digestion with EcoRI. In the unmutated plasmids an EcoRI digest drops out a 1.407Kbp fragment, which is associated with EcoRI sites within the native pBLCAT3 vector, insertion of an EcoRI site in replacement of the EMS 5 at position –588bp within the *Slc11a1* promoter causes the apperance of a 0.960Kbp band. (B) & (C) pHB4M6M & pHB4Sp1M: 1 or 2µl of DNA were incubated at 37°C for 1 hour with either 12U EcoRI, 10U HindIII, 10U BamHI or 10U HindIII and 10U BamHI restriction endonucleases (Promega, UK). Mutation of both the EMS#6 at position –91bp (pHB4M6M) and the Sp1 site at –27bp (pHB4Sp1M) introduces an extra EcoRI site into the plasmids, enabling easy identification of clones. EcoRI digestion will drop out the previously described 1.407Kbp fragment and a fragment of 0.463Kbp and 0.399Kbp for pHB4M6M and pHB4Sp1M respectively. Digestion with BamHI will linearise the plasmids, HindIII will produce a fragment of 0.711Kbp corresponding to the HindIII site within the MCS at the 5' end of the *Slc11a1* promoter and the HindIII site within the *Slc11a1* promoter, whereas the BamHI/HindIII digests should drop the same 0.711Kbp fragment and a 0.961Kbp fragment corresponding to the HindIII site within the *Slc11a1* promoter and the synthetic BamHI site at the 3' end of the *Slc11a1* promoter Digests were loaded on a 1% Agarose-TBE gel containing 0.01% Ethidium Bromide, and run at 100V for 30-60 minutes. (1), (4), (10), (11) & (17), 1Kbp DNA ladder (Promega, UK); (2), pHB4-EcoRI; (3), pHB4M5M-EcoRI; (5), pHB4M6M-Uncut; (6), pHB4M6M-EcoRI; (7), pHB4M6M-HindIII; (8), pHB4M6M-BamHI; (9), pHB4M6M-HindIII/BamHI; (12), pHB4Sp1M-Uncut; (13), pHB4Sp1M-EcoRI; (14), pHB4Sp1M-HindIII; (15), pHB4Sp1M-BamHI; (16), pHB4Sp1M-HindIII/BamHI.

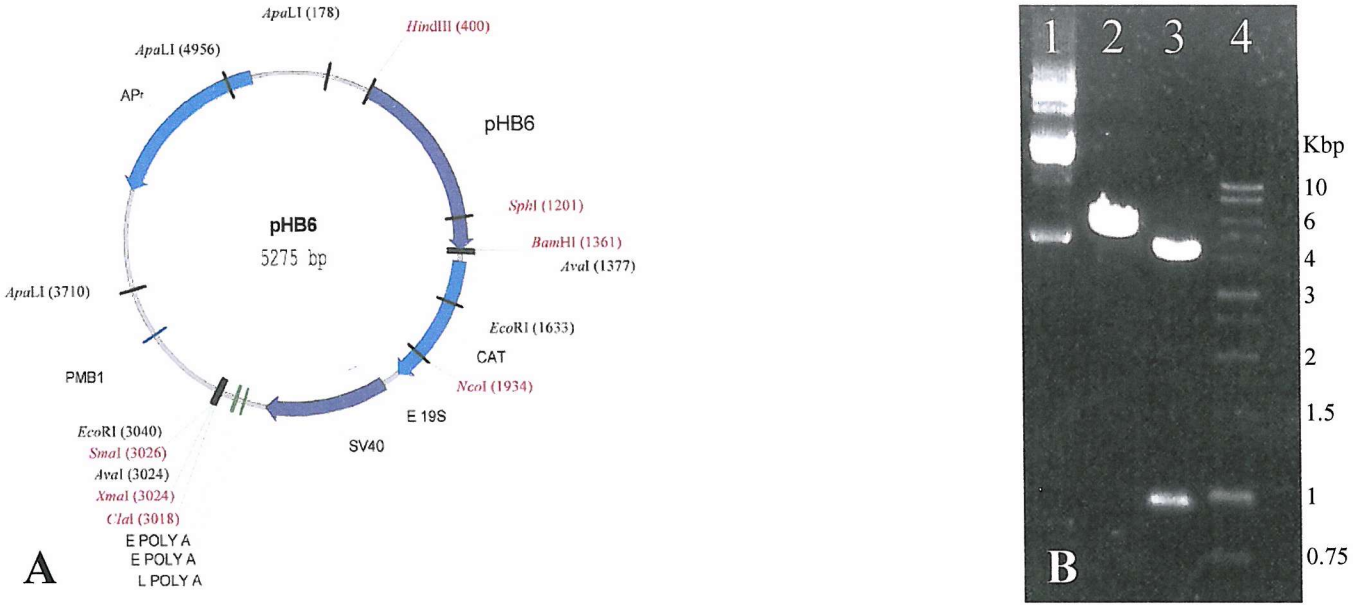

FIGURE 3.2.6 Plasmid Map and Restriction Digests Confirming pHB6 Clones. (A) Plasmid map of pHB6 indicating size (5.275Kbp) and restriction endonuclease recognition sites, unique sites are highlighted in red. (B) 1 or 2µl of DNA mini-preparations were incubated at 37°C for 1 hour with 10U of HindIII or 10U HindIII and 10U of BamHI restriction endonucleases (Promega, UK), if correct HindIII will linearise the plasmid whereas the HindIII/BamHI digests should drop out a 0.961Kbp fragment corresponding to the HindIII site at the 5' end of the *Slc11a1* promoter and the synthetic BamHI site at the 3' end of the *Slc11a1* promoter. Digests were loaded on a 1% Agarose-TBE gel containing 0.01% Ethidium Bromide, and run at 100V for 30-60 minutes. (1), pHB6 uncut; (2), pHB6-HindIII; (3), pHB6-HindIII/BamHI; (4), 1Kbp DNA ladder (Promega, UK)

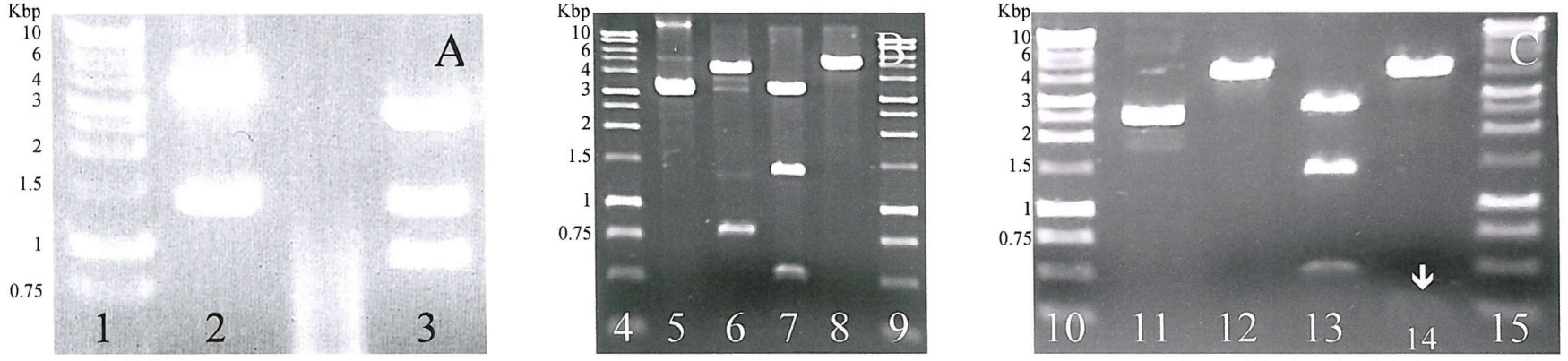

FIGURE 3.2 Restriction Digests Confirming pHB6M5M pHB6M6M and pHB6Sp1M Clones. (A) pHB6M5M: 1µl of DNA was incubated at 37°C for 1 hour with 12U of the EcoRI restriction endonuclease (Promega, UK). Mutation of EMS #5 at position –588bp inserts an EcoRI site in replacement of EMS enabling identification of clones via the pattern of digestion with EcoRI. In the unmutated plasmids an EcoRI digest drops out a 1.407Kbp fragment, which is associated with EcoRI sites within the native pBLCAT3 vector, insertion of an EcoRI site in replacement of the EMS 5 at position –588bp within the *Slc11a1* promoter causes the apperance of a 0.960Kbp band. (B) & (C) pHB6M6M & pHB6Sp1M: 1 or 2µl of DNA were incubated at 37°C for 1 hour with either 12U EcoRI, 10U HindIII, 10U BamHI or 10U SphI and 10U BamHI restriction endonucleases (Promega, UK). Mutation of both the EMS#6 at position –91bp (pHB4M6M) and the Sp1 site at –27bp (pHB4Sp1M) introduces an extra EcoRI site into the plasmids, enabling easy identification of clones. EcoRI digestion will drop out the previously described 1.407Kbp fragment and a fragment of 0.463Kbp and 0.399Kbp for pHB4M6M and pHB4Sp1M respectively. Digestion with BamHI will linearise the plasmids, HindIII will produce a fragment of 0.711Kbp corresponding to the HindIII site within the MCS at the 5' end of the *Slc11a1* promoter and the HindIII site within the *Slc11a1* promoter, whereas SphI/BamHI produces a 0.164Kbp corresponding to the synthetic BamHI site at the 3' end of the *Slc11a1* promoter and the SphI site within the *Slc11a1* promoter. Digests were loaded on a 1% Agarose-TBE gel containing 0.01% Ethidium Bromide, and run at 100V for 30-60 minutes. (1), (4), (9), (10) & (15), 1Kbp DNA ladder (Promega, UK); (2), pHB6-EcoRI; (3), pHB6M5M-EcoRI; (5), pHB6M6M-Uncut; (6), pHB6M6M-HindIIII; (7), pHB6M6M-EcoRI; (8), pHB4M6M-BamHI; (11), pHB6Sp1M-Uncut; (12), pHB6Sp1M-BamHII; (13), pHB4Sp1M-EcoRI; (14), pHB4Sp1M-SphI/BamHI.

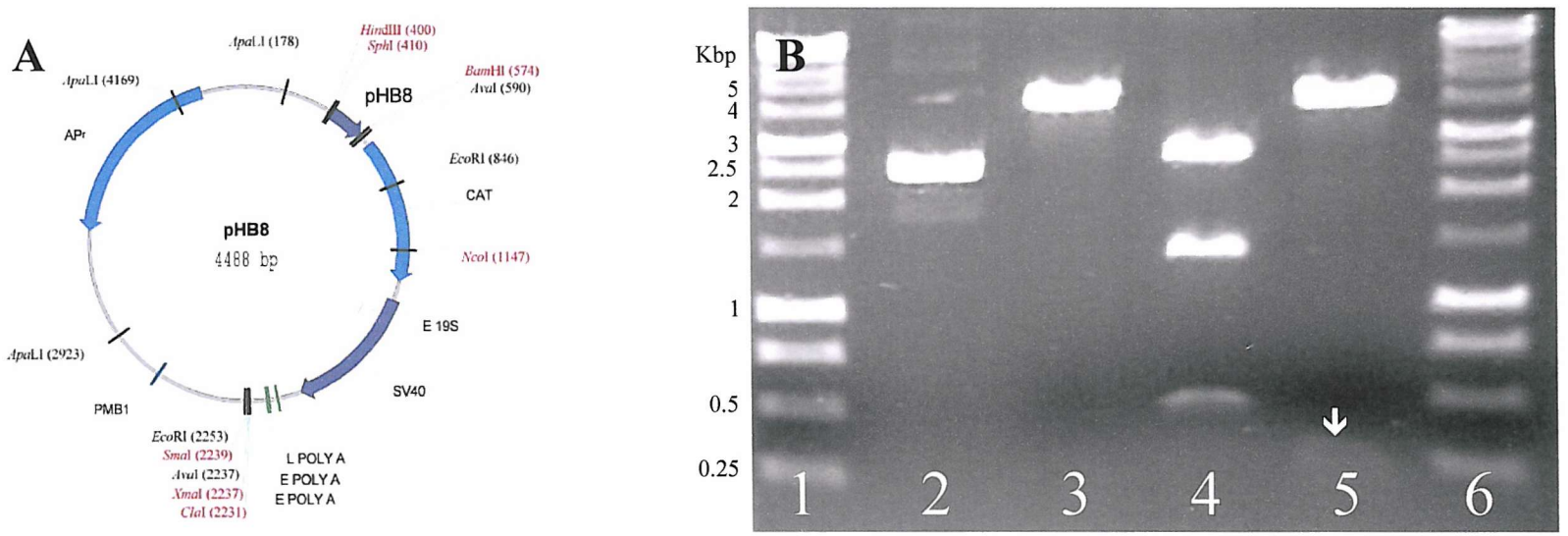

FIGURE 3.2.9 Plasmid Map and Restriction Digests Confirming pHB8 Clones. (A) Plasmid map of pHB8 indicating size (4.488Kbp) and restriction endonuclease recognition sites, unique sites are highlighted in red. (B) Restriction analysis of pHB8Sp1M clones: 1 or 2µl of DNA were incubated at 37°C for 1 hour with either 10U BamHI, 12U EcoRI, or 10U BamHI and 10U SphI restriction endonucleases (Promega, UK). Mutation of the Sp1 site at –27bp (pHB4Sp1M) introduces an extra EcoRI site into the plasmid, enabling easy identification of clones. EcoRI digestion will drop out a 1.407Kbp fragment, which is associated with EcoRI sites within the native pBLCAT3 vector, insertion of an EcoRI site in replacement of the Sp1 site at position –27bp within the *Slc11a1* promoter causes the appearance of a 0.399Kbp band. Digestion with BamHI will linearise the plasmid, whereas SphI/BamHI produces a 0.164Kbp fragment (indicated by a white arrow ⇩) corresponding to the synthetic BamHI site at the 3' end of the *Slc11a1* promoter and the SphI site within the *Slc11a1* promoter. Digests were loaded on a 1% Agarose-TBE gel containing 0.01% Ethidium Bromide, and run at 100V for 30-60 minutes. (1) & (6), 1Kbp DNA ladder (Promega, UK); (2), pHB8Sp1M-Uncut; (3), pHB8Sp1M-BamHI; (4), pHB8Sp1M-EcoRI; (5), pHB8Sp1M-SphI/BamHI.

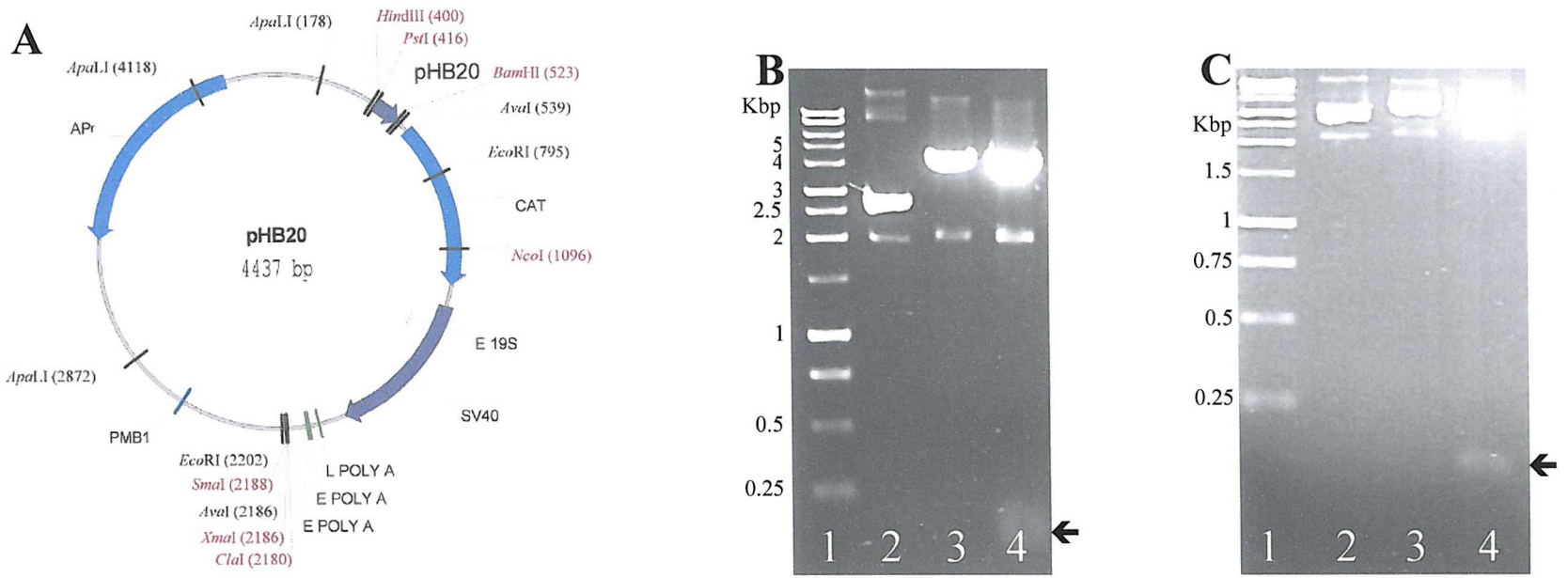

FIGURE 3.2.10 Plasmid Map and Restriction Digests Confirming pHB20 Clones. (A) Plasmid map of pHB20 indicating size (4.437Kbp) and restriction endonuclease recognition sites, unique sites are highlighted in red. (B) & (C) 1 or 2µl of DNA mini-preparations were incubated at 37°C for 1 hour with 10U of BamHI or 10U BamHI and 10U of HindIII restriction endonucleases (Promega, UK), if correct BamHI will linearise the plasmid whereas the BamHI/HindIII digests should drop out a 0.107Kbp (indicated by an arrow ←) fragment corresponding to the HindIII site within the MCS at the 5' end of the *Slc11a1* promoter and the synthetic BamHI site at the 3' end of the *Slc11a1* promoter. Digests were loaded on a (B) 1% or (C) 2% Agarose-TBE gel containing 0.01% Ethidium Bromide, and run at 100V for 30-60 minutes. (1), 1Kbp DNA ladder (Promega, UK); (2), pHB20 uncut; (3), pHB20-BamHI; (4), pHB20-BamHI/HindIII.

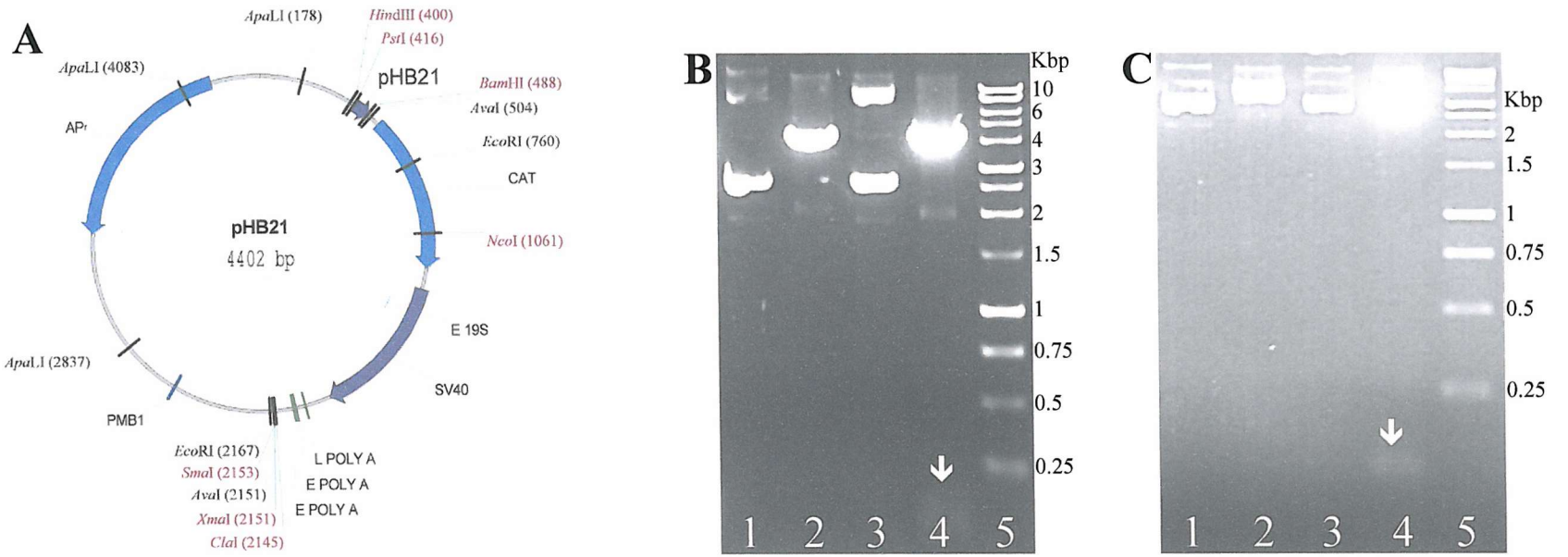

FIGURE 3.2.11 Plasmid Map and Restriction Digests Confirming pHB21 Clones. (A) Plasmid map of pHB21 indicating size (4.402Kbp) and restriction endonuclease recognition sites, unique sites are highlighted in red. (B) & (C) 1 or 2µl of DNA mini-preparations were incubated at 37°C for 1 hour with 10U of BamHI, 10U SalI or 10U BamHI and 10U of HindIII restriction endonucleases (Promega, UK), if correct BamHI will linearise the plasmid, SalI should not cut as the restriction site is not reconstituted, whereas the BamHI/HindIII digests should drop out a 0.088Kbp (indicated by a white arrow ⇩) fragment corresponding to the HindIII site within the MCS at the 5' end of the *Slc11a1* promoter and the synthetic BamHI site at the 3' end of the *Slc11a1* promoter. Digests were loaded on a (B) 1% or (C) 2% Agarose-TBE gel containing 0.01% Ethidium Bromide, and run at 100V for 30-60 minutes. (1), pHB21 uncut; (2), pHB21-BamHI; (3), pHB21-SalI; (4), pHB21-BamHI/HindIII; (5), 1Kbp DNA ladder (Promega, UK).

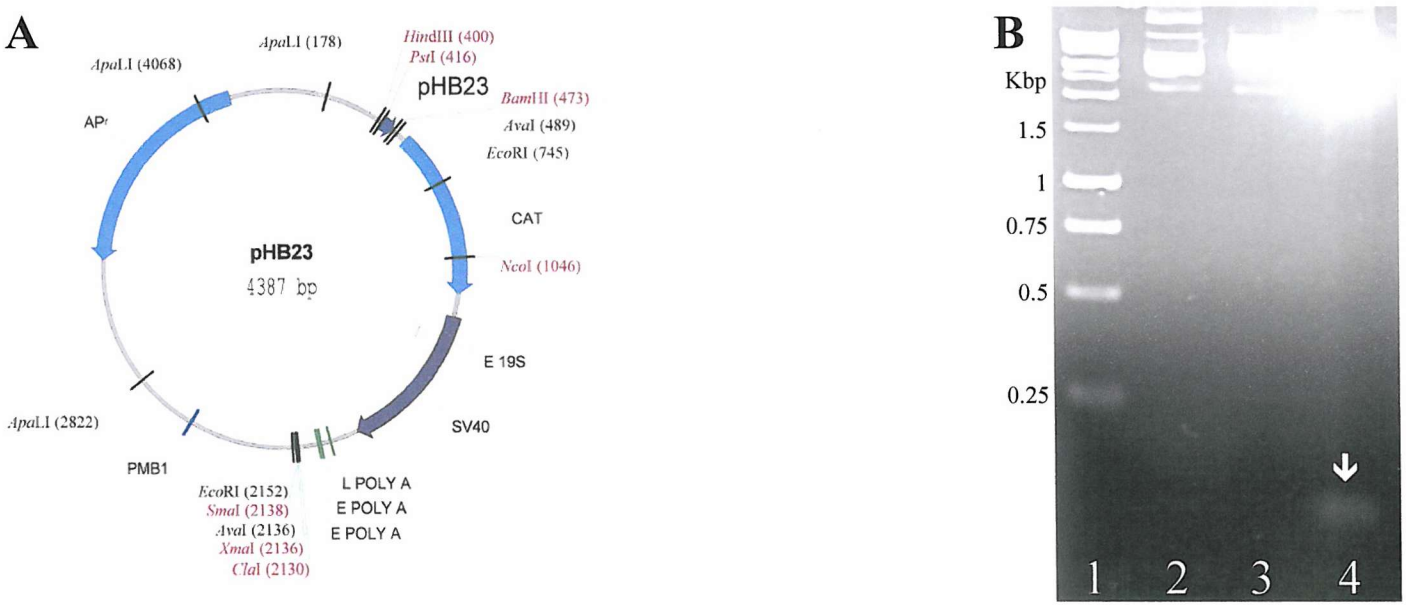

FIGURE 3.2.12 Plasmid Map and Restriction Digests Confirming pHB23 Clones. (A) Plasmid map of pHB23 indicating size (4.4387Kbp) and restriction endonuclease recognition sites, unique sites are highlighted in red. (B) 1 or 2µl of DNA mini-preparations were incubated at 37°C for 1 hour with 10U of BamHI, or 10U BamHI and 10U of HindIII restriction endonucleases (Promega, UK), if correct BamHI will linearise the plasmid, whereas the BamHI/HindIII digests should drop out a 0.073Kbp (indicated by a white arrow ⇩) fragment corresponding to the HindIII site within the MCS at the 5' end of the *Slc11a1* promoter and the synthetic BamHI site at the 3' end of the *Slc11a1* promoter. Digests were loaded on a 1% Agarose-TBE gel containing 0.01% Ethidium Bromide, and run at 100V for 30-60 minutes. (1), 1Kbp DNA ladder (Promega, UK); (2), pHB23 uncut; (3), pHB23-BamHI; (4), pHB23-BamHI/HindIII.

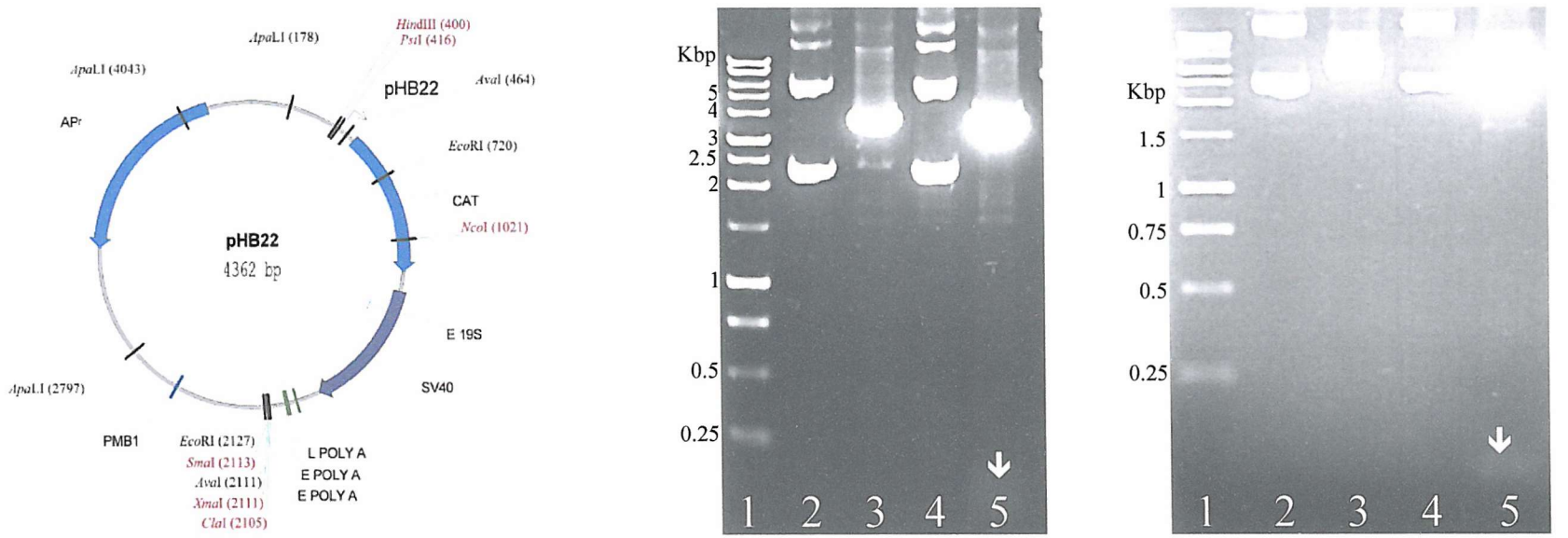

FIGURE 3.2.13 Plasmid Map and Restriction Digests Confirming pHB22 Clones. (A) Plasmid map of pHB22 indicating size (4.362Kbp) and restriction endonuclease recognition sites, unique sites are highlighted in red. (B) & (C) 1 or 2µl of DNA mini-preparations were incubated at 37°C for 1 hour with 10U of BamHI, 8-12U XbaI or 10U BamHI and 10U of HindIII restriction endonucleases (Promega, UK), if correct BamHI will linearise the plasmid, XbaI should not cut as the restriction site is not reconstituted, whereas the BamHI/HindIII digests should drop out a 0.048Kbp (indicated by a white arrow ⇩) fragment corresponding to the HindIII site within the MCS at the 5' end of the *Slc11a1* promoter and the synthetic BamHI site at the 3' end of the *Slc11a1* promoter. Digests were loaded on a (B) 1% or (C) 2% Agarose-TBE gel containing 0.01% Ethidium Bromide, and run at 100V for 30-60 minutes. (1), pHB21 uncut; (2), pHB21-BamHI; (3), pHB21-SalI; (4), pHB21-BamHI/HindIII; (5), 1Kbp DNA ladder (Promega, UK).

(A)

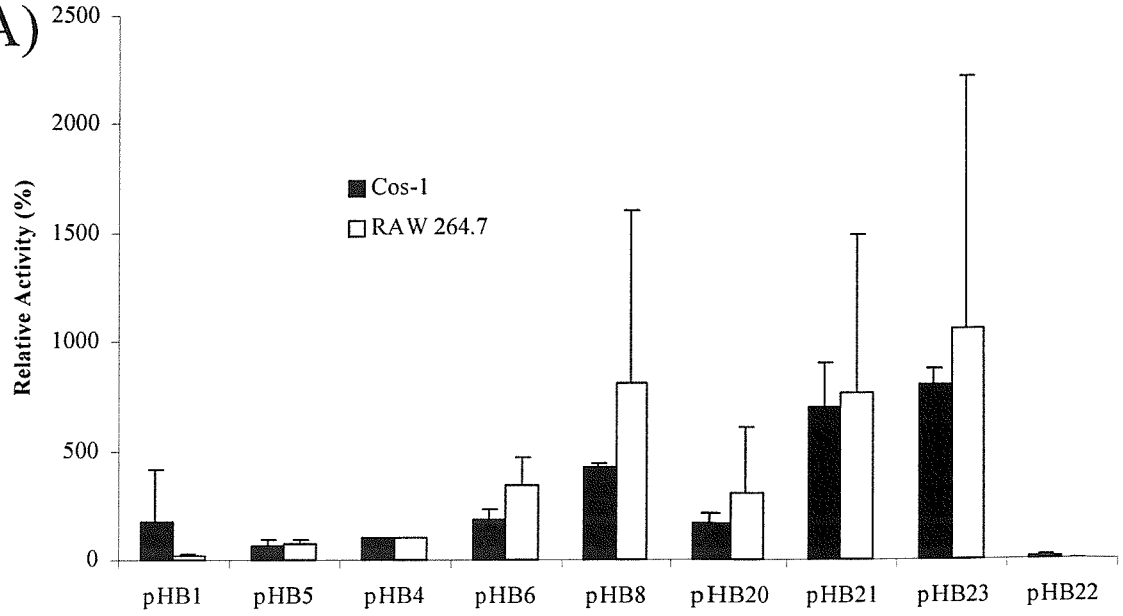
2500
2000
1500
1000
500
0
Relative Activity (%)
Cos-1
RAW 264.7
pHB1
pHB5
pHB4
pHB6
pHB8
pHB20
pHB21
pHB23
pHB22

(B)

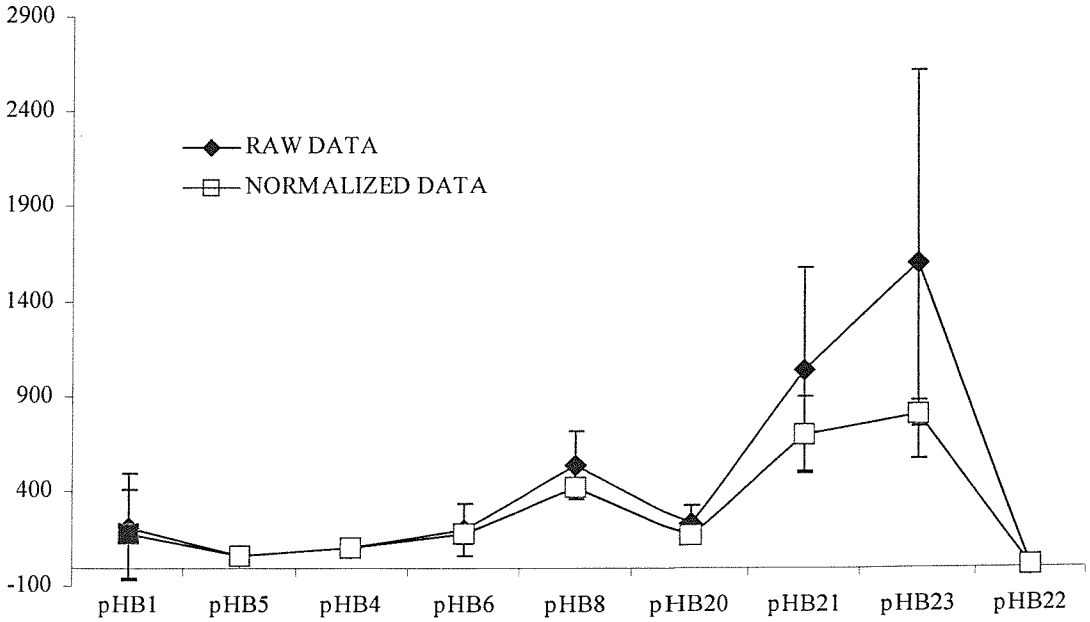
2900
2400
1900
1400
900
400
-100
RAW DATA
NORMALIZED DATA
pHB1
pHB5
pHB4
pHB6
pHB8
pHB20
pHB21
pHB23
pHB22

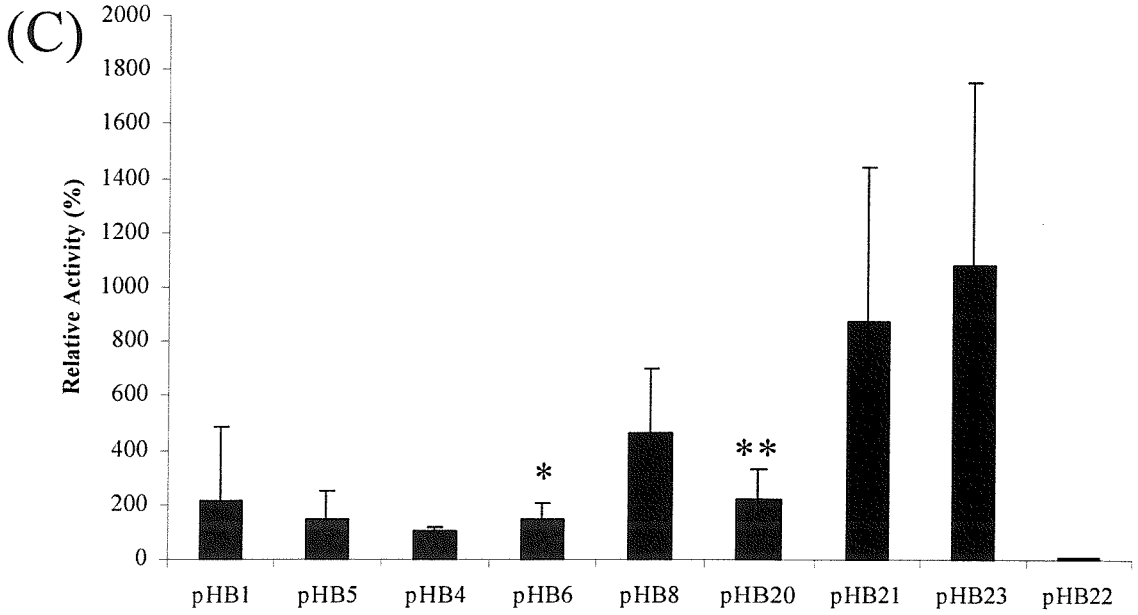

FIGURE 3.2.14 Expression of the *Slc11a1* Promoter Constructs in the Cos-1 and RAW 264.7 Cell Lines. Cells were transfected with 2μg of the *Slc11a1* promoter constructs and 1μg of the pGL3-Control luciferase vector (Promega, UK) ((A) & (B)) as described (section 2.2.7). Expression of the CAT reporter gene was detected by performing a CAT assay (37^0C; 6 hours) on 50μg (RAW 264.7) and 20μg (Cos-1) protein extract from each transfection. CAT activity was normalised to luminescence produced by the luciferase internal control and all activities were subsequently calculated relative to pHB4 activity. (A) Activity of the *Slc11a1* promoter constructs in both the Cos-1 (closed bars) and RAW 264.7 (open bars) cell lines. (B) Comparison of Raw data and normalised (to luciferase activity) data in the Cos-1 cell line. (C) Activity of the *Slc11a1* promoter constructs in the Cos-1 cell line. Students T-test comparing pHB6 & pHB8 * P=0.00066, and pHB8 & pHB20 ** P=0.007.

(A) & (B) n=2, (C) n=2-18.

(A)

NAME	OLIGONUCLEOTIDE	LENGTH
pHB6		-868 to +99bp
REP#1	5' GCTCTAGATTCACTAAGTTGTTTAGA 3'	-763 to +99bp
REP#2	5' GCTCTAGACCGTCATATGTATCCACT 3'	-673 to +99bp
REP#3	5' GCTCTAGAGGAGGTTTTTGTTTGGAC 3'	-583 to +99bp
REP#4	5' GCTCTAGAATCTGAGTGAGACCCTCA 3'	-493 to +99bp
REP#5	5' GCTCTAGACAGACTGAGATGAAAGAC 3'	-403 to +99bp
pHB8		-71 to +99bp

FIGURE 3.2.15 Expression of the *Slc11a1* REP Promoter Constructs in the Cos-1 Cell Line. (A) Table summarising REP constructs including the 5' oligonucleotides used to amplify fragments and the region of the *Slc11a1* promoter these correspond to. (B) Schematic of the *Slc11a1* promoter construct REP series indicating sequences of interest and the Initiator driven start site of transcription (see key). (C) Cells were transfected with 2μg of the *Slc11a1* REP promoter constructs as described (section 2.2.7). Expression of the reporter gene was detected by performing a CAT assay (37^0C; 1 hour) on 20μg protein extract from each transfection, all activities were subsequently calculated relative to pHB4 activity; n=2.

(B)

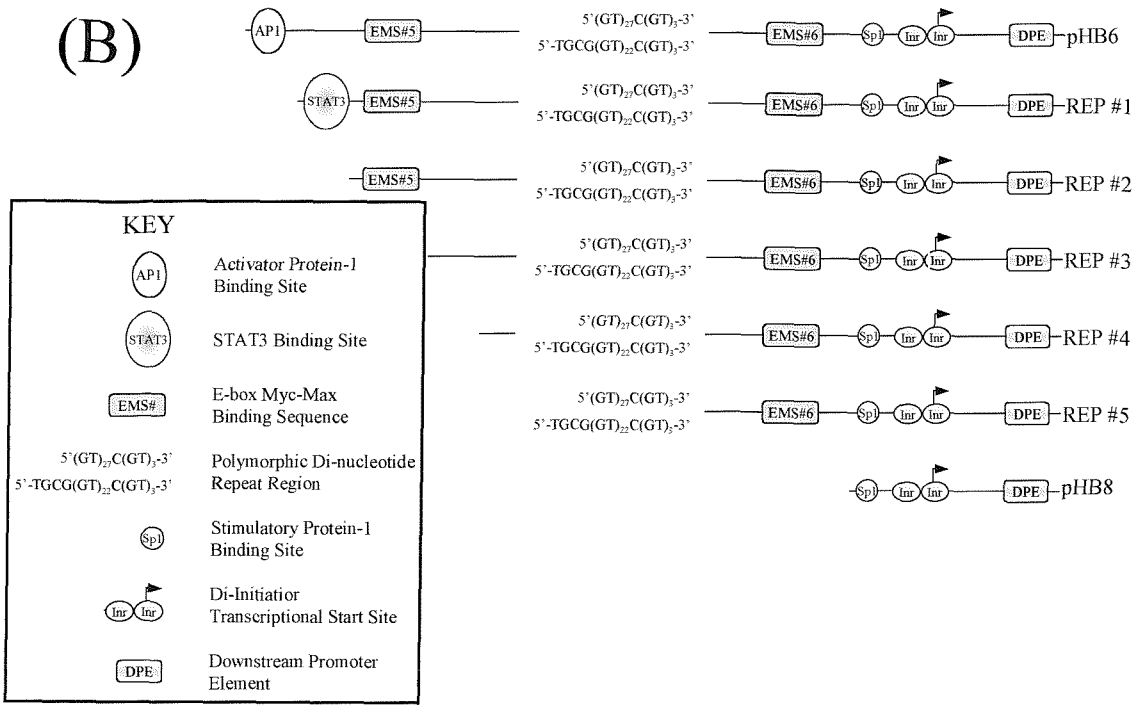
KEY
Activator Protein-1 Binding Site
STAT3 Binding Site
E-box Myc-Max Binding Sequence
Polymorphic Di-nucleotide Repeat Region
Stimulatory Protein-1 Binding Site
Di-Initiatior Transcriptional Start Site
Downstream Promoter Element
pHB6
REP #1
REP #2
REP #3
REP #4
REP #5
pHB8

(C)

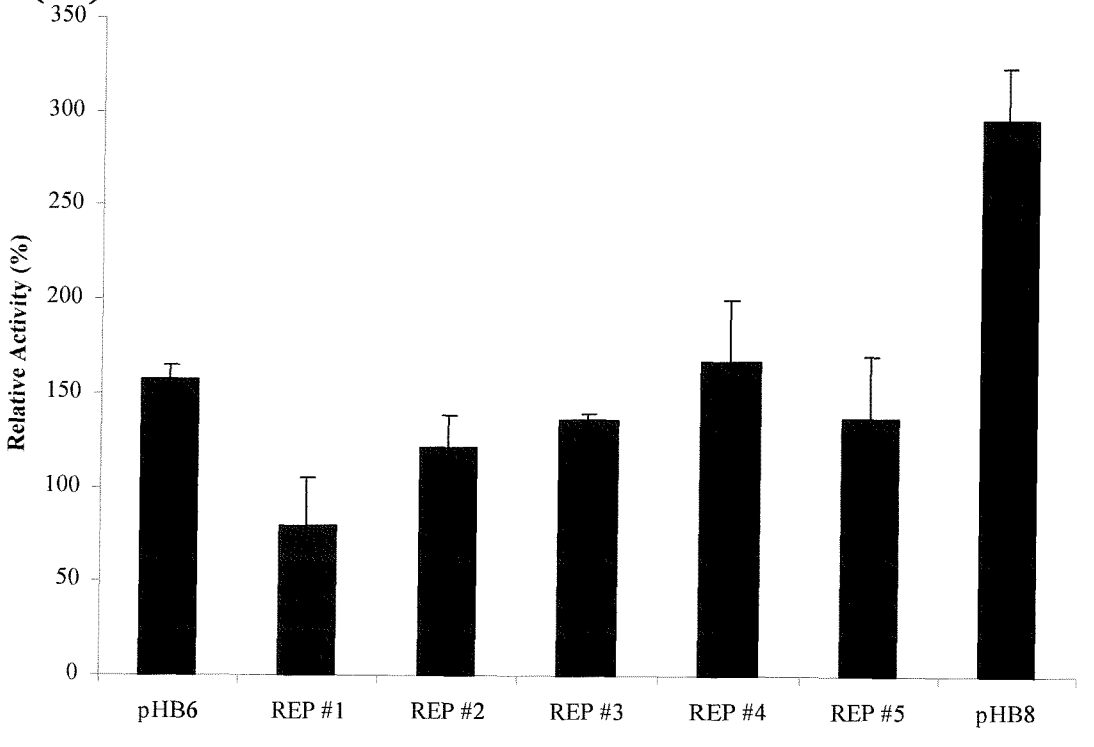
Relative Activity (%)
350
300
250
200
150
100
50
0
pHB6
REP #1
REP #2
REP #3
REP #4
REP #5
pHB8

FIGURE 3.2.16 Expression of the *Slc11a1* Promoter Constructs in the Cos-1 and RAW 264.7 Cell Lines. Cells were transfected with 2μg of the Slc11a1 promoter constructs as described (section 2.2.7). Expression of the reporter gene was detected by performing a CAT assay 37^0C for 6 hours on 50μg protein extract (RAW 264.7) and 37^0C for 1 hour on 20μg protein extract (Cos-1). All activities were subsequently calculated relative to pHB4 activity. (A) pHB4 and mutants. Student T-test in Cos-1 cells comparing pHB4 & pHB4M6M * P=0.0079, and pHB4 & pHB8 ** P=0.0002. n= 8 (Cos-1) & 2 (RAW 264.7). (B) pHB6 and mutants. Students T-test in Cos-1 cells comparing pHB6 & pHB6M6M * P=0.005, and pHB6 & pHB8 ** P=0.000659. n=4 (Cos-1) & 2 (RAW 264.7).

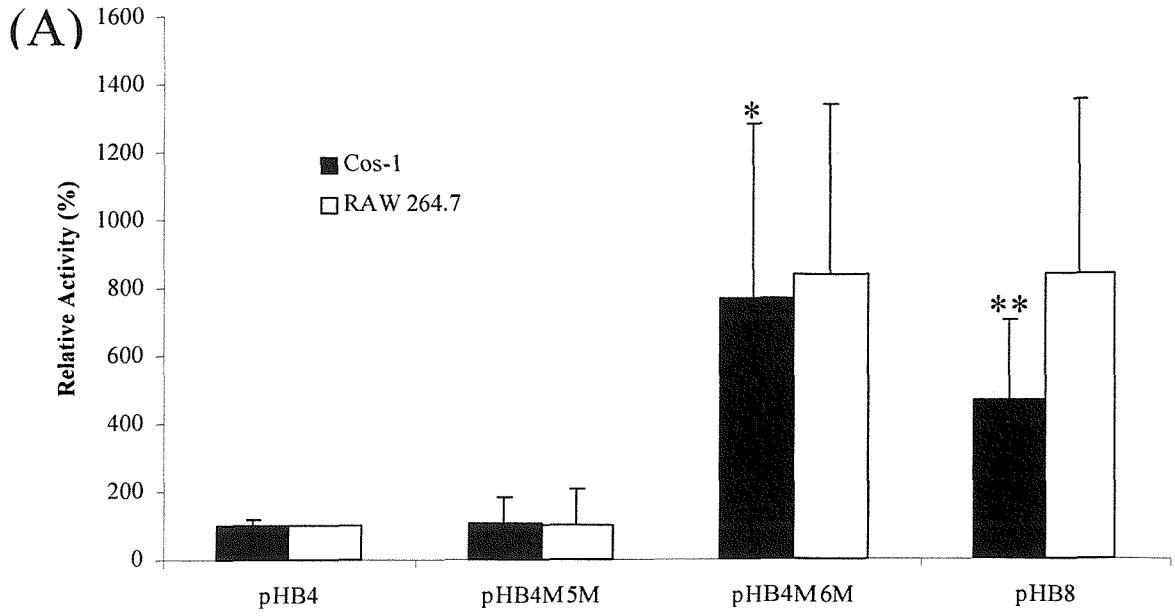
(A)
1600
1400
1200
1000
800
600
400
200
0
Relative Activity (%)
Cos-1
RAW 264.7
*
**
pHB4
pHB4M5M
pHB4M6M
pHB8

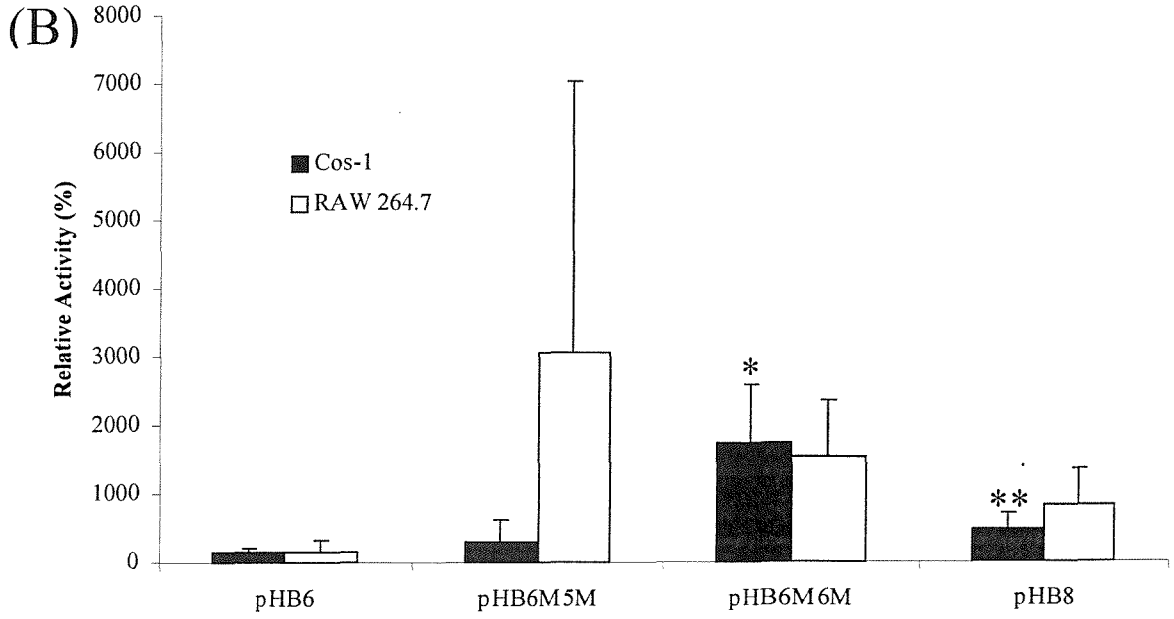
(B)
8000
7000
6000
5000
4000
3000
2000
1000
0
Relative Activity (%)
Cos-1
RAW 264.7
*
**
pHB6
pHB6M5M
pHB6M6M
pHB8

FIGURE 3.2.17 Comparison of *Slc11a1* Promoter Activity to LKCAT2 Activity in the Cos-1 and RAW 264.7 Cell Lines. Cells were transfected with 2μg of the *Slc11a1* promoter constructs as described (section 2.2.7). Expression of the reporter gene was detected by performing a CAT assay 37^0C; 6 hours on 50μg (RAW 264.7) and 37^0C; 2 hours 20μg (Cos-1) protein extract from each transfection. Total CAT conversion was calculated as CAT conversion/μg protein/hour for each sample and *Slc11a1* promoter activity calculated as a percentage of the activity of the β-actin promoter (LKCAT2). The β-actin promoter is assumed to be equally active in both cell types. (A) Comparison of pHB4 activity between Cos-1 and RAW 264.7 cells. n=19 (Cos-1) and 5 (RAW 264.7). (B) Comparison of pHB4, pHB5, pHB8 & pHB23 activities between Cos-1 (closed bars) and RAW 264.7 (open bars) cells, activity of constructs within the Cos-1 cell line were also calculated as a percentage of construct activity within the RAW 264.7 cell line (line). n=2.

(A)

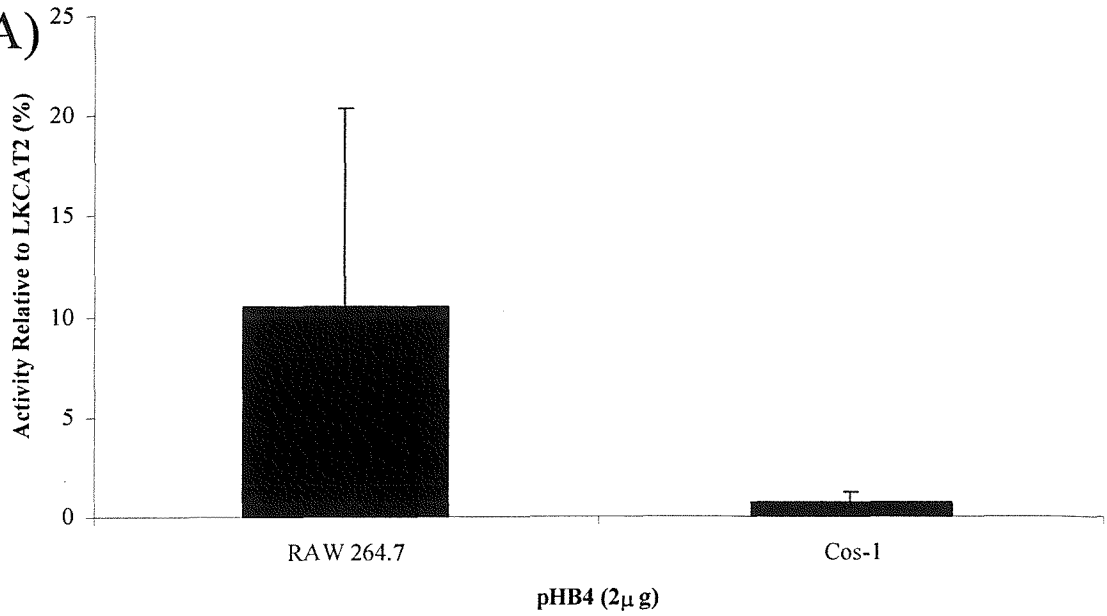
Activity Relative to LKCAT2 (%)
25
20
15
10
5
0
RAW 264.7
Cos-1
pHB4 (2μg)

(B)

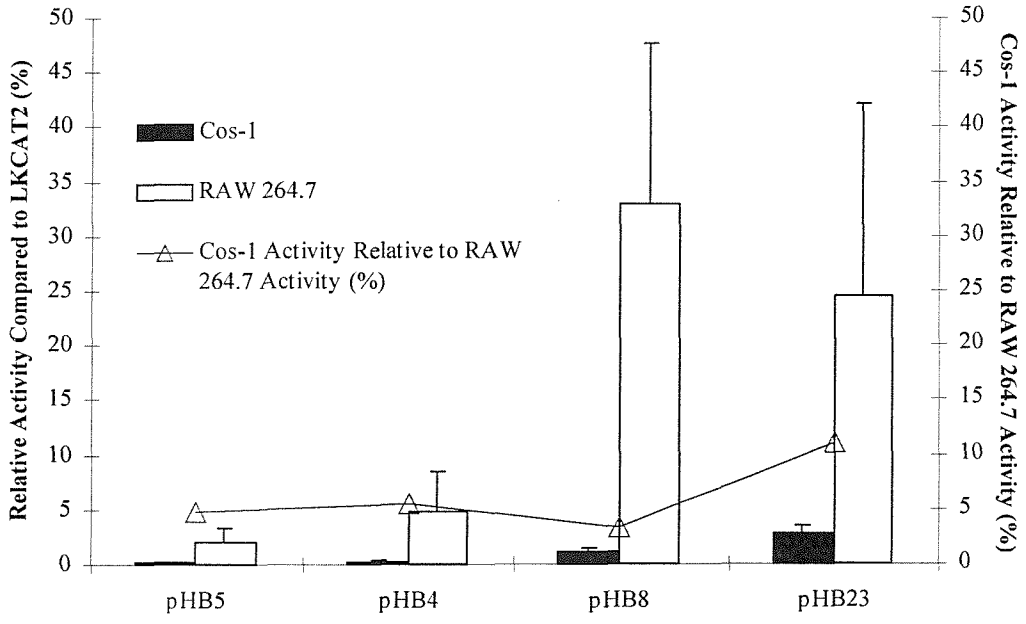
Relative Activity Compared to LKCAT2 (%)
Cos-1 Activity Relative to RAW 264.7 Activity (%)
50
45
40
35
30
25
20
15
10
5
0
Cos-1
RAW 264.7
Cos-1 Activity Relative to RAW 264.7 Activity (%)
pHB5
pHB4
pHB8
pHB23

FIGURE 3.2.18 Expression of the *Slc11a1* Sp1 Mutant Promoter Constructs in the Cos-1 and RAW 264.7 Cell Lines. Cells were transfected with 2μg of the *Slc11a1* promoter constructs and 1μg of the pGL3-Control luciferase vector (Promega, UK) ((A) & (B)) as described (section 2.2.7). Expression of the CAT reporter gene was detected by performing a CAT assay (37^0C; 6 hours) on 50μg (RAW 264.7) and 20μg (Cos-1) protein extract from each transfection. All activities were calculated relative to pHB4 activity. (A) Comparison of pHB4 & pHB4Sp1M activity in both the Cos-1 (closed bars) and RAW 264.7 (open bars) cells. (B) Comparison of pHB6 & pHB6Sp1M activity in both the Cos-1 (closed bars) and RAW 264.7 (open bars) cells. (C) Comparison of pHB8 & pHB8Sp1M activity in both the Cos-1 (closed bars) and RAW 264.7 (open bars) cells.

(A)

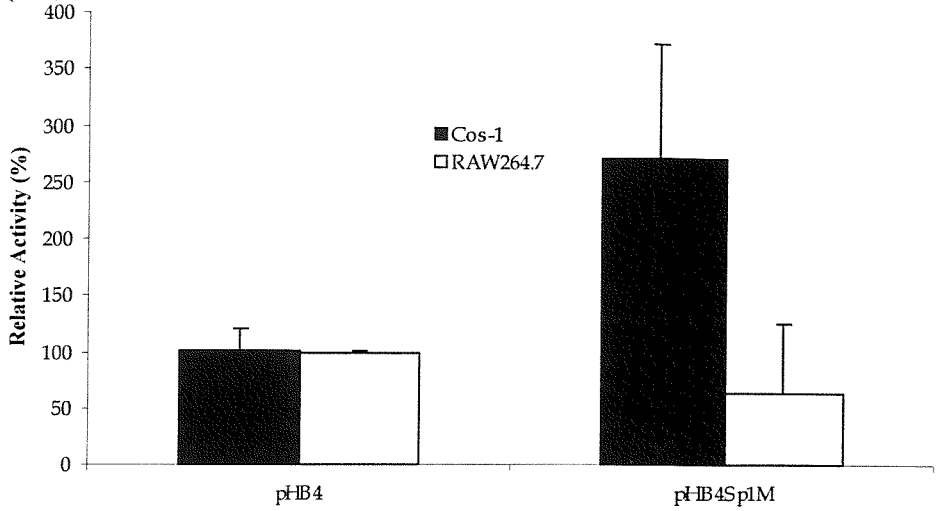
400
350
300
250
200
150
100
50
0
Relative Activity (%)
Cos-1
RAW264.7
pHB4
pHB4Sp1M

(B)

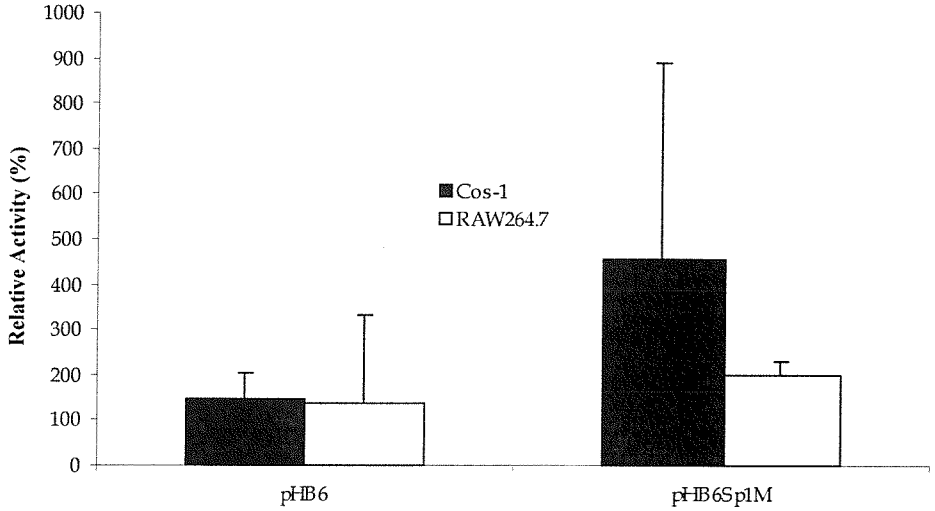
1000
900
800
700
600
500
400
300
200
100
0
Relative Activity (%)
Cos-1
RAW264.7
pHB6
pHB6Sp1M

(C)

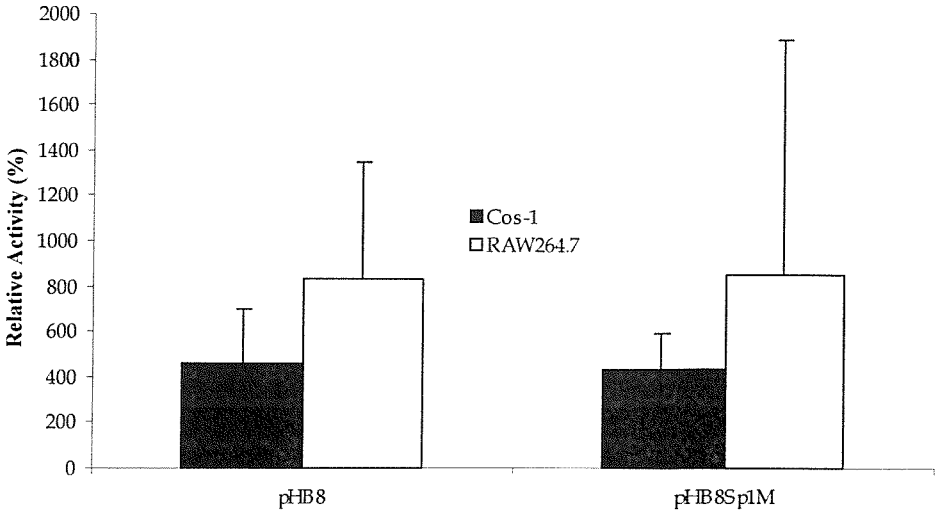
2000
1800
1600
1400
1200
1000
800
600
400
200
0
Relative Activity (%)
Cos-1
RAW264.7
pHB8
pHB8Sp1M

FIGURE 3.2.19 Comparison of *Slc11a1* Promoter Activity to LKCAT2 Activity in the Cos-1 and RAW 264.7 Cell Lines. Cells were transfected with 2μg of the *Slc11a1* promoter constructs as described (section 2.2.7). Expression of the reporter gene was detected by performing a CAT assay 37^0C; 6 hours on 50μg (RAW 264.7) and 37^0C; 2 hours 20μg (Cos-1) protein extract from each transfection. Total CAT conversion was calculated as CAT conversion/μg protein/hour for each sample and *Slc11a1* promoter activity calculated as a percentage of the activity of the β-actin promoter (LKCAT2) in both the Cos-1 (closed bars) and RAW 264.7 (open bars) cell lines. Activity of the promoter constructs within the Cos-1 cells was also calculated as a percentage of construct activity within the RAW 264.7 cells. The β-actin promoter is assumed to be equally active in both cell types. (A) Comparison of pHB4 & pHB4Sp1M activity between Cos-1 and RAW 264.7 cells. (B) Comparison of pHB6 & pHB6Sp1M activity between Cos-1 and RAW 264.7 cells. (C) Comparison of pHB8 & pHB8Sp1M activity between Cos-1 and RAW 264.7 cells.
n=2.

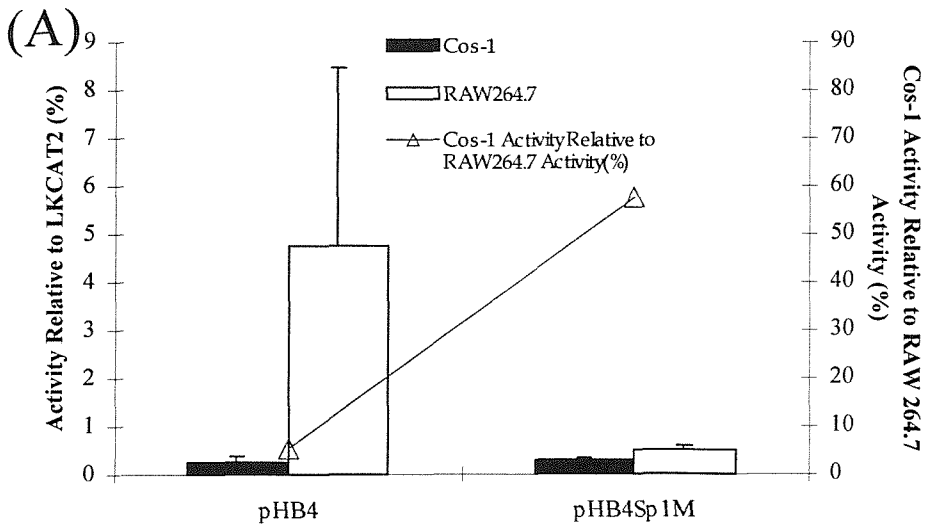
(A)
Cos-1
RAW264.7
Cos-1 Activity Relative to RAW264.7 Activity(%)
Activity Relative to LKCAT2 (%)
Cos-1 Activity Relative to RAW 264.7 Activity (%)
0
1
2
3
4
5
6
7
8
9
0
10
20
30
40
50
60
70
80
90
pHB4
pHB4Sp1M

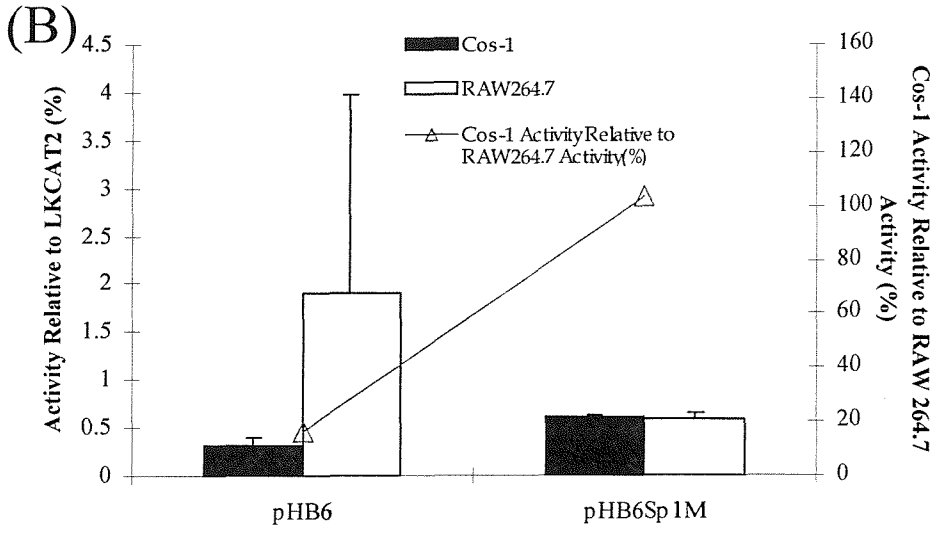
(B)
Cos-1
RAW264.7
Cos-1 Activity Relative to RAW264.7 Activity(%)
Activity Relative to LKCAT2 (%)
Cos-1 Activity Relative to RAW 264.7 Activity (%)
0
0.5
1
1.5
2
2.5
3
3.5
4
4.5
0
20
40
60
80
100
120
140
160
pHB6
pHB6Sp1M

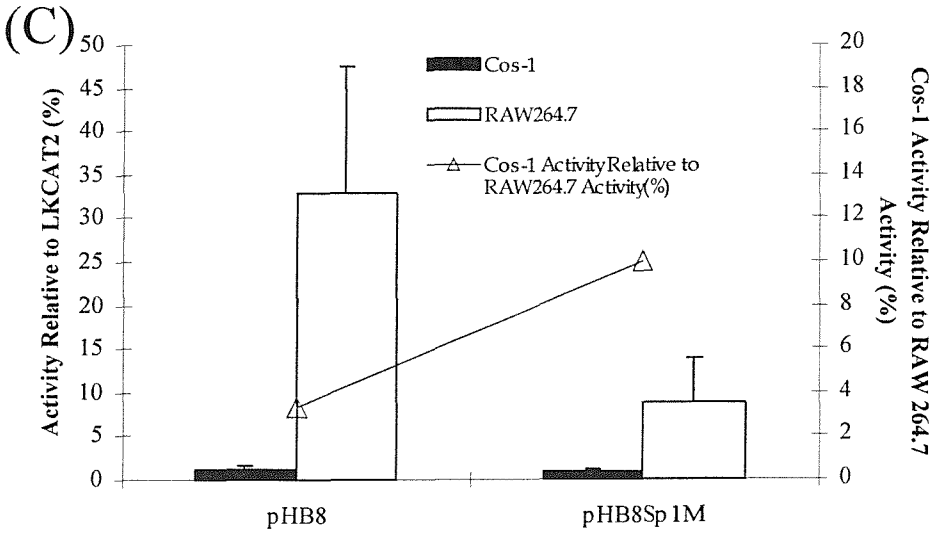
(C)
Cos-1
RAW264.7
Cos-1 Activity Relative to RAW264.7 Activity(%)
Activity Relative to LKCAT2 (%)
Cos-1 Activity Relative to RAW 264.7 Activity (%)
0
5
10
15
20
25
30
35
40
45
50
0
2
4
6
8
10
12
14
16
18
20
pHB8
pHB8Sp1M

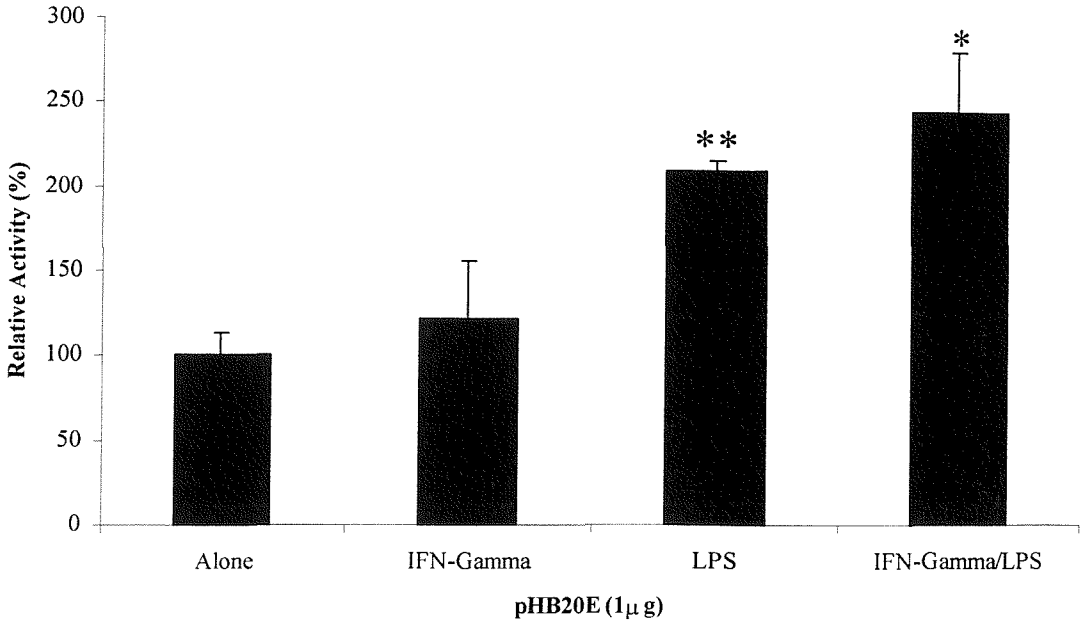

FIGURE 3.2.20 Upregulation of Slc11a1 Promoter Activity by the Proinflammatory Cytokines IFNγ and LPS in the RAW 264.7 Cell Line. RAW 264.7 Cells were transfected with 2μg of the *Slc11a1* promoter construct pHB20E as described (section 2.2.7) Cells were incubated for 24 hours before a 24 hour treatment with IFNγ (50U/ml), LPS (100ng/ml) or a combination of both, untreated pHB20E transfected cells were used as a control. Expression of the reporter gene was detected by performing a CAT assay (37^0C; 6 hours) on 50μg protein extract from each transfection. Promoter activity for each sample was calculated as a percentage of the average value obtained from the control (pHB20E Alone). *P=0.011 **P=0.0015

n=3 (2 for LPS treated)

3.3 DISCUSSION

The data presented in this chapter expand on the previous findings about the sequence and nature of the *Slc11a1* promoter. Previous work by Govoni *et al.* (1995) described the proximal region (-265bp to +180bp) of the *Slc11a1* promoter, mapping the major transcriptional start to two Inr elements lying at -7bp to -16bp and -5bp to +3bp, with a cluster of minor start site located around -50bp. A TATA-less promoter and multiple start sites are characteristic of genes displaying myeloid-specific expression (Clarke and Gordon, 1998). Govoni *et al.* (1995) also reported the presence of multiple transcription factor recognition sites associated with driving macrophage specific expression. Data within this chapter describe the isolation and characterisation of a promoter fragment spanning the -6197bp to +2408bp region of the *Slc11a1* gene. Computer assisted analysis of this region identified a large number of potential transcription factor binding sites associated with myeloid-specific expression, adding to and expanding on the number, and type of transcription factor binding sites previously described by Govoni *et al.* (1995), these data are summarised in figure 3.2.1. These data confirm on a transcriptional level the numerous studies looking at *Slc11a1* mRNA and protein expression (see section 1.1.5).

The promoter data and expression studies have established myeloid-specific expression of the *Slc11a1* gene *in vivo* and *in vitro*. However in our studies, comparison the 1.6Kbp *Slc11a1* promoter construct pHB4 with the strong *β-actin* promoter construct LKCAT2 in both the RAW 264.7 and Cos-1 cells lines suggests that there is a preferential expression in the RAW 264.7 cell line although this difference is not statistically significant. During these experiments it is assumed the *β-actin* promoter that is abundantly expressed in all non-muscle cells, drives equal expression in both cell lines used (Gunning *et al.* 1987). If activity were higher in the RAW 264.7 cell line, relative pHB4 activity would be less, thereby accounting for the apparent lack of myeloid specificity observed. A second explanation could be that 1.6Kbp region of the *Slc11a1* promoter was not enough to confer macrophage specificity. In gene transfer studies Govoni *et al.* (1996) achieved macrophage specific expression of the $Slc11a1^{G169}$ transgene using an expression construct containing a 5Kbp region of the *Slc11a1* promoter. Many of the identified

transcription factor binding sites proposed to drive myeloid specific expression are found within the region between -5Kbp and -1.6Kbp suggesting that this region may be essential in directing such expression. However throughout the deletion series activity of the *Slc11a1* promoter constructs within the Cos-1 cell line remain at a constant 4.56±1.1% compared with activity within the RAW 264.7 cell line (see figure 3.2.17-B). These data suggest that sequences between –6197 and –71bp are not the major determinant of the macrophage specific expression observed for the *Slc11a1* gene. Deletion of the region between –71 and –19bp increased the activity within the Cos-1 cell to 11% of the activity within the RAW 264.7 cell line, suggesting that sequences within this region are influencing the macrophage specific expression of the *Slc11a1* gene. Sequence analysis of the region between –71 and –19bp identified a consensus Sp1-binding site at –27bp. Sp1 sites have been reported to be essential for both Inr driven transcription (reviewed Smale, 1997) and myeloid specific gene expression (reviewed Clarke and Gordon, 1998; Black *et al.* 2001). Unexpectedly mutation of the consensus Sp1-binding site at –27bp did not significantly alter expression levels, however mutation did abolish the difference in relative expression levels between the Cos-1 and RAW 264.7 cells, thereby suggesting that the presence of an Sp1-binding site is important in driving the macrophage specific expression of the *Slc11a1* gene. A possible explanation of this is that different proteins within the two cell types occupy the Sp1-binding site. It has been suggested that Sp1 achieves tissue-specific expression through post-translational modifications such as phosphorylation, acetylation and glycosylation (reviewed Clarke and Gordon, 1998; Black *et al.* 2001). Therefore, in the macrophage-like cell line RAW 264.7 Sp1 maybe bound specifically by the modified Sp1 transcription factor, whereas in the Cos-1 cell line the same site maybe unoccupied or occupied by other members of the Sp1 family of transcription factors, such as Sp3 which can function as both an activator and repressor of transcription (reviewed Black *et al.* 2001). Considering this possibility, deletion of the Sp1-binding would lead to a decrease in promoter activity within the RAW 264.7 cells as any enhancement of activity induced by Sp1 binding is removed. Conversely in the Cos-1 cell line deletion of the Sp1-binding site would be predicted to either have no effect on activity as no factors are bound to this site, or lead to enhancement of activity as any repression induced as a result of negatively activity factors such as Sp3 would be removed. In support of this hypothesis, Sp1 has

been reported to bind in a myeloid-specific fashion *in vivo,* with Sp1 binding to the consensus Sp1-binding site in the *CD11b* promoter in myeloid cells but not in non-myeloid cervical carcinoma cells (Chen *et al.* 1993). Furthermore it was proposed that binding of a myeloid-specific factor such as PU.1 allows the binding of general transcription factors such as Sp1, thereby contributing to the myeloid-specific expression of target genes. It is therefore possible that PU.1 can discriminate between unmodified and modified Sp1, allowing only the latter to bind. Govoni *et al.* (1995) previously reported a PU.1 binding site at –170bp within the Slc11a1 promoter suggesting a similar model of activation for *Slc11a1.*

Despite this apparent lack of specificity a 0.105Kbp *Slc11a1* promoter construct, pHB20E, spanning -71bp to +34bp is responsive to LPS and IFNγ/LPS treatment but not to IFNγ treatment alone. IFNγ and LPS are pro-inflammatory cytokines that specifically induce macrophage activation pathways and responsiveness to these cytokines is therefore a mark of myeloid specific expression. Activation of *Slc11a1* expression induced by LPS and IFNγ/LPS treatment is however low compared to reported levels of stimulation (maximum of 16-fold; Govoni *et al.* 1997). One explanation for this could be the time course of our experiments, cell were treated for 24 hours before harvesting. Optimisation experiments (Govoni *et al.* 1997) revealed that LPS causes rapid induction of *Slc11a1* mRNA within 2 hours with levels peaking between 8-12 hours, declining thereafter. Furthermore it was shown that concomitant treatment with IFNγ and LPS did not increase levels above the maximum seen for LPS alone, with synergy only being seen when cells were "primed" with IFNγ for 24 hours before incubation with LPS for a further 8 hours. It would therefore be appropriate to test the *Slc11a1* promoter constructs for IFNγ and LPS responsiveness under the optimised conditions. However, computer assisted analysis of the -71bp to +34bp region of the *Slc11a1* promoter identifies no IFNγ or LPS responsive transcription factor binding sites. Responsiveness to IFNγ and LPS may therefore be a consequence of adding an enhancer element to the expression construct; it is therefore advisable to test the effects of IFNγ and LPS on both the enhancer-less pHB20 construct and the enhancer alone.

Deletion analysis of the *Slc11a1* promoter region revealed that substantial activity is maintained in a 53bp construct, pHB23, which contains only 19bp of the promoter confirming the findings of Govoni *et al.* (1995) that the two identified Inr elements constitute the major transcriptional start site. One striking feature of the deletion analysis is the significant increase in promoter activity induced by the deletion from -868bp to -71bp, constructs pHB6 to pHB8 respectively. One interpretation of this is that there is a repressor/silencer sequence within this region. Sequence analysis of this region indicates that 2 of the 6 non-canonical EMS sites lie within this region, EMS sequences are widely reported to mediate transactivation of target genes however, there are reports that EMS sequences can negatively regulate promoter activity. An EMS motif within the proximal *ATP-binding cassette transporter A1* (*ABCA1*) promoter has been shown to negatively regulate basal activity of the *ABCA1* gene (Yang *et al.* 2002), whereas a non-canonical EMS element suppresses the mitogen-induced expression of the fibroblast growth factor binding protein (Harris *et al.* 2000). In both cases mutation of the EMS resulted in increased promoter activity. Figure 3.2.16 shows that mutation of EMS #6 at position –127bp, but not EMS #5 at position –588bp, results in a 9.89±5.3-fold increase in promoter activity, resulting in an expression levels in the pHB4 derived construct pHB4M6M that is not-significantly different to pHB8. These data show that EMS #6 at –127bp is repressing the basal activity of the *Slc11a1* gene. How this EMS is affecting basal promoter activity is unclear however, in the case of the *ABCA1* promoter a complex of upstream factor (USF)-1, USF2 and fos related antigen (Fra)-2 were specifically bound to the EMS. USF-1 & -2 were both able to transactivate the *ABCA1* promoter whereas Fra-2 resulted in a downregulation of promoter expression, whether USF-1 &-2 and Fra-1 can regulate *Slc11a1* expression is the subject of ongoing research within our laboratory. Alternatively binding of c-Myc-Max heterodimers to EMS #6 maybe affecting promoter activity by preventing the assembly of the basal transcriptional machinery, possibly via an association with the myc-interacting zinc finger protein –1 (Miz-1).

A second interesting feature of the *Slc11a1* promoter construct deletion series was the 1.898±0.61-fold decrease in promoter activity that is observed by the deletion from pHB8 to pHB20. pHB8 and pHB20 comprise of the same 5' sequence however they

differ in their 3' region, with pHB20 being truncated by 66bp compared with pHB8. The basis for this decrease in promoter activity is not known however it is proposed that it is due to disruption or deletion of a conserved downstream promoter element (DPE). The DPE was first identified in the *Drosophila Antennapedia* P2 and *Jockey* promoters as a 7bp downstream analogue of the TATA-box (Burke *et al.* 1998). TFIID has been found bound to these elements and in conjugation with the Inr it is believed to mediate basal transcription from TATA-less promoters. In *Drosophila* the DPE is located at about +30bp relative to the transcriptional start site and conforms to the consensus $^{A}/_{G}G^{A}/_{T}CGTG$, in humans however the DPE does not have a good consensus (Burke *et al.* 1998). The basis of this proposal is that in *Dropsophila* the Inr sequences conform to a much more distinct consensus (Arkhipova 1995) than in mammals (Javahery *et al.* 1994). In the *Slc11a1* downstream promoter region there are no sequences that fit the *Drosophila* consensus but there are sequences that may fit to a looser consensus sequence such as Pu Pu $^{A}/_{T}$ Py Pu Py Pu. Assuming the presence of a DPE within the *Slc11a1* gene, the truncation from pHB8 to pHB20 may interrupt DPE function thereby reducing promoter activity.

CHAPTER 4

Repression of the *Slc11a1* Promoter by c-Myc

4.1 INTRODUCTION

Cellular Myelocytomatosis (c-Myc) has been the focus of much research since its initial identification in the early 1980's as being the cellular homologue of the transforming element in the oncogenic retrovirus MC29. c-Myc has subsequently been shown to be deregulated in a wide range of human cancers (reviewed Grandori *et al.* 2000) contributing to one seventh of cancer related deaths in the U.S (Dang. 1999). c-Myc is the best-studied member of a functionally redundant family that includes N-Myc, L-Myc and B-Myc (reviewed Nasi *et al.* 2001), all of which have the potential to induce oncogenesis. The *c-Myc* gene encodes 3 c-Myc proteins of 67kDa, 64kDa (Hann *et al.* 1988) and 45kDa (Spotts *et al.* 1997) respectively which are all produced by differential translational initiation at in-frame non-AUG and AUG-codons respectively. Under normal growth conditions the 64kDa protein is the predominant isoform, as cells reach confluence methionine deprivation results in transcriptional initiation from the non-AUG-codon and levels of the 67kDa protein rise dramatically (Hann *et al.* 1992). *c-Myc* encodes an immediate early gene that is absent in quiescent cells, but is strongly induced within 30 minutes of the addition of various mitogens. Furthermore, c-Myc expression is downregulated by a variety of compounds known to inhibit proliferation such as transforming growth factor-β (TGF-β) and interferon-γ (IFN-γ) (reviewed Nasi *et al.* 2001). It is widely accepted that the *c-Myc* gene is a key gene involved in promoting cellular growth and proliferation, terminal differentiation and apoptosis. Direct involvement of c-Myc in cellular growth and differentiation has been shown by gene knockout (Mateyak *et al.* 1997) and various over-expression studies (reviewed Grandori *et al.* 2000). c-Myc (and N-Myc) null fibroblast cell lines exhibit cell cycle times 3-fold slower than control cells with elongated G1 and G2 phases (Mateyak *et al.* 1997), whereas Myc null embryos are smaller, retarded in development, and show pathological abnormalities in various organs (Davies *et al.* 1993). Conversely expression of endogenous c-Myc in cultured fibroblasts promotes S-phase entry and shortens the G1 phase (Eilers *et al.* 1989), and can inhibit terminal differentiation in various cell types (reviewed Grandori *et al.* 2000), including myeloid cells (Larsson *et al.* 1988). c-Myc promotes cell growth by stimulating the expression of growth enhancing genes, such as those involved in cell cycle regulation, glucose metabolism and protein synthesis,

and by inhibiting expression of growth repressing genes, such as those involved in terminal differentiation (reviewed Classen and Hann 1999; Dang *et al.* 1999; Nasi *et al.* 2001). In order to influence gene expression c-Myc must heterodimerize with its cellular partner Myc-Associated factor-X (Max). Interactions between the bHLH/LZ domain of Max with the C-terminal bHLH/LZ domain of c-Myc produce a transcriptionally active heterodimer. The basic regions of c-Myc and Max diverge from the bundle of four helices to contact specific DNA sequences (Soucek *et al.* 1998) known as E-box Myc sites (EMS) (Blackwell *et al.* 1993) within the promoter region of target genes. The EMS consensus is 5'-CACGTG-3' however, c-Myc-Max heterodimers have also been shown to bind both *in vitro* and *in vivo* to non-canonical EMS sequences (5'-CANNTG-3') (Blackwell *et al.* 1993) such as those found in the *Slc11a1* promoter, 5'-CACATG-3', 5'-CACTTG-3' and 5'-CATGTG-3'. Transactivation of target genes is mediated via the N-terminal 143 amino acids, termed the transactivation domain (TAD). The TAD contains regions of high sequence conservation between Myc proteins termed Myc box (MB)-I and MBII (Atchley and Fitch 1995). Binding of the TRRAP protein to c-Myc via MBII (McMahon *et al.* 1998) leads to the recruitment of the histone acetyltransferase hGCN5 (McMahon *et al.* 2000) leading to local acetylation of histone H4 (Frank *et al.* 2001). Histone acetylation promotes transcriptional activation by decreasing inter-nucleosomal and nucleosomal DNA association, thereby increasing the accessibility of DNA to the basal transcriptional machinery and other positively acting cofactors. The mechanism of c-Myc regulation repression of gene transcription is however less well understood; although the binding sequences for repression have been mapped near the start site of transcription, and in many instances is thought to involve the Initiator (Inr) element. Inr elements are pyrimidine rich sequences at the start site of many TATA-less promoters and indicate the start site of transcription within these genes (Javahery *et al.* 1994). A limited number of Inr binding proteins have been identified including TFII-D, TFII-I, YY-1 (reviewed Smale 1997) and Miz-1 (Peukert *et al.* 1997). Binding of factors such as TFII-I to Inr elements is followed by sequential addition of the basal transcriptional machinery, providing a mechanism for initiation of transcription from TATA-less promoters. c-Myc can bind to, and form a complex with, TFII-I preventing further binding of basal transcriptional machinery, thereby preventing transcriptional activation from the Inr (reviewed Eisenman 2001). A similar mechanism of action has been observed between the novel Myc-interacting

zinc finger protein 1 (Miz-1) and c-Myc (Schneider *et al.* 1997; Peukert *et al.* 1997, Staller *et al.* 2001; Seoane *et al.* 2001).

In 1999 Wu *et al.* showed a direct, co-ordinated regulation of the iron controlling genes H-ferritin and Iron-regulatory protein (IRP) 2 by c-Myc. H-ferritin is the heavy subunit of the iron storage protein ferritin, whereas IRP2 binds to hairpin loop structures, termed iron-response elements (IRE), within the target mRNA. Binding to of IRP2 to IREs within the 5'UTR of ferritin mRNA and the 3'UTR of the transferrin receptor mRNA causes an increase in cellular iron levels by blocking translation and enhancing mRNA stability respectively. In a mechanism that was independent of c-Myc induced changes in cell-cycle activity, exogenous c-Myc could down-regulate H-ferritin RNA levels. Conversely but co-ordinately, exogenous c-Myc caused a five-fold increase in IRP2 gene-expression. These results indicated that c-Myc co-ordinately regulates genes controlling intracellular iron concentrations, resulting in increased iron levels required for c-Myc mediated cellular growth and proliferation. This was of interest, as results from our laboratory report that *Slc11a1*^{G169} expressing cell lines display both lower cytoplasmic iron levels (Atkinson and Barton 1998 & 1999; Barton *et al.* 1999; Baker *et al.* 2000), and reduced growth rates (Baker ST unpublished results), than their non-expressing, *Slc11a1*^{D169}, counterparts. The findings that both c-Myc and *Slc11a1* can regulate cellular growth rates and cytoplasmic iron levels, but in opposite directions, suggested a role for c-Myc in the regulation of *Slc11a1*.

This chapter reports a temporal link between cell growth, c-Myc expression and the onset of *Slc11a1* expression in primary bone marrow derived macrophages. Furthermore exogenous c-Myc expression within both the Cos-1 African green monkey kidney cell line and the RAW 264.7 murine leukaemic monocyte/macrophage cell line induces dose dependent repression of murine *Slc11a1* promoter expression. Deletion studies show that this repression is mediated via the Inr element and is independent of the EMS as has been shown for the other c-Myc repressed genes *C/EBPα* (Li *et al.* 1994), *AdMLP* (Li *et al.* 1994; Peukert *et al.* 1997), *Cyclin D* (Peukert *et al.* 1997), *Caveolin-1* (Park *et al.* 2001) and *p15*^{ink4b} (Staller *et al.* 2001).

4.2 RESULTS

4.2.1 *Slc11a1* Expression Correlates with the Onset of Differentiation in *Slc11a1*$^{G169/D169}$-expressing Primary Macrophages.

Bone marrow cells were prepared from MF1 *Slc11a1*$^{G169/D169}$-expressing mice, and placed in culture with granulocyte/macrophage colony-stimulating factors (GM-CSF) to induce differentiation into mature macrophages. On successive days (Days 1-6) samples were taken and analysed for Slc11a1 protein expression via western blotting using an antibody directed against the N-terminal region of the Slc11a1 protein (Atkinson and Barton, 1998) (figure 4.2.1-A). Immunoreactive Slc11a1 is detected on day 3 (figure 4.2.1-A; lane 3) after which levels increase until reaching a steady state at day 6 (figure 4.2.1-A; lane 6). Confirmation protein was loaded onto all tracks is provided by amido black staining the Immobilon membrane after immunodetection (figure 4.2.1-B). These results confirm Slc11a1 expression correlates with the onset of differentiation. Figure 4.2.1 is a representative experiment of n=3.

4.2.2 A Temporal Link between Cellular Growth and the Onset of Slc11a1 Expression in the N11 Cell Line[5]

Murine N11 macrophage cells were incubated in serum free medium for 24 hours to synchronise cells in the G0 phase and subsequently exposed to fresh medium containing 10% foetal bovine serum (FBS) to simultaneously stimulate cellular growth. Cell were harvested periodically after the addition of FBS (0, 8, 24, 32, 48 and 56 hours), and analysed for Slc11a1 protein expression via western blotting using an antibody directed against the N-terminal region as before (figure 4.2.2-A). Serum starvation decreased Slc11a1 protein levels, addition of FBS for 8 hours further decreased protein levels below the level of detection. Sustained exposure of the cells to FBS, 8 hours +, saw Slc11a1 protein levels returning back to basal levels. Confirmation protein was loaded onto all tracks is provided by amido black staining the Immobilon membrane after immunodetection (figure 4.2.2-B). These results

[5] These data were obtained and provided by Dr C Howard Barton.

suggest a negative link between the onset of DNA synthesis within proliferating cells and Slc11a1 protein expression. Figure 4.2.2 is a representative experiment of n=2.

4.2.3 A Temporal Link between Cellular growth, c-Myc Expression, and Slc11a1 Expression in Differentiating Bone Marrow Cells

Bone marrow cells were prepared from MF1 (4.2.3-B&C) or CBA (figure 4.2.3-A) *Slc11a1*^{G169} expressing mice, and placed in culture with GM-CSF to induce differentiation into mature macrophages. On successive days (Days 1-5/7) samples were taken for c-Myc and Slc11a1 western blotting (figures 4.2.3-B&C respectively) and cell numbers assessed by a colorimetric assay and DNA synthesis quantitated by BrdU incorporation (figure 4.2.3-A)[6]. c-Myc protein levels were maximal on days 1-2, when no Slc11a1 protein could be detected (figures 4.2.3-B&C, lanes 3-4). c-Myc degradation products start to appear on day 3, as does immunoreactive Slc11a1 (figures 4.2.3-B&C, lane 5). With the disappearance of full-length c-Myc immunoreactivity, there is a corresponding increase in detectable Slc11a1. Slc11a1 protein levels reach a steady state at days 6-7, immunoreactive c-Myc was not detectable at this time (figures 4.2.3-B&C, lanes 8-9). The growth and DNA synthesis over this time course are shown in figure 4.2.1-A in parallel cultures. Over 5 days in culture the number of cells, using the colorimetric assay, gradually increase however, there is a peak of DNA synthesis that precedes the appearance of Slc11a1 immunoreactivity. After the peak in DNA synthesis levels remain higher than at day 1. These data indicate that induction of *Slc11a1* occurs after the proliferative spurt when c-Myc levels are declining and the cells are displaying a more differentiated phenotype. Figure 4.2.3 is a representative experiment of n=3.

4.2.4 c-Myc Represses a 1.6Kbp Region of the *Slc11a1* Promoter in the Cos-1 Cell Line

The *Slc11a1* promoter construct pHB4 was transfected into the Cos-1 cell line using the LipofectAMINE (LA) reagent (see section 2.2.7). Cells were co-transfected with

[6] The cell number and DNA synthesis data used for figure 4.2.3-A were obtained and provided by Dr. Thelma E Biggs.

a constant amount (1μg) of the *Slc11a1* promoter construct pHB4 and increasing amounts of pEF-c-Myc DNA (c-Myc)[7] (0, 0.1, 0.2, 0.5, 1, 1.5 and 2μg), the DNA concentrations were normalised to 3μg using the pBABE empty vector. Cells were left for 48 hours before being assayed for CAT activity (see section 2.2.9). c-Myc causes a dose-dependent inhibition of pHB4 promoter activity (see figure 4.2.4-A), and all doses a c-Myc above 0.2μg induced a significant decrease in promoter activity ($P<0.05$). A 48.8±18.9% reduction in promoter activity was observed with 1μg of c-Myc. To determine that the inhibition observed by c-Myc titration was a specific effect, the experiment was repeated with a plasmid containing the CAT reporter gene under the control of the human *β-actin* promoter, LKCAT2. Figure 4.2.4-B shows there was a 23.67±5.71% and a 26.01±12.02% reduction in promoter activity following the addition of 0.5μg and 1μg c-Myc DNA respectively with increased DNA concentrations having no significant effect on *β-actin* promoter activity (LKCAT2). These results indicate the c-Myc induced dose dependent decrease in promoter activity is specific to *Slc11a1*, specifically the pHB4 promoter construct.

4.2.5 c-Myc Represses the *Slc11a1* Promoter in the RAW 264.7 Cell Line

To evaluate whether the *Slc11a1* promoter, specifically pHB4, was also subjected to inhibition by c-Myc in the macrophage derived RAW 264.7 cell line, the use of quantitative digital microscopy was evaluated. Two control experiments were performed firstly increasing amounts (0, 1, 2, 5, 10, 20μg) of peGFPN3 DNA (Clontech) were transfected into the RAW 264.7 cells by electroporation (see section 2.2.7). This experiment revealed a plasmid DNA dose dependent increase in fluorescence intensity (figure 4.2.5-A). A 2-log unit increase in fluorescence was observed between the transfection of 1μg and 20μg of peGFFN3 plasmid DNA. Next the stability of the eGFP fluorophore was examined. peGFPN3 transfected RAW 264.7 cells were exposed to a persistent light for 10 minutes and images captured at 30second intervals. Analysis of the fluorescent output revealed remarkable stability for 0-5 minutes, after which a 13.13±0.41% drop in fluorescent output was observed between 6-7 minutes, increasing to a 46.26±9.38% drop in fluorescent output between

[7] The pEF-c-Myc expression construct was kindly provided by Yongfeng Shang at the Dana-Farber Cancer Institute, Boston, USA.

9-10 minutes (figure 4.2.5-B). Together these experiments show the technique is suitable to quantitate reporter gene activity in transiently transfected cells.

A pHB4 related construct, with the promoter driving eGFP expression was prepared, (pHB15 (see section 3.2.2)), and transfected into the RAW 264.7 cells as before with a range of c-Myc doses. As with the experiments conducted in Cos-1 cells, increasing amounts of c-Myc induced a dose-dependent reduction in *Slc11a1* promoter, pHB15, activity ($P<0.01$) (figure 4.2.6-A&B). These results indicate that the inhibitory effects of c-Myc on *Slc11a1* expression are not restricted to the Cos-1 cell line, but are a feature of the *Slc11a1* promoter within its natural setting, a macrophage lineage cell.

Production of a 0.105Kb *Slc11a1* promoter fragment corresponding to the region -71bp to +34bp, attached to both an enhancer sequence and the CAT reporter gene, pHB20E (see section 3.2.2), has enabled confirmation of these findings using the more efficient LA method of gene transfer, and CAT reporter gene detection. c-Myc was again seen to induce a dose dependent reduction in promoter activity ($P<0.05$) (figure 4.2.7). 1μg of c-Myc induced a 70±19.1% inhibition of pHB20E activity.

4.2.6 c-Myc Repression is Maintained in a Reporter Construct Containing 19bp of the *Slc11a1* Promoter Sequence

c-Myc can both transactivate and transrepress target genes depending on the presence of, and context of, specific sequences within the promoter. The *Slc11a1* promoter contains 6 non-canonical EMS and 2 Inr elements, the target sequences of c-Myc transactivation and transrepression respectively. In order to determine where c-Myc was having its effects a deletion series of the *Slc11a1* promoter driving the CAT reporter gene was produced (see section 3.2.2). The *Slc11a1* promoter constructs were transfected into the Cos-1 cell line as before. Cells were co-transfected with a constant amount (1μg) of the *Slc11a1* promoter constructs (pHB4, pHB6, pHB8, pHB20 and pHB23) and increasing amounts of c-Myc DNA (0, 0.1, 0.5, 1 and 2μg), the DNA concentrations were normalised to 3μg using the pBABE empty vector. c-Myc induced a dose dependent decrease in promoter activity in all promoter constructs (figure 4.2.8-B), with 2μg c-Myc inducing a comparable level of repression

of the *Slc11a1* promoter constructs averaging 5.87±2.07-fold for all 5 constructs (figure 4.2.8-C). As expected pHB22 was inactive at the level of sensitivity used to measure the activity of the other constructs, furthermore its activity was not modulated by c-Myc (data not shown). These data suggest that c-Myc is repressing *Slc11a1* promoter activity through sequences contained within the region between -19bp and +34bp (pHB23). This 53bp region of the *Slc11a1* promoter contains both of the Inr elements but not any of the putative EMS sites, suggesting c-Myc is repressing *Slc11a1* expression via the Inr elements and the EMS sites are not involved in this repression. Grouping of the promoter constructs into those containing both EMS and Inr sites (pHB4 and pHB6), and those containing only Inr sites (pHB8, pHB20 and pHB23), shows c-Myc induces a significant repression of promoter activity in both groups $P<0.00025$ (Students T-test). Removal of the EMS sites has no effect on c-Myc induced repression at higher doses of c-Myc as the activity of the two groups after the addition of both 1 and 2μg c-Myc is not significantly different (see figure 4.2.8-D). However, small doses of c-Myc DNA, 0.1-0.2μg induced a small non-significant induction of pHB4 promoter activity, whereas larger doses. 0.5μg and above, induce a significant decrease in promoter activity, this dose dependent bi-phasic response was not observed with the smaller non-EMS containing constructs (figure 4.2.9-B). It can be concluded from the c-Myc co-transfection studies that in the Cos-1 cell line, c-Myc represses the *Slc11a1* promoter in a dose dependent fashion via a mechanism involving the Inr elements. However, at small doses of c-Myc this Inr mediated repression is antagonised by the presence of upstream EMS. These findings can be extended to include the RAW 264.7-macrophage cell line considering the c-Myc titration studies on pHB20E (figure 4.2.7), a promoter construct extending from -71bp to +34bp. Like pHB23, pHB20E contains both of the Inr elements but none of the putative EMS sites.

4.2.7 Differential Regulation of the *NCAM* Promoter by c-Myc.

The neural cell adhesion molecule (NCAM) is involved in cell-cell adhesion, it was therefore proposed that downregulation of NCAM could contribute to increased metastatic potential in neuroblastoma cells. Furthermore it was shown that N-Myc overexpression in the neuroblastoma cell line decreased both NCAM mRNA and

protein expression (Akeson and Bernards, 1990). Transcription from the NCAM promoter is mediated via an Inr element (Barton *et al.* 1990), and sequence analysis reveals that like the *Slc11a1* promoter, in addition to the Inr the *NCAM* promoter contains multiple non-canonical EMS sites (EMS#1 –930 to –935bp; EMS#2 –873 to –878bp; EMS#3 –180 to –185bp) and a single GC-box Sp1 binding site (figure 4.2.10-B). In light of the findings of Akeson and Bernards (1990) and the presence of both EMS and Inr elements it was asked whether c-Myc could repress *NCAM* promoter expression in transient transfection studies and whether repression was mediated via the EMS of the Inr element? The *NCAM* promoter constructs (Barton *et al.* 1990) were transfected into the Cos-1 cell line using the LipofectAMINE (LA) reagent (see section 2.2.7). Cells were co-transfected with a constant amount (1μg) of the *NCAM* promoter constructs NCAM1 and NCAM6 (figure 4.2.10-A) and increasing amounts of c-Myc DNA (0, 0.5, 1 and 2μg), the DNA concentrations were normalised to 3μg using the pBABE empty vector. Cells were left for 48 hours before being assayed for CAT activity (see section 2.2.9). c-Myc repressed NCAM1 promoter activity, this repression was maximal with 1μg of c-Myc DNA which induced a 72±13.86% decrease in activity. c-Myc was not able to repress the NCAM6 promoter construct, with a slight increase in promoter activity being observed (figure 4.2.11). NCAM1 contains both EMS and Inr elements, whereas NCAM6 contains only an Inr element (figure 4.2.10-A). These data therefore suggest that unlike *Slc11a1,* the repression of *NCAM* expression by c-Myc is mediated via a mechanism involving the EMS, however cooperation between the EMS and Inr element cannot be discounted.

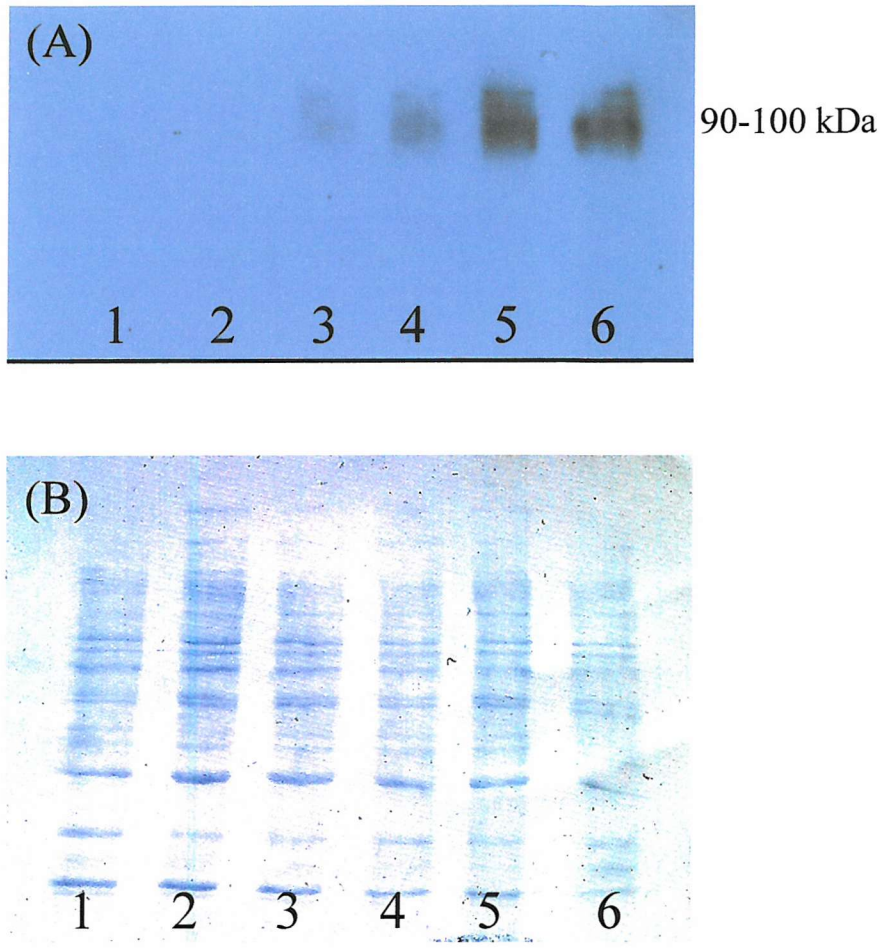

FIGURE 4.2.1 ***Slc11a1*** **Expression Correlates with the Onset of Differentiation in** ***Slc11a1***^{G169}**-expressing Primary Macrophages.** Primary bone marrow derived macrophages were obtained from the MF1 *Slc11a1*^{G169} expressing mice and cultured in media enriched with Granulocyte/Macrophage colony stimulating factors (GM-CSF). Samples were harvested on successive days (Days 1-6) for analysis by western blotting (As described sections 2.2.10-12) using antibodies specific to the N-terminal region (amino acids 1-82) of the Slc11a1 protein (Atkinson and Barton, 1998). (1), MFI day 1; (2), Day 2; (3), Day 3; (4), Day 4; (5), Day 5; (6), Day 6.

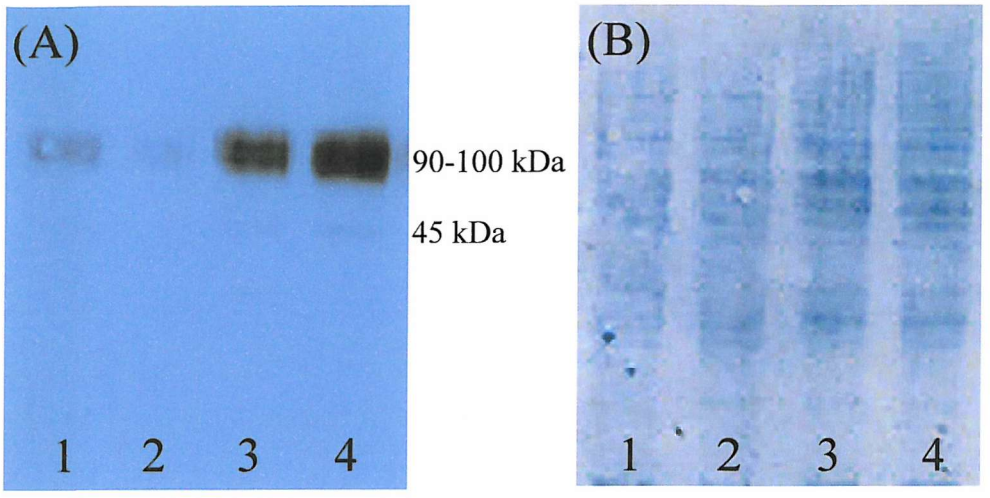

FIGURE 4.2.2 A Temporal Link Between Cellular Growth and *Slc11a1* Expression in the *Slc11a1*^{G169}-expressing Macrophage Cell Line N11. Cells were serum starved for 24 hours to synchronise growth, after which time cells were re-exposed to serum to simultaneously stimulate cellular growth. Samples were subsequently taken periodically after the addition of serum for analysis via western blotting as described (section 2.2.10-12). (A) Western blot using an antibody specific to the N-terminal region (amino acids 1-82) of the Slc11a1 protein (Atkinson and Barton, 1998). (B) Amido-black stained membrane. (1), 24 hours serum starved; (2), 8 hours + serum; (3), 24 hours + serum; (4), 32 hours + serum.

FIGURE 4.2.3 A Temporal Link Between Cell Growth and *c-Myc* Expression and the Onset of *Slc11a1* Expression. Primary bone marrow derived macrophages were obtained from *Slc11a1*^{G169} expressing mice ((A) CBA; (B) & (C) MF1) and cultured in media enriched with Granulocyte/Macrophage colony stimulating factors (GM-CSF). Samples were harvested on successive days (Days 1-7) for BrdU incorporation studies (A) and analysis by western blotting (B & C). MF1 primary macrophage samples were analysed by western blotting (as described sections 2.2.10-12) using (B) A commercial antibody directed against the C-terminal region of c-Myc (Santacruz) or (C) An antibody directed against an N-terminal region (amino acids 1-82) of the Slc11a1 protein (Atkinson and Barton, 1998) (1), Parental RAW 264.7 cells (*Slc11a1*^{D169}); (2), 37 RAW 264.7 engineered to express *Slc11a1*^{D169}; (3), MFI day 1; (4), Day 2; (5), Day 3; (6), Day 4; (7), Day 5; (8), Day 6; (9), Day 7.

(A)

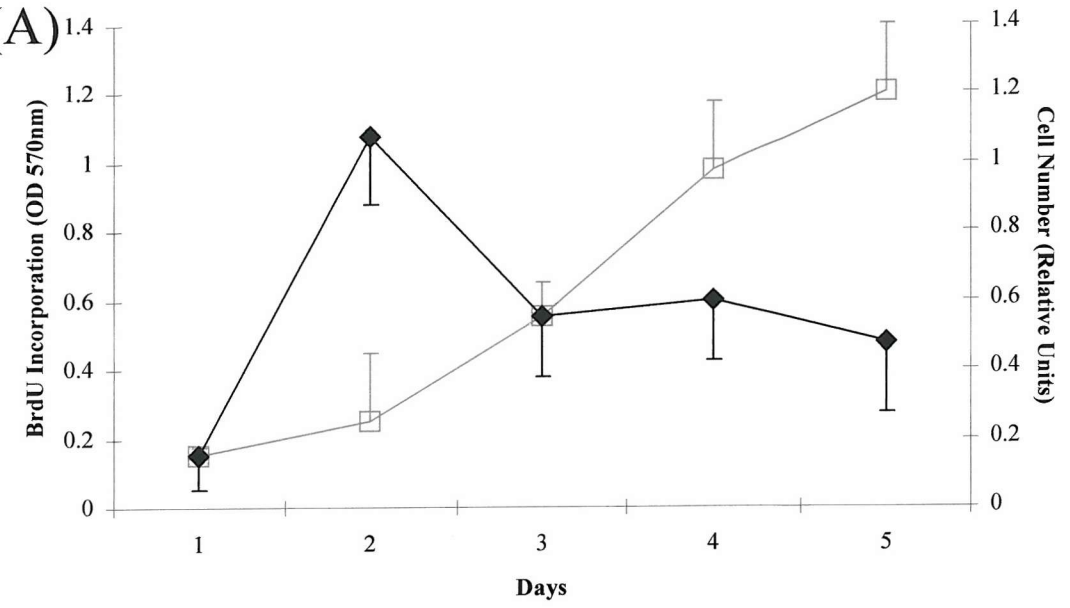

(B)

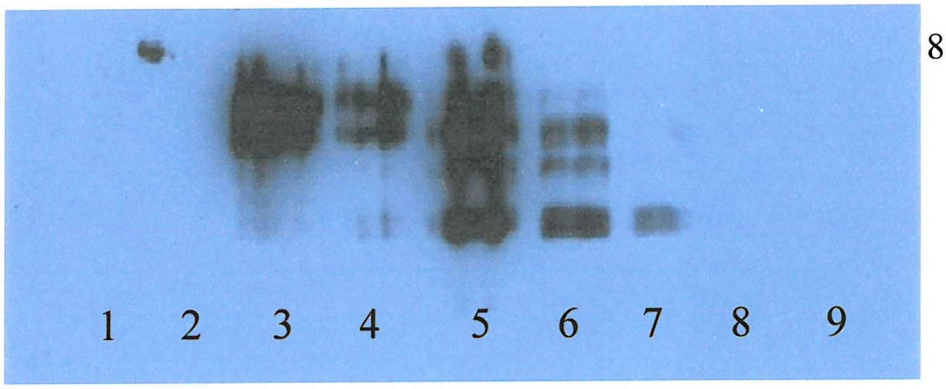

80 kDa

(C)

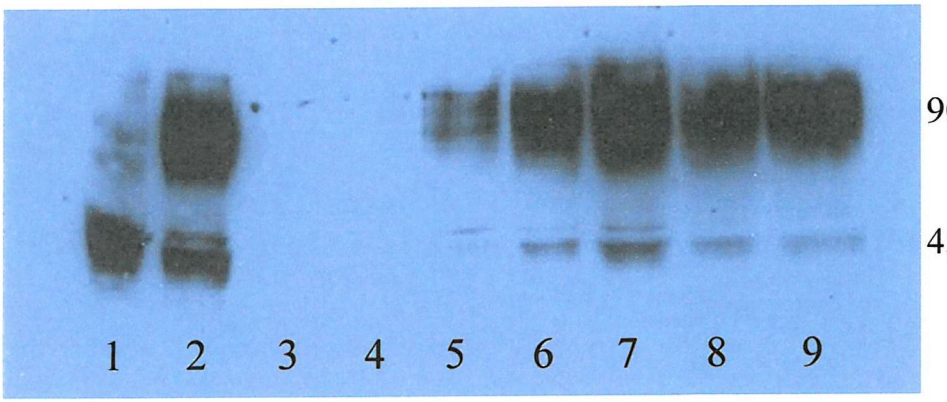

90-100 kDa

45 kDa

FIGURE 4.2.4 Repression of the *Slc11a1* Promoter Construct with c-Myc in the Cos-1 Cell Line. Cos-1 Cells were co-transfected using the LipofectAMINE (LA) reagent as described (section 2.2.7) with (A) 1μg of the *Slc11a1* promoter construct pHB4 and increasing amounts of c-Myc DNA (0, 0.1, 0.2, 0.5, 1, 1.5 and 2μg), (B) 1μg of the *β-actin* promoter construct LKCAT2 and increasing amounts of c-Myc DNA (0, 0.5, 1, 1.5 and 2μg), DNA concentrations were made up to 3μg with the pBABE empty vector. Expression of the reporter gene was detected by performing a CAT assay at 37^0C for 6 hours on 20μg protein extract (pHB4) and 37^0C for 1 hour on 1μg protein extract (LKCAT2). Promoter activity for each sample was calculated as a percentage of the average value obtained from the control (pHB4 & LKCAT2 Alone respectively). (A) Students T-Test compared with pHB4 alone *P=0.023 **P=0.012 ***P=0.0015 ****P=0.00021; n=10. (A) Students T-Test compared with LKCAT2 alone *P=0.03 **P=0.04; n=2 (3 for 1μg c-Myc DNA).

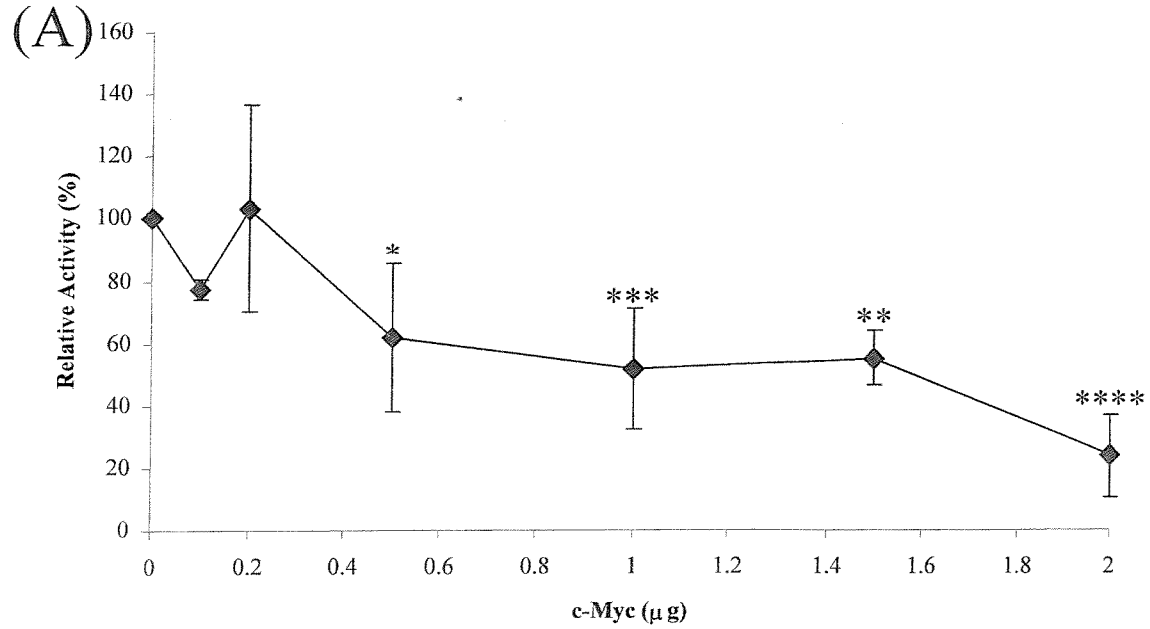
(A)
160
140
120
100
80
60
40
20
0
Relative Activity (%)
*
***
**
****
0
0.2
0.4
0.6
0.8
1
1.2
1.4
1.6
1.8
2
c-Myc (μg)

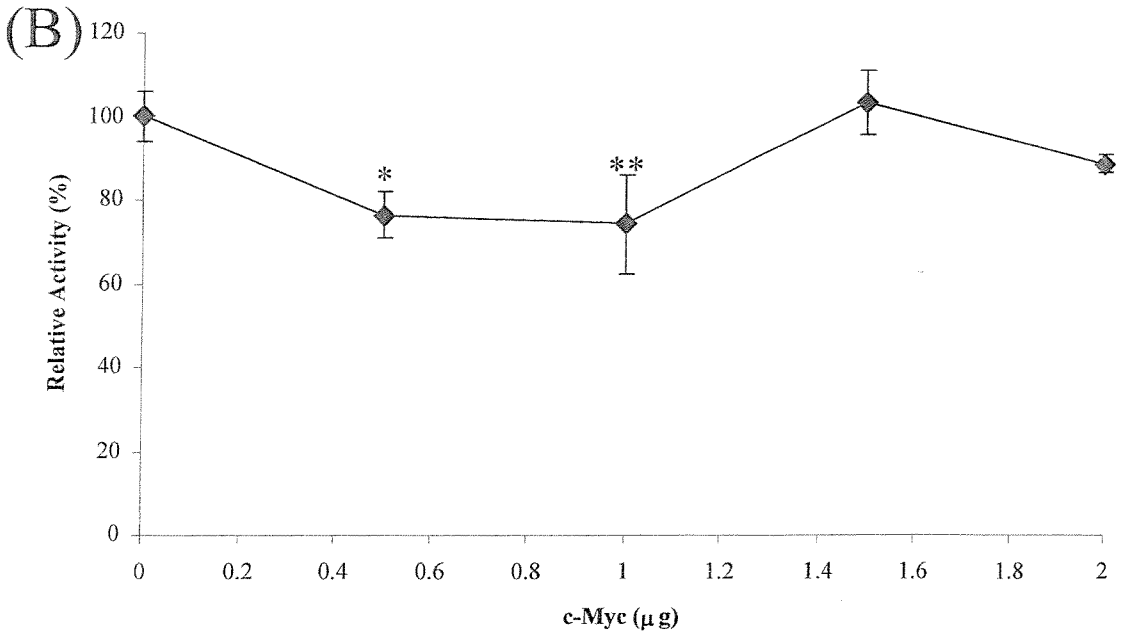
(B)
120
100
80
60
40
20
0
Relative Activity (%)
*
**
0
0.2
0.4
0.6
0.8
1
1.2
1.4
1.6
1.8
2
c-Myc (μg)

FIGURE 4.2.5 Assessing The Use Of Semi-Quantitative Digital Microscopy. RAW 264.7 Cells were transfected by electroporation as described (section 2.2.7) plated onto cover slips. After 48 hours reporter gene activity was measured using the Metamorph Imaging System. (A) Increasing amounts (0, 1, 2, 5, 10 and 20μg) of pN3GFP control vector were transfected to assess whether increasing amounts of reporter gene gave a linear increase in fluorescence intensity. (B) Cells transfected with 10μg pN3GFP control vector were subjected to constant fluorescent light for 10 minutes, images were captured at 30 second time points to determine the rate of degradation of the GFP fluorescence. . In all experiments DNA concentrations were made a constant 20μg with the pBABE empty vector.

(A)

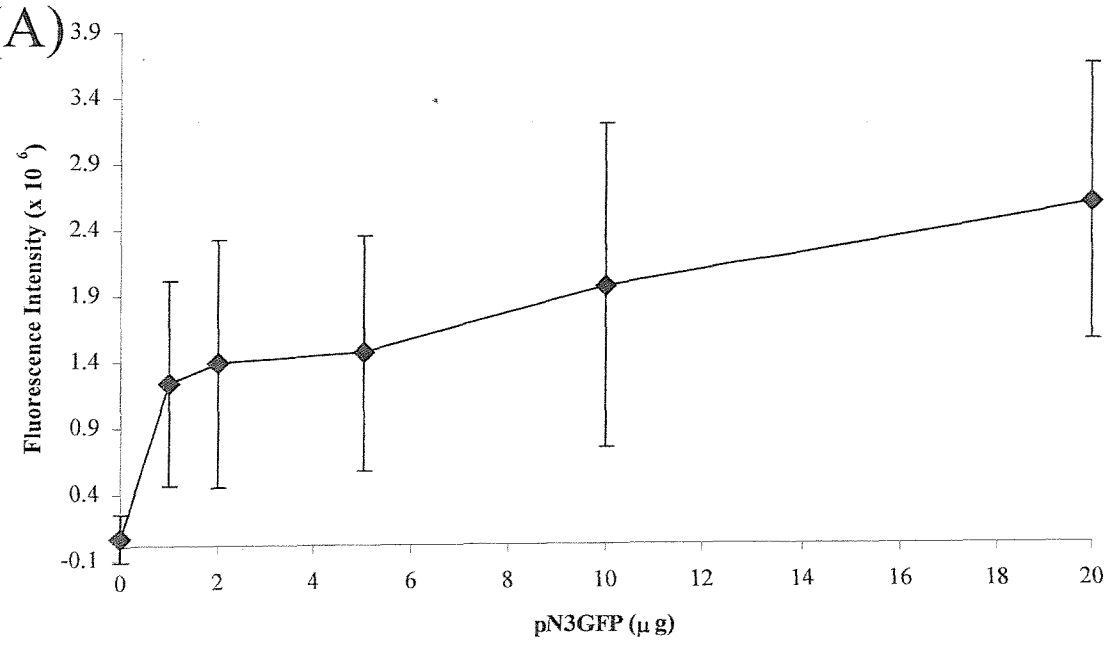
3.9
3.4
2.9
2.4
1.9
1.4
0.9
0.4
-0.1
Fluorescence Intensity (x 10 6)
0
2
4
6
8
10
12
14
16
18
20
pN3GFP (µg)

(B)

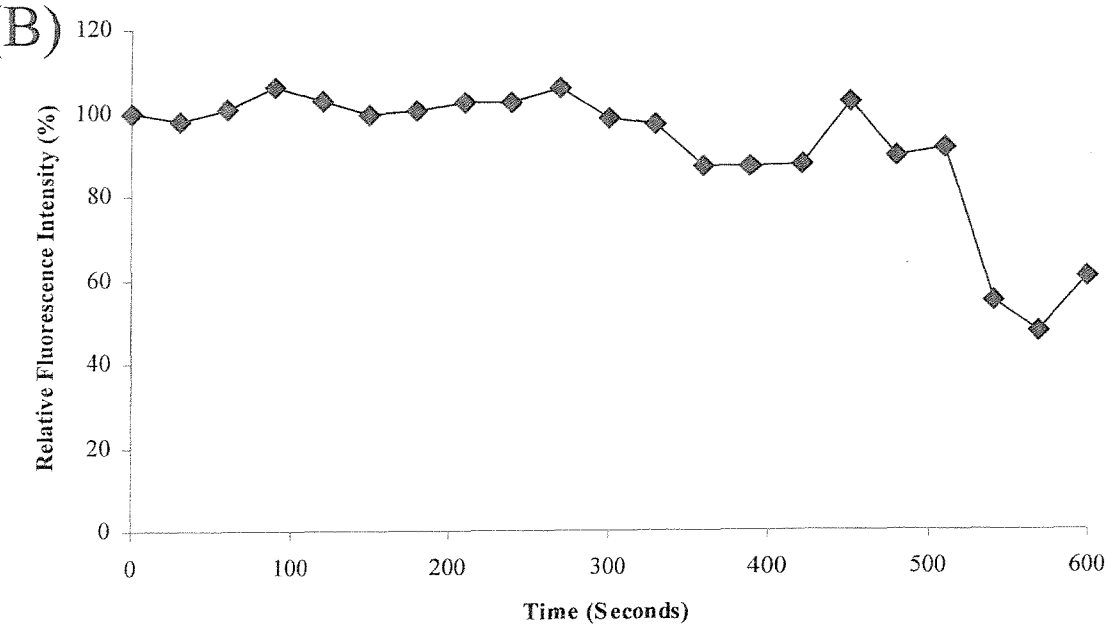
120
100
80
60
40
20
0
Relative Fluorescence Intensity (%)
0
100
200
300
400
500
600
Time (Seconds)

FIGURE 4.2.6 Repression Of The *Slc11a1* Promoter Construct pHB15 with c-Myc In The RAW 264.7 Cell Line. RAW 264.7 Cells were transfected by electroporation as described (section 2.2.7) plated onto cover slips. After 48 hours reporter gene activity was measured using the Metamorph Imaging System. (A) 10μg of the *Slc11a1* promoter construct was transfected either alone or in the presence of 10μg c-Myc DNA. Students T-Test ***P=0.00239. n= 15 (pHB15) and 13 (pHB15 + c-Myc). (B) 10μg of the *Slc11a1* promoter construct was co-transfected with increasing amounts of c-Myc DNA (0, 1, 2, 5, 10μg). Students T-Test *P=0.0085 **P=0.002 ***P=0.00019. n=13. In all experiments DNA concentrations were made a constant 20μg with the pBABE empty vector.

(A)

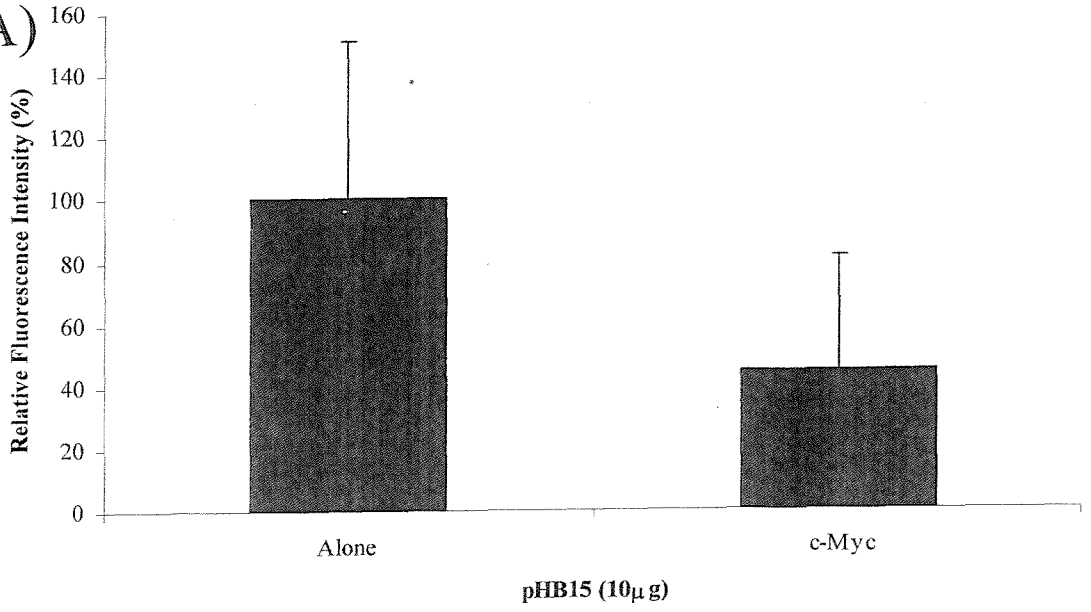
160
140
120
100
80
60
40
20
0
Relative Fluorescence Intensity (%)
Alone
c-Myc
pHB15 (10μg)

(B)

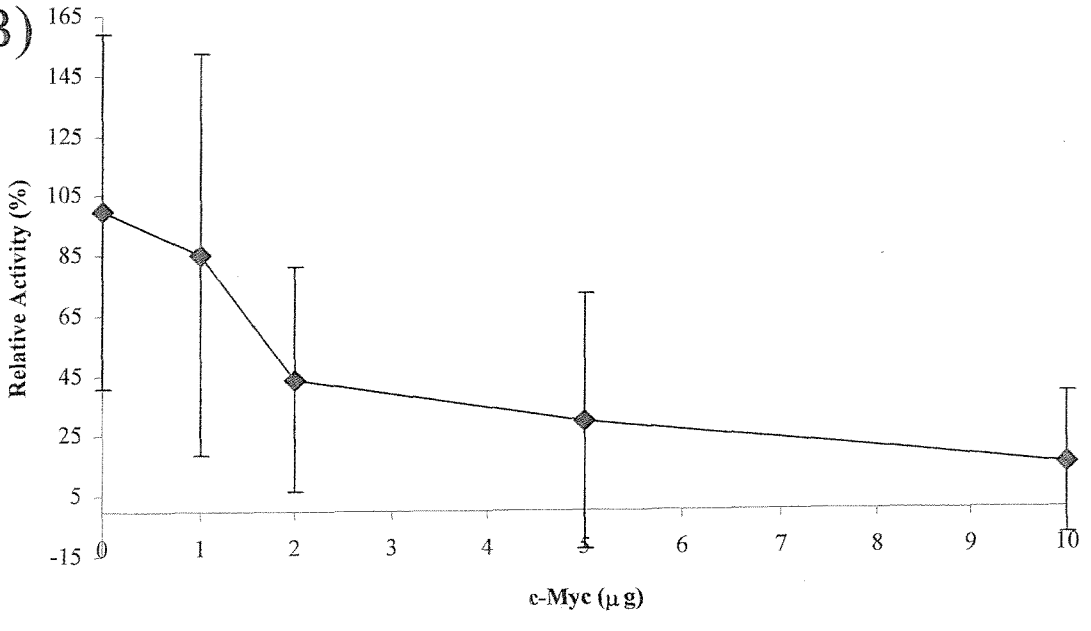
165
145
125
105
85
65
45
25
5
-15
Relative Activity (%)
0
1
2
3
4
5
6
7
8
9
10
c-Myc (μg)

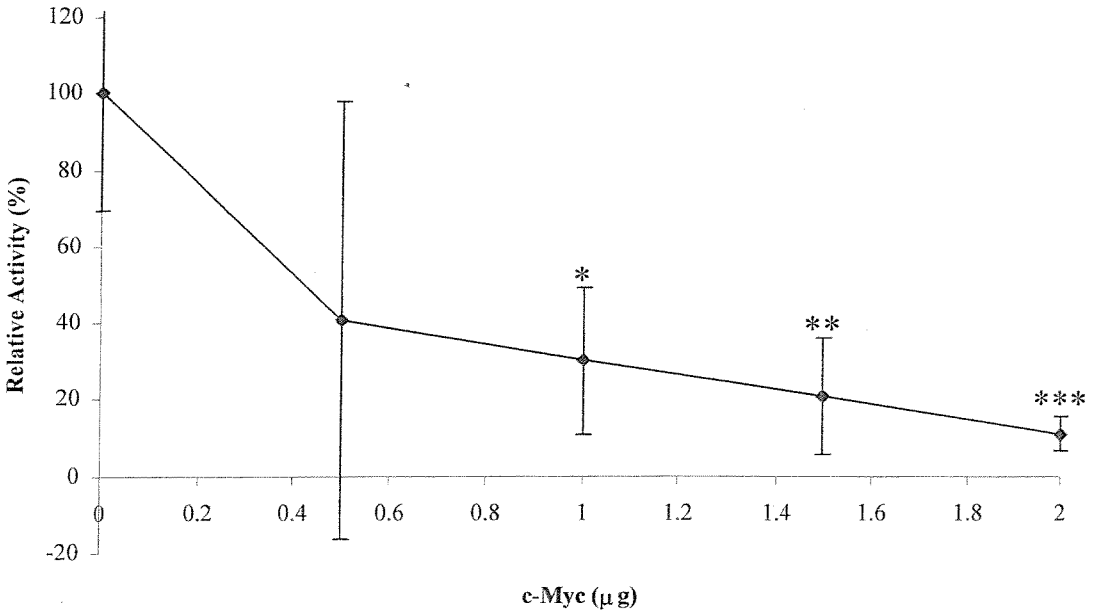

FIGURE 4.2.7 Repression of the *Slc11a1* Promoter Construct pHB20E with c-Myc in the RAW264.7 Cell Line. RAW 264.7 Cells were co-transfected using LA as described (section 2.2.7) with 1μg of the Slc11a1 promoter construct pHB20E and increasing amounts of c-Myc DNA (0, 0.5, 1, 1.5 and 2μg), DNA concentrations were made up to 3μg with the pBABE empty vector. Expression of the reporter gene was detected by performing a CAT assay (37^0C; 6 hours) on 50μg protein extract from each transfection. Promoter activity for each sample was calculated as a percentage of the average value obtained from the control (pHB20E Alone). Students T-Test compared with pHB20E alone *P=0.037 **P=0.03 ***P=0.035; n=3.

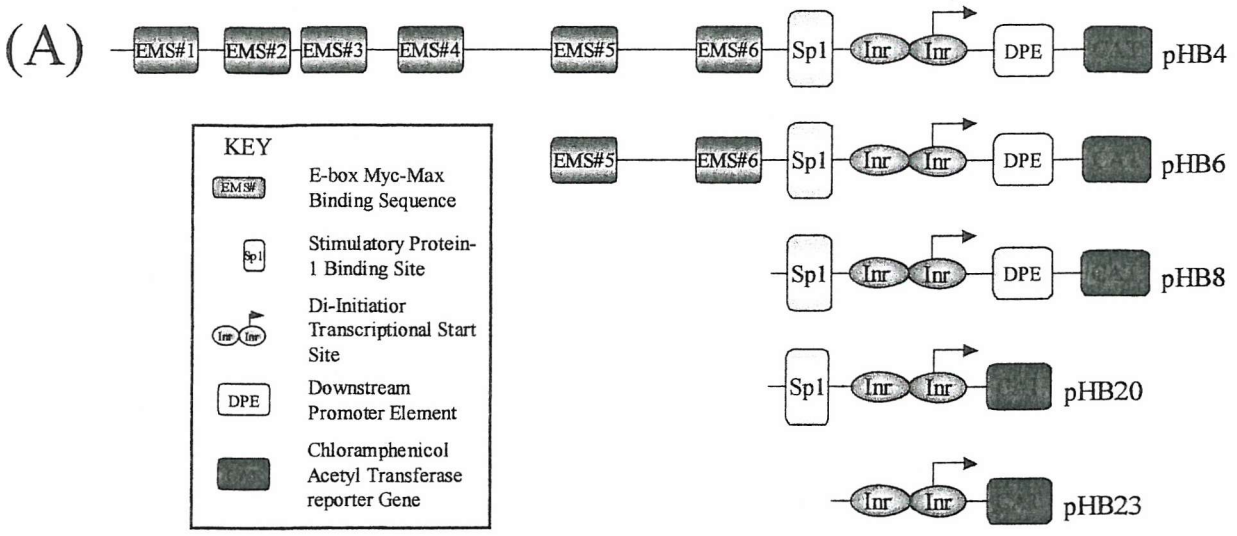

FIGURE 4.2.8 Repression of the *Slc11a1* Promoter Construct Deletion Series with c-Myc in the Cos-1 Cell Line. Cos-1 Cells were co-transfected using the LipofectAMINE (LA) reagent as described (section 2.2.7) with 1μg of the *Slc11a1* promoter constructs and increasing amounts of c-Myc DNA (0, 0.1, 0.5, 1 and 2μg), DNA concentrations were made up to 3μg with the pBABE empty vector. Expression of the reporter gene was detected by performing a CAT assay (37^0C; 2 hours) on 20μg protein extract from each transfection. Promoter activity for each sample was calculated as a percentage of the average value obtained from the control (*Slc11a1* promoter construct alone). (A) Illustration of the *Slc11a1* promoter constructs (see key). (B) c-Myc titration on the *Slc11a1* promoter construct deletion series. (C) Comparison of fold repression induced by 2μg c-Myc, grey bars represent relative activity compared to the promoter constructs alone, and fold repression is illustrated with a black line. (D) *The Slc11a1* promoter constructs were classified into two groups according to type of c-Myc binding site contained within the construct, either EMS + Inr containing (pHB4 and pHB6-black bars), or Inr containing (pHB8, pHB20 and pHB23-open bars). Students T-Test compared with Promoter activity without c-Myc *P<0.0005.

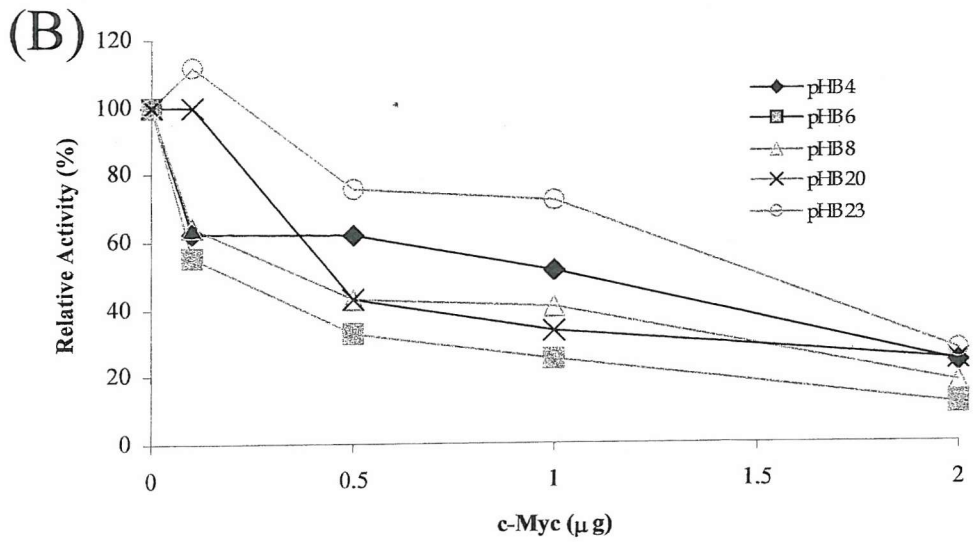
(B)
120
100
80
60
40
20
0
Relative Activity (%)
pHB4
pHB6
pHB8
pHB20
pHB23
0
0.5
1
1.5
2
c-Myc (μg)

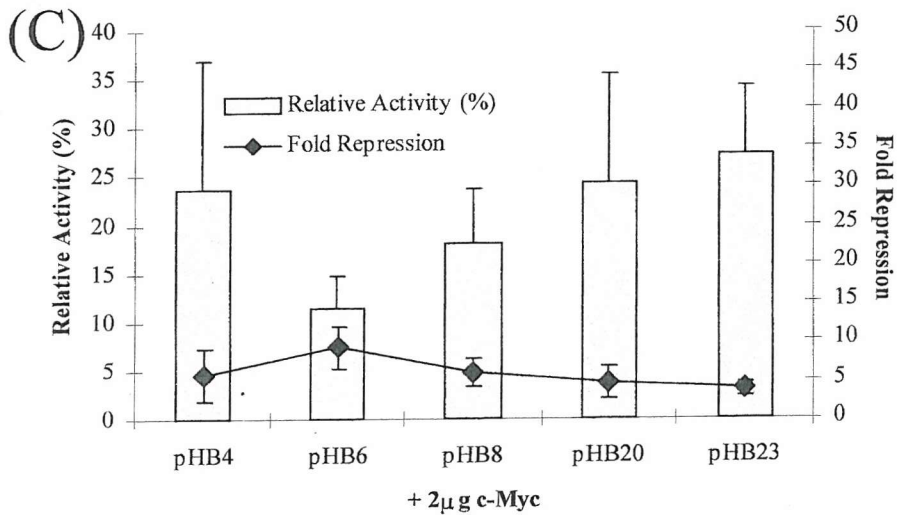
(C)
40
35
30
25
20
15
10
5
0
Relative Activity (%)
Relative Activity (%)
Fold Repression
50
45
40
35
30
25
20
15
10
5
0
Fold Repression
pHB4
pHB6
pHB8
pHB20
pHB23
+ 2μg c-Myc

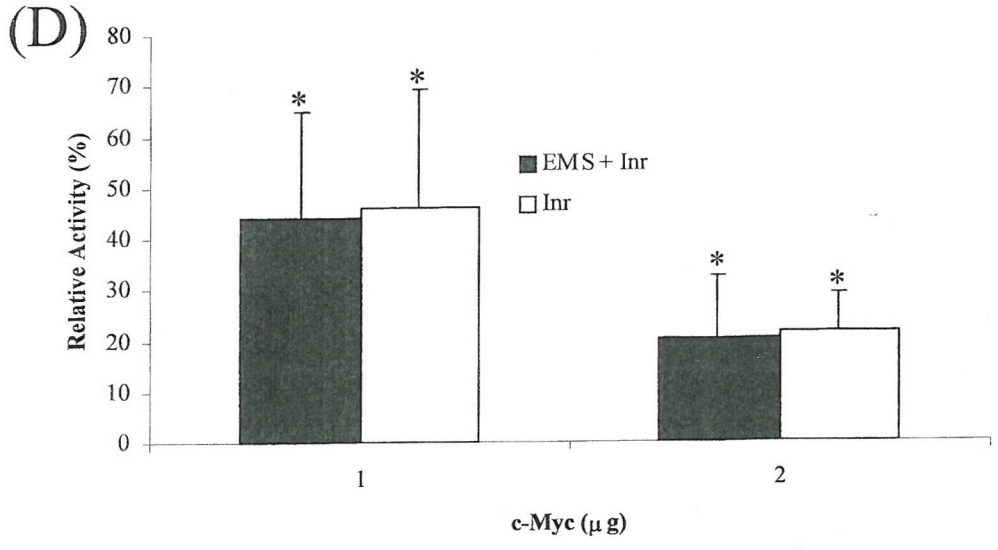
(D)
80
70
60
50
40
30
20
10
0
Relative Activity (%)
*
*
*
*
EMS + Inr
Inr
1
2
c-Myc (μg)

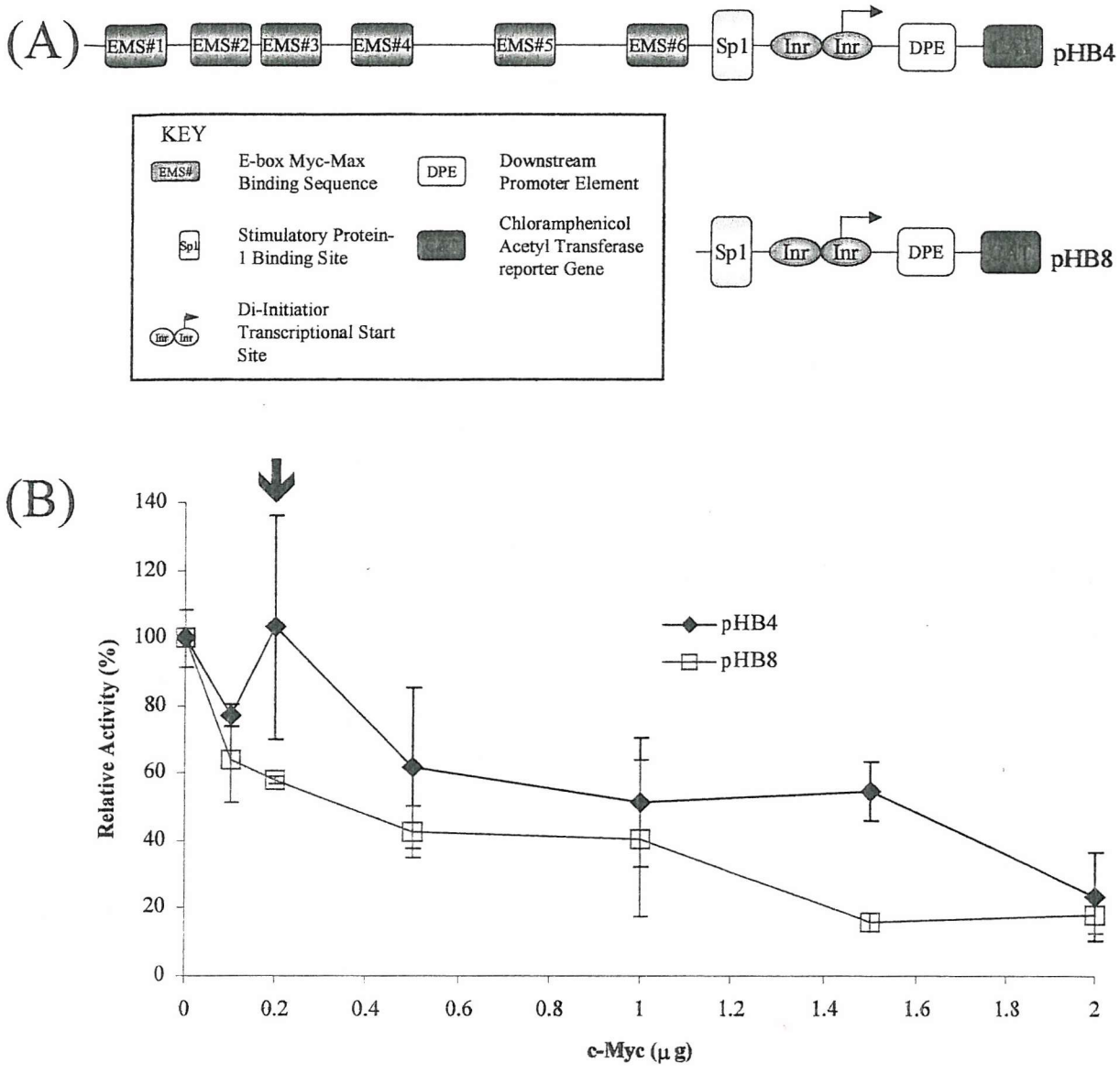

FIGURE 4.2.9 A Bi-phasic Response of the *Slc11a1* Promoter Construct pHB4 to c-Myc in the Cos-1 Cell Line. Cos-1 Cells were co-transfected using the LipofectAMINE (LA) reagent as described (section 2.2.7) with 1μg of the *Slc11a1* promoter constructs and increasing amounts of c-Myc DNA (0, 0.1, 0.2, 0.5, 1, 1.5 and 2μg), DNA concentrations were made up to 3μg with the pBABE empty vector. Expression of the reporter gene was detected by performing a CAT assay (37^0C; 2 hours) on 20μg protein extract from each transfection. Promoter activity for each sample was calculated as a percentage of the average value obtained from the control (*Slc11a1* promoter construct alone). (A) Illustration of the *Slc11a1* promoter constructs (see key). (B) c-Myc titration on the *Slc11a1* promoter constructs pHB4 & pHB8. Student T-test comparing with pHB8 Alone for all concentrations c-Myc $P<0.005$; $n=5$, for pHB4 values see figure 4.2.4.

FIGURE 4.2.10 Sequence of the 1.392Kbp *NCAM* Promoter Construct NCAM 1. (A) Illustration of the *NCAM* promoter constructs (see key). (B) Annotated sequence of the 1.392Kbp *NCAM* promoter sequence from the PstI site at position -1198bp to the ATG translational initiation site at +194bp. Transcription factor binding sites on the sense-strand have been indicated above the sequence. The initiator element (Inr) at and around position +1 are highlighted in bold with the major transcriptional initiation site being indicated with a big arrow  , the transcribed sequence is underlined. The translational initiation ATG codon at position +95 is indicated with an arrow  .

(A)

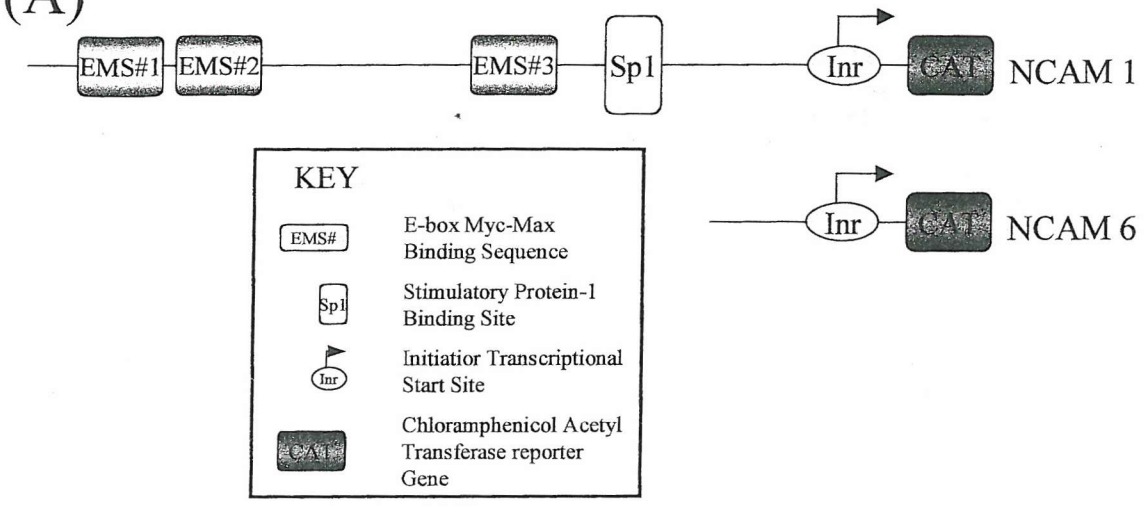

(B)

-1198

CTGCAGCCTGGGCGACAGAGCGAGGCTCCATCTCAAAAAAACAAAACAGAAACAAAACAAAACAAAACA
AAACAAAAAACCTGCTACAGGAGTGGGGAGGCCGACCTTTGAAGAAAAACGGAGTACCCGGTAACATTA
GTGCTTTAATGCCTTTGAACTTATGCAGACTTCCTCTGTTAGAGGGTTTCAGTGTTCTAGGCTAATGGG

-991 EMS #1

TTAACCTGACATCTAGAACACCTTTCTCACATTAGTTCCTTACATACCCAAGCCTT**CAGGTG**CTGAGAC

-922 EMS #2

ATGATTCTTTTCACCCCGCTTTCTCCACCCCCTACTTTTGAAAA**CACGGG**TGGAATTTTAATTAAAGCC
TATTGTGTTGGTACCTCAGTAATATTATACATTAATATCTTTAAGAATTAAGGTCACGTCCCCATGTAA
GAAAATATTATTTAATGACGCTTCTATATCATAATACCTATATAAAAGCCTGGCTATTTTAATAAAGAG
ACCACAGATTTCAGAATTTATAAACAGGAAAACATTTTCTTCGGGTTATTTCTGGAAATCTCTTCCAAA
CATCGGAGTTTTCTTCTAACTTAAGTCTCTTCCCACCTCCTTCCCAGGGGATCTGCTGAAGGGTGTTGT
ATGTCTCTCTGTGGGAGAGCAAACTTCACAGTTAGGATAAAACAAACAAACAAACAATATCCAAACAAC
ACCCAGGCCAACGGCAACCCCCATCCCTCTCCAAAGTTCTAATTTCCCGCACTTAAAGTCCTGGGCTAT
CCTTGTGTTGCAAGGATCTTAGAATCGAAATGGAGGGATTTGACAACTTTACCTAACCAAATCTAAAAT
TTTGCTTTTATTATTTACTAGTTATCAAAATATGCAAACTGCTGATTAAGGAAGGCTGGGTAGCAGGAG
CGCCTGCGAAGGCGTAGGGTAGAAGTGTGAAAAGAAATCCCAGCTCTCCCAGGGAGACTGCGTGTGAAA

-232 EMS #3

GAGCCCGGCTCCCCCAAAAGCTCCAGGCCGCGTTTTGCAGGCTTCCG**CATCTG**CCTCCCCTGTCTCTCT
TACCTCCTTGATGTTCGGCACTATTTGTGGCCGGCGTGGTGGAAGGACACAGTGAGGTTCTCACCC**CCG**

Sp1

CCCCCCGCTCCTCGCTCCCATCCCAGTTCCATCAAAACGAA***CCCGGG***CCAGCGCAAGGATCTCCGAGTT

-25 Inr

GCGAGTGTGCTGAGGCTGGGACTG**TCACTCATT**CTCCGATCAGCGCGTGAACCGAGCTCGGCTCGGCTG

+45

GCGAGAAACAATTCTGCAAAAATAATCATACTCAGCCTGGCAATTGTCTGCCCCTAGGTCTGTCGCTCA
GCCGCCGTCCACACTCGCTGCAGGGGGGGGGGCACAGAATTTACCGCGGCAAGAACATCCCTCCCAGCC

+183

AGCAGATTACA **ATG**

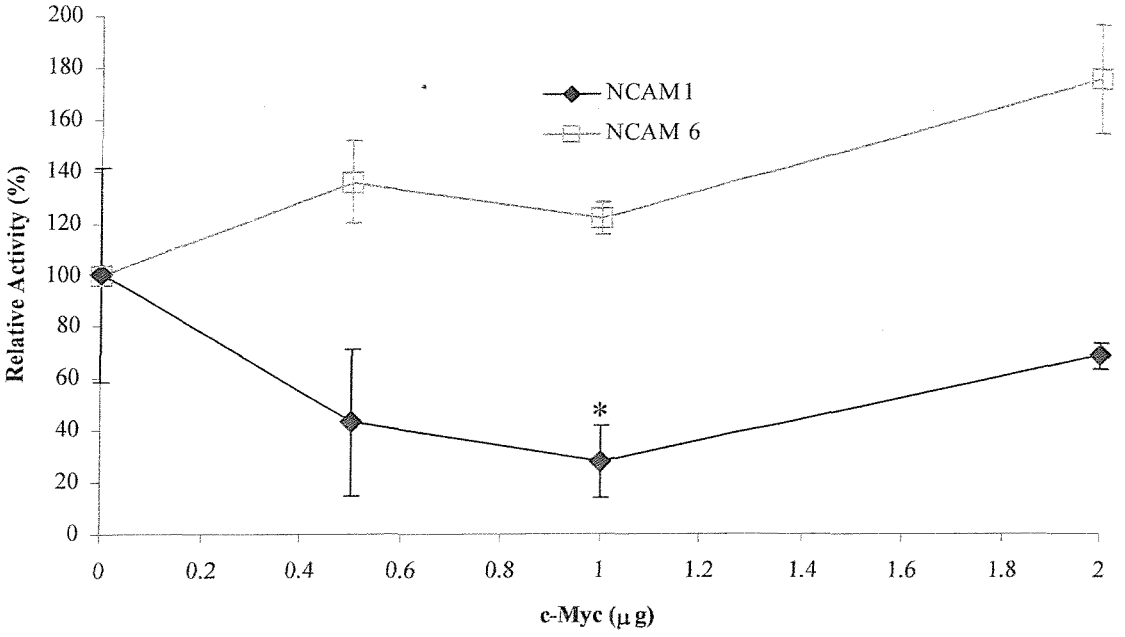

FIGURE 4.2.11 Differential Regulation of the *NCAM* Promoter Construct with c-Myc in the Cos-1 Cell Line. Cos-1 Cells were co-transfected using the LipofectAMINE (LA) reagent as described (section 2.2.7) with 1μg of the *NCAM* promoter constructs NCAM1 & NCAM6 and increasing amounts of c-Myc DNA (0, 0.5, 1 and 2μg), DNA concentrations were made up to 3μg with the pBABE empty vector. Expression of the reporter gene was detected by performing a CAT assay at 37^0C for 15 minutes on 0.1μg (NCAM1) and 10μg (NCAM6) protein extract from each transfection. Promoter activity for each sample was calculated as a percentage of the average value obtained from the control (NCAM1 & NCAM6 alone). Student T-test comparing NCAM1 & NCAM6 *P=0.036; n=2.

4.3 DISCUSSION

The data presented here outline a linkage between endogenous and exogenous *c-Myc* expression and *Slc11a1* expression in both primary cells and cell lines. Serum starvation of the N11 macrophage cell line for 24 hours, followed by the subsequent re-supplementation with 10% serum, correlates with a reduction in basal levels of the Slc11a1 protein, which is followed by a further decrease in protein levels between 0-8 hours of serum exposure. Slc11a1 protein expression returns to basal levels with prolonged exposure of serum (figure 4.2.2). Similar observations have been made for the c-Myc repressed *platelet derived growth factor-β receptor (pdgf-βR)* (Oster *et al.* 2000). Serum starvation of cells synchronises the cells by inducing growth arrest within the G1 phase of the cell cycle. Addition of essential growth factor containing serum stimulates the G1/S cell cycle progression via the activation of a transient (2 hours) increase in c-Myc expression. c-Myc contributes toward the G1/S cell cycle progression by activating transcription of the genes required for DNA synthesis. It is this transient increase in c-Myc expression that is thought responsible for the observed decrease in *Slc11a1* and *pdgf-βR* expression upon re-exposure to serum. Differential c-Myc and Slc11a1 expression are also observed within maturing BMM cells, and furthermore expression is seen to correlate with cellular growth (figure 4.2.1 & 4.2.3). Maximal cellular proliferation at day 2 decreases to a steady state level between days 3-5, a pattern mirrored by c-Myc expression levels. Conversely, Slc11a1 immunoreactivity appears on day 3 with steady state levels being achieved between days 4-7. These results suggest a temporal link between *Slc11a1* expression and endogenous *c-Myc* expression.

We also report that exogenous *c-Myc* expression is capable of repressing *Slc11a1* promoter driven reporter constructs. Deletion studies have shown that c-Myc-mediated repression is maintained in a reporter construct containing only 19bp of the *Slc11a1* promoter, pHB23 (figure 4.2.8-B). The data further go on to show that there is no significant difference between c-Myc-induced repression of *Slc11a1* promoter constructs containing both the EMS and Inr sequences, pHB4 and pHB6, and those containing only the Inr sequences, pHB8, pHB20 and pHB23 (figure 4.2.8-D). These data suggest that c-Myc is repressing *Slc11a1* expression via the initiator element as

has been noted for other c-Myc repressed genes including *Cyclin D* (Peukert *et al.* 1997), *AdMLP* (Li *et al.* 1994; Peukert *et al.* 1997) and *p15^{ink4b}* (Staller *et al.* 2001). The differential effect of exogenous *c-Myc* on the *Slc11a1, NCAM* (figure 4.2.11) and no effect on *β-actin* (figure 4.2.4-B) suggests that the effects of *c-Myc* on *Slc11a1* gene expression are specific (at the Inr) and not a consequence of *c-Myc* over-expression.

c-Myc repression of the *Slc11a1I* promoter construct pHB4, but not the smaller construct pHB8, was seen to induce a dose dependent bi-phasic response (figure 4.2.4 & 4.2.9). Small doses of c-Myc DNA, 0.1-0.2μg induced a small non-significant increase in promoter activity, whereas larger doses. 0.5μg and above, induce a significant decrease in promoter activity. Such a bi-phasic response has also been reported for the c-Myc-mediated repression of both the *AdMLP* (Li *et al.* 1994) and *Cyclin D* (Peukert *et al.* 1997) reporter constructs, like these reporter constructs, pHB4 contains both EMS and Inr sequences, pHB8 contains only Inr sequences. It was suggested that the presence of both these c-Myc recognition sequences may subject the promoter to both activation and repression signals from c-Myc (Li *et al.* 1994) and the data presented here are supportive of this proposal. However, we (data not shown), and others (Claassen and Hann, 2000) have also observed differential effects of c-Myc dependent upon the density of the cells prior to transfection and the method of transfection used. Furthermore, Claassen and Hann (2000) report higher endogenous c-Myc levels after transient transfection. A possible explanation for the differential effects of c-Myc at varying cell densities maybe a result of an altered ratio of the c-Myc isoforms. The *c-Myc* gene encodes two major translational products a 67kDa and a 64kDa protein termed c-Myc1 and c-Myc2 respectively (Hann *et al.* 1988). In proliferating cells c-Myc2 is the predominant isoform, as cells reach confluence methionine deprivation results in transcriptional initiation from the non-AUG-codon, and levels of the c-Myc1 protein rise 5-10-fold reaching levels comparable to that of c-Myc2 (Hann *et al.* 1992). The ratio of the two major c-Myc isoforms have also been reported to be affected in tumour cells, with an increase in the shorter c-Myc2 isoform being observed in neoplastic cells (Hann and Eisenmann, 1984), and disruption of the c-Myc1 isoform in Burkitt's Lymphoma (Hann *et al.* 1988). In addition it has been shown that the ratio of c-Myc isoforms can affect the

transactivating ability of c-Myc, with efficient transactivation of *E-cadherin* only being observed when both c-Myc isoforms are expressed. Furthermore expression of either isoform alone lead to repression of the *E-caherin* promoter driven reporter constructs (Batsche and Crémisi, 1999). The switch from transactivation to repression a high cellular densities may represent a protective mechanism whereby the downregulation of growth promoting genes prevents proliferation when conditions are not optimal and c-Myc1 but not c-Myc2 has been shown to inhibit cellular growth (Hann *et al.* 1994). Furthermore, c-Myc1 but not c-Myc2 can strongly transactivate the Rous Sarcoma virus long terminal repeat through C/EBP sequences within the EFII enhancer element (Hann *et al.* 1994). As the table in figure 3.2.1 shows there are multiple C/EBP binding sites within the *Slc11a1* promoter, it is therefore possible that when cells are transfected at a high density the altered ratio of c-Myc1:c-Myc2 results is transactivation mediated by c-Myc1 through C/EBP sequences. In order to elucidate the main factor influencing the bi-phasic response observed c-Myc titrations would have to be performed on the *Slc11a1* promoter construct deletion series with transfection being performed at a variety of cellular densities.

CHAPTER 5

Regulation of the *Slc11a1* Promoter by Miz-1

5.1 INTRODUCTION

Chapter 4 describes repression of the *Slc11a1* promoter by the proto-oncogene c-Myc. The DNA sequence responsible for the repression was mapped to a 19bp region of the *Slc11a1* promoter that includes 1 Inr element, 1 Inr-like element and consensus Sp1 binding site. Inr elements are pyrimidine rich sequences at the start site of many TATA-less promoters however, they can function synergistically with TATA-elements further enhancing transcription from these so called 'combinatorial' promoters. The mechanism of TATA-box directed transcription initiation has been well characterised (reviewed Smale, 1997; Dvir *et al.* 2001), however the mechanism for Inr mediated transcriptional initiation is less well understood (reviewed Smale, 1997). Whereas the TATA-box is recognised by the ubiquitous TATA-box binding protein (TBP), the Inr is recognised and bound by multiple proteins including TFII-D, TFII-I, YY-1, RNA Polymerase II (reviewed Smale, 1997), USF1&2 (Du *et al.* 1993), c-Myc (Roy *et al.* 1993) and Miz-1 (Peukert *et al.* 1997). How transcription is initiated is unclear but two potential mechanisms of action have been proposed (Javahery *et al.* 1994). The first model proposes that several distinct classes of Inr exist and that each class is recognised by a different protein, possibly in a spatially and temporally specific manner. The second proposal suggests a model similar to that observed for TATA-box dependent transcription, with a universal protein recognising the Inr-element and then specific Inr-binding proteins augmenting promoter strength in conjunction with this universal protein. The loose but consistent consensus of the Inr-elements tested (Javahery *et al.* 1994) is supportive of the latter proposal of a universal Inr binding protein. Of the Inr binding proteins identified to date both TFII-I (Roy *et al.* 1993) and Miz-1 (Peukert *et al.* 1997) interact with c-Myc, and repress target gene transcription.

Miz-1 was isolated as novel c- and N-Myc interacting protein when the C-terminal bHLH/LZ region of c-Myc was used as bait in a two-hybrid screen of a HeLa cDNA library (Schneider *et al.* 1997; Peukert *et al.* 1997). Analysis of the isolated clone revealed the encoded Miz-1 polypeptide to be highly conserved (92% amino acid identity between human and mouse) and ubiquitously expressed in mice. Sequence analysis of the isolated clone suggested the 803 amino acid polypeptide might

function as a transcription factor. Miz-1 contains 13 zinc fingers, 12 clustered and the 13th at the C-terminus of the protein, and N-terminal BTB/POZ (Broad-complex, Tramtrack, and Bric-a-brac/ poxvirus and zinc finger) and acidic activation domains. BTB/POZ domains are evolutionarily conserved sequences of approximately 120 amino acids in length, found at the extreme N-terminus of some C_2H_2-type zinc finger transcription factors, BTB/POZ domains promote protein-protein interactions (Bardwell and Treisman 1994; reviewed Collins *et al.* 2001). To influence gene expression transcription factors must first translocate to the nucleus, complex with DNA and/or members of the transcriptional initiation complex to promote or suppress transcription of the target gene. Miz-1 contains no functional nuclear localisation signal (NLS) suggesting a cytoplasmic localisation. Preliminary immunofluorescent studies showed Miz-1 within the cytoplasm and microtubule association (Peukert *et al.* 1997). Immunofluorescence and co-precipitation studies have confirmed this latter finding (Ziegelbauer *et al.* 2001). Results from our laboratory however suggest a nuclear expression of a Miz-1-GFP fusion protein within the Cos-1 cell line (Barton CH, unpublished results). How Miz-1 translocates to the nucleus is still unclear, however ectopic expression of either c-Myc or p300 could induce efficient import of the co-transfected Miz-1 into the nucleus (Peukert *et al.* 1997; Staller *et al.* 2001), as could drug induced (T113242) destabilisation of the microtubules (Ziegelbauer *et al.* 2001). Despite its apparent cytoplasmic localisation, Miz-1 antagonises the c-Myc-induced repression of selected Inr-containing promoter constructs (Schneider *et al.* 1997; Peukert *et al.* 1997; Staller *et al.* 2001; Seoane *et al.* 2001). Studies involving the AdML and cyclin D1 promoters suggest that the binding of c-Myc to Miz-1 induces a conformational change within Miz-1 thereby exposing latent BTB/POZ activity, resulting in the formation of insoluble subnuclear foci (Peukert *et al.* 1997). The findings that Miz-1 can itself cause transactivation of the c-Myc repressed genes *Cyclin D1* (Peukert *et al.* 1997), *p15^{ink4b}* (Staller *et al.* 2001; Seoane *et al.* 2001), *LDLR* (Ziegelbauer *et al.* 2001), *p21^{cip1}* (Herold *et al.* 2002; Seoane *et al.* 2002) and *Mad4* (Kime and Wright, 2002), and that Miz-1-c-Myc-Max trimers specifically bind to the Inr elements of target genes suggest an alternative mode of action, that c-Myc antagonises the function of Miz-1. The c-Myc interacting domain of Miz-1 overlaps both the TAD and the p300-binding domain of Miz-1 (Peukert *et al.* 1997). Binding of c-Myc to Miz-1 through a putative α-helix located between amino acids 638 and

715 obscures the TAD, inhibiting the recruitment of p300 and the subsequent binding of basal transcriptional machinery, thereby preventing transcription of the target gene. Similarities have been drawn between c-Myc and the adenovirus E1A oncoprotein (reviewed Claassen and Hann, 1999). E1A is known to bind to a p300 co-activator complex and prevent its activity, thereby repressing general transcription. It is possible that c-Myc represses target genes not only by blocking Miz-1 recruitment of p300, a potent cellular co-activator, to the site of transcriptional initiation, but also by simultaneously sequestering p300. However, such a broad, non-specific suppression of p300 by c-Myc does seem unlikely, as it would have profound effects on the cell.

p300 was identified as a protein targeted by the adenovirus E1A oncoprotein (Eckner *et al.* 1994), and was subsequently shown to interact with CREB binding protein (CBP). p300 and CBP are extremely large, 268kDa and 271kDa respectively, proteins of high sequence identity that can bind a large number of diverse transcription factors (reviewed Man Chan and Thangue, 2001; Vo and Goodman, 2001). The p300/CBP transcriptional co-activator proteins participate in co-ordinating and integrating the activities of hundreds of different transcription factors, thereby regulating many physiological processes including proliferation, differentiation and apoptosis. Despite the high sequence identity p300 and CBP are not redundant in their function. Subtle differences in expression during development, and the observations that null alleles produce a severe phenotype, indicate that although they have many overlapping functions they are not interchangeable (reviewed Man Chan and Thangue, 2001; Vo and Goodman, 2001; Blobel 2002). p300 is thought to perform 3 major roles in transcriptional regulation, histone (and transcription factor) acetylation, bridging promoter bound transcription factors, and acting as a scaffold for the assembly of multi-protein complexes, and at any one promoter p300 may perform all 3 or just selected roles (reviewed Man Chan and Thangue, 2001). However, the exact mechanism of p300 regulation is still to be determined, one of the complicating factors is that p300 has been reported to perform dual, antagonistic roles in the regulation of certain transcription factors. An example of this is the regulation of the pro-apoptotic factor p53 (reviewed Man Chan and Thangue, 2001). p300 can augment p53-dependent apoptosis and cell cycle arrest by promoting p53 complexes with stabilising proteins such as JMY and HIF1a. Conversely by promoting p53-MDM2 complex formation p300 promotes the

ubiquitin-mediated degradation of p53 protein, thereby diminishing the pro-apoptotic activity of p53. Owing to such diverse effects of p300 it has been proposed that p300 is a versatile transcriptional integrator, with the mechanism of action depending on both the pattern of transcription factor expression and the context of the target promoter. For example, transcriptional synergy between nuclear factors bound to the same regulatory region has been proposed to result in co-operative assembly of a multi-component complex (called an enhanceosome) in which multiple activation domains contribute to p300/CBP recruitment to the target gene (Merika *et al.* 1998).

The importance of Stimulatory protein-1 (Sp1) binding sites, adjacent to Inr-elements (Javahery *et al.* 1994; reviewed Smale, 1997), in directing lineage specific gene expression (Chen *et al.* 1993; Zhang *et al.* 1994; reviewed Tenen *et al.* 1997; reviewed Clarke and Gordon, 1998), is well documented. In light of this, and the ability of Sp1 to activate the *transforming growth factor-β (TGFβ)-1* and the *TGFβ-Receptor* genes in mammalian cells (reviewed Black *et al.* 2001), the Sp1 transcription factor has been proposed to be involved in c-Myc/Miz-1 mediated transcriptional regulation of the TGFβ responsive gene $p15^{ink4b}$ (Seoane *et al.* 2001). Sp1 was the first mammalian transcription factor to be cloned (Kadonaga et al., 1987), and has subsequently been found to be a member of the large Sp/Krüppel-like factor (KLF) family of C_2H_2-zinc finger containing transcription factors. Sp and KLF proteins preferentially bind to GC-boxes (5'-GGGCGG-3') and GT-boxes (5'-CACCC-3') respectively, but do have the ability to bind to basal transcriptional elements (reviewed Black *et al.* 2001). Sp/KLF proteins are associated with transcriptional activation however, a limited number of the family can act as both activators and repressors of transcription (see Black *et al.* 2001, Table 1), and as such it has become apparent that the mode of action of the Sp/KLF family of proteins is highly context dependent, an example of this is in directing the myeloid specific expression of target genes. Unlike the myeloid specific transcription factor PU.1, Sp1 is a highly expressed ubiquitous protein, so how it directs the myeloid specific expression of target genes is unclear. Sp1 binds specifically to the consensus Sp1 site in the CD11b promoter in myeloid cells, but not in non-myeloid cervical carcinoma cells. It is proposed that binding of the myeloid specific factor PU.1 causes a conformational change in chromatin structure enabling access to the Sp1 site only in

myeloid cells (Chen *et al.* 1993). Furthermore, posttranslational modifications alter the binding specificity of the Sp/KLF proteins (Clarke and Gordon, 1998). Sp1 proteins undergo extensive posttranslational modifications such as phosphorylation, and glycosylation (reviewed Black *et al.* 2001), and reports indicate that there is a higher ratio of phosphorylated Sp1 in myeloid cells compared to non-myeloid cells (Zhang *et al.* 1994). It was initially thought that Sp/KLF-binding sites were basal promoter elements involved in the expression of 'housekeeping genes', however it is now accepted that they perform multiple regulatory roles in controlling gene expression, dependent upon posttranslational modifications cell type and promoter context.

This chapter reports that Miz-1 can antagonise the repressive effects of c-Myc on the *Slc11a1* promoter; furthermore Miz-1 can transactivate the *Slc11a1* promoter constructs in a consensus Sp-1 binding site-dependent fashion, and this transactivation is antagonised by the presence of EMS sequences within the promoter or the addition of exogenous c-Myc. Miz-1 has been proposed to recruit p300 to the start site of transcription (Staller *et al.* 2001). We report here that exogenous p300 can transactivate the *Slc11a1* promoter in an EMS independent but a consensus Sp-1 binding site-dependent manner. The data reported here suggest that p300 may function to bridge Miz-1 with the consensus Sp-1 binding site bound protein, thereby enhancing transcription.

5.2 RESULTS

5.2.1 Miz-1 Relieves c-Myc Mediated Repression of the *Slc11a1* Promoter

Miz-1 causes cell growth arrest, antagonising the effect of c-Myc on cell growth and proliferation. Furthermore, Miz-1 transactivates c-Myc-repressed genes. In order to see if Miz-1 is a positive regulator of *Slc11a1* expression, the *Slc11a1* promoter construct pHB4 (1μg) was co-transfected increasing amounts (0, 0.1, 0.2, 0.5, 1, 1.5 and 2μg), of pCMV-Miz-1 (Miz-1)[7]. Miz-1 was unable to transactivate the *Slc11a1* promoter construct pHB4 at any of the given doses in the Cos-1 cell line (figure 5.2.1-A). However, co-transfection of both Myc (1μg) and Miz-1 (1μg) with pHB4 (1μg) revealed that Miz-1 could overcome the c-Myc induced repression of *Slc11a1* expression (figure 5.2.1-B). 1μg of the pHB4 *Slc11a1* promoter construct was transfected into the Cos-1 cell line either alone or with 1μg Myc, 1μg of c-Myc and 1μg of Max, 1μg of c-Myc and 1μg of pCMV-Miz-1ΔPOZ[7], 1μg of c-Myc and 1μg of Miz-1, or 1μg Miz-1, DNA concentrations were made up to 3μg using the pBABE empty vector. 1μg of c-Myc induced a significant (P=0.0015 Students T-test) 2.45±1.59 fold repression of promoter activity, co-transfection of 1μg Max further decreased promoter activity inducing a significant (P=0.0.33 Students T-test) 6.21±3.26 fold reduction in activity. Co-transfection of 1μg Miz-1, but not the Miz-1ΔPOZ mutant, restored promoter activity back to control levels (pHB4 alone); the resultant activity was significantly different from the addition of c-Myc alone (P=0.036). It can be concluded from the Miz-1 co-transfection studies in the Cos-1 cell line, although Miz-1 is unable to transactivate a 1.6Kbp *Slc11a1* promoter construct, addition of Miz-1 can relieve a c-Myc mediated repression of *Slc11a1* activity.

5.2.2 Miz-1 can Transactivate *Slc11a1* Promoter Constructs Devoid of EMS

Reviewing the literature published on Miz-1 transactivation (Peukert *et al.* 1997) revealed that the studies had been performed on promoter constructs starting

[7] The pCMV-Miz-1 & pCMV-Miz-1ΔPOZ expression vectors were a kind gift from Frank Hänel at the Hans-Knöll Institute, Germany.

downstream of the documented EMS. In order to elucidate whether the presence of EMS within the promoter constructs was affecting Miz-1 induced transactivation, responsiveness to Miz-1 was compared between two *Slc11a1* promoter constructs pHB4 and pHB20 which differ in the number of EMS within the sequence, 6 and 0 respectively. Co-transfection with the *Slc11a1* promoter constructs pHB4 and pHB20 with increasing amounts of Miz-1 (0, 0.5, 1, 1.5 and 2μg) shows differential regulation of the two promoter constructs by Miz-1 in the Cos-1 cell line (figure 5.2.2-B). Responsiveness of pHB4 and pHB20 to 1 and 1.5μg Miz-1 were significantly different, P=0.04 and P=0.036 respectively. Figure 5.2.2-C shows that co-transfection of the *Slc11a1* promoter construct pHB20 with 0.1 and 0.2μg of Miz-1 induces a significant (P<0.05) 9.6±5.36 and 9.6±4.5-fold induction in promoter activity respectively. Increasing Miz-1 concentration still significantly transactivates the *Slc11a1* promoter construct pHB20 (P≤0.025) but to a lesser extent, 4.37±0.39, 2.98±0.52 and 2.5±0.19 for 0.5, 1 and 1.5μg Miz-1 respectively. These data suggest that the presence of EMS within the promoter can affect responsiveness to Miz-1.

5.2.3 Responsiveness to Miz-1 is Inversely Proportional to the Number of EMS

In order to assess whether the effect of EMS responsiveness was due to a specific EMS or whether the effect was a result of cooperation between EMS, Miz-1 responsiveness was compared between *Slc11a1* promoter constructs containing differing numbers of EMS sites. Co-transfection of the *Slc11a1* promoter constructs pHB4, pHB6, pHB6M5M, pHB6M6M and pHB20, which differ in the number of EMS (figure 5.2.3-A&D), with 0, 0.1 and 0.2μg Miz-1 illustrates that Miz-1 responsiveness is inversely proportional to the number of EMS sites within the promoter construct (figure 5.2.3-B&C). Figure 5.2.3-C does suggest that EMS#6 plays a bigger role in influencing responsiveness to 0.2μg Miz-1 as mutation of this site (pHB6M6M) induces a promoter activity that is significantly different from pHB6M6M alone (P=0.031), whereas mutation of EMS#5 (pHB6M5M) does not. These data suggest that factors binding to the EMS sites within the *Slc11a1* promoter interfere with Miz-1 responsiveness.

5.2.4 The Microtubule Destabilising Compound, Nocodazole, Increases both Transcription and Protein Expression of *Slc11a1* in the RAW 264.7 and N11 Macrophage-like Cell Lines Respectively

Miz-1 does not contain a functional NLS (Peukert *et al.* 1997) and is reported to localise to the cytoplasm where it is associates with microtubules (Peukert *et al.* 1997; Ziegelbauer *et al.* 2001). Association of Miz-1 with either c-Myc or p300 has been shown to induce nuclear import (Peukert *et al.* 1997), as has microtubule destabilisation (Ziegelbauer *et al.* 2001). Furthermore microtubule destabilisation led to a Miz-1 dependent transactivation of the *low-density lipoprotein receptor* and α_2-*integrin* genes (Ziegelbauer *et al.* 2001). As Miz-1 has the ability to transactivate the *Slc11a1* promoter (figure 5.2.2), the involvement of microtubule destabilisation in *Slc11a1* gene regulation was assessed. RAW 264.7 cells were transfected with the *Slc11a1* promoter construct pHB4 for 24 hours before treatment for a further 24 hours with the microtubule stabilising compound taxol, and the microtubule destabilising compound nocodazole. 1μM nocodazole led to a significant (P=0.01) ≈15-fold increase in promoter activity (figure 5.2.4-A), the same nocodazole concentration led to an ≈5.6-fold increase in protein expression in the N11 cell line (figure 5.2.4-B, lane 10 & 5.2.4-D). The microtubule stabilising compound taxol had no significant effect on either *Slc11a1* transcription or protein expression in either the RAW 264.7 or the N11 cell lines. These data suggest that in macrophage-like cell lines, the microtubule destabilising compound nocodazole can increase both *Slc11a1* mRNA and protein levels. Figure 5.2.4-B&C is a representative experiment of n=3.

5.2.5 The Microtubule Stabilising Compound and LPS Mimetic, Taxol, Upregulates Slc11a1 Protein Expression in Primary Bone Marrow Derived Macrophages

Bone marrow cells prepared from MF1 *Slc11a1*^{G169} expressing mice were treated for 24 hours with 10μM taxol and 1μM nocodazole. After this time samples were analysed for Slc11a1 protein expression via western blotting using an antibody directed against the N-terminal region of the Slc11a1 protein (Atkinson and Barton, 1998) (figure 5.2.5-A). Immunoreactive Slc11a1 is detected in all samples however, the microtubule stabilising compound and LPS mimetic, taxol, induces a marked

upregulation of Slc11a1 protein expression (figure 5.2.5-A, Lane 3). Confirmation protein was loaded onto all tracks is provided by amido black staining the Immobilon membrane after immunodetection (figure 5.2.5-B). Figure 5.2.5 is a representative experiment of n=3.

5.2.6 Exogenous Sp1 cannot Transactivate the *Slc11a1* Promoter in the Cos-1 cell line

The involvement of Sp1 binding sites in Inr-mediated transcription (Javahery *et al.* 1994; reviewed Smale, 1997), and in directing lineage specific gene expression (Chen *et al.* 1993; reviewed Clarke and Gordon, 1998) is well documented. Furthermore the Sp1 transcription factor has been proposed to be involved in c-Myc/Miz-1 mediated transcriptional regulation of the TGFβ responsive gene $p15^{ink4b}$ (Seoane *et al.* 2001). In light of these data we were interested to see if Sp1 was able to directly transactivate the *Slc11a1* promoter. In order to see if Sp1 is a positive regulator of *Slc11a1* expression, the *Slc11a1* promoter constructs pHB4, pHB20 and pHB23 were co-transfected with increasing amounts (0, 0.1, 0.2, 0.5, 1, 1.5 and 2μg), of pPAC-Sp1[8]. Figure 5.2.6 illustrates that Sp1 alone was unable to transactivate the *Slc11a1* promoter and that neither deletion of the EMS (figure 5.2.6-C) nor deletion of the consensus Sp1 binding site (figure 5.2.6-D) affected this. It has been documented that endogenous Sp1 is in excess within the cell and that it needs to be activated by TGFβ in order to influence gene regulation (Feng *et al.* 2002). Figure 5.2.7 shows that although Cos-1 cells are responsive to TGFβ treatment (figure 5.2.7-A[9]), TGFβ treatment does not lead to enhanced activity of the pHB4 *Slc11a1* promoter construct (figure 5.2.7-B). These data suggest that exogenous Sp1 alone cannot transactivate the *Slc11a1* promoter in the Cos-1 cell line.

5.2.7 Deletion/ Mutation of the Consensus Sp1-Binding Site at –27bp Decreases Responsiveness to Miz-1

The above data (section 5.2.6) suggests that addition of exogenous Sp1 is unable to transactivate the *Slc11a1* promoter; deletion or mutation of the consensus Sp1-binding

[8] pPAC-Sp1 was kindly by R. Tjian (Courtney and Tjian, 1988).
[9] Dr. C. H. Barton provided the data for figure 5.2.7-A.

site does however affect responsiveness to Miz-1. Deletion from the construct pHB20 to pHB23, the –71bp to –19bp region of the *Slc11a1* promoter, prevented Miz-1 induced transactivation (figure 5.2.8). The difference in responsiveness of pHB20 and pHB23 to Miz-1 was found to be significant in two independent experiments ($P<0.05$). The –71bp to –19bp deletion does not specifically remove the consensus Sp1-binding site, other transcription factor binding sites are also removed, these include binding sites for the myeloid zinc finger protein, the GA-binding protein and the aryl hydrocarbon heterodimer. To elucidate whether the observed abrogation of Miz-1 responsiveness was due to deletion of the consensus Sp1-binding site at –27bp, this site was mutated in the context of pHB4, pHB6 and pHB8 (see section 3.2.2). Figure 5.2.9 shows that unlike deletion of the consensus Sp1-binding site, mutation of this site only leads to a reduced response to Miz-1 as opposed to a complete inhibition. These data suggest that factors binding to the consensus Sp1-binding site are influencing responsiveness of the *Slc11a1* promoter to Miz-1 but other factor binding sites are also involved.

5.2.8 p300 Functions both Alone and Synergistically with Miz-1 to Transactivate the *Slc11a1* Promoter

p300 has been implicated as the possible cofactor involved in Miz-1 transactivation and it was subsequently shown that exogenous p300 could transactivate the $p15^{ink4b}$ gene alone, and that this activity could further be increased by the addition of exogenous Miz-1 (Staller *et al.* 2001). To elucidate whether p300 could transactivate the *Slc11a1* promoter and whether p300 and Miz-1 could act synergistically, pHB4 was co-transfected with 1μg of the *Slc11a1* promoter construct pHB4 and either, a constant 1μg Miz-1 with increasing p300[10] (0, 0.1, 0.2, 0.5 and 1μg), or, a constant 1μg of p300 with increasing Miz-1 (0, 0.1, 0.2, 0.5 and 1μg). DNA concentrations were made up to 3μg with the pBABE empty vector. Co-transfection of a constant amount of Miz-1 with increasing p300 produced no significant increase pHB4 activity (figure 5.2.10-A). However, co-transfection of a constant amount of p300 with increasing Miz-1 resulted in a biphasic transactivation of the promoter. A maximal

[10] The pCMV-HA-p300 expression construct was kindly provided by Issay Kitabayashi at the National Cancer Center Research Institute, Tokyo, Japan.

4.3-fold induction of promoter activity was produced by the co-transfection of 1μg p300 with 0.1μg Miz-1; increasing amounts of Miz-1 resulted in promoter activities less than 1μg p300 alone. Figure 5.2.10-B further illustrates these results, comparing the effects of adding 0.1μg Miz-1, 1μg Miz-1, 1μg p300, 1μg p300/0.1μg Miz-1, and 1μg p300/1μg Miz-1 with the activity of pHB4 alone. Together these data suggest that transactivation of the EMS containing *Slc11a1* promoter construct, pHB4, by Miz-1 requires the co-expression of p300, whereas p300 is able to transactivate *Slc11a1* expression alone. Figure 5.2.11-B confirms this latter statement, showing co-transfection with a constant amount (1μg) of the *Slc11a1* promoter construct pHB4 with increasing amounts (0, 0.5, 1, 1.5 and 2μg) of p300, induces a dose dependent increase in promoter activity that was significant over all doses tested ($P<0.05$). It can be concluded from these data that p300 can transactivate the *Slc11a1* promoter, and that this transactivation can be augmented by the co-transfection of Miz-1.

5.2.9 Responsiveness to Low Concentrations of p300 is Decreased by EMS

Unlike Miz-1, figure 5.2.11-B shows that p300 can transactivate an EMS containing *Slc11a1* promoter construct, pHB4, suggesting that factors binding to the EMS are not having a dramatic affect on p300 responsiveness. Comparison of the response of pHB4 and pHB20 to p300 (figure 5.2.11-B) shows that although both constructs are efficiently transactivated by p300, the effect of 0.5μg of p300 is significantly higher for pHB20 than for pHB4 ($P=0.01$). These data suggest that factors binding to EMS sites may alter the response to low concentrations (≤0.5μg) of p300. This proposal is supported by the data presented in figure 5.2.11-C, which illustrated that the response to low concentrations (0.5μg) of p300 correlates with the number of EMS site within the construct (figure 5.2.11-D). As was the case for Miz-1 responsiveness (see section 5.2.3), EMS#6 appears to play a bigger role that any of the other EMS in influencing the response to p300 (figure 5.2.11-C).

5.2.10 Responsiveness to p300 is Dependent upon the Presence of the Consensus Sp1-Binding Site at –27bp

Miz-1 mediated transactivation has been proposed to involve both p300 (Staller *et al.* 2001) and Sp1 (Seoane *et al.* 2001). As mutation of the consensus Sp1 binding site at position –27bp led to a marked reduction in the response of the *Slc11a1* promoter to Miz-1 (section 5.2.7), we were interested to see what affects these mutations would have on p300-mediated transactivation. Figure 5.2.12-B shows that deletion of the consensus Sp-1-binding site at position –27bp results in a significant loss of p300 responsiveness at all concentrations tested ($P<0.05$), whereas mutation of the Sp-1 consensus binding site (figure 5.2.12-C) resulted in a loss of p300 responsiveness that was significant ($P<0.05$) at 0.1 and 0.5μg of p300. These data suggest that factors binding to the consensus Sp1-binding site are essential for p300-mediated transactivation of the *Slc11a1* promoter.

FIGURE 5.2.1 Cotransfection of Miz-1 with the *Slc11a1* Promoter Construct pHB4 in the Cos-1 Cell Line. Cos-1 cells were co-transfected using the LipofectAMINE (LA) reagent as described (section 2.2.7). Expression of the reporter gene was detected by performing a CAT assay (37^0C; 6 hours) on 20μg protein extract from each transfection. Promoter activity for each sample was calculated as a percentage of the average value obtained from the control (pHB4 Alone). (A) 1μg of the *Slc11a1* promoter construct pHB4 and increasing amounts of Miz-1 DNA (0, 0.1, 0.2, 0.5, 1, 1.5 and 2μg), DNA concentrations were made up to 3μg with the pBABE empty vector. n=15. (B) 1μg of the *Slc11a1* promoter construct pHB4 either alone or with 1μg c-Myc DNA, 1μg of c-Myc DNA and 1μg of Max DNA, 1μg of c-Myc DNA and 1μg of Miz-1ΔPOZ DNA, 1μg of c-Myc DNA and 1μg of Miz-1 DNA, or 1μg Miz-1 DNA respectively, DNA concentrations were made up to 3μg with the pBABE empty vector. Student T-test compared with either pHB4 Alone (*) or pHB4 + 1μg of c-Myc DNA (♦) $P<0.05$; $n\approx3$.

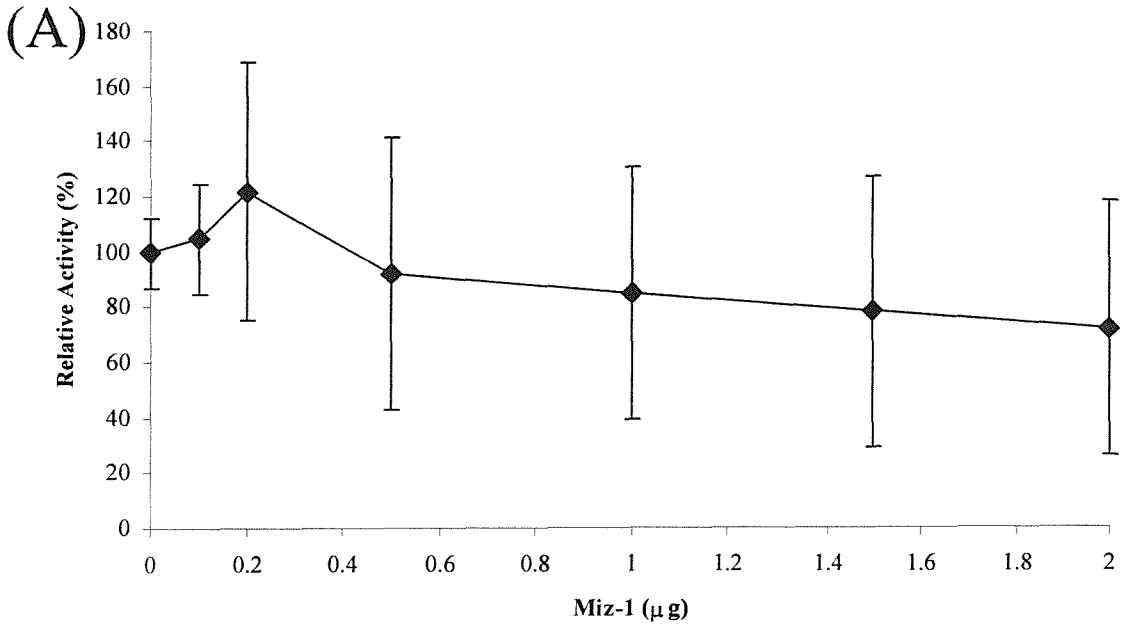
(A)
Relative Activity (%)
180
160
140
120
100
80
60
40
20
0
0
0.2
0.4
0.6
0.8
1
1.2
1.4
1.6
1.8
2
Miz-1 (μg)

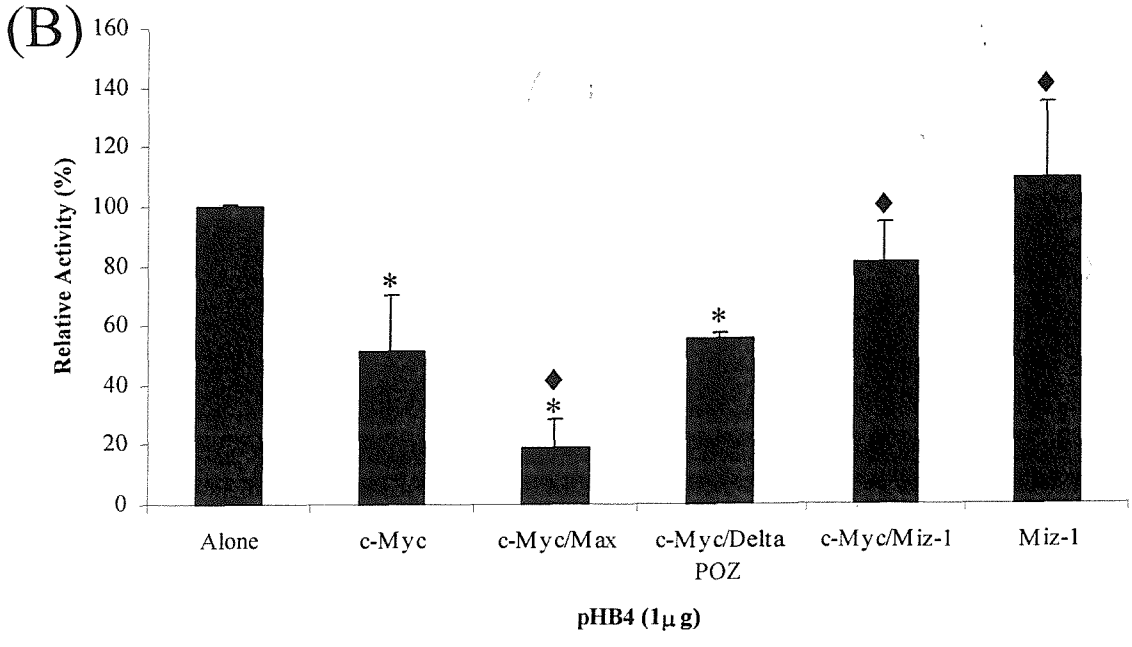
(B)
Relative Activity (%)
160
140
120
100
80
60
40
20
0
Alone
c-Myc
c-Myc/Max
c-Myc/Delta POZ
c-Myc/Miz-1
Miz-1
pHB4 (1μg)

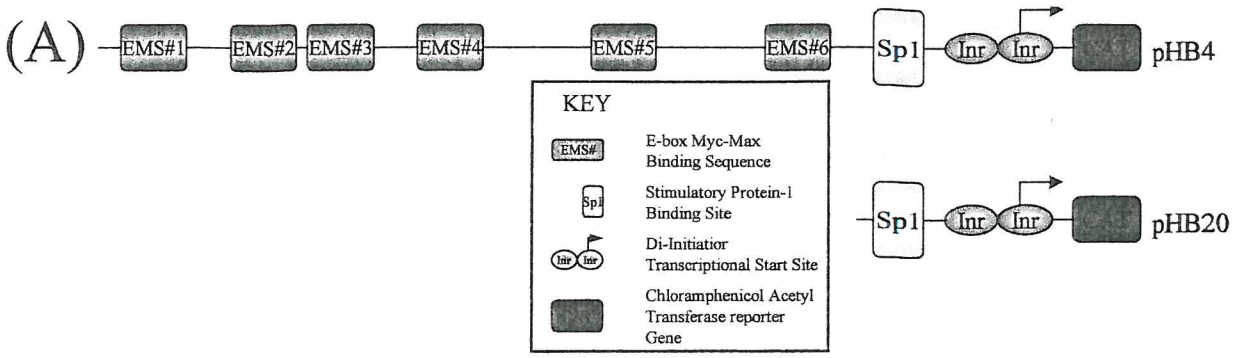

FIGURE 5.2.2 Differential Regulation of the *Slc11a1* Promoter Constructs pHB4 & pHB20 by Miz-1 in the Cos-1 Cell Line. Cos-1 cells were co-transfected using the LipofectAMINE (LA) reagent as described (section 2.2.7). Expression of the reporter gene was detected by performing a CAT assay (37^0C; 2 hours) on 20µg protein extract from each transfection. Promoter activity for each sample was calculated as a percentage of the average value obtained from the control (pHB4 & pHB20 Alone). (A) Illustration of the pHB4 & pHB20 *Slc11a1* promoter constructs (see key). (B) 1µg of the *Slc11a1* promoter constructs pHB4 (Closed Diamonds) & pHB20 (Open Squares) were co-transfected with increasing amounts of Miz-1 DNA (0, 0.5, 1, 1.5 and 2µg), DNA concentrations were made up to 3µg with the pBABE empty vector. Student T-test comparing the responses of pHB4 & pHB20 to Miz-1 ♦ $P<0.05$; n=2. (C) 1µg of the Slc11a1 promoter construct pHB20 was co-transfected with increasing amounts of Miz-1 DNA (0, 0.1, 0.2, 0.5, 1, 1.5 and 2µg), DNA, concentrations were made up to 3µg with the pBABE empty vector. Student T-test compared with pHB20 Alone *$P<0.05$, **$P<0.025$, ***$P<0.005$; n=2-6.

(B)

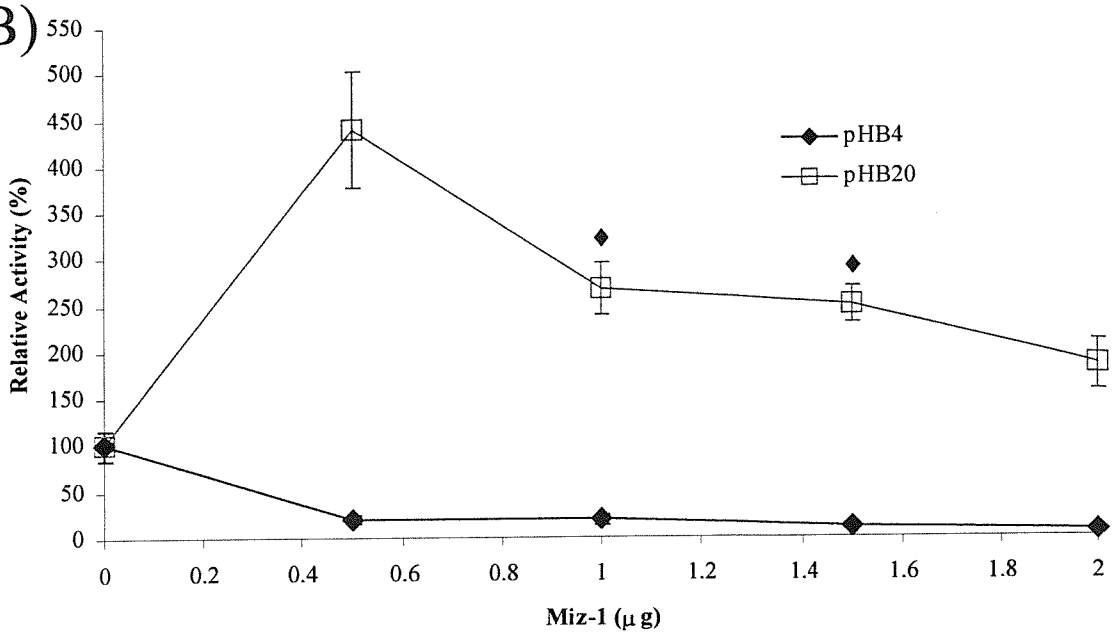
Relative Activity (%)
550
500
450
400
350
300
250
200
150
100
50
0
pHB4
pHB20
0
0.2
0.4
0.6
0.8
1
1.2
1.4
1.6
1.8
2
Miz-1 (μg)

(C)

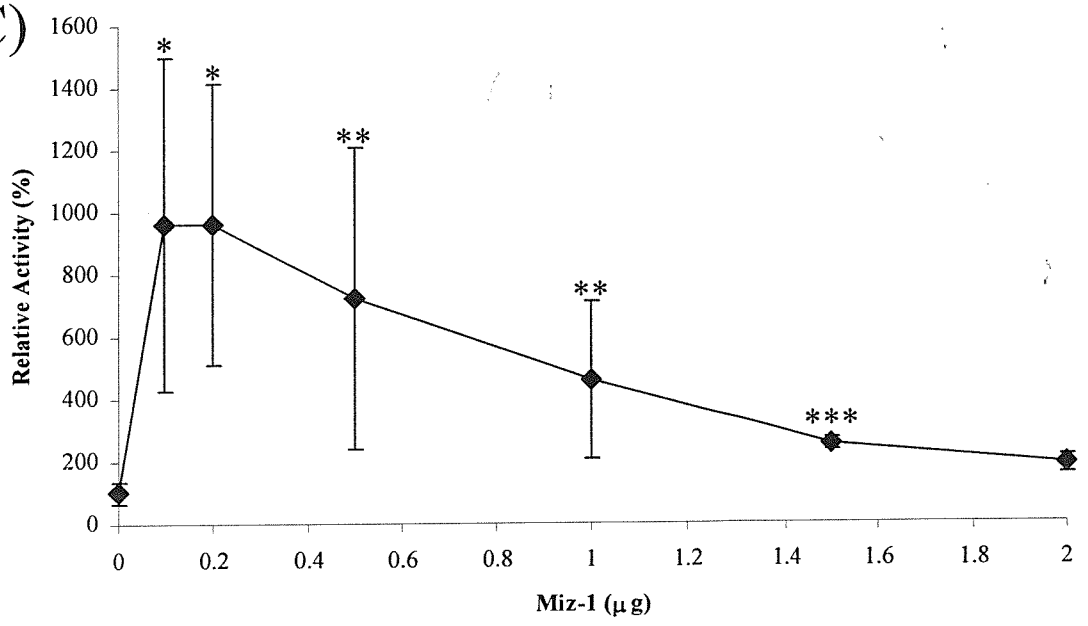
Relative Activity (%)
1600
1400
1200
1000
800
600
400
200
0
*
*
**
**
***
0
0.2
0.4
0.6
0.8
1
1.2
1.4
1.6
1.8
2
Miz-1 (μg)

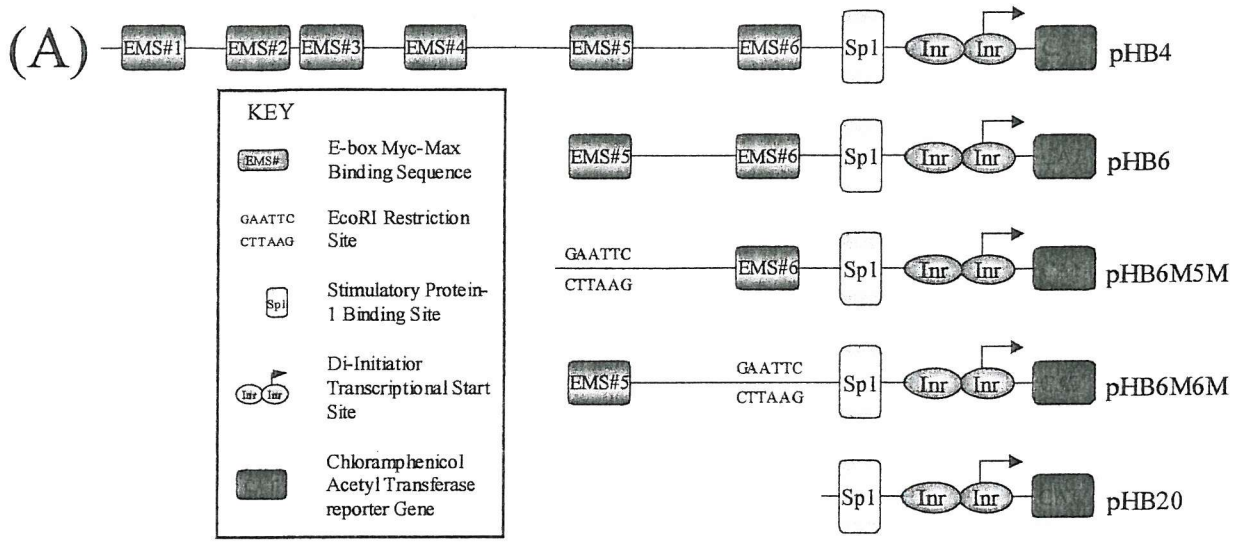

FIGURE 5.2.3 Effect of EMS on Responsiveness of the *Slc11a1* Promoter to Miz-1. Cos-1 cells were co-transfected using the LipofectAMINE (LA) reagent as described (section 2.2.7). Expression of the reporter gene was detected by performing a CAT assay (37^0C; 2 hours) on 20µg protein extract from each transfection. Promoter activity for each sample was calculated as a percentage of the average value obtained from the control (*Slc11a1* promoter construct alone). (A) Illustration of the *Slc11a1* promoter constructs (see key). (B) 1µg of the *Slc11a1* promoter constructs pHB4, pHB6, pHB6M5M, pHB6M6M & pHB20 were co-transfected with increasing amounts of Miz-1 DNA (0, 0.1 and 0.2µg), DNA concentrations were made up to 3µg with the pBABE empty vector. (C) Comparison of responsiveness to 0.2µg Miz-1. Students T-Test compared with Promoter activity without Miz-1 *P=0.0053 **P=0.031; n=2 (pHB6M6M), 4 (pHB6 & pHB20), & 6 (pHB4 & pHB6M5M). (D) Table summarising the number of EMS sequences within each of the *Slc11a1* promoter constructs.

(B)

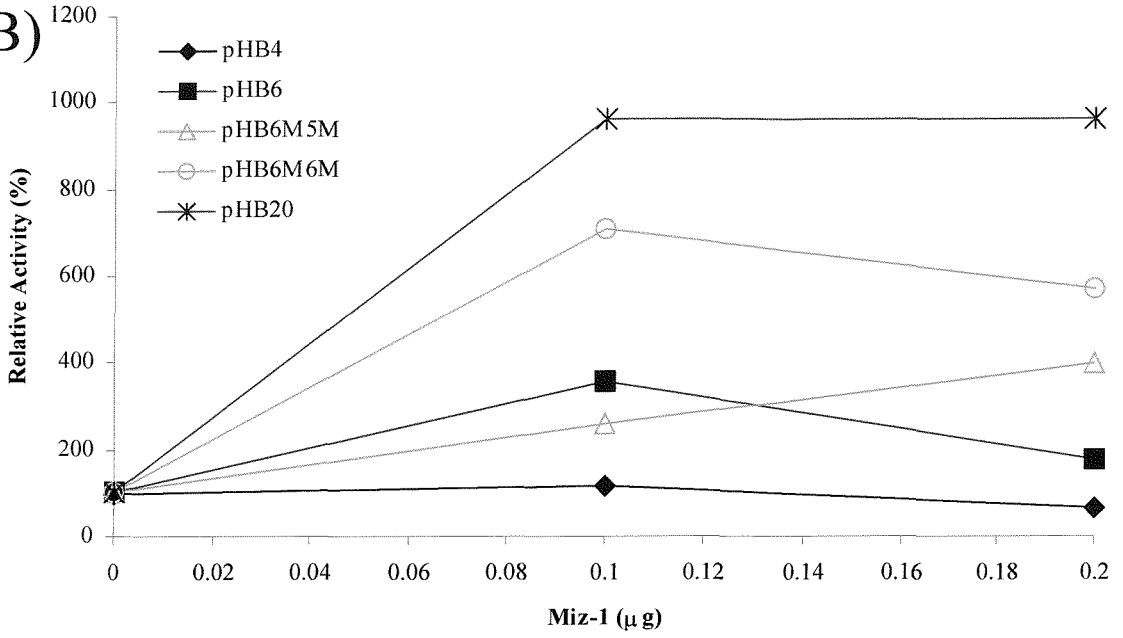

(C)

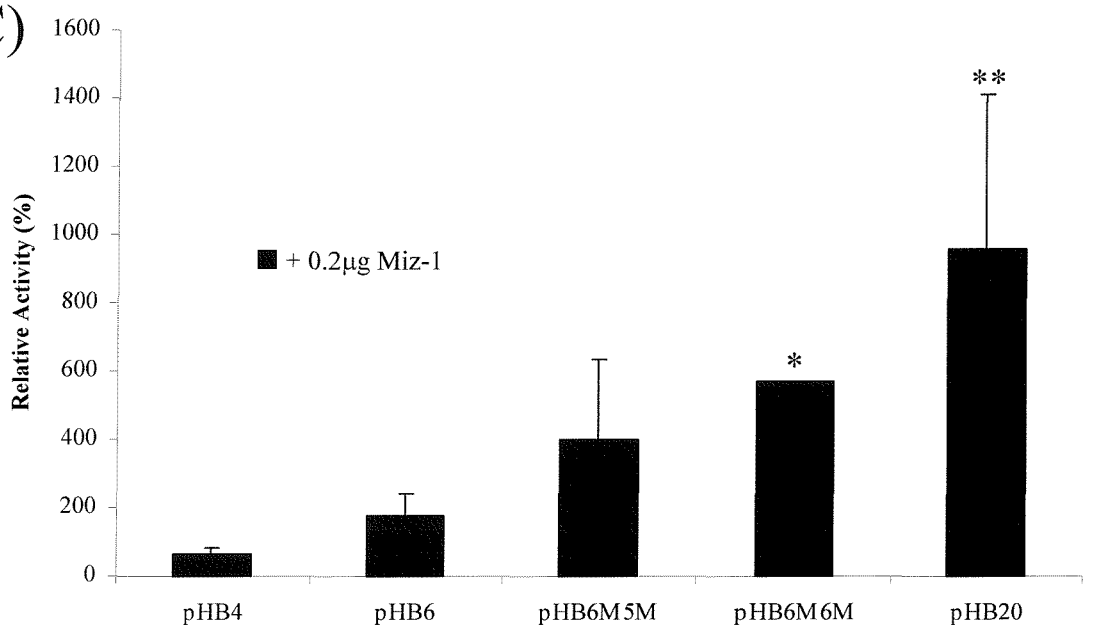

(D)

	pHB4	pHB6	pHB6M5M	pHB6M6M	pHB20
Number of EMS Sites	6	2	1	1	0

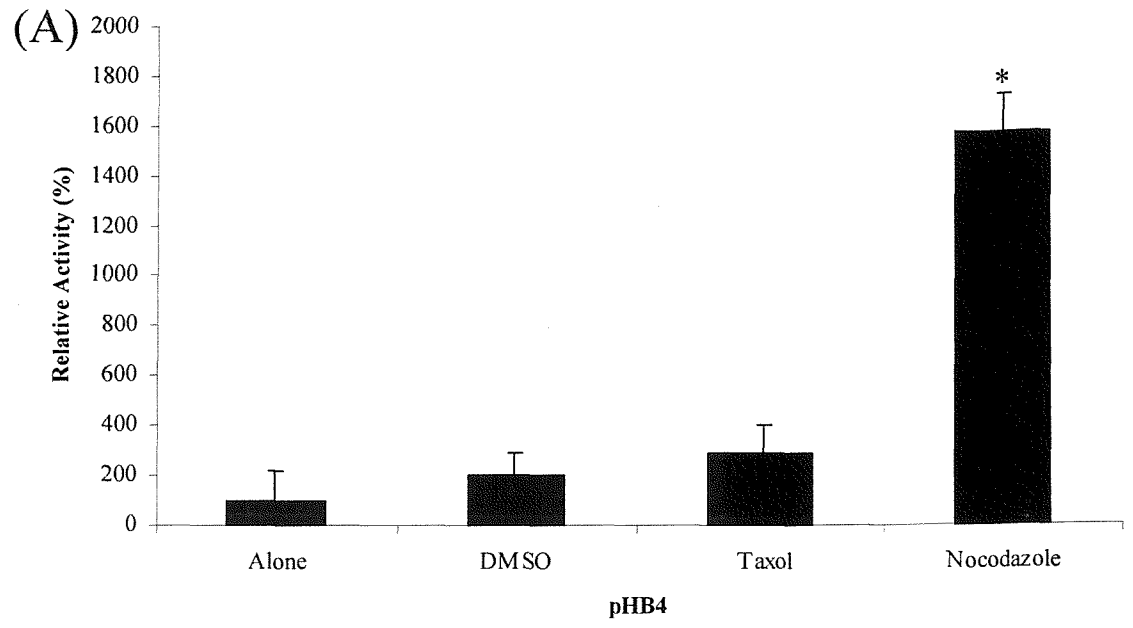

FIGURE 5.2.4 The Microtubule Destabilising Compound Nocodazole Increases *Slc11a1* Expression in the Macrophage-Like Cell Lines RAW 264.7 & N11. (A) RAW 264.7 Cells were co-transfected using LA as described (section 2.2.7) with 1μg of the *Slc11a1* promoter construct pHB4 for 24 hours before the addition 100% DMSO (Sigma, UK), 10μM Taxol (Alexis Biosciences) or 1μM Nocodazole (Alexis Biosciences) for a further 24 hours. Expression of the reporter gene was detected by performing a CAT assay (37^0C; 6 hours) on 50μg protein extract from each transfection. Promoter activity for each sample was calculated as a percentage of the average value obtained from the control (pHB4 Alone). (B, C & D) N11 Microgial cells were treated with increasing concentrations of either Taxol or Nocodazole for 24 hours after which samples were taken for analysis via western blotting as described (section 2.2.10-12). (B) Western blot using an antibody specific to the N-terminal region (amino acids 1-82) of the Slc11a1 protein (Atkinson and Barton, 1998). (C) Amido-black stained membrane. (1), Untreated; (2), 2μl DMSO; (3), 10μl DMSO; (4), 20μl DMSO; (5), 1μM Taxol; (6), 5μM Taxol; (7), 10μM Taxol; (8), 0.1μM Nocodazole; (9), 0.5μM Nocodazole; (10), 1μM Nocodazole. (D) Intensity of immunoreactive bands (B) were quantitated using the Quantity One programme and values calculated relative to the untreated cells (lane 1), the table indicates the lanes represented in the graph.

(B)

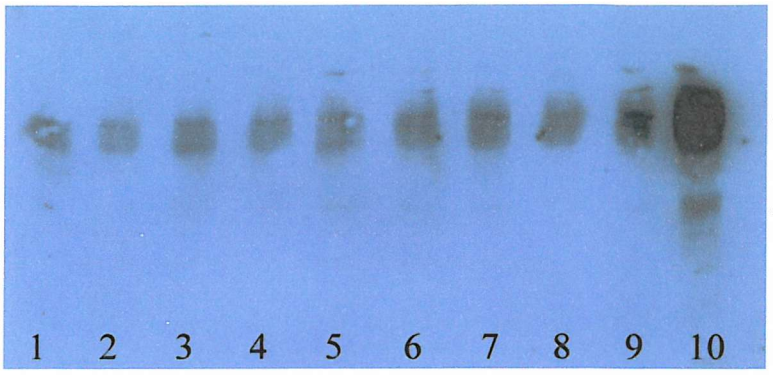

(C)

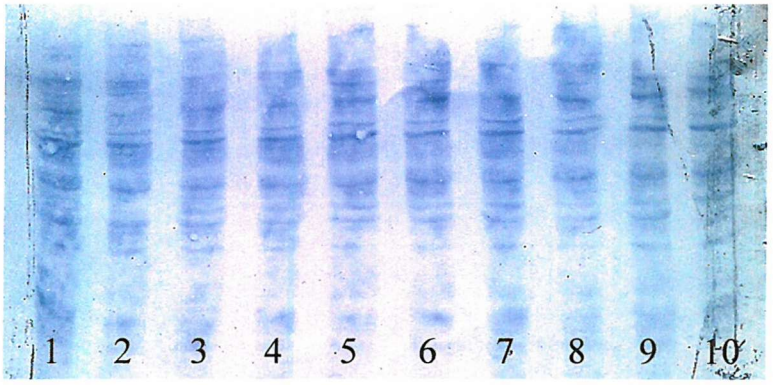

(D)

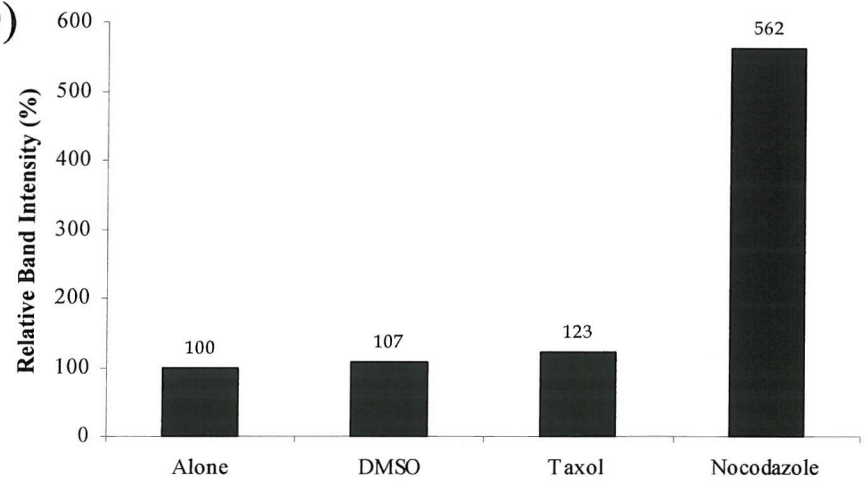

Lane Number	1	4	7	10

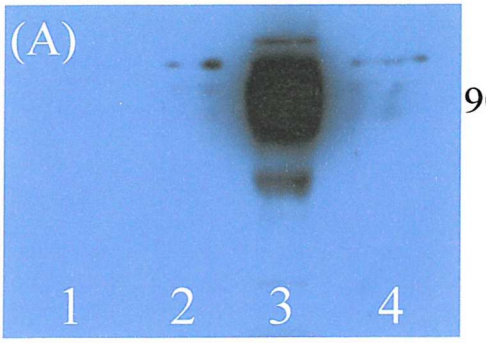

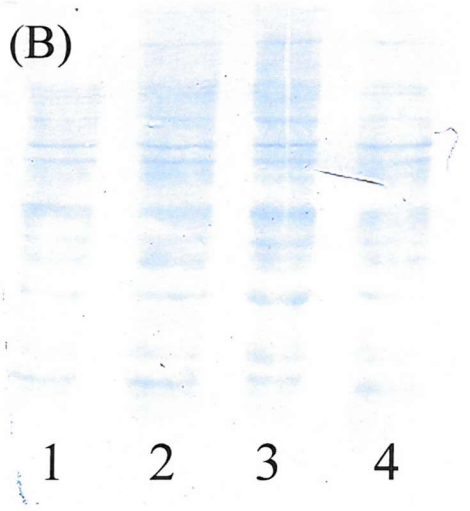

FIGURE 5.2.5 The LPS-mimetic and Microtubule Stabilising Agent Taxol Stimulates *Slc11a1* Expression in *Slc11a1*^{G169}-expressing Primary Macrophages. Primary bone marrow derived macrophages were obtained from the MF1 *Slc11a1*^{G169} expressing mice and cultured in media enriched with Granulocyte/Macrophage colony stimulating factors (GM-CSF) for 14 days. After this time cells were treated for 24 hours with either 100% DMSO (Sigma, UK), 10μM Taxol (Alexis Biosciences) or 1μM Nocodazole (Alexis Biosciences), after this time cells were harvested for analysis via western blotting as described (section 2.2.10-12). (A) Western blot using an antibody specific to the N-terminal region (amino acids 1-82) of the Slc11a1 protein (Atkinson and Barton, 1998). (B) Amido-black stained membrane. (1), Untreated; (2), DMSO; (3), Taxol; (4), Nocodazole.

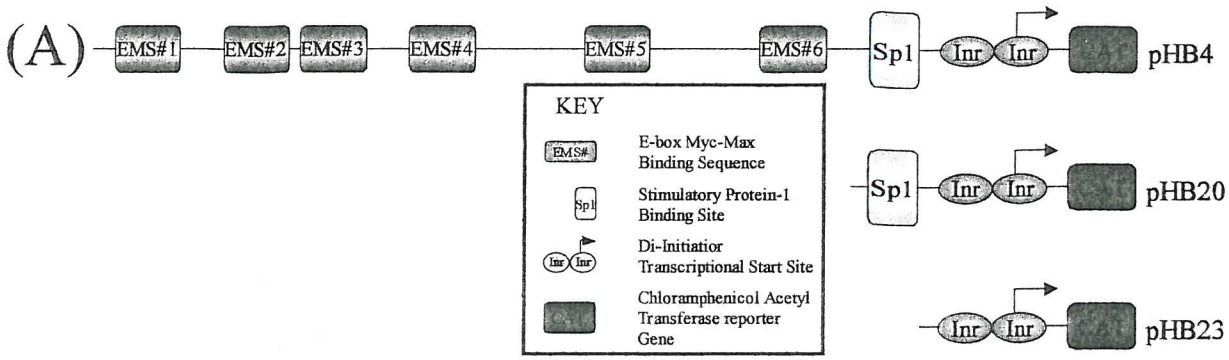

FIGURE 5.2.6 Exogenous Sp1 Fails to Trans-activate the *Slc11a1* Promoter Miz-1 in the Cos-1 Cell Line. Cos-1 cells were co-transfected using the LipofectAMINE (LA) reagent as described (section 2.2.7). Expression of the reporter gene was detected by performing a CAT assay (37^0C; 2 hours) on 20μg protein extract from each transfection. Promoter activity for each sample was calculated as a percentage of the average value obtained from the control (*Slc11a1* promoter alone). (A) Illustration of the pHB4, pHB20 & pHB23 *Slc11a1* promoter constructs (see key). (B) 1μg of the *Slc11a1* promoter constructs pHB4 was co-transfected with increasing amounts of Sp1 DNA (0, 0.1, 0.2, 0.5, 1, 1.5 and 2μg), DNA concentrations were made up to 3μg with the pBABE empty vector, n=4. (C) 1μg of the *Slc11a1* promoter constructs pHB20 was co-transfected with increasing amounts of Sp1 DNA (0, 0.1, 0.2, 0.5 and 1μg), DNA concentrations were made up to 2μg with the pBABE empty vector, n=2. (D) 1μg of the *Slc11a1* promoter constructs pHB23 was co-transfected with increasing amounts of Sp1 DNA (0, 0.1, 0.2, 0.5 and 1μg), DNA concentrations were made up to 2μg with the pBABE empty vector, n=2.

(B)

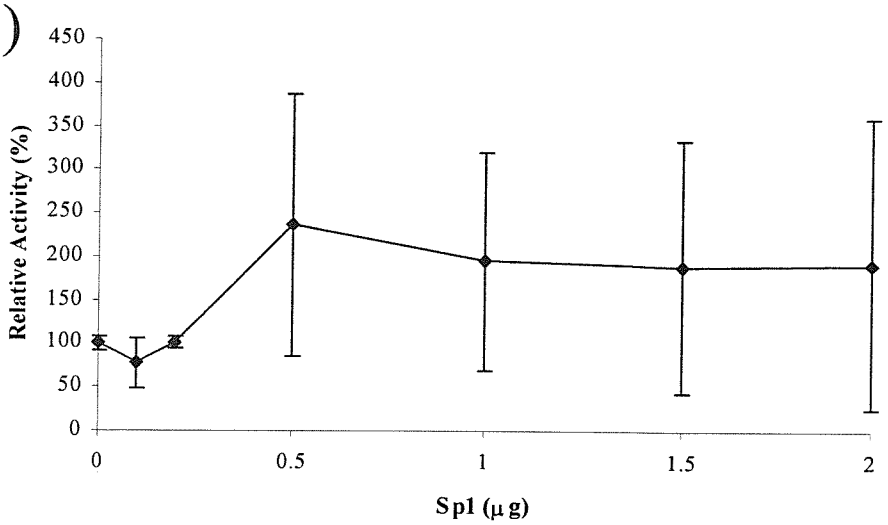
Relative Activity (%)
450
400
350
300
250
200
150
100
50
0
0
0.5
1
1.5
2
Sp1 (μg)

(C)

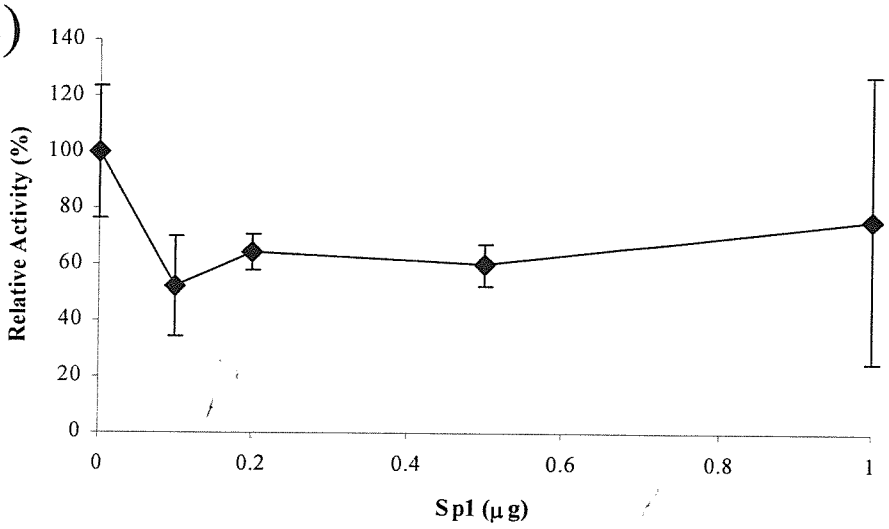
Relative Activity (%)
140
120
100
80
60
40
20
0
0
0.2
0.4
0.6
0.8
1
Sp1 (μg)

(D)

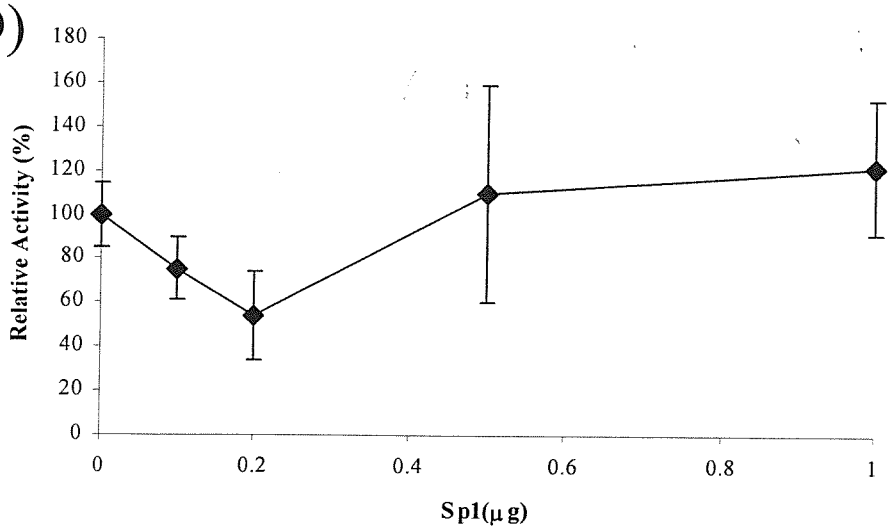
Relative Activity (%)
180
160
140
120
100
80
60
40
20
0
0
0.2
0.4
0.6
0.8
1
Sp1(μg)

FIGURE 5.2.7 TGFβ Fails to Trans-activate the *Slc11a1* Promoter Miz-1 in the Cos-1 Cell Line. Cos-1 cells were co-transfected using the LipofectAMINE (LA) reagent as described (section 2.2.7). Expression of the reporter gene was detected by performing a CAT assay (37^0C; 2 hours) on 20μg protein extract from each transfection. Promoter activity for each sample was calculated as a percentage of the average value obtained from the control. (A) 1μg of the *Slc11a1* promoter constructs pHB4 was co-transfected with increasing amounts of Sp1 DNA (0, 0.1, 0.2, 0.5, 1, 1.5 and 2μg), DNA concentrations were made up to 3μg with the pBABE empty vector, n=4. (B) Cos-1 cells were transfected with 1μg of the *Slc11a1* promoter constructs pHB4 for 30 hours before the addition of 10pg/ml TGFβ for a further 18 hours.

(A)

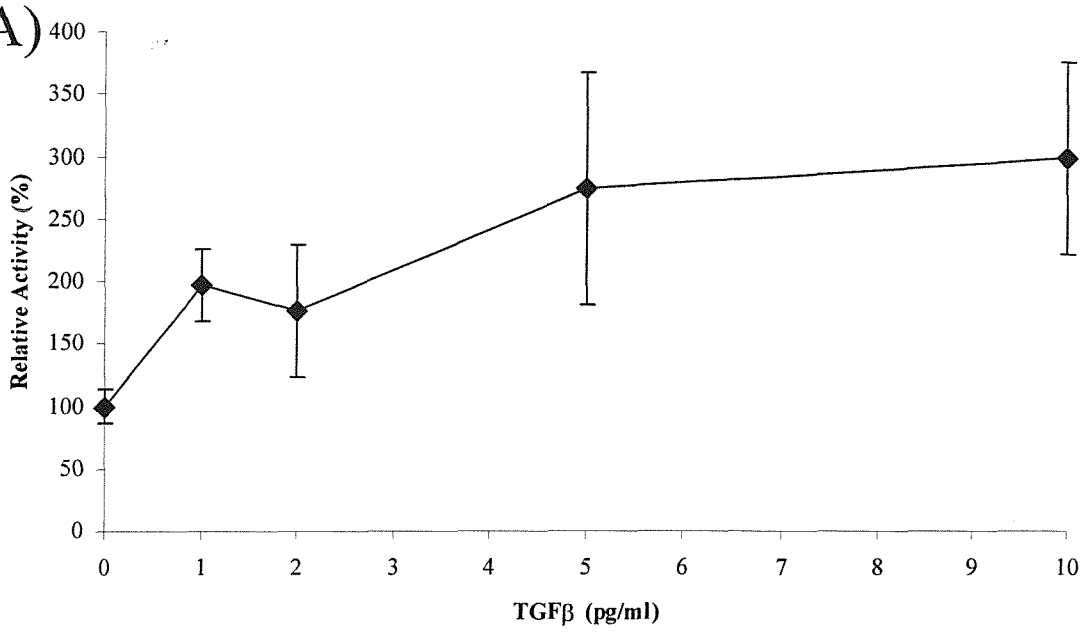
Relative Activity (%)
400
350
300
250
200
150
100
50
0
0
1
2
3
4
5
6
7
8
9
10
TGFβ (pg/ml)

(B)

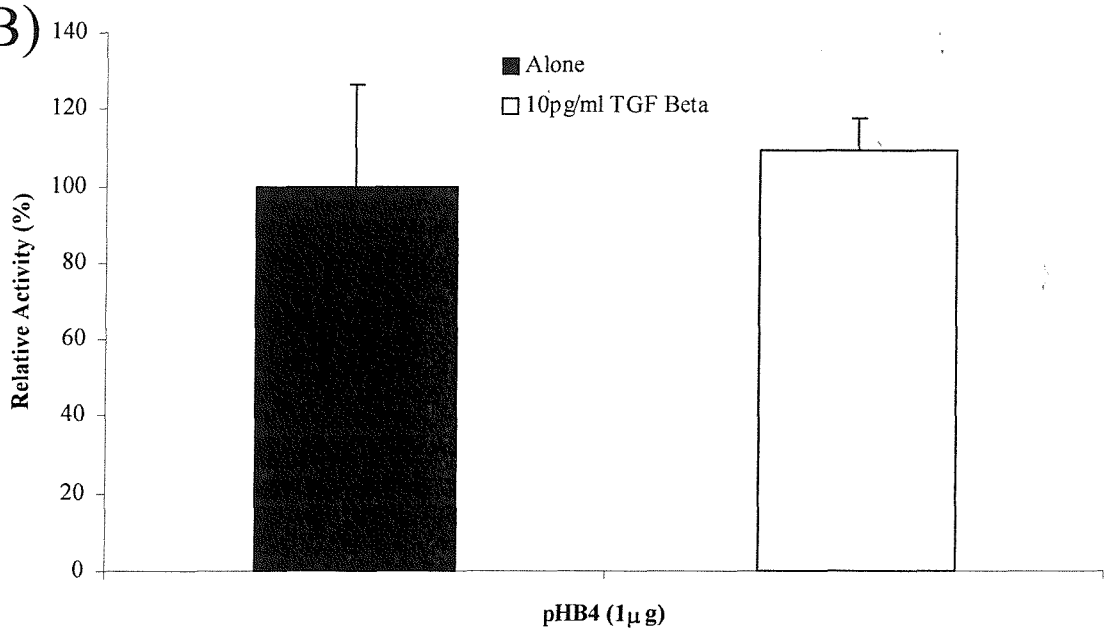
Relative Activity (%)
140
120
100
80
60
40
20
0
Alone
10pg/ml TGF Beta
pHB4 (1μg)

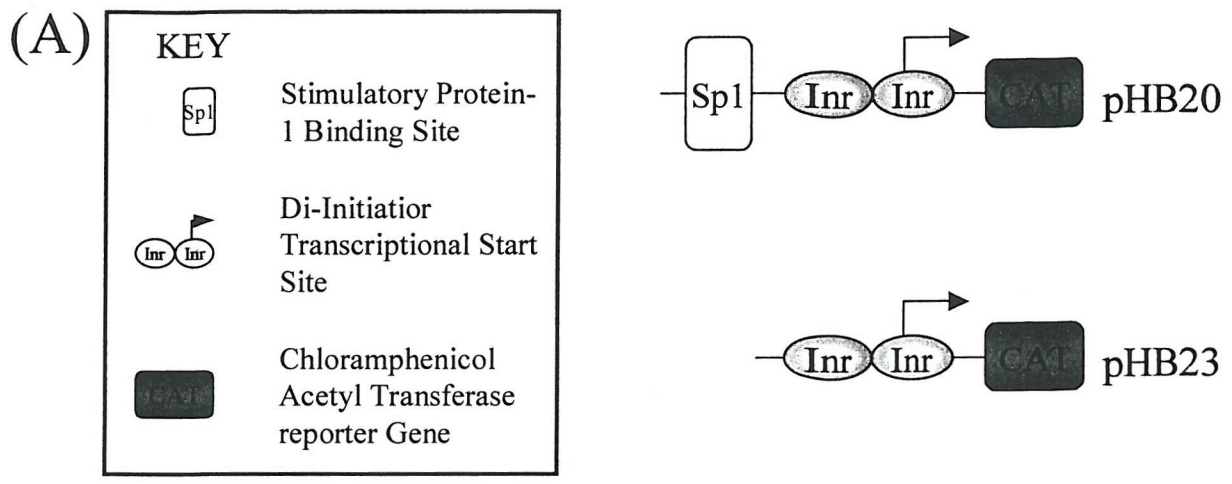

FIGURE 5.2.8 Deletion of the Sp1 Binding Site at –27bp Abrogates Responsiveness of the *Slc11a1* Promoter to Miz-1. Cos-1 cells were co-transfected using the LipofectAMINE (LA) reagent as described (section 2.2.7). Expression of the reporter gene was detected by performing a CAT assay (37^0C; 2 hours) on 20μg protein extract from each transfection. Promoter activity for each sample was calculated as a percentage of the average value obtained from the control (*Slc11a1* promoter construct alone). (A) Illustration of the pHB20 & pHB23 *Slc11a1* promoter constructs (see key). (B & C) 1μg of the *Slc11a1* promoter constructs pHB20 & pHB23 were co-transfected with increasing amounts of Miz-1 DNA (0, 0.1, 0.2, 0.5 and 1μg), DNA concentrations were made up to 2μg with the pBABE empty vector. (B) Students T-test comparing Miz-1 responsiveness of pHB20 to pHB23 *P=0.00086 **P=0.0069; n=2. (C) Students T-test comparing Miz-1 responsiveness of pHB20 to pHB23 ***P=0.035; n=2.

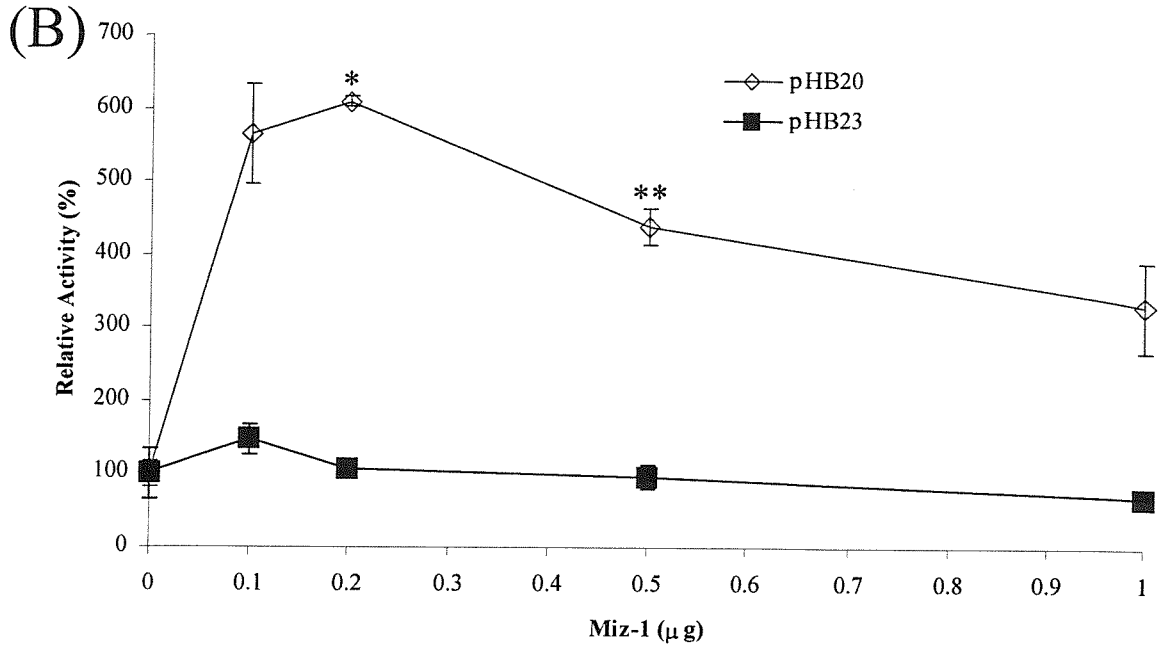
(B)
700
600
500
400
300
200
100
0
Relative Activity (%)
*
**
pHB20
pHB23
0
0.1
0.2
0.3
0.4
0.5
0.6
0.7
0.8
0.9
1
Miz-1 (μg)

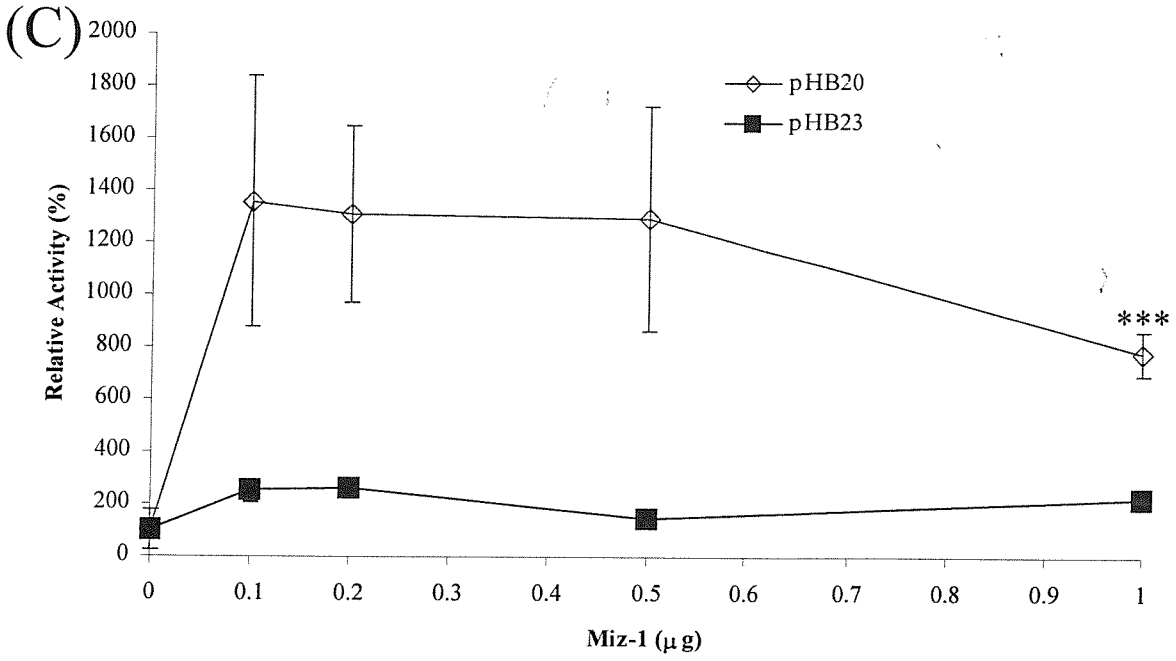
(C)
2000
1800
1600
1400
1200
1000
800
600
400
200
0
Relative Activity (%)
pHB20
pHB23
***
0
0.1
0.2
0.3
0.4
0.5
0.6
0.7
0.8
0.9
1
Miz-1 (μg)

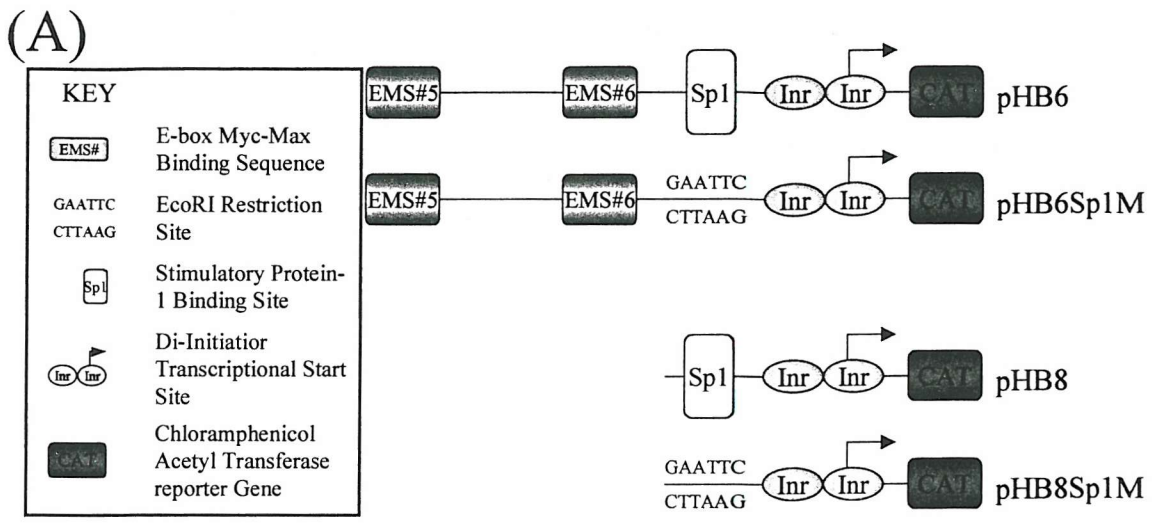

FIGURE 5.2.9 Mutation of the Sp1 Binding Site at –27bp Reduces Responsiveness of the *Slc11a1* Promoter to Miz-1. Cos-1 cells were co-transfected using the LipofectAMINE (LA) reagent as described (section 2.2.7). Expression of the reporter gene was detected by performing a CAT assay (37^0C; 2 hours) on 20μg protein extract from each transfection. Promoter activity for each sample was calculated as a percentage of the average value obtained from the control (*Slc11a1* promoter construct alone). (A) Illustration of the pHB6, pHB6Sp1M, pHB8 & pHB8Sp1M *Slc11a1* promoter constructs (see key). (B & C) 1μg of the *Slc11a1* promoter constructs were co-transfected with increasing amounts of Miz-1 DNA (0, 0.1 and 0.2μg), DNA concentrations were made up to 2μg with the pBABE empty vector. (B) 1μg of the *Slc11a1* promoter constructs pHB6 & pHB6Sp1M were co-transfected with increasing amounts of Miz-1 DNA (0, 0.1 and 0.2μg), DNA concentrations were made up to 2μg with the pBABE empty vector. Students T-test comparing Miz-1 responsiveness of pHB6 to pHB6Sp1M *P=0.01; n=4. (C) 1μg of the *Slc11a1* promoter constructs pHB8 & pHB8Sp1M were co-transfected with increasing amounts of Miz-1 DNA (0, 0.1 and 0.2μg), DNA concentrations were made up to 2μg with the pBABE empty vector, n=2.

(B)

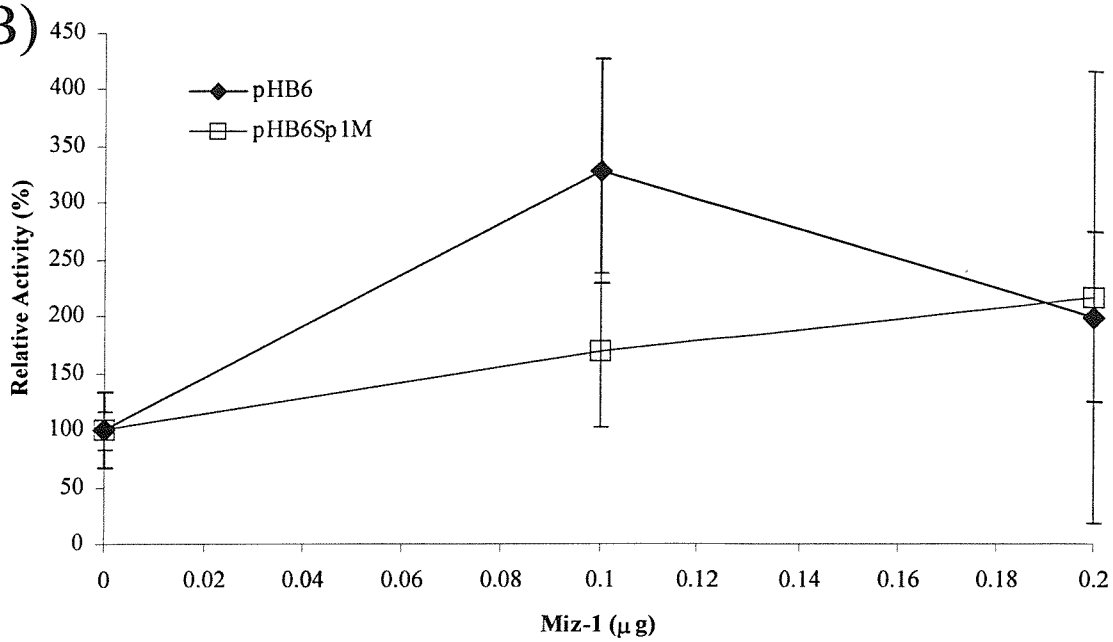
pHB6
pHB6Sp1M
Relative Activity (%)
450
400
350
300
250
200
150
100
50
0
0
0.02
0.04
0.06
0.08
0.1
0.12
0.14
0.16
0.18
0.2
Miz-1 (μg)

(C)

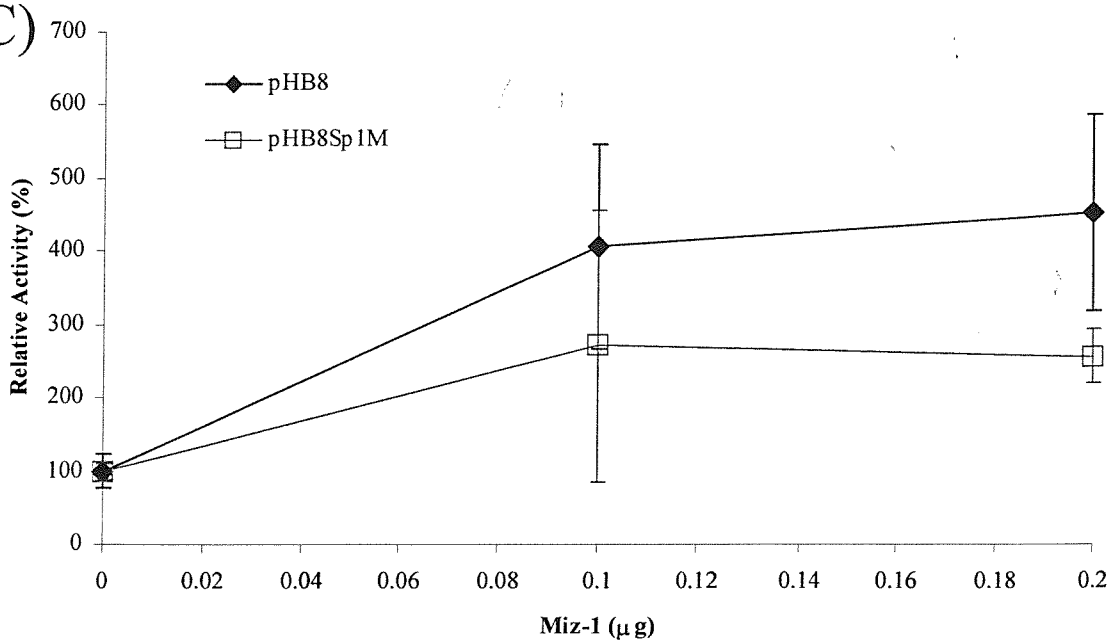
pHB8
pHB8Sp1M
Relative Activity (%)
700
600
500
400
300
200
100
0
0
0.02
0.04
0.06
0.08
0.1
0.12
0.14
0.16
0.18
0.2
Miz-1 (μg)

FIGURE 5.2.10 Cotransfection of Miz-1 and p300 with the *Slc11a1* Promoter Construct pHB4 in the Cos-1 Cell Line. Cos-1 cells were co-transfected using LA as described (section 2.2.7) and expression of the reporter gene was detected by performing a CAT assay (37^0C; 6 hours) on 20μg protein extract from each transfection. Promoter activity for each sample was calculated as a percentage of the average value obtained from the control (pHB4 Alone) (A) 1μg of the Slc11a1 promoter construct pHB4 either, a constant 1μg Miz-1 DNA with increasing p300 DNA (0, 0.1, 0.2 0.5 and 1μg), or, a constant 1μg of p300 DNA with increasing Miz-1 DNA 1μg of Miz-1 DNA (0, 0.1, 0.2 0.5 and 1μg), DNA concentrations were made up to 3μg with the pBABE empty vector. n= 1. (B) 1μg of the Slc11a1 promoter construct pHB4 either, 0.1μg Miz-1, 1μg Miz-1, 1μg p300, 1μg p300 and 0.1μg Miz-1, or 1μg p300 and 1μg Miz-1, DNA concentrations were made up to 3μg with the pBABE empty vector. Student T-Test Compared with pHB4 control *P=0.015 **P=0.005. Student T-Test pHB4 + 1μg Miz-1 compared with pHB4 + 1μg p300/1μg Miz-1 ♦P=0.013; n= 4 (0.1μg Miz-1); 8 (1μg Miz-1); 5 (1μg p300); 1 (1μg p300/ 0.1μg Miz-1); 3 (1μg p300/1μg Miz-1).

(A)

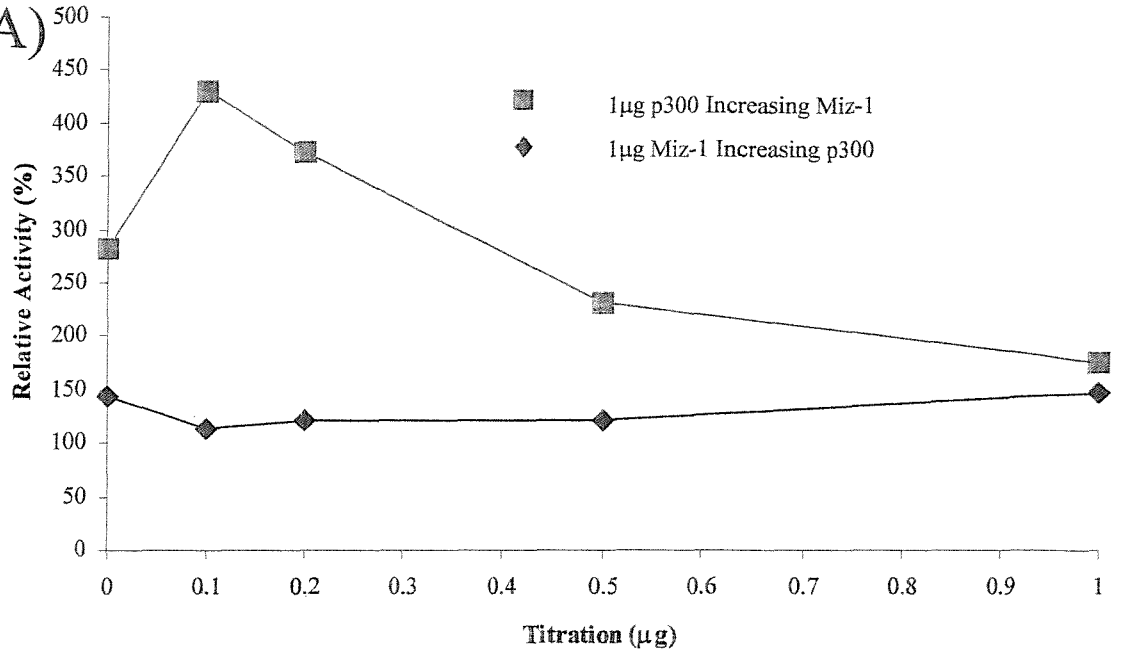
500
450
400
350
300
250
200
150
100
50
0
Relative Activity (%)
1µg p300 Increasing Miz-1
1µg Miz-1 Increasing p300
0
0.1
0.2
0.3
0.4
0.5
0.6
0.7
0.8
0.9
1
Titration (µg)

(B)

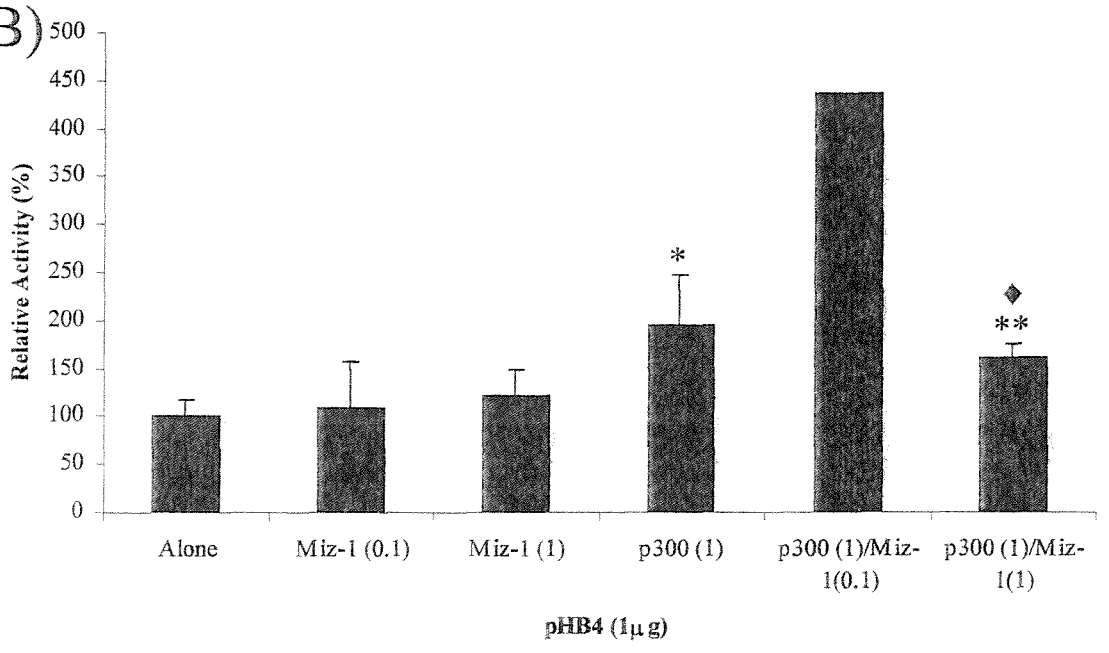
500
450
400
350
300
250
200
150
100
50
0
Relative Activity (%)
*
**
Alone
Miz-1 (0.1)
Miz-1 (1)
p300 (1)
p300 (1)/Miz-1(0.1)
p300 (1)/Miz-1(1)
pHB4 (1µg)

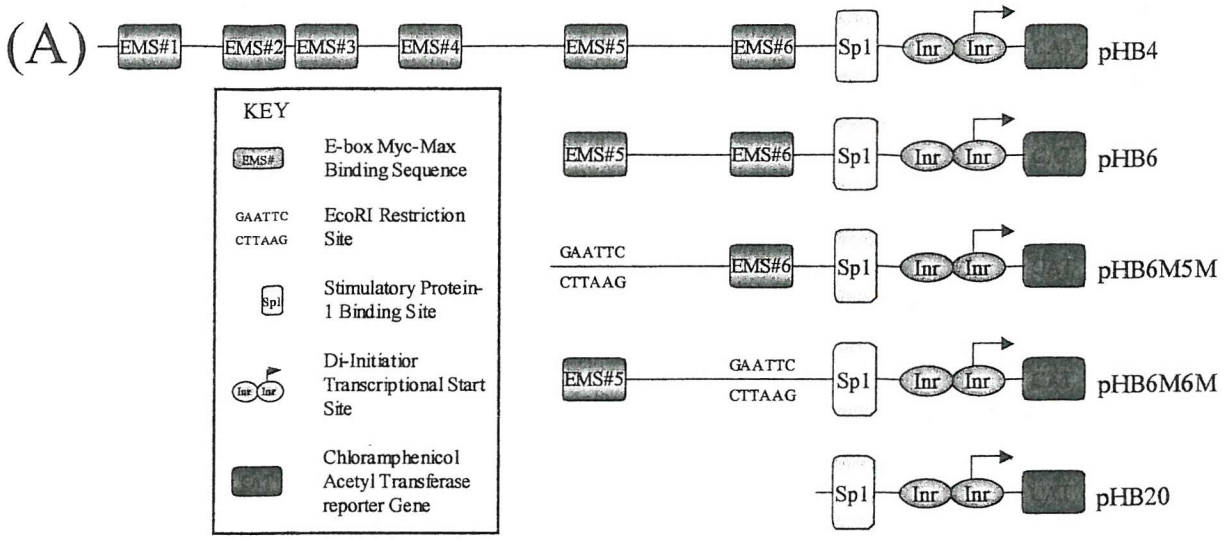

FIGURE 5.2.11 Effect of EMS on Responsiveness of the *Slc11a1* Promoter to p300. Cos-1 cells were co-transfected using the LipofectAMINE (LA) reagent as described (section 2.2.7). Expression of the reporter gene was detected by performing a CAT assay (37^0C; 2 hours) on 20μg protein extract from each transfection. Promoter activity for each sample was calculated as a percentage of the average value obtained from the control (*Slc11a1* promoter construct alone). (A) Illustration of the *Slc11a1* promoter constructs (see key). (B) 1μg of the *Slc11a1* promoter constructs pHB4 & pHB20 were co-transfected with increasing amounts of p300 DNA (0, 0.5, 1, 1.5 and 2μg), DNA concentrations were made up to 3μg with the pBABE empty vector. Students T-test comparing pHB4 & pHB20 responsiveness to p300, *P=0.01, **P=0.025, ***P=0.008; n=4. (C) 1μg of the *Slc11a1* promoter constructs pHB4, pHB6, pHB6M5M, pHB6M6M & pHB20 were co-transfected with 0.5μg of p300 DNA concentrations were made up to 2μg with the pBABE empty vector. n=2 (pHB6, pHB6M5M & pHB6M6M) & n=4 (pHB4 & pHB20). (D) Table summarising the number of EMS sequences within each of the *Slc11a1* promoter constructs.

(B)

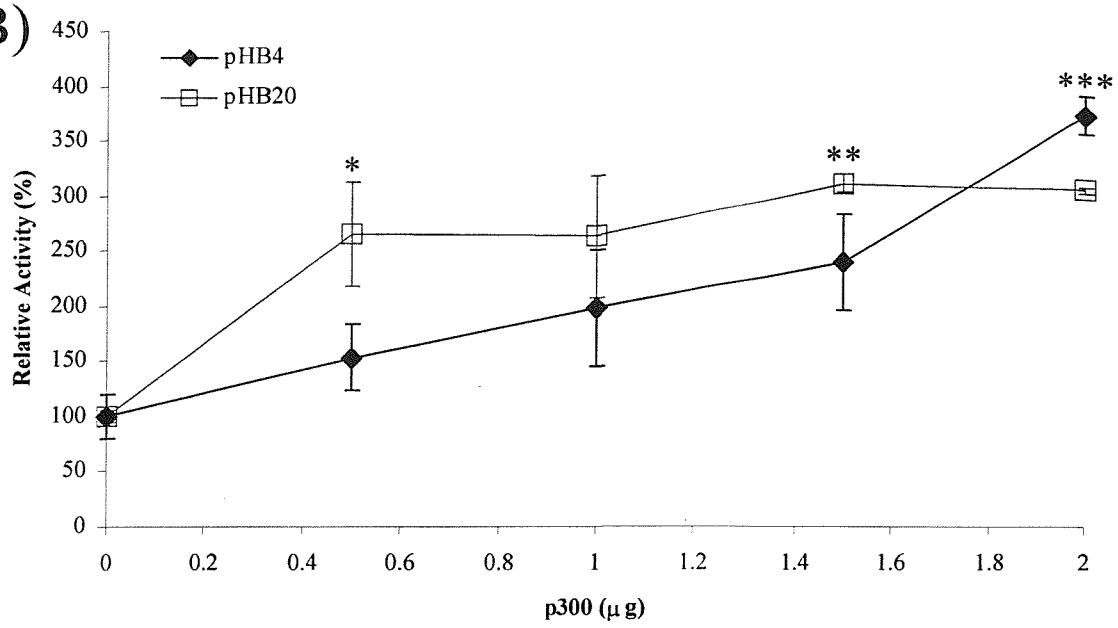

(C)

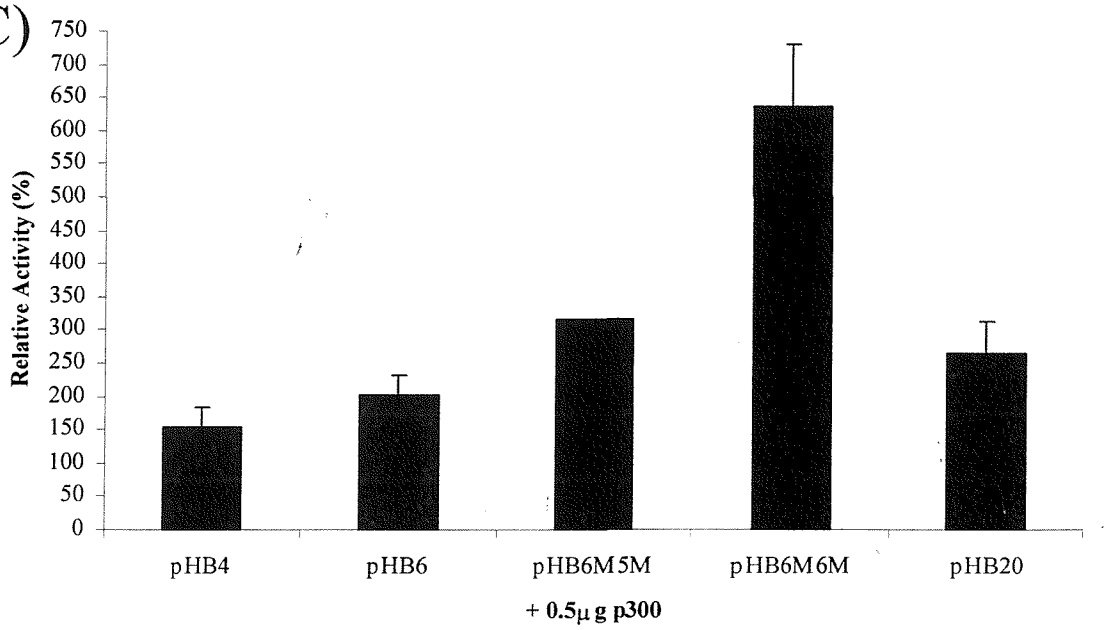

(D)

	pHB4	pHB6	pHB6M5M	pHB6M6M	pHB20
Number of EMS Sites	6	2	1	1	0

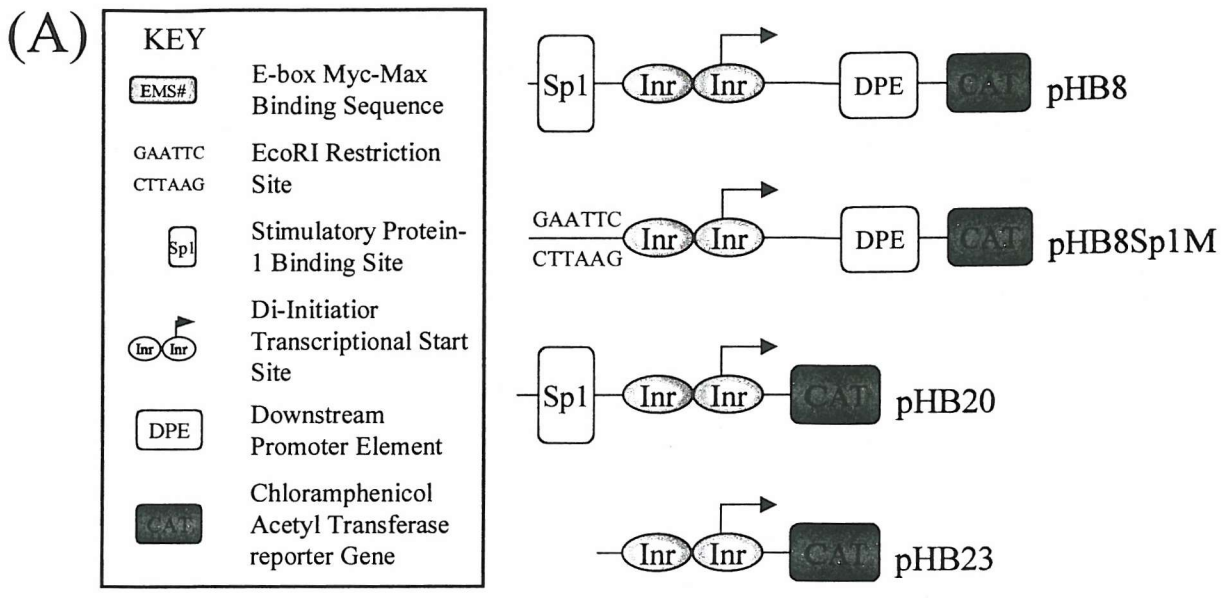

FIGURE 5.2.12 Deletion or Mutation of the Sp1 Binding Site at –27bp Abrogates Responsiveness of the *Slc11a1* Promoter to p300. Cos-1 cells were co-transfected using the LipofectAMINE (LA) reagent as described (section 2.2.7). Expression of the reporter gene was detected by performing a CAT assay (37^{0}C; 2 hours) on 20μg protein extract from each transfection. Promoter activity for each sample was calculated as a percentage of the average value obtained from the control (*Slc11a1* promoter construct alone). (A) Illustration of the pHB8, pHB8Sp1M, pHB20 & pHB23 *Slc11a1* promoter constructs (see key). (B) 1μg of the *Slc11a1* promoter constructs pHB20 & pHB23 were co-transfected with increasing amounts of p300 DNA (0, 0.1, 0.2, 0.5, 1, 1.5 and 2μg), DNA concentrations were made up to 3μg with the pBABE empty vector. Students T-test comparing p300 responsiveness of pHB20 and pHB23 *P<0.05, **P<0.005, ***P<0.0005; n=4. (C) 1μg of the *Slc11a1* promoter constructs pHB8 & pHB8Sp1M were co-transfected with increasing amounts of p300 DNA (0, 0.1, 0.2, 0.5, 1, 1.5 and 2μg), DNA concentrations were made up to 3μg with the pBABE empty vector, Students T-test comparing p300 responsiveness of pHB8 and pHB8Sp1M ♦P<0.05, ♦♦P<0.005; n=2-4.

(B)

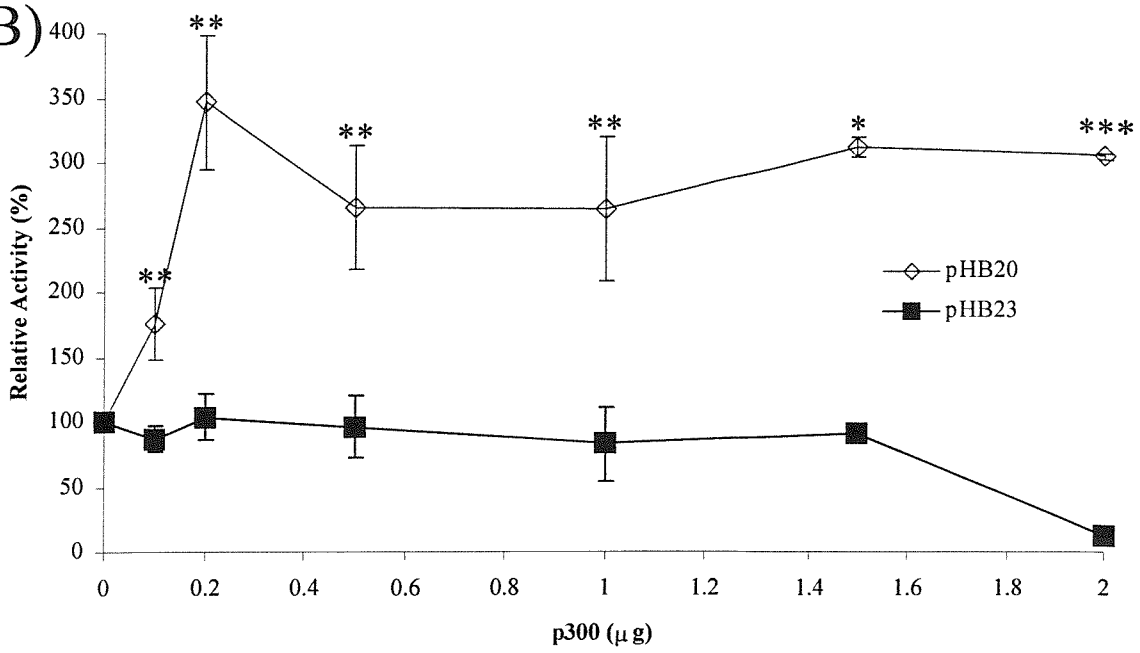
Relative Activity (%)
400
350
300
250
200
150
100
50
0
0
0.2
0.4
0.6
0.8
1
1.2
1.4
1.6
1.8
2
p300 (μg)
**
**
**
**
*
***
pHB20
pHB23

(C)

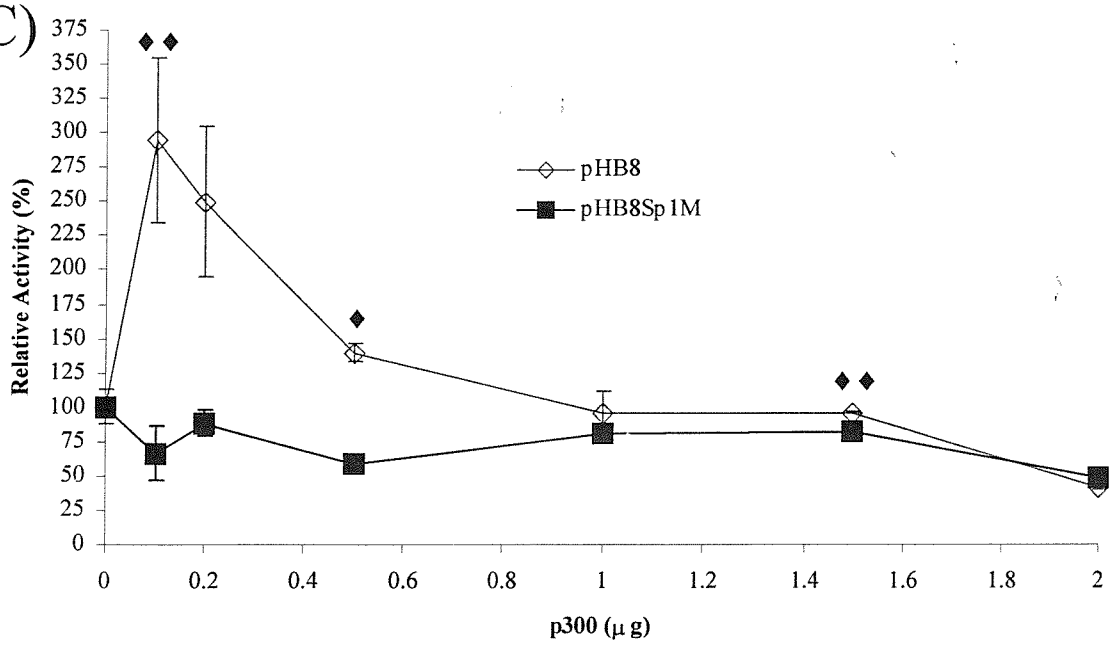
Relative Activity (%)
375
350
325
300
275
250
225
200
175
150
125
100
75
50
25
0
0
0.2
0.4
0.6
0.8
1
1.2
1.4
1.6
1.8
2
p300 (μg)
pHB8
pHB8Sp1M

5.3 DISCUSSION

Chapter 4 established that the proto-oncogene c-Myc can repress transcription of the *Slc11a1* gene. Promoter studies on the *AdMLP* (Peukert *et al.* 1997) and $p15^{ink4b}$ (Staller *et al.* 2001) genes, which are both repressed by c-Myc via a mechanism involving the Inr element, have implicated the transcription factor Miz-1 as being involved in gene regulation. Data presented here show that overexpression of exogenous Miz-1 was able to overcome the repressive effects of c-Myc on the *Slc11a1* promoter (figure 5.2.1-B); and furthermore Miz-1 was able to transactivate the *Slc11a1* promoter (figure 5.2.2). However, efficient transactivation was only observed in *Slc11a1* promoter constructs devoid of EMS, with levels of transactivation being inversely proportional to the number of EMS sites within the promoter (figure 5.2.3). Interestingly the previously reported Miz-1 transactivation studies were performed on EMS-less promoters, in the *AdMLP* studies (Peukert *et al.* 1997) a promoter construct used contained the Inr element but none of the documented EMS sites, whereas the $p15^{ink4b}$ promoter was not reported to contain any EMS sites (Staller *et al.* 2001). These data suggest that the presence of EMS sequences within the promoter interfere with the ability of Miz-1 to transactivate the *Slc11a1* promoter, although the ability of Miz-1 to antagonise c-Myc-induced repression is maintained. As c-Myc can repress transcription in a mechanism that involves interference of Miz-1 function, the reasoning that EMS within the promoter would affect this is may be due to EMS bound c-Myc binding to, and preventing efficient transactivation by, Inr bound Miz-1. c-Myc is commonly used to transform primary cells, therefore in many cell lines the levels of endogenous c-Myc, USF and Max, are higher than would be seen in primary cells (Littlewood *et al.* 1992). c-Myc levels are also reported to be increased immediately after transfection (Claassen and Hann, 2000). Therefore in cell lines, especially after transfection, c-Myc levels are elevated above what would be expected in primary cells. *In vivo Slc11a1* is expressed in fully differentiated macrophage cells (see section 1.1.5) where *c-Myc* levels are downregulated (reviewed Nasi *et al.* 2001; figure 4.2.3) or uncoupled from its protein partner Max (Ayer and Eisenman, 1993). Under these conditions Miz-1 would be expected to transactivate the endogenous EMS containing *Slc11a1* promoter, as you would expect minimal interference by endogenous c-Myc. Miz-1 does not contain a

functional NLS (Peukert *et al.* 1997) therefore both the endogenous and the exogenous protein are reported to localise to the cytoplasm (Peukert *et al.* 1997; Ziegelbauer *et al.* 2001). Association of Miz-1 with either c-Myc or p300 has been shown to induce nuclear import (Peukert *et al.* 1997), as has microtubule destabilisation (Ziegelbauer *et al.* 2001). Miz-1 nuclear entry in therefore tightly controlled, and this tight regulation enables regulation within the nucleus by elevated endogenous proteins, such as c-Myc, a situation that does not normally occur within over-expression studies.

In agreement with this proposal the microtubule destabilising drug nocodazole increased both *Slc11a1* promoter activity and protein expression in macrophage-like cell lines (figure 5.2.4). However, within primary bone marrow derived macrophages nocodazole had only a very slight effect on Slc11a1 protein expression (figure 5.2.5, lane 4), furthermore the microtubule stabilising drug, taxol, which was used as a control dramatically induced Slc11a1 protein expression (figure 5.2.5, lane 3). In macrophages taxol (paclitaxel) is documented to be a mimetic of bacterial LPS, inducing normal host responses (Manthey *et al.* 1992). The basis for the discrepancy between the responses of macrophage cell lines and primary macrophages to microtubule altering drugs is unclear. However it may indicate that primary bone marrow derived macrophages are more primed for activation than macrophage cell lines.

c-Myc represses transcription by binding to Miz-1 and preventing recruitment of the coactivator p300, as the binding sites for c-Myc and p300 on Miz-1 overlap (Staller *et al.* 2001). Data presented within this report show that p300 can transactivate the *Slc11a1* promoter alone (figure 5.2.11-B) and furthermore, can cooperate with Miz-1 to further enhance transcription (figure 5.2.10). Unlike Miz-1, the presence of EMS within the promoter do not dramatically affect the p300-mediated transactivation of the *Slc11a1* promoter (figure 5.2.11-B), possibly due to higher nuclear levels of exogenous p300 than Miz-1. However the presence of the EMS does appear to alter the amount of p300 required to induce similar levels of induction, increasing with the number of EMS present within the sequence (figure 5.2.11-C), suggesting that c-Myc bound to the EMS is interfering with transactivation. This maybe due to binding of endogenous c-Myc to endogenous Inr bound Miz-1, preventing p300 recruitment.

Alternatively endogenous c-Myc may bind to and sequester p300, again preventing recruitment of p300 to the start site of transcription. The effect of EMS on Miz-1 transactivation is more pronounced than the effect of EMS on p300 transactivation, however the opposite is observed by mutation of the consensus Sp1-binding site.

Deletion of the region between –71bp to –19bp removes the consensus Sp1 binding site, this deletion abrogates both the Miz-1 (figure 5.2.8) and p300 (figure 5.2.12-B) mediated transactivation of the *Slc11a1* promoter. Mutation of this site however only reduces Miz-1-mediated transactivation of the *Slc11a1* promoter (figure 5.2.9) whereas it completely abrogates the p300-mediated transactivation (figure 5.2.12-C). Deletion of the region between –71bp to –19bp does not specifically remove the consensus Sp1-binding site, other transcription factor binding sites are also removed by this deletion, these include binding sites for the Myeloid zinc finger protein, the GA-binding protein and the aryl hydrocarbon heterodimer The difference observed between deletion and mutation of the consensus Sp1-binding site on Miz-1 mediated transactivation is possibly due to the removal of other transcription factor binding sites, suggesting that proteins binding to at least one other site, apart from the consensus Sp1-binding site, are important in the Miz-1 mediated transactivation. Abrogation of p300 induced transactivation by deletion or mutation of the consensus Sp1-binding site suggests that p300 is involved in complex formation at the promoter as opposed to just augmenting the nuclear import of Miz-1.

Sp1 cannot transactivate the *Slc11a1* promoter alone (figure 5.2.6). A possible explanation for this is that Sp1 levels within the cell are reported to be in excess and constitutively bound to sites within target genes (reviewed Black *et al.* 2001). In order for Sp1 to transactivate target genes it is required to be activated by a second signal, such as that from TGFβ. Treatment of cells with TGFβ (figure 5.2.7-B) or TGFβ and exogenous Sp1 (data not shown) had no effect on promoter activity, suggesting that, in the Cos-1 cell line at least, Sp1 is unable to transactivate the *Slc11a1* promoter. The reason for this is unclear, however it is well documented that although ubiquitous Sp1 is preferentially expressed in haematopoietic cells (Saffer *et al.* 1991). Sp1 is also intimately involved in promoting the temporal and spatial expression of target genes, in particular in directing the expression of myeloid specific

genes (reviewed Black *et al.* 2001; Tenen *et al.* 1997). The mechanism of this has not been fully elucidated but it has been reported to be due to selective promoter binding (Chen *et al.* 1993) and/ or posttranslational modifications of Sp1, specifically phosphorylation (Zhang *et al.* 1994). Data presented here suggests that binding to the consensus Sp1-binding site does occur, as deletion/ mutation of the consensus Sp1-binding site affects both Miz-1 and p300 mediated transactivation of the *Slc11a1* promoter. Whether the factor bound to the consensus Sp1-binding site is Sp1, and if so whether this protein is in its active form is the subject of ongoing research.

CHAPTER 6

Slc11a1 Promoter Polymorphism

6.1 INTRODUCTION

The human SLC11A1 gene was isolated using a mouse *Slc11a1* cDNA probe to screen a human spleen cDNA library, and the isolated cDNA was subsequently mapped to a region of conserved synteny on the long arm of human chromosome 2g35 using synthetic oligonucleotides derived from the human SLC11A1 cDNA (Cellier *et al.* 1994). The isolated SLC11A1 cDNA encodes a highly hydrophobic 550 amino acid protein with high sequence similarity to the murine Slc11a1 protein (82% identical, 93% overall sequence similarity). The hydrophobic core is highly conserved between the two proteins, with the amino and carboxy terminals showing the most variation. Furthermore the substitutions observed are clustered within discreet domains. Hydropathy profiles suggest that like the murine protein human SLC11A1 contains a minimum of 10 and a maximum of 12 TMD. The "binding protein-dependent transport system inner membrane component signature" (CTM) locates to the intra-cytoplasmic loop between TMD 6 and 7 (residues 373-392), whereas the putative sites for N-linked glycosylation are located on the extra-cytoplasmic loop between TMD 5-6 (residues 224 and 238). The predicted PKC phosphorylation sites within the hydrophobic core of the murine Slc11a1 protein are not conserved within the human protein. However, one of the 3 putative PKC phosphorylation sites found within the amino terminal of the murine Slc11a1 protein (Barton *et al.* 1994) is conserved at position 54 within the human protein. Like the murine Slc11a1 protein, expression studies isolate SLC11A1 mRNA from peripheral blood leukocytes (PBL) and cells of the reticuloendothelial system (spleen and liver), unlike the murine protein, high expression levels are also observed in the lungs. Considering, the pattern of expression observed it is concluded that like the murine protein, human SLC11A1 is restricted to cells of the monocyte/macrophage lineage. *In vitro* studies using cell lines representative of immature precursors of the myelomonocytic lineage blocked by immortalisation/transformation at different stages of differentiation, and a T-cell leukaemia cell line, detect SLC11A1 expression in all of the cells tested (Cellier *et al.* 1994; Kishi *et al.* 1996). Furthermore, commitment of cell toward phagocytic type correlates with SLC11A1 expression, the more committed the cell, the higher the expression (Cellier *et al.* 1994). These data are

confirmed by Cannone-Hergaux *et al.* (2002), who show that human SLC11A1 expression does not occur until late in neutrophil maturation.

Population genetics reveal that the SLC11A1 gene, and in some cases specific SLC11A1 alleles, are associated with a variety of infectious and autoimmune diseases including, rheumatoid arthritis (Shaw *et al.* 1996), Crohn's disease and ulcerative colitis (Kojima *et al.* 2000), multiple sclerosis (Kotze *et al.* 2001), tuberculosis and leprosy (reviewed Blackwell *et al.* 2001). As yet, no mutation has been found within the human SLC11A1 protein that is comparable with the G169D mutation found within the murine protein however, population genetics have identified a polymorphic potential Z-DNA forming dinucleotide repeat within the 5' promoter region of the SLC11A1 gene (figure 6.1.1) (Blackwell *et al.* 1995) and a highly polymorphic region within the 3'UTR (Lui *et al.* 1995). Reporter gene studies on the four identified alleles provide evidence that the promoter polymorphism is a functional polymorphism, with all four allele driving differential expression of the reporter gene (Searle and Blackwell, 1999). Alleles 1, 2 and 4 drive poor expression, whereas allele 3 drives high expression of the luciferase reporter gene. Furthermore, alleles 2 and 3, which represent the two most common alleles in the population studied, (gene frequencies of 0.2-0.25 and 0.75-0.8 respectively), are differentially regulated by bacterial LPS. LPS represses allele 2 driven expression, whereas it enhances allele 3 driven expression. Upregulation of allele 3 by bacterial LPS indicates it may be play a protective role against infectious disease susceptibility however, allele 3 has also been linked to autoimmune disease susceptibility (Searle and Blackwell, 1999; Kotze *et al.* 2001). A role for SLC11A1 allele 3 (and possibly alleles 5 and 7) in autoimmune disease susceptibility has been proposed due to the highly conserved sequence and expression patterns between the murine and human proteins. As discussed, the murine Slc11a1 protein has many pleiotropic effects on macrophage activation and cellular iron levels (reviewed Blackwell *et al.* 2000; Blackwell *et al.* 2001). It is these effects of Slc11a1 that potentially contribute to the inflammatory response and pathology associated with diseases such as rheumatoid arthritis (RA), Multiple sclerosis (MS), and the inflammatory bowel diseases (IBS) Crohn's disease and ulcerative colitis. High levels of SLC11A1 expression driven by specific promoter alleles could potentially lead to chronic macrophage activation, thereby triggering the onset of autoimmune disease. The potential role of SLC11A1 in

protection against infectious disease is however less well understood, although a clear association has been made between SLC11A1 alleles and pulmonary tuberculosis in man, the murine *Slc11a1* gene confers no protection to primary infection with *Mycobacterium tuberculosis* to the mice (reviewed North and Medina, 1998). In a Malawian population, vaccination against BCG also provides an SLC11A1 associated protection against *M. leprae* (leprosy) in a number of individuals. This has led to the proposal that SLC11A1 maybe functionally linked to the priming/vaccinating exposures to specific infectious diseases.

This chapter describes the identification of a potential Z-DNA forming dinucleotide repeat within the murine *Slc11a1* promoter region within a region that aligns with the polymorphic region of the human SLC11A1 promoter. The identified repeat is biallelic and appears to be in linkage disequilibrium with the point mutation causing the G169D amino acid substitution within the coding region of the gene. Reporter studies have revealed the polymorphism is functional, with the D169-linked allele driving 3-fold higher expression than the G169-linked allele.

ALLELE	SEQUENCE	REFERENCE
1	$T(GT)_5AC(GT)_5AC(GT)_{11}GGCAGA(G)_6$	Blackwell *et al.*1995
2	$T(GT)_5AC(GT)_5AC(GT)_{10}GGCAGA(G)_6$	Blackwell *et al.*1995
3	$T(GT)_5AC(GT)_5AC(GT)_{09}GGCAGA(G)_6$	Blackwell *et al.*1995
4	$T(GT)_5AC(GT)_5$----------$GGCAGA(G)_6$	Blackwell *et al.*1995
5	$T(GT)_4AC(GT)_5AC(GT)_{11}GGCAGA(G)_6$	Graham *et al.*2000
6	$T(GT)_5AC(GT)_5AC(GT)_4AT(GT)_4GGCAGA(G)_7$	Graham *et al.*2000
7	$T(GT)_5AC(GT)_5AT(GT)_{11}GGCAGA(G)_6$	Kojima *et al.* 2001

FIGURE 6.1.1 Summary of the 5' Promoter Polymorphisms Alleles within the Human *SLC11A1* Promoter. Table summarising the polymorphic sequence for each of the 7 identified alleles.

6.2 RESULTS

6.2.1 Analysis of the *Slc11a1* Gene between Inbred Strains of Mice: Identification of a Biallelic Promoter Polymorphism

Analysis of the pS3 murine *Slc11a1* promoter sequence identified a GT repeat region between -315bp and -368bp. Computer assisted analysis (figure 6.2.1) reveals that this region aligns with the human SLC11A1 promoter polymorphism, which lies between -274bp and -317bp (Searle and Blackwell, 1999). pS3 was isolated from a B6/CBAF1Jλ FixII library, in order to ascertain whether the murine GT repeat was polymorphic, as is the case with the human repeat, it was necessary to clone and sequence the -315bp to -368bp region of the murine *Slc11a1* promoter from a variety of inbred strains of mice.

pHB-BALB/c, pHB-DBA, pMP-C57BL/6, pMP-CBA and pMP-C3H

Genomic DNA was isolated from 5 strains of inbred mice, BALB/cJ, DBA1/J, C57BL/6J, CBA/J and C3H/HeJ (section 2.2.13). A 0.7Kbp region of the *Slc11a1* promoter spanning from EMS#5 at position -588bp to the ATG translational start site immediately downstream of exon 1 at position +99bp was amplified from the genomic DNA using the synthetic oligonucleotides 5'-MYC5S (5'-CATTGCTGTAAACAT**GAATTC**GAGGTTTTTGTTTGG-3') and 3'-HB#1 (5'-ATGC**GGATCC**TAATCAAGAGGACGCAGG-3'). The resulting 0.7Kbp fragments obtained from the genomic DNA of the inbred mice were TA-cloned into the pGEM-T-EASY vector (Promega, UK). The resulting plasmids were designated pHB-BALB/c, pHB-DBA, pMP-C57BL/6, pMP-CBA and pMP-C3H respectively[11].

The plasmids were sequenced using the Sanger dideoxy method as described (section 2.2.14), using the GT-AS synthetic oligonucleotide (5'-TCCATAATAAGTCTGGCC-3'), gels were visualised via autoradiography, an example gel can be seen in figure 6.2.2-B. Sequence analysis revealed the identified GT repeat region to be biallelic furthermore, as summarised in figure 6.2.2-A, the two identified alleles appear to be in linkage with the G169D Slc11a1 protein mutation.

[11] Michael Patterson, an undergraduate project student 2000-2001, produced pMP-C57BL/6, pMP-CBA and pMP-C3H.

The two alleles have been termed the G169-linked Allele (CBA/J and C3H/HeJ), and the D169-linked Allele (BALB/c, DBA and C57BL/6). The G169-linked Allele contains the sequence 5'-TGCG$(GT)_{22}C(GT)_3$-3', whereas the D169-linked Allele contains the sequence 5'$(GT)_{27}C(GT)_3$-3'. This polymorphism results in the D169-linked allele being 6bp longer than the G169-linked allele. A 6bp difference in promoter length introduces a 216^0 angular difference and a $20.4A^0$ spatial difference between distal and proximal promoter binding sites between the two alleles.

6.2.2 The G169-Linked and D169-Linked Alleles Promote Differential Reporter Gene Expression

Sequence analysis of the promoters from inbred strains of mice has revealed that the pS3 sequence is derived from the C57BL/6J inbred stain of mouse. The *Slc11a1* promoter constructs pHB1, pHB4, pHB5, pHB6, pHB8, pHB20, pHB21, pHB22 and pHB23 are therefore also of C57BL/6J origin and contain the D169-linked Allele. In order to determine whether the identified polymorphism within the murine *Slc11a1* promoter is a functional one, an *Slc11a1* promoter construct containing the G169-linked Allele driving the CAT reporter gene was produced.

pHBC11 and pHBC12

A 1.654Kbp region from an XbaI site at –1555bp to a synthetic BamHI introduced immediately downstream of exon 1 at position +99bp was amplified from CBA genomic DNA via the PCR, using the synthetic oligonucleotides 5'-HB#2 (5'-TTTGCT**TCTAGA**ATGTTG-3') and 3'-HB#1. HB#2 inserts an XbaI restriction endonuclease recognition site, where as HB#1 inserts a BamHI restriction endonuclease recognition site. The insertion of this synthetic BamHI site also converts the ATG translational initiation codon to TTG. The amplified region of the promoter was cloned via XbaI and BamHI into the plasmid pBS (pHBC12) for subcloning, and into the CAT reporter plasmid pBLCAT3 (pHBC11-see figure 6.2.3-A). pHBC11 is the CBA/J derivative of pHB4.

The *Slc11a1* promoter constructs pHB4 and pHBC11 were transfected into the Cos-1 cell line using the LipofectAMINE (LA) (section 2.2.7). Figure 6.2.4 illustrates pHB4 (D169-linked allele) promotes a 2.99±0.85-fold higher basal reporter gene

activity (P=0.0000283) than pHBC11 (G169-linked allele) in the Cos-1 cell line (closed bars), this pattern of expression in mirrored in the RAW 264.7 cell line (open bars).

6.2.3 Deletion of the Polymorphic Region Abolishes the Difference in Promoter Activity between the Two Alleles

The difference in activity observed between the two *Slc11a1* promoter alleles is predicted to be due to the polymorphic region between -315bp and -368bp. If this is the case then deletion of this region should abrogate the differences observed between the two alleles. In order to assess this a derivative of the G169-Linked Allele *Slc11a1* promoter construct lacking the polymorphic region was produced.

pHBC25

An SphI restriction digest on pHBC11 removes the 1.484Kb region from the 5'-vector arm SphI site, immediately upstream of the XbaI site at -1555bp, to the SphI site at -71bp (see figure 6.2.3-B). This 5' truncation removes all 6-candidate E-box c-Myc-Max binding sites and the di-nucleotide GT-repeat. pHBC25 is the CBA/J derivative of pHB8.

The *Slc11a1* promoter constructs pHB8 and pHBC25 were transfected into the Cos-1 cell line using the LipofectAMINE (LA) (section 2.2.7). Preliminary data (figure 6.2.5) suggests that the activity of pHB8 (D169-linked allele) and pHBC25 (G169-linked allele) are not different in either the Cos-1 (closed bars) or the RAW 264.7 (open bars) cells lines. A summary of relative promoter activity between the two identified alleles, the D169-Linked Allele (C57BL/6J) and the G169-Linked Allele (CBA/J), can be seen in figure 6.2.6. These data suggest that the difference in promoter activity observed between the 1.645Kbp *Slc11a1* promoter alleles, pHB4 and pHBC11, is due to the polymorphic di-nucleotide repeat between –315bp and –368bp, as deletion of this region removes the observed difference.

6.2.4 The Two Alleles are repressed equally by c-Myc

The *Slc11a1* promoter constructs pHB4 and pHBC11 were transfected into the Cos-1 cell line using the LipofectAMINE reagent following the manufacturers' instructions (section 2.2.7). Cells were co-transfected with a constant amount (1μg) of the *Slc11a1* promoter constructs and increasing amounts of c-Myc DNA (0, 0.5, 1, 1.5 and 2μg), the DNA concentrations were made up to 3μg using the pBABE empty vector. Cells were left for 48 hours before being assayed for CAT activity (section 2.2.9). Figure 6.2.7-A shows that the difference in activity between the two promoter constructs becomes insignificant with increasing c-Myc. Furthermore, calculating promoter activities relative to the controls (either pHB4 alone or pHBC11 alone) for each sample shows no significant difference between the samples (Figure 6.2.7-B). The promoters from the two alleles are therefore equally responsive to the repressive effects of c-Myc.

6.2.5 Responsiveness of the 1.654Kbp *Slc11a1* Promoter Constructs to Miz-1 is Unaffected by the Polymorphism

The *Slc11a1* promoter constructs pHB4 and pHBC11 were transfected into the Cos-1 cell line using the LipofectAMINE reagent (section 2.2.7). Cells were co-transfected with a constant amount (1μg) of the *Slc11a1* promoter constructs and increasing amounts of Miz-1 DNA (0, 0.5, 1, 1.5 and 2μg); the DNA concentrations were made up to 3μg using the pBABE empty vector. Cells were left for 48 hours before being assayed for CAT activity (section 2.2.9). Figure 6.2.8 shows there is no significant difference in the response of the two promoter alleles to Miz-1, suggesting that it is the EMS sites downstream of the polymorphism (EMS#5 and EMS#6) that are most influential in controlling responsiveness to Miz-1.

FIGURE 6.2.1 Sequence Alignment of the Murine and Human *Slc11a1* Promoters. Human (top line) and Mouse (bottom line) *Slc11a1* promoter sequences were aligned. The position of the GT dinucleotide repeat has been highlighted in light grey, and the conserved consensus Sp1-binding site in dark grey. Transcribed sequences are underlined, and the translational start codon highlighted in bold. Double dots (:) indicate conserved nucleotides.

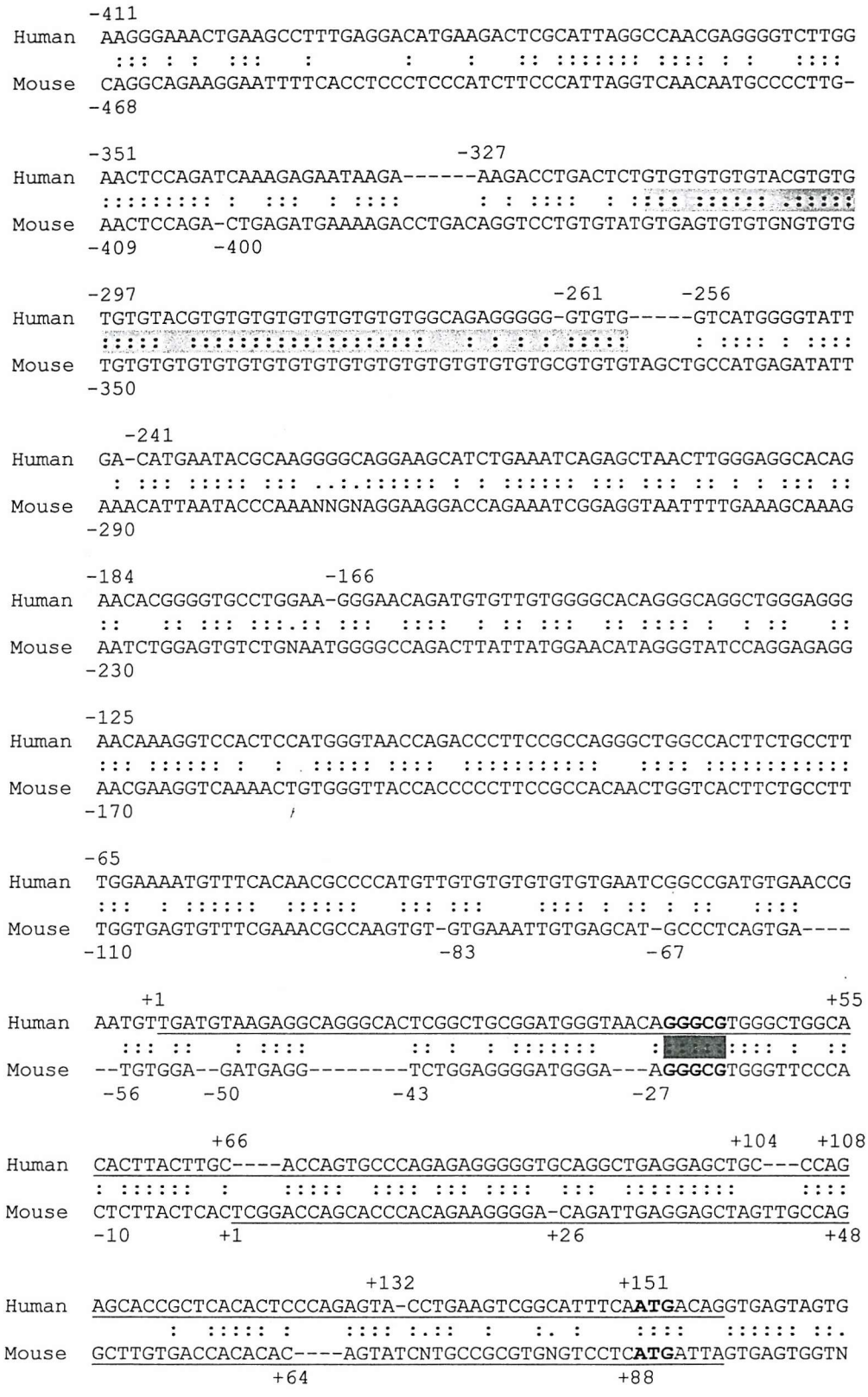
-411
Human AAGGGAAACTGAAGCCTTTGAGGACATGAAGACTCGCATTAGGCCAACGAGGGGTCTTGG
Mouse CAGGCAGAAGGAATTTTCACCTCCCTCCCATCTTCCCATTAGGTCAACAATGCCCCTTG-
-468
-351 -327
Human AACTCCAGATCAAAGAGAATAAGA------AAGACCTGACTCTGTGTGTGTGTACGTGTG
Mouse AACTCCAGA-CTGAGATGAAAAGACCTGACAGGTCCTGTGTATGTGAGTGTGTGNGTGTG
-409 -400
-297 -261 -256
Human TGTGTACGTGTGTGTGTGTGTGTGTGGCAGAGGGGG-GTGTG-----GTCATGGGGTATT
Mouse TGTGTGTGTGTGTGTGTGTGTGTGTGTGTGTGTGCGTGTGTAGCTGCCATGAGATATT
-350
-241
Human GA-CATGAATACGCAAGGGGCAGGAAGCATCTGAAATCAGAGCTAACTTGGGAGGCACAG
Mouse AAACATTAATACCCAAANNGNAGGAAGGACCAGAAATCGGAGGTAATTTTGAAAGCAAAG
-290
-184 -166
Human AACACGGGGTGCCTGGAA-GGGAACAGATGTGTTGTGGGGCACAGGGCAGGCTGGGAGGG
Mouse AATCTGGAGTGTCTGNAATGGGGCCAGACTTATTATGGAACATAGGGTATCCAGGAGAGG
-230
-125
Human AACAAAGGTCCACTCCATGGGTAACCAGACCCTTCCGCCAGGGCTGGCCACTTCTGCCTT
Mouse AACGAAGGTCAAAACTGTGGGTTACCACCCCCTTCCGCCACAACTGGTCACTTCTGCCTT
-170
-65
Human TGGAAAATGTTTCACAACGCCCCATGTTGTGTGTGTGTGTGAATCGGCCGATGTGAACCG
Mouse TGGTGAGTGTTTCGAAACGCCAAGTGT-GTGAAATTGTGAGCAT-GCCCTCAGTGA----
-110 -83 -67
+1 +55
Human AATGTTGATGTAAGAGGCAGGGCACTCGGCTGCGGATGGGTAACAGGGCGTGGGCTGGCA
Mouse --TGTGGA--GATGAGG--------TCTGGAGGGGATGGGA---AGGGCGTGGGTTCCCA
-56 -50 -43 -27
+66 +104 +108
Human CACTTACTTGC----ACCAGTGCCCAGAGAGGGGGTGCAGGCTGAGGAGCTGC---CCAG
Mouse CTCTTACTCACTCGGACCAGCACCCACAGAAGGGGA-CAGATTGAGGAGCTAGTTGCCAG
-10 +1 +26 +48
+132 +151
Human AGCACCGCTCACACTCCCAGAGTA-CCTGAAGTCGGCATTTCAATGACAGGTGAGTAGTG
Mouse GCTTGTGACCACACAC----AGTATCNTGCCGCGTGNGTCCTCATGATTAGTGAGTGGTN
+64 +88

(A)

STRAIN	RESISTANCE TO INTRACELLULAR INFECTIONS	AMINO ACID AT POSITION 169	GT DINUCLEOTIDE REPEAT SEQUENCE.
BALB/cJ	**S**	**Asp**	5'$(GT)_{27}C(GT)_3$-3'
DBA1/J	**S**	**Asp**	5'$(GT)_{27}C(GT)_3$-3'
C57BL/6J	**S**	**Asp**	5'$(GT)_{27}C(GT)_3$-3'
CBA/J	**R**	**Gly**	5'-TGCG$(GT)_{22}C(GT)_3$-3'
C3H/HeJ	**R**	**Gly**	5'-TGCG$(GT)_{22}C(GT)_3$-3'

FIGURE 6.2.2 Sequence Analysis of the *Slc11a1* Promoter from a Range of Inbred Strains of Mice. Cloned DNA from 5 inbred strains of mice, BALB/cJ, DBA1/J, C57BL/6J, CBA/J and C3H/HeJ, were sequenced using the Sanger dideoxy method (section 2.2.14). (A) Table to summarise the strain of mouse, the resistance (R) or susceptibility (S) of the mouse to intracellular infections, the amino acid at position 169, and the GT repeat sequence between -315bp and -368bp of the *Slc11a1* promoter. (B) An example of the sequence obtained from a $Slc11a1^{D169}$ expressing mouse (C57BL/6J) and from a $Slc11a1^{G169}$ expressing mouse (CBA).

(B)

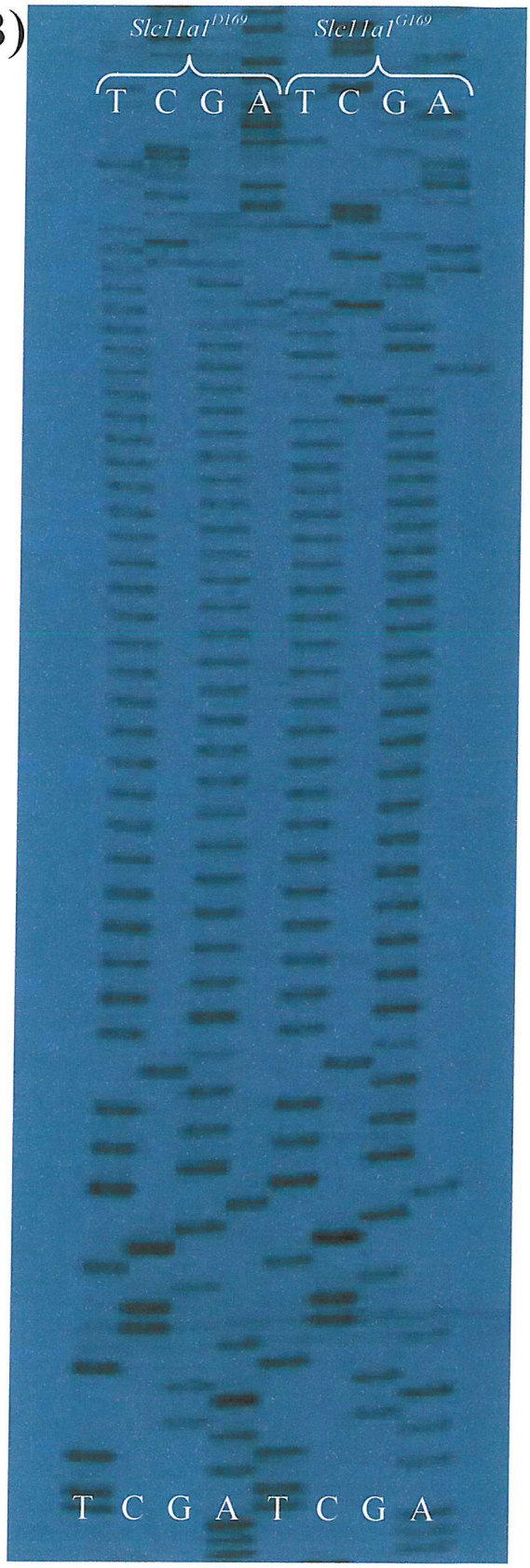

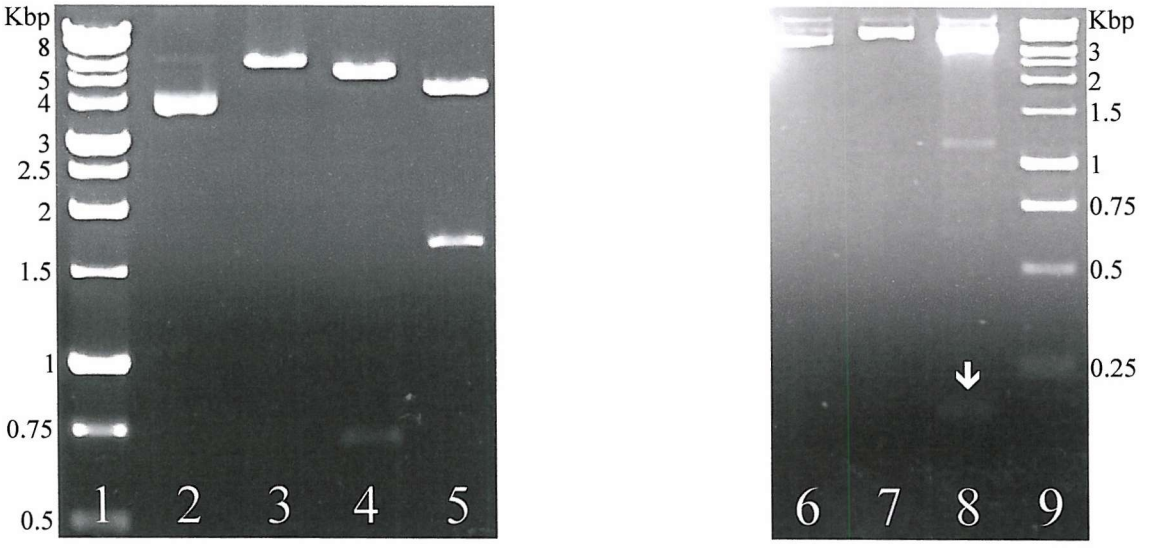

FIGURE 6.2.3 Restriction Digests Confirming the CBA Derived Clones pHBC11 & pHBC25. (A) pHBC11: 1µl of DNA mini-preparations were incubated at 37°C for 1 hour with 10U HindIII, 10U BamHI, or 10U BamHI and 8-12U XbaI restriction endonucleases (Promega, UK). Digests were loaded on a 1% Agarose-TBE gel containing 0.01% Ethidium Bromide, and run at 100V for 30-60 minutes. BamHI linearises the plasmid, HindIII drops out a 0.711Kbp fragment corresponding to the HindIII site within the 5' MCS and a HindIII site within the *Slc11a1* promoter, whereas BamHI/XbaI produces a 1.648Kbp fragment corresponding to the XbaI site at the 5' end of the *Slc11a1* promoter and the BamHI site within the multiple cloning site (MCS). (B) pHBC25: 1µl or 5µl of DNA mini-preparations were incubated at 37°C for 1 hour with 10U BamHI, or 10U BamHI and 10U SphI restriction endonucleases (Promega, UK). Digests were loaded on a 2% Agarose-TBE gel containing 0.01% Ethidium Bromide, and run at 100V for 30-60 minutes. BamHI linearises the plasmid whereas BamHI/SphI produces a 0.164Kbp fragment (indicated by a white arrow ⇩) corresponding to the synthetic BamHI site at the 3' end of the *Slc11a1* promoter and the SphI site within the *Slc11a1* promoter. (1), 1Kbp DNA ladder (Promega, UK); (2), pHBC11 uncut; (3), pHBC11-BamHI; (4), pHBC11-HindIII; (5), pHBC11-BamHI/XbaI; (6), pHBC25 uncut; (7), pHBC25-BamHI; (8), pHBC25-BamHI/SphI; (9), 1Kbp DNA ladder (Promega, UK).

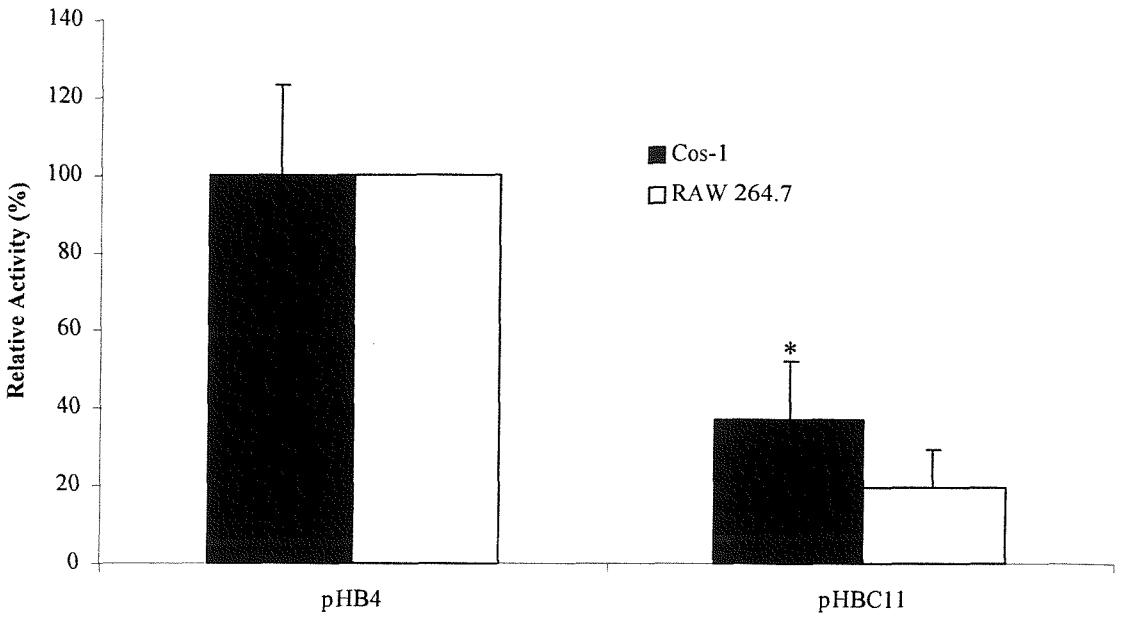

FIGURE 6.2.4 Expression of the *Slc11a1* Promoter Constructs pHB4 and pHBC11 within the Cos-1 & RAW 264.7 Cell Lines. Cos-1 (closed bars) & RAW 264.7 (open bars) cells were transfected as described (section 2.2.7) with 1μg of the *Slc11a1* promoter constructs pHB4 and pHBC11. Expression of the reporter gene was detected by performing a CAT assay at 37^{0}C for 2 hours on 20μg protein extract (Cos-1 cells) or at 37^{0}C for 6 hours on 50μg protein extract (RAW 264.7 cells). Promoter activity for each sample was calculated relative to pHB4. Students T-Test comparing pHB4 and pHBC11 in the Cos-1 cell line *P=0.0000283; n= 8 (Cos-1) & n=2 (RAW 264.7 cells).

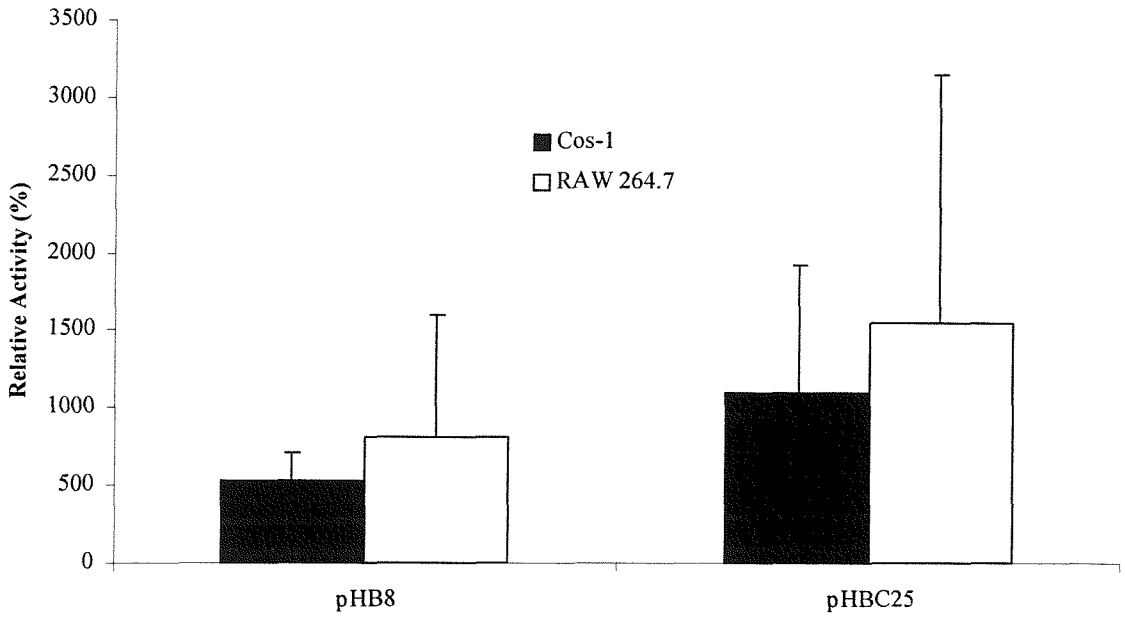

FIGURE 6.2.5 Expression of the *Slc11a1* Promoter Constructs pHB8 and pHBC25 within the Cos-1 & RAW 264.7 Cell Lines. Cos-1 (closed bars) & RAW 264.7 (open bars) cells were transfected as described (section 2.2.7) with 1μg of the *Slc11a1* promoter constructs pHB8 and pHBC25. Expression of the reporter gene was detected by performing a CAT assay at 37^{0}C for 2 hours on 20μg protein extract (Cos-1 cells) or at 37^{0}C for 6 hours on 50μg protein extract (RAW 264.7 cells), promoter activity for each sample was calculated relative to pHB4; n=2.

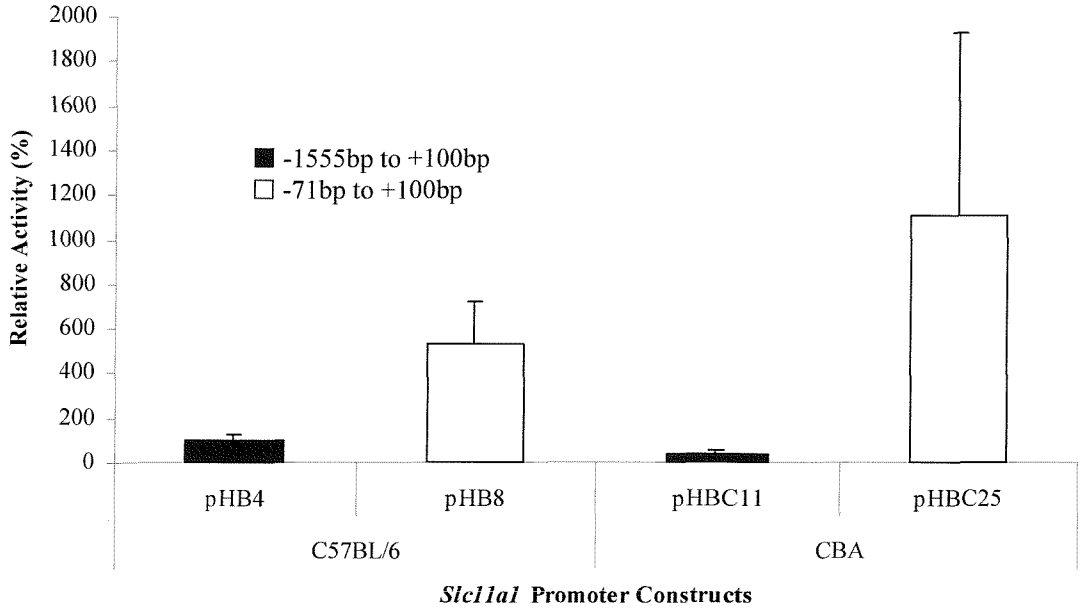

FIGURE 6.2.6 Comparison of the C57BL/6 & CBA *Slc11a1* Promoter Constructs pHB4, pHB8, pHBC11 & pHBC25 within the Cos-1 Cell Line. Cos-1 cells were transfected as described (section 2.2.7) with 1μg of the *Slc11a1* promoter constructs. Expression of the reporter gene was detected by performing a CAT assay at 37^0C for 2 hours on 20μg protein, Promoter activity for each sample was calculated relative to pHB4.

FIGURE 6.2.7 Repression of the *Slc11a1* Promoter Constructs pHB4 and pHBC11 with c-Myc in the Cos-1 Cell Line. Cos-1 Cells were co-transfected as described (section 2.2.7) with 1μg of the *Slc11a1* promoter construct (pHB4-Black diamonds/ pHBC11-Grey squares) and increasing amounts of c-Myc DNA (0, 0.5, 1, 1.5 and 2μg), DNA concentrations were made up to 3μg with the pBABE empty vector. Expression of the reporter gene was detected by performing a CAT assay (37^0C; 6 hours) on 20μg protein extract from each transfection. (A) Comparison of pHB4 & pHBC11 activity in response to c-Myc. Students T-Test comparing pHB4 with pHBC11, 0μg c-Myc ***P=0.00018; 0.5μg c-Myc **P=0.0295; 1μg c-Myc *P=0.01746; 1.5μg c-Myc P=0.0534; 2μg c-Myc P=0.087. (B) Promoter activity for each sample was calculated as a percentage of the average value obtained from the control (*Slc11a1* promoter construct alone). Students T-test comparing relative activity of pHB4 & pHBC25 0μg c-Myc P=0.654047; 0.5μg c-Myc P=0.228853; 1μg c-Myc P=0.065989; 1.5μg c-Myc P=0.275296; 2μg c-Myc P=0.865792. Students T-Test compared with pHBC11 alone ♦P<0.02; n= 9 (pHB4) and 3 (pHBC11)

(A)

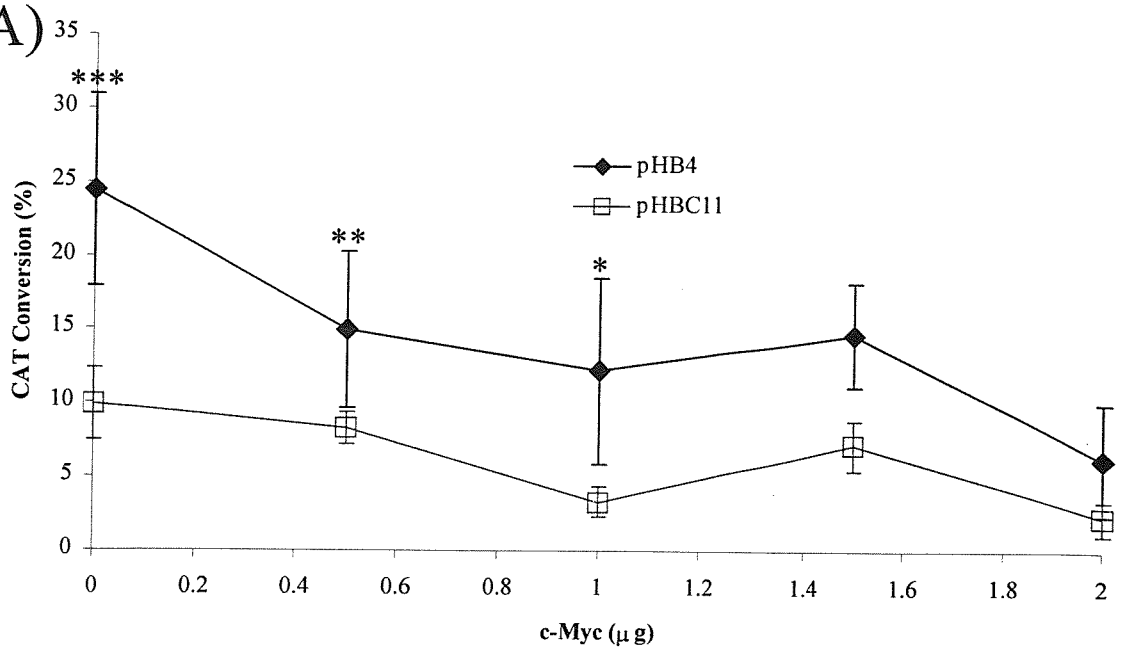
35
30
25
20
15
10
5
0
***
**
*
pHB4
pHBC11
CAT Conversion (%)
0
0.2
0.4
0.6
0.8
1
1.2
1.4
1.6
1.8
2
c-Myc (μg)

(B)

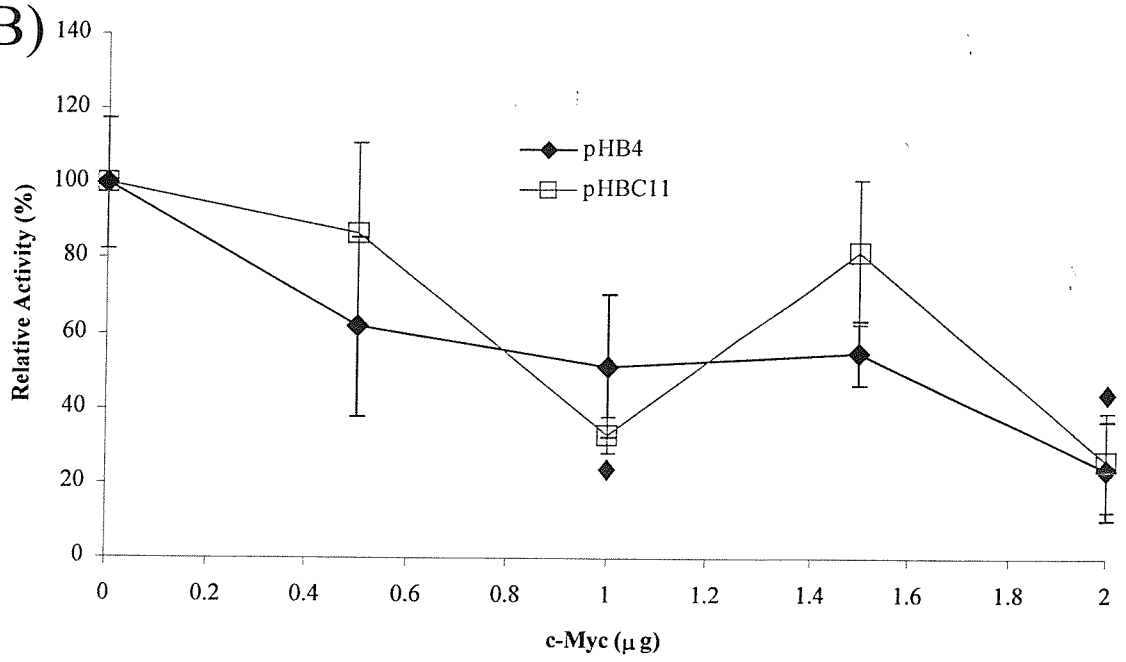
140
120
100
80
60
40
20
0
pHB4
pHBC11
Relative Activity (%)
0
0.2
0.4
0.6
0.8
1
1.2
1.4
1.6
1.8
2
c-Myc (μg)

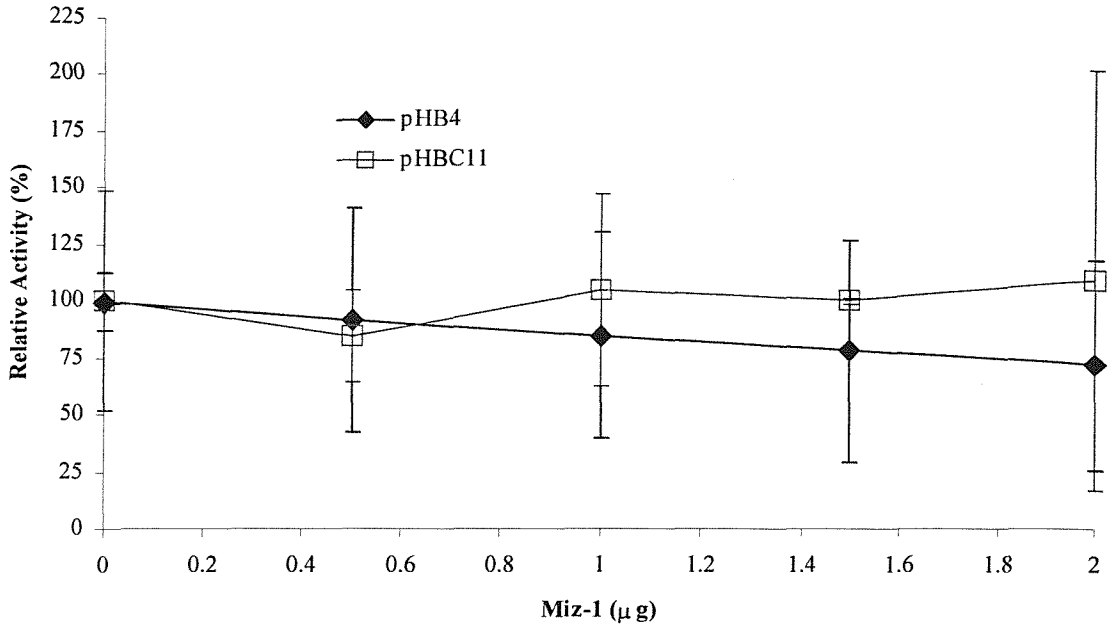

FIGURE 6.2.8 Effect of Miz-1 on the *Slc11a1* Promoter Constructs pHB4 and pHBC11 in the Cos-1 Cell Line. Cos-1 Cells were co-transfected as described (section 2.2.7) with 1μg of the *Slc11a1* promoter construct (pHB4-Black diamonds/ pHBC11-Grey squares) and increasing amounts of Miz-1 DNA (0, 0.5, 1, 1.5 and 2μg), DNA concentrations were made up to 3μg with the pBABE empty vector. Expression of the reporter gene was detected by performing a CAT assay (37^0C; 6 hours) on 20μg protein extract from each transfection. Student T-test comparing Miz-1 response between pHB4 & pHBC11 0μg Miz-1 P=0.993077; 0.5μg c-Myc P=0.732037; 1μg c-Myc P=0.6231; 1.5μg c-Myc P=0.276527; 2μg c-Myc P=0.667628; n=17 (pHB4) & n=2 (pHBC11).

6.3 DISCUSSION

The data presented here describe the identification of a GT dinucleotide repeat within the promoter region of the murine *Slc11a1* gene. Sequence analysis (figure 6.2.1) shows that this repeat region can be aligned with the polymorphic GT-repeat identified in human SLC11A1 (Blackwell *et al.* 1995). Analysis of this region from 5 inbred strains of mice have revealed this repeat to be polymorphic, with preliminary data suggesting the polymorphism may be biallelic, and that these two alleles may be in linkage with the G169D mutation within the *Slc11a1* protein (figure 6.2.2-A). Studies using *Slc11a1* promoter driven reporter constructs suggest that the polymorphism is a functional one; the D169-linked allele drives higher reporter gene expression than the G169-linked allele (figure 6.2.4). Deletion of the polymorphic region removes the difference in promoter activity between the two alleles (figure 6.2.5). These data confirm that the observed difference in promoter activity is a result of a functional promoter polymorphism. The polymorphism introduces a 6bp difference in promoter length, with the D169-linked allele being 6bp longer than the G169-linked allele. Transcription factor binding sites upstream of the promoter polymorphism therefore differ by an angle of 216^0, approximately half a turn of the helix, between the two alleles. The data suggest that upstream transcription factor binding sites within the D169-linked allele are appropriately situated to cooperate with the basal transcriptional machinery, thereby enhancing promoter activity. Corresponding sites within the G169-linked allele are therefore predicted to be in a position that does not enable such cooperation, thereby decreasing basal promoter activity. The situation may however be reversed for induced promoter activity. Many of the predicted binding sites for transcription factors involved in both the LPS/IFNγ and TGFβ-mediated signalling pathways lie upstream of the di-nucleotide repeat. It would therefore be of interest to see if the two murine alleles differ in their ability to be induced by such signalling pathways, a situation which has been observed between the human SLC11A1 promoter alleles (Searle and Blackwell, 1999).

The functional difference between the two alleles was also abrogated by the addition of c-Myc DNA in a dose dependent fashion (figure 6.2.7-A), furthermore the response of the alleles to c-Myc was not significantly different (figure 6.2.7-B), these

observations confirm the findings presented in chapter 4, that the 5 EMS sequences located upstream of the GT-repeat are not involved in the c-Myc mediated repression of *Slc11a1* expression. An equivalent response to Miz-1 treatment was also observed between the two alleles (figure 6.2.7-B), confirming the findings in chapter 5 that EMS#6 is most instrumental of the 6 EMS in mediating the Miz-1 response.

As mentioned, different levels of expression of the human SLC11A1 gene driven by the different promoter alleles have been linked to a variety of infectious and autoimmune diseases including, rheumatoid arthritis (Shaw *et al.* 1996), Crohn's disease and ulcerative colitis (Kojima *et al.* 2000), multiple sclerosis (Kotze *et al.* 2001), tuberculosis and leprosy (reviewed Blackwell *et al.* 2001). However, the human SLC11A1 protein does not have a non-conservative mutation equivalent to the G169D mutation seen within the murine protein, it is for this reason that the functional difference seen between the murine promoter polymorphism alleles may be of no significance. If the two alleles identified are in tight linkage with the G169D mutation within the protein, the stronger D196-linked promoter allele will be driving expression of a functionally null protein; the polymorphism would therefore have no functional consequence to gene expression. However, the polymorphism would be of functional consequence if the stronger D169-linked promoter allele were to drive expression of the G169-functional protein. It can be hypothesised that such a finding would provide a mouse model of the human SLC11A1 promoter polymorphism allele 3, which has been proposed to provide protection against infectious disease but susceptibility to autoimmune disease (Searle and Blackwell, 1999). Current models of autoimmune disease in mice are provided by the SJL and NOD mice which are genetically susceptible to experimental autoimmune encephalomyelitis (EAE) and insulin dependent diabetes (IDD) respectively, EAE provides a murine model of MS. Autoimmune diseases in humans and rodents are multigenic in nature, in which several gene products interact to initiate and propagate disease, and genome linkage analysis has suggested both MHC (H2) and non-MHC genes are associated with the autoimmune disease EAE (Butterfield *et al.* 1998). In order to assess the effects of non-MHC genes on susceptibility and progression of EAE the SJL/J and B10.S strains of mice are commonly used, both strains have the $H2^S$ haplotype but are susceptible and resistant to EAE respectively. One notable difference between the SJL and B10 strains is that they differ in their resistance to infectious disease, containing the

Slc11a1^{G169} and *Slc11a1*^{D169} alleles respectively (Plant and Glynn, 1974; Bradley, 1974; Gros *et al.* 1981; Malo *et al.* 1994). In humans, it is generally thought that a triggering event, such as a viral infection, combined with a genetic predisposition may trigger the onset of disease. If a similar situation occurs in the models of autoimmune disease provided by the SJL and NOD mice, a role for *Slc11a1* in the onset of disease can be proposed. If in the SJL and NOD mice functional Slc11a1 protein expression is driven by the stronger D169-linked promoter allele, the subsequent chronic macrophage activation resulting from high level Slc11a1 expression, induced by a pathogenic infection may, in a combination with other genetic factors, trigger the onset of an autoimmune response. Sequence analysis of the promoter region of the *Slc11a1* gene within the SJL and NOD inbred strains of mice may provide evidence to support this hypothesis.

CHAPTER 7

General Discussion and Future Work

7.1 GENERAL DISCUSSION

In this thesis the factors regulating *Slc11a1* expression have been examined, and a particular focus has been c-Myc and its associating proteins. This avenue of research has been pursued, following publication of a role for c-Myc in the control of genes that regulate the labile iron pool within cells (Wu *et al.* 1999). Previous work by our group has shown *Slc11a1* reduces the extent of iron within this pool (Atkinson and Barton, 1998 & 1999; Baker *et al.* 2000). The data presented here provide evidence for a temporal link between cellular growth, *c-Myc* expression and the onset of *Slc11a1* expression. Furthermore, *Slc11a1* promoter deletion studies have revealed that the basal activity of the promoter is repressed by factors, putatively c-Myc, but chromatin immunoprecipitation experiments will confirm this, binding to EMS#6 at –127bp. Deletion and mutagenesis of EMS#6 causes an increase in basal promoter activity. Similar observations have been made for the *fibroblast growth factor-binding protein (FGF-BP)* and *ABCA1* genes (Harris *et al.* 2000; Yang *et al.* 2002). Mitogen-induced expression of *FGF-BP* is transcriptionally repressed via a non-canonical EMS element (5'-AACGTG-3') and deletion of the EMS, which binds c-Myc, results in enhanced responsiveness to TPA treatment (Harris *et al.* 2000). Whereas an EMS motif within the proximal *ABCA1* promoter negatively regulates basal activity (Yang *et al.* 2002). Together these data can be applied to formulate a model for *Slc11a1* gene regulation involving transcriptional repression upon binding of c-Myc to EMS#6. However, deletion analysis of the *Slc11a1* promoter shows that c-Myc repression is maintained in the smallest active *Slc11a1* promoter construct, pHB23, which contains only 19bp of promoter sequence (figure 4.2.8-B). pHB23 contains the two identified Inr elements (Govoni *et al.* 1995), but none of the identified EMS sites. These data indicate that the dominant element for c-Myc repression is the Inr, however, the repressive activity is potentiated by EMS element(s) in cis.

During the course of these studies two alleles of the murine *Slc11a1* gene were identified that align with the functional variants in human (Searle and Blackwell, 1999). Furthermore, like the human promoter variants the two mouse alleles are also functionally polymorphic, and they are equally repressed by c-Myc, suggesting that c-

Myc mediates repression downstream of the promoter polymorphism. Together these data indicate that c-Myc represses the *Slc11a1* promoter via a mechanism involving the Inr, as has been noted for other c-Myc repressed genes (Peukert *et al.* 1997; Li *et al.* 1994; Peukert *et al.* 1997; Staller *et al.* 2001).

Studies into the mechanism of c-Myc induced repression have suggested that binding of c-Myc to Inr-bound Miz-1 blocks transcriptional activation by interfering with the recruitment of co-activators, such as p300, to the site of transcriptional initiation (Peukert *et al.* 1997; Seaone *et al.* 2001; Staller *et al.* 2001). Feng *et al.* (2002) have also reported that c-Myc can block transcription by forming a stable nucleoprotein complex with the Smad and Sp1 proteins at the $p15^{ink4b}$ gene promoter. Data presented within this thesis show that exogenous Miz-1 can overcome c-Myc induced repression of the *Slc11a1* promoter and that exogenous Miz-1 can transactivate *Slc11a1* in an EMS and consensus Sp-1 binding site-dependent fashion. The described model is probably also applicable to *Slc11a1*, as Miz-1-mediated transactivation is augmented by exogenous p300. p300 mediated transactivation of *Slc11a1* is EMS–independent, but dependent on a consensus Sp1 binding site. Comparison of these findings with the published data on the regulation of expression of other c-Myc-repressed genes has enabled us to propose a model of *Slc11a1* gene regulation under conditions of both active proliferation and differentiation, integrating known signalling pathways with Slc11a1 function.

Growth factors induce *c-Myc* expression within actively proliferating cells that drives G1-S phase progression, by a dual mechanism of gene activation and gene repression. Evidence that *Slc11a1* contributes to cell cycle arrest is from studies associated with ectopic expression of *Slc11a1* in which expressing cells show reduced proliferation. Two potential mechanisms for this repression have been proposed. The first mechanism involves a single c-Myc-Max heterodimer binding to EMS#6 and forming a complex with upstream proteins, potentially the Smad proteins, and the downstream Miz-1 molecule, thereby blocking gene expression (figure 7.1.1-A). The second involves two c-Myc-Max heterodimers binding to the *Slc11a1* promoter, one to EMS#6 and one to Inr-bound Miz-1. EMS#6 bound c-Myc forms a complex with, and blocks activation by upstream factors, possibly the Smad and Sp1 proteins as is the case for $p15^{ink4b}$ (Feng *et al.* 2002), whereas the Miz-1 bound c-Myc-Max

sterically blocks p300 recruitment by Miz-1, the overall result being transcriptional repression (figure 7.1.2-B).

The proposed model for the regulation of *Slc11a1* expression within differentiated cells is illustrated in figure 7.1.2 and is based on the proposed model of $p15^{ink4b}$ gene regulation (Seoane *et al.* 2001). Within differentiated cells c-Myc levels are low and c-Myc-repressed and –activated genes will be at high and low levels respectively. A decrease in c-Myc levels relieves the repression of Miz-1, allowing co-activators, such as p300, to bind and activate the basal transcriptional machinery (figure 7.1.2-A).

Slc11a1 expression is induced by ROS, IFNγ and LPS (Govoni *et al.* 1995; Atkinson *et al.* 1997; Govoni *et al.* 1997; Baker *et al.* 2000), and induction via the latter two is via a mechanism that mimics the *in vivo* response to intracellular infection. IFNγ and LPS signals are transduced via the Janus kinase (JAK)/ signal transducer and activator of transcription (STAT) signalling pathway (reviewed Lau and Horvath, 2002), whereas ROS signals can be transduced via both the JAK/STAT pathway and the MAP kinase pathway. Many STAT binding sites have been identified within the *Slc11a1* promoter (figure 3.2.1), and STAT1 and STAT3 are reported to interact with the Inr binding protein, TFII-I, in GST pull-down assays (Kim *et al.* 1998). Furthermore phosphorylation by JAK2 activates TFII-I, and this interaction is required for TFII-I to interact with the ERK proteins of the MAP kinase pathway (Kim *et al.* 2001). STAT1, the STAT protein involved in IFNγ signalling, is also reported to interact with p300 and Sp1 (reviewed Lau and Horvath, 2002), factors that have been implicated in promoting *Slc11a1* expression. Together these data suggest that under conditions of intracellular infection, signals transduced by both the JAK/STAT and MAP kinase signalling pathways could upregulate *Slc11a1* gene expression via activation of TFII-I.

Slc11a1 expression can also be induced by exogenous iron and RBC (Baker *et al.* 2000; Biggs *et al.* 2001), and a role for *Slc11a1* in iron homoeostasis and erythrophagocytosis has been proposed. Senescent erythrocytes do not undergo apoptosis as they don't express cytochrome C and do not contain nuclei or mitochondria. However, it is established that the presence of PS on the cell surface of

an erythrocyte triggers their recognition and clearance by resident macrophages within the spleen (reviewed Bratosin *et al.* 1998). Like removal of apoptotic cells, uptake of senescent erythrocytes is efficient and non-inflammatory. Inflammation is actively suppressed via the production of TGFβ, prostaglandin-E_2 (PGE_2) and IL-10. The PS-PS receptor interaction has been implicated in immunosuppression during apoptotic cell removal (reviewed Henson *et al.* 2001). Exposure of PS by senescent erythrocytes may not only trigger the cell for uptake by resident macrophages, but may also trigger the production of TGFβ, thereby preventing an inflammatory response. Here a role for TGFβ in the regulation of *Slc11a1* gene expression is proposed. Upon erythrophagocytosis of senescent erythrocytes the PS-PS receptor interaction induces the production of TGFβ, which activates the Smad signal transduction pathway. Activated Smad proteins bind with Sp1, p300 and Miz-1 at the promoter, forming an enhanceosome complex. Enhanceosomes form a stable platform for the recruitment of RNA polymerase, thereby driving transcription (figure 7.1.2-C).

There is much evidence to support a role for TGFβ in the regulation of *Slc11a1* gene expression. (i) The Slc11a1 protein has been implicated in iron homeostasis and RBC recycling (Baker *et al.* 2000; Biggs *et al.* 2001; Mulero *et al.* 2002), a process which stimulates the production of TGFβ. (ii) TGFβ transcriptionally represses *c-Myc* gene expression (reviewed Dennier *et al.* 2002). (iii) Vitamin D treatment enhances SLC11A1 gene expression (Roig *et al.* 2002). Vitamin D treatment also increases TGFβ production in neuroblastoma cells (Veenstra *et al.* 1997). (iv) Sequence analysis of the *Slc11a1* promoter identified both Smad and NFI binding sites, both of which are transcription factors involved in TGFβ signalling. Recently the Ets and C/EBP transcription factors have been implicated in the TGFβ induced activation of the IgA1 and IgA2 promoters (reviewed Dennier *et al.* 2002). (v) Chromatin immunoprecipitation (ChIP) assays and electophoretic mobility shift assays (EMSA) have shown the Miz-1, c-Myc and Max are all bound to the Inr region of the $p15^{ink4b}$ promoter before, but not after TGFβ treatment (Staller *et al.* 2001; Seoane *et al.* 2001). Data within this thesis highlight similarities between *Slc11a1* gene regulation and regulation of the $p15^{ink4b}$ gene, a gene which is stimulated by TGFβ.

This proposed model is however quite controversial as TGFβ functions as an anti-inflammatory agent and it is established that *Slc11a1* expression is upregulated by the pro-inflammatory agents IFNγ and LPS (Govoni *et al.* 1995; Atkinson *et al.* 1997; Govoni *et al.* 1997; Baker *et al.* 2000). During erythrophagocytosis an inflammatory reaction could lead to autoimmunity against erythrocytes, therefore TGFβ is protective against autoimmune disease. However, TGFβ has been implicated in T-helper (Th) subset differentiation, with a tendency to promote differentiation of $CD4^+$ cells into IFNγ producing Th1 cells (Cerwenka and Swain, 1999) and actively down regulate Th2 differentiation (Heath *et al.* 2000). Excessive Th1 activity is associated to autoimmune disease. Furthermore, Smad3-deficient mice exhibit chronic infection (Yang *et al.* 1999) and display impaired inflammatory responses (Ashcroft *et al.* 1999) suggesting TGFβ is involved in protection against infection. The functions of TGFβ are therefore not clear-cut and its actions are highly context dependent, with specific responses being influenced by both the local balance of cytokines stimulating target cells, and the balance between coactivators and corepressors at the site of transcription (reviewed Dennier *et al.* 2002).

Many transcription factor binding sites, including those for STATs and SMADs, lie upstream of the polymorphic GT repeat (figure 3.2.1) within the *Slc11a1* promoter. It is therefore possible that the two identified alleles are differentially responsive to different signalling pathways, as is the case for the human SLC11A1 promoter alleles, which are differentially regulated by bacterial LPS (Searle and Blackwell, 1999). The size difference between the D169-linked allele and the G169-linked allele is 6bp (60% of one complete helical turn). The consequence of this phase shift between transcription factor binding sites positioned proximal and distal to the GT-repeat between the two alleles is that proteins bound to sites upstream of the polymorphism may be able to co-operate only with the core promoter transcriptional initiation complex in one, but not the other promoter allele, the converse may be observed for different transcription factors and signalling pathways (figure 7.1.3).

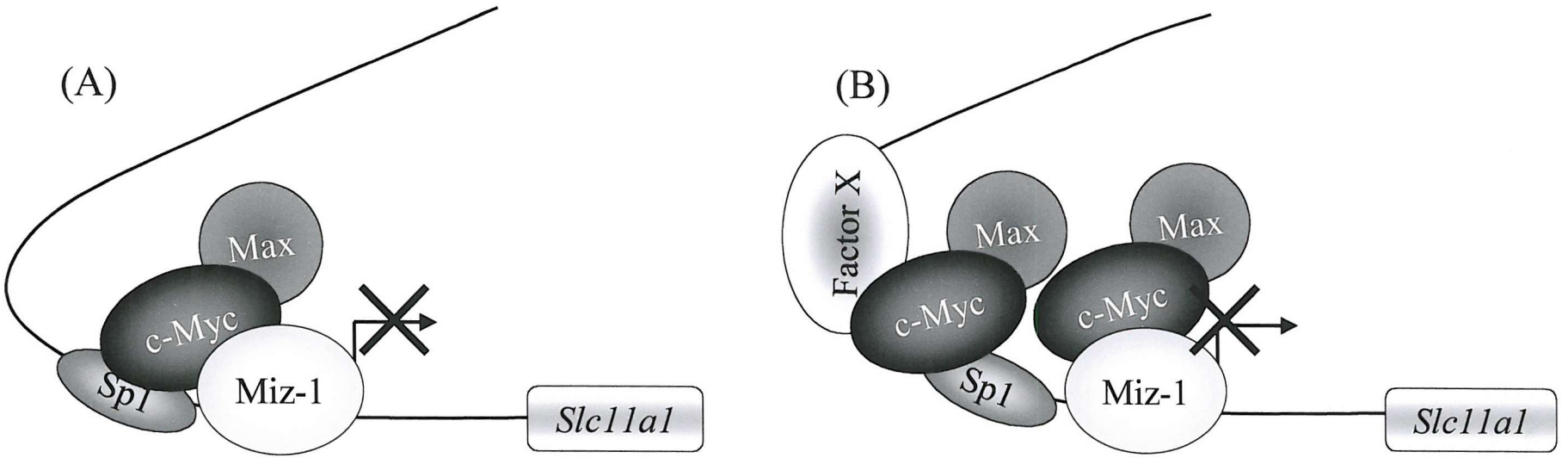

FIGURE 7.1.1 Proposed Models of c-Myc-Mediated Repression of *Slc11a1* Expression. Based on data presented within this report and proposed models of c-Myc-mediated regulation of $p15^{ink4b}$ expression (Seoane *et al.* 2001; Staller *et al.* 2001; Feng *et al.* 2002) a model of *Slc11a1* promoter regulation by c-Myc during cell growth and proliferation can be proposed. (A) c-Myc bound to EMS#6 forms a stable complex with Sp1 and Miz-1 at the *Slc11a1* promoter inhibiting transcription. (B) One c-Myc-Max heterodimer binds to EMS#6 and forms a stable complex with Sp1 and possibly upstream factors (factor X), a second c-Myc-Max hereodimer binds to Inr-bound Miz-1. The two c-Myc-heterodimers act synergistically to repress the *Slc11a1* expression.

FIGURE 7.1.2 Proposed Model of *Slc11a1* Regulation. Based on data presented within this report and proposed models of regulation of $p15^{ink4b}$ expression (Seoane *et al.* 2001; Staller *et al.* 2001; Feng *et al.* 2002) a model of *Slc11a1* promoter regulation can be proposed. (A) Upon cellular differentiation c-Myc levels are decreased by degradation via the ubiquitinylation process. "Removal" of c-Myc enables access of the p300 coactivator to the site of transcription, the formation of a pre-initiation complex/enhanceosome and the subsequent recruitment of RNA polymerase II, enabling transcription of basal levels of the *Slc11a1* gene. (B) During intracellular infection c-Myc levels are decreased by IFNγ/LPS. IFNγ/LPS activates the STAT proteins, and TFII-I, which both complex with Sp1 and p300 at the site of transcription, inducing the formation of a pre-initiation complex/enhanceosome and the subsequent recruitment of RNA polymerase II, enabling high level transcription of the *Slc11a1* gene. (C) During apoptotic cell phagocytosis c-Myc levels are decreased by TGFβ mediated transcriptional repression. TGFβ activates the SMAD proteins, and Miz-1, which both complex with Sp1 and p300 at the site of transcription, inducing the formation of a pre-initiation complex/enhanceosome and the subsequent recruitment of RNA polymerase II, enabling high level transcription of the *Slc11a1* gene.

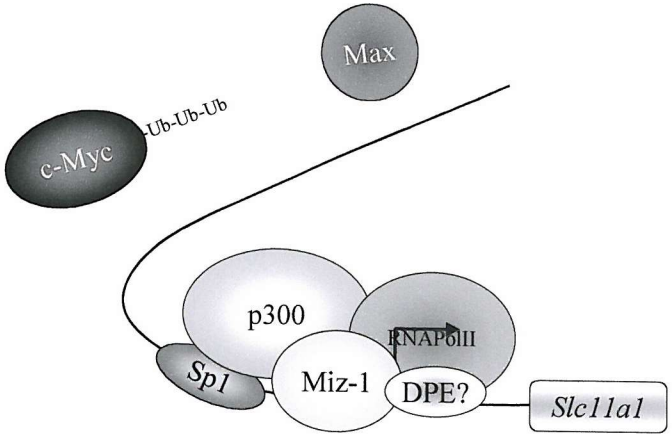

(A) Differentiation

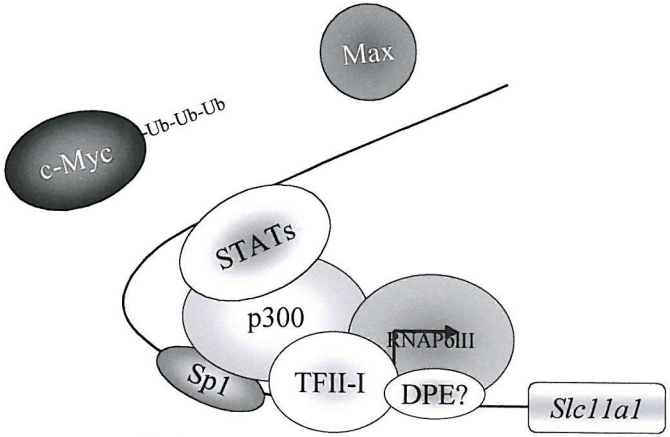

(B) Intracellular Infection

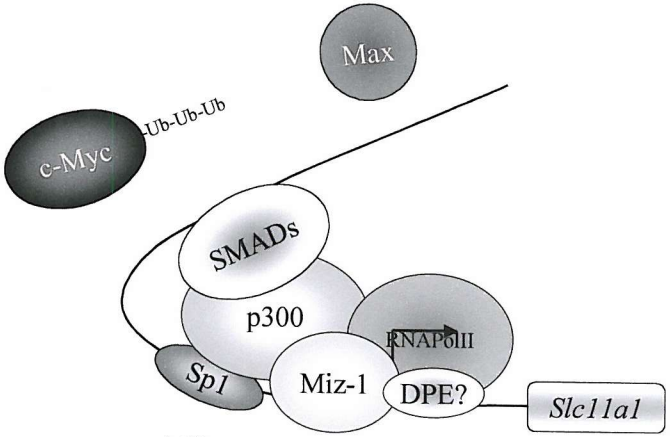

(C) Erythrophagocytosis

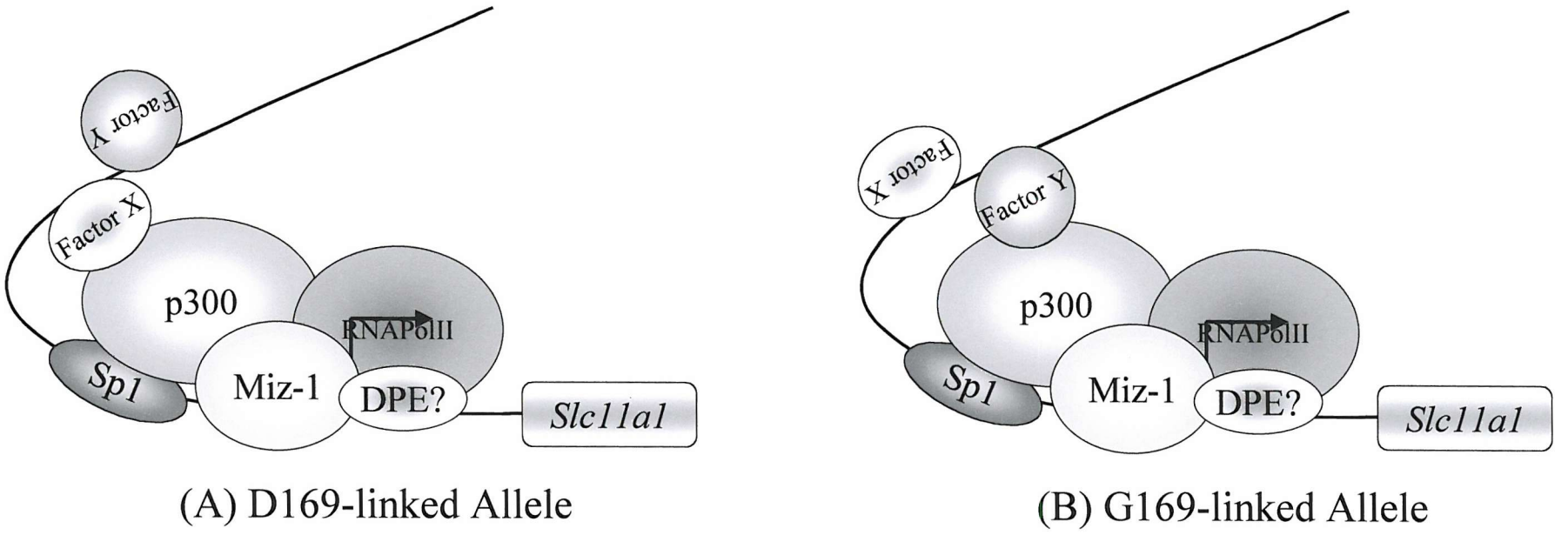

FIGURE 7.1.3 Proposed Effect of the Promoter Polymorphism on *Slc11a1* Regulation. Based on data presented within this report and a model illustrating the potential effect the polymorphism may have on different signalling pathways. (A) Transcriptions factor binding sites upstream of the polymorphic region are positioned in such a way factor X, but not factor Y, can cooperate with the basal transcriptional machinery and activate transcription. (B) Transcriptions factor binding sites upstream of the polymorphic region are positioned in such a way factor Y, but not factor X, can cooperate with the basal transcriptional machinery and activate transcription.

7.2 FUTURE WORK

Transcriptional Regulation of *Slc11a1* Expression

In order to confirm and complement the results presented within this thesis, both chromatin immunoprecipitation (ChIP) and RNA interference (RNAi) could be performed. ChIP assays will establish whether the factors described within this thesis are binding to the endogenous *Slc11a1* promoter. Whereas RNAi could be used to decrease *c-Myc* and *Miz-1* mRNA levels to assess what effects loss-of-function of the endogenous genes has on transiently transfected *Slc11a1* promoter constructs. RNAi could also be used to "knock-down" the endogenous levels of other transcription factors implicated in the regulation of *Slc11a1* gene expression such as STATs and SMADS, enabling assessment of involvement in the absence of specific expression constructs. Such RNAi "knock-down" studies will help elucidate which pathways (JAK/STAT, SMAD, MAP kinase) are regulating *Slc11a1* expression under different cellular conditions such as intracellular infection and erythrophagocytosis.

A role for *Slc11a1* in intracellular infection is well documented, as is the upregulation of *Slc11a1* by proinflammatory agents such as IFNγ and bacterial LPS, however the molecular mechanisms of induction remain elusive. IFNγ and bacterial LPS signals are transduced to the nucleus via the JAK/STAT signalling pathway, although the ability of specific proteins within this pathway to transactivate *Slc11a1* has not been shown. Furthermore, proteins within the JAK/STAT pathway are reported to bind to and activate TFII-I, therefore it would be of interest to investigate a role for TFII-I in *Slc11a1* gene expression.

Comparison of data within this thesis with the published findings of $p15^{ink4b}$ gene regulation has suggested a role for TGFβ in the regulation of *Slc11a1* gene expression. Treating cells with exogenous TGFβ and assessing both RNA and protein levels will establish whether TGFβ regulates *Slc11a1*. If a regulatory role for TGFβ is established, RNAi targeting specific proteins within known signalling pathways could be used to elucidate the mechanism of regulation.

The *Slc11a1* Promoter Polymorphism

Isolation and sequencing of the polymorphic promoter region of the *Slc11a1* gene from a wider array of inbred strains of mice, specifically the SJL and NOD strains could be performed. Such analysis may confirm the hypothesis that in these mice that are highly susceptible to autoimmune disease the strong D169-linked *Slc11a1* promoter allele drives expression of the G169-functional protein. Alternatively these studies may identify new alleles, which will themselves could be tested for functionality.

The methods of real time PCR or allele specific oligonucleotide hybridisation (ASOH), using F1 strains of mice could be used to confirm that these polymorphisms constitute a functional difference in the context of the endogenous gene. Such experiments could be performed to establish whether the polymorphism induces differential responses to inflammatory cytokines, as is the case with the human promoter polymorphisms (Searle and Blackwell, 1999).

REFERENCES

Akeson R and Bernards R. (1990) N-myc down regulates neural cell adhesion molecule expression in rat neuroblastoma. *Mol Cell Biol.* 10(5):2012-6.

Alcantara O, Obeid L, Hannun Y, Ponka P and Boldt DH (1994) Regulation of protein kinase C (PKC) expression by iron: effect of different iron compounds on PKC-β and PKCα expression and role of the 5' flanking region of the PKC-β gene in the response to ferric transferrin. *Blood.* 84, 3510-3517

Allen TM, Williamson P and Schlegel RA. (1988) Phosphatidylserine as a determinant for reticuloendothelial recognition of liposome models of the erythrocyte surface. *Proc Natl Acad Sci U S A.* 85, 8067-8071.

Arias M, Rojas M, Zabaleta J, Rodriguez JI, Paris SC, Barrera LF and Garcia LF. (1997). Inhibition of virulent Mycobacterium tuberculosis by Bcg(r) and Bcg(s) macrophages correlates with nitric oxide production. *J.Infect.Dis.* 176, 1552-1558

Arkhipova IR. (1995) Promoter elements in *Drosophila melanogaster* revealed by sequence analysis. *Genetics.* 139, 1359.

Ashcroft GS, Yang X, Glick AB, Weinstein M, Letterio JL, Mizel DE, Anzano M, Greenwell-Wild T, Wahl SM, Deng C and Roberts AB. (1999) Mice lacking Smad3 show accelerated wound healing and an impaired local inflammatory response. *Nat. Cell. Biol.* 1, 260-266

Atchley WR, Fitch WM. (1995) Myc and Max: molecular evolution of a family of proto-oncogene products and their dimerization partner. *Proc Natl Acad Sci U S A.* 92(22):10217-21.

Atkinson PG, Blackwell JM and Barton CH. (1997) *Nramp1* locus encodes a 65 kDa interferon-gamma-inducible protein in murine macrophages. *Biochem.J.* 325, 779-786.

Atkinson PGP and Barton CH. (1998) Ectopic expression of *Nramp1* in Cos-1 cells modulates iron accumulation. *FEBS Letters.* 425, 239-242

Atkinson PGP and Barton CH. (1999) High-level expression of $Nramp1^{G169}$ in RAW 264.7 cell transfectants: analysis of intracellular iron transport. *Immunology.* 96, 656-662

Ayer DE and Eisenman RN. (1993) A swith from Myc:Max to Mad:Max heterocomplexes accompanies monocyte/macrophage differentiation. *Genes and Devel.* 7, 2110-2119.

Baker ST, Barton CH, and Biggs TE. (2000) A negative autoregulatory link between Nramp1 function and expression. *J.Leuk.Biol.* 67, 501-507.

Barrera LF, Kramnik I, Skamene E and Radzioch D. (1994). Nitrite production by macrophages derived from BCG-resistant and –susceptible congenic mouse strains in response to IFN-gamma and infection with BCG. *Immunol.* 82,457-464

Barrera LF, Kramnik I, Skamene E and Radzioch D. (1997). I-A beta gene expression regulation in macrophages derived from mice susceptible or resistant to infection with *M. bovis* BCG. *Mol. Immunol.* 34, 343-355

Barton CH, Mann DA and Walsh FS. (1990) Characterisation of the human N-CAM promoter. *Biochem. J.* 268, 161-168.

Barton CH, White JK, Roach TIA, and Blackwell JM. (1994). NH_2-terminal sequence of macrophage-expressed natural resistance-associated macrophage protein (Nramp) encodes a proline/serine-rich putative Src homology 3-binding domain. *J.Exp.Med.* 179, 1683-1687.

Barton CH, Whitehead SH and Blackwell JM. (1995) *Nramp* transfection transfers *Ity/Lsh/Bcg*-related pleiotropic effects on macrophage activation: Influence on oxidative burst and nitric oxide pathways. *Mol. Med.* 1(3), 267-279.

Barton CH, Biggs TE, Baker ST, Bowen H and Atkinson PGP. (1999) *Nramp1*: a link between intracellular iron transport and innate resistance to intracellular pathogens. *J. Leuk. Biol.* 66, 757-762.

Biggs TE, Bowen H, Phillips ES, Perry VH, Mann DA and Barton CH. (2003) Divalent cation transport in macrophages: Role of Nramp1 (Natural resistance-associated protein). *Research Signpost.* Submitted.

Batsche E and Cremisi C. (1999) Opposite transcriptional activity between the wild type c-Myc gene coding for c-Myc1 and c-Myc2 proteins and c-Myc1 and c-Myc2 separately. *Oncogene.* 18, 5662-5671.

Bellamy R. (1999) The natural resistance-associated marophage protein and susceptibility to intracellular pathogens. *Microbes and Infection.* 1, 23-27

Benjamin WH, Hall P, Roberts SJ and Briles DE. (1990) The primary effect of the *Ity* locus is on the rate of growth of *Salmonella typhimurium* that are relatively protected from killing. *J. Immunol.* 144, 1683-1687

Biggs TE, Baker ST, Botham MS, Barton CH and Perry VH. (2001). *Nramp1* modulates iron homoeostasis *in vivo* and *in vitro*: evidence for a role in cellular iron releases involving de-acidifcation of intracellular vesicles. *Eur.J.Immunol.* 31, 2060-2070.

Black AV, Black JD and Azizkhan-Clifford J. (2002) Sp1 and Kruppel-like factor family of transcription factors in cell growth regulation and cancer. *J. Cell. Physiol.* 188, 143-160.

Blackwell TK, Huang J, Ma A, Kretzner L, Alt FW, Eisenman, RN, and Weintraub H. (1993) Binding of myc proteins to canonical and non-canonical DNA sequences. *Mol. Cell. Biol.* 13, 5216-5224

Blackwell JM, Barton CH, White JK, Roach TI, Shaw MA, Whitehead SH, Mock BA, Searle S, Williams H and Baker AM. (1994) Genetic regulation of leishmanial and mycobacterial infections: The *Ity/Lsh/Bcg* gene story continues. *Immunol. Lett.* 43, 99-107.

Blackwell JM, Barton CH, White JK, Searle S, Baker AM, William H and Shaw MA. (1995) Genomic organisation and sequence of the human NRAMP gene: Identification and mapping of a promoter region polymorphism. *Mol. Med.* 1, 194-205

Blackwell JM, Searle S, Goswami T and Miller EN. (2000) Understanding the multiple functions of Nramp1. *Microbes and Infection.* 2, 317-321

Blackwell JM, Goswami T, Evans CAW, Sibthorpe D, Papo N, White JW, Searle S, Miller EN, Peacock CS, Mohammed H and Ibrahim M. (2001) SLC11A1 (formerly NRAMP1) and disease resistance. *Cell. Microbiol.* 3(12), 773-784

Blobel GA. (2002) CBP and p300: Versatile coregulators with important roles in hematopoietic gene expression. *J. Leuk. Biol.* 71, 545-556

Bradley DJ (1974). Genetic control of natural resistance to *Leishmania donovani. Nature.* 250, 353-354

Bradley DJ (1977). Genetic control of *Leishmania* populations within the host. II. Genetic control of acute susceptibility of mice to *L. donovani* infections. *Clin. Exp. Immunol.* 30, 130-140.

Bradley DJ (1979). Regulation of *Leishmania* populations within the host. IV. Parasite and host cell kinetics studied by radioisotope labelling. *Acta. Trop.* 36, 171-179

Bratosin D, Mazurier J, Tissier JP, Estaquier J, Huart JJ, Ameisen JC, Aminoff D and Montreuil J. (1998) Cellular and molecular mechanisms of senescent erythrocyte phagocytosis by macrophages. A review. *Biochimie.* 80, 173-195

Bratton DL, Fadok VA, Richter DA, Kailey JM, Frasch SC, Nakamura T and Henson PM. (1999) Polyamine regulation of plasma membrane phospholipid flip-flop during apoptosis. *J Biol Chem.* 274(40), 28113-20.

Brown D, Faris M, Hilburger M and Zwilling BS. (1994) The induction of persistence of I-A expression by macrophages from Bcgr mice occurs via a protein kinase C-dependent pathway. *J. Immunol.* 152, 1323-1331.

Brown DH, Lafuse W and Zwilling BS. (1995) Cytokine-mediated activation of macrophages from *Mycobacterium bovis* BCG-resistant and -susceptible mice: Differential effects of corticosterone on antimycobacterial activity and expression of the *Bcg* gene (candidate *Nramp*). *Infect. and Immun.* 63(8), 2983-2988

Brown DH, Lafuse WP and Zwilling BS. (1997) Stabikised expression of mRNA is associated with mycobacterial resistance controlled by *Nramp1*. *Infect. Immun.* 65(2), 597-603.

Brown AJ, Dusso A and Slatopolsky E. (1999) Vitamin D. *Am. J. Physiol.* 277, F157–F175.

Burke TW, Willy PJ, Kutach AK, Butler JEF and Kadonaga JT. (1998) The DPE, a conserved downstream core promoter elements that is functionally ananogous to the TATA box. *Cold Spring Harbour Symposia on Quantitative Biology.* LXIII, 75-82.

Butterfield RJ, Sudweeks JD, Blankenhorn EP, Korngold R, Marinin JC, Todd JA, Roper RJ and Teuscher C. (1998) New genetic loci that control susceptibility and symptoms of experimental allergic encephalomyelitis in inbred mice. *J. Immunol.* 161, 1860-1867

Canonne-Hergaux F, Calafat J, Richer E, Cellier M, Grinstein S, Borregaard N and Gros P. (2002) Expression and subcellular localisation of NRAMP1 in human neutrophil granules. *Blood.* 100(1), 268-275

Cellier M, Govoni G, Vidal S, Kwan T, Groulx N, Liu J, Sanchez F, Skamene E, Schurr E and Gros P. (1994) Human natural resistance associated macrophage protein: cDNA cloning, chromosomal mapping, genomic organisation, and tissue specific expression. *J. Exp. Med.* 180, 1741-1752

Cellier M, Prive G, Belouchi A, Kwan T, Rodrigues V, Chia W and Gros P. (1995) Nramp defines a family of member proteins. *Proc. Natl. Acad. Sci. USA.* 92, 10089-10093

Cerwenka A and Swain SL. (1999) TGFβ1: immunosuppressant and viability factor for T-lymphocytes. *Microbes Infect.* 1, 1291-1296

Channon JY, Roberts MB, and Blackwell JM. (1984). A study of the differential respiratory burst activity elicited by promastigotes and amastigotes of Leishmania donovani in murine resident peritoneal macrophages. *Immunol.* 53, 345-355

Chen HM, Pahl HL, Scheibe RJ, Zhang DE and Tenen DG. (1993) The Sp1 transcription factor binds to the CD11b promoter specifically in myeloid cells in vivo and is essential for myeloid-specific promoter activity. *J. Biol. Chem.* 268(11), 8230-8239.

Claassen GF and Hann SR. (1999) Myc-mediated transformation: the repression connection. *Oncogene,* 18, 2925-2933

Claassen GF and Hann SR. (2000) A role for transcriptional repression of $p21^{cip1}$ by c-Myc in overcoming transforming growth factor β-induced cell-cycle arrest. *Proc. Natl. Acad. Sci. USA.* 97(17), 9498-9503

Clarke S and Gordon S. (1998) Myeloid-specific gene expression. *J. Leuk. Biol.* 63, 153-168

Connor J, Pak CC and Schroit AJ. (1994) Exposure of phosphatidylserine on the outer leaflet of human red blood cells. Relationship to cell density, cell age and clearance by mononuclear cells. *J. Biol. Chem.* 269, 2399-2404.

Courey AJ and Tjian R. (1988) Analysis of Sp1 in vivo reveals multiple transcriptional domains, including a novel glutamine-rich activation motif. *Cell.* 55(5), 887-98.

Dang CV. (1999) c-Myc target genes involved in cell growth, apoptosis and metabolism. *Mol. Cell. Biol.* 19(1), 1-11

Davies AC, Wims M, Spotts GD, Hann SR and Bradley A. (1993) A null c-Myc mutation causes lethality before 10.5 days of gestation in homozygous and reduced fertility in heterozygous female mice. *Genes Dev.* 7, 671-682

Denis M., Forget A., Pelletier M and Skamene E. (1988a) Pleiotropic effects of the Bcg gene. I. Antigen presentation in genetically susceptible and resistant congenic mouse strains. *J. Immunol.* 140, 2395-2400.

Denis M, Buschman E, Forget A, Pelletier M, and Skamene E. (1988b). Pleiotropic effects of the Bcg gene. II. Genetic restriction of responses to mitogens and allogeneic targets. *J.Immunol.* 141, 3988-3993

Denis M., Forget A., Pelletier M and Skamene E. (1988c). Pleiotropic effects of the Bcg gene: III. Respiratory burst in Bcg-congenic macrophages. *Clin.Exp.Immunol.* 73, 370-375

Dennier S, Goumans MJ and ten Dijke P. (2002) Transforming growth factor β siganl transduction. *J. Leuk. Biol.* 71, 731-740

Diaz C, Morkowski J and Schroit AJ. (1996) Generation of phenotypically aged phosphatidylserine exposed erythrocytes by dilauroyl phosphatidylcholine induced vesiculation. *Blood.* 87, 2956-2961.

Dlaska M and Weiss G. (1999) Central Role of Transcription Factor NF-IL6 for Cytokine and Iron-Mediated Regulation of Murine Inducible Nitric Oxide Synthase Expression1. *J. Immunol*, 162, 6171–6177.

Du H, Roy AL and Roeder RG. (1993) Human transcription factor USF stimulates transcription through the initiator elements of the HIV-1 and Ad-ML promoters. *EMBO J.* 12, 501-511.

Dvir A, Weliky Conaway J and Conaway RC. (2001) Mechanisms of transcriptional initiation and promoter escape by RNA polymerase II. *Curr. Opin. Gen. Devel.* 11, 209-214.

Eckner R, Ewen ME, Newsome D, Gerdes M, DeCaprio JA, Lawrence JB and Livingston DM. (1994) Molecular cloning of the adenovirus E1A-associated 300KDa protein (p300) reveals a protein with properties of a transcriptional adapter. *Genes Dev.* 8, 869-884

Eilers M, Picard D, Yamamoto KR and Bishop JM. (1989) Chimeras of Myc oncoproteins and steroid receptors cause hormone dependent transformation of cells. *Nature.* 340, 66-68

Eisenman RN. (2001) Deconstructing Myc. *Genes and Devel.* 15, 2023-2030

Evans CA, Harbuz MS, Ostenfeld T, Norrish A and Blackwell JM. (2001). Nramp1 is expressed in neurons and is associated with behavioural and immune responses to stress. *Neurogen.* 3, 69-78

Feng X-H, Liang Y-Y, Liang M, Zhai W and Lin X. (2002) Direct interaction of c-Myc with Smad 2 and 3 to inhibit TGF-β-mediated induction of the CDK inhibition $p15^{ink4b}$. *Mol. Cell.* 9, 133-143

Ferre-D'Amare AR, Prendergast GC, Ziff EB, Burley SK. (1993) Recognition by Max of its cognate DNA through a dimeric b/HLH/Z domain. *Nature.* 363(6424):38-45.

Fleming MD, Trenor CC, Su MA, Foernzler D, Beier DR, Dietrich WF and Andrews NC. (1997) Microcytic anaemia mice have a mutation in *Nramp2*, a candidate iron transporter gene. *Nat. Gen.* 16, 383-386.

Forbes JR and Gros P. (2001) Divalent-metal transport by NRAMP proteins at the interface of host-pathogen interactions. *TRENDS in Microbiol.* 9(8), 397-403

Formica S, Roach TI and Blackwell JM. (1994). Interaction with extracellular matrix proteins influences Lsh/Ity/Bcg (candidate Nramp) gene regulation of macrophage priming/activation for tumour necrosis factor-alpha and nitrite release. *Immunol.* 82, 42-50

Frank SR, Schroeder M, Fernandez P, Taubert S, Amati B. (2001) Binding of c-Myc to chromatin mediates mitogen-induced acetylation of histone H4 and gene activation. *Genes Dev.* 15(16):2069-82.

Frehel C, Cannone-Hergaux F, Gros P and de Chastellier C. (2002) Effect of *Nramp1* on bacterial replication and on maturation of *Mycobacterium avium*-containing phagosomes in bone marrow-derived mouse macrophages. *Cell. Microbiol.* 4(8), 541-556.

Gomes MS, Dom G, Pedrosa J, Boelaert J and Appleberg R. (1998) Effects of iron deprivation on Mycobacterium avium growth. *Tuber Lung Dis.* 1999;79(5):321-8.

Gomes MS and Appelberg R. (1998). Evidence for a link between iron metabolism and *Nramp1* gene function in innate resistance against *mycobacterium avium. Immunol.* 95, 165-168.

Gomes MS and Appelberg R. (2002). NRAMP1- or cytokine-induced bacteriostasis of *Mycobacterium avium* by mouse macrophages is independent of the respiratory burst. *Microbiol.* 148, 3155-3160.

Goswami T, Bhattacharjee AA, Babal P, Searle S, Moores E, Li M and Blackwell JM (2001). Nramp1 is an H+/bivalent cation antiporter. *Biochem.J.* 354, 511-5119.

Goto Y, Buschman E and Skamene E. (1989) Regulation of host resistance to *Mycobacterium intracellulare in vivo* and *in vitro* by the *Bcg* gene. *Immunogenetics.* 30, 218-221

Gunning P, Leavitt J, Muscat G, Ng S-Y and Kedes L. (1987) A human β-actin expression vector system directs high-level accumulation of antisense transcripts. *Proc. Natl. Acad. Sci. USA.* 84, 4831-4835

Gunshin H, Mackenzie B, Berger UV, Gunshin Y, Romero MF, Boron WF, Nussberger S, Gollan JL and Hediger MA. (1997) Cloning and characterisation of a mammalian proton-coupled metal-ion transporter. *Nature.* 388, 482-488.

Govoni G, Vidal S, Gauthier S, Skamene E, Malo D, and Gros P. (1994). The *Bcg/Ity/Lsh* locus: genetic transfer of resistance to infections in C57BL/6J mice transgenic for the Nramp1 Gly169 allele. *Infect.Immun.* 64, 2923-2929.

Govoni G, Vidal S, Cellier M, Lepage P, Malo D, and Gros P. (1995) Genomic structure, promoter sequence, and induction of expression of the mouse *Nramp1* gene in macrophages. *Genomics*, 27, 9-19

Govoni G, Vidal S, Gauthier S, Skamene E, Malo D and Gros P. (1996) The *Bcg/Ity/Lsh* Locus: genetic transfer of resistance to infections in C57BL/6J mice transgenic for the $Nramp1^{G169}$ allele. *Infect. and Immun.* 64(8), 2923-2929

Govoni G, Gauthier S, Billia F, Iscove NN and Gros P. (1997) Cell-specific and inducible *Nramp1* gene expression in mouse macrophage in vitro and in vivo. *J. Leuk. Biol.* 62, 277-286

Govoni G, Canonne-Hergaux F, Pfeifer CG, Marcus SL, Mills SD, Hackman DJ, Grinstein S, Malo D, Finlay BB and Gros P. (1999) Functional expression of Nramp1 In vitro in the murine macrophage line RAW 264.7. *Infect. and Immun.* 67(5), 2225-2232

Grandori C. *et al.* (2000) The Myc/Max/Mad network and the transcriptional control of cell behavior. *Annu. Rev. Cell Dev. Biol,* 16, 653-699

Gros P, Skamene E and Forget AI. (1981) Genetic control of natural resistance to *Mycobacterium bovis* (BCG) in mice. *J.Immunol.* 127, 2417-2421

Gros P, Skamene E and Forget A. (1983) Cellular mechanisms of genetically-controlled host resistance to *Mycobacterium bovis* (BCG). *J. Immunol.* 131, 1966-1973

Gruenheid S, Pinner E, Desjardins M and Gros P. (1997). Natural resistance to infection with intracellular pathogens: the Nramp1 protein is recruited to the membrane of the phagosome. *J.Exp.Med.* 185,: 717-730.

Gruenheid S, Cannone-Hergaux S, Gauthier S, Hackman DJ, Grinstein S and Gros P. (1999) The iron transporter Nramp2 is an integral membrane protein that colocalises with transferring in recycling endosomes. *J. Exp. Med.* 189, 831-841.

Hackman DJ, Rotstein OD, Zhang W-j, Gruenheid S, Gros P and Grinstein S. (1998) Host resistance to intracellular infection: Mutation of natural resistance-associated macrophage protein 1 (*Nramp1*) impairs phagosomal acidification. *J. Exp. Med.* 188(2), 351-364.

Hann SR and Eisenman RN. (1984) Proteins encoded by the human c-myc oncogene: differential expression in neoplastic cells. *Mol Cell Biol.* 4(11):2486-97.

Hann SR, King MW, Bentley DL, Anderson CW, Eisenman RN. (1988) A non-AUG translational initiation in c-myc exon 1 generates an N-terminally distinct protein whose synthesis is disrupted in Burkitt's lymphomas. *Cell.* 52(2):185-95.

Hann SR, Sloan-Brown K, Spotts GD. (1992) Translational activation of the non-AUG-initiated c-myc 1 protein at high cell densities due to methionine deprivation. *Genes Dev.* 6(7):1229-40.

Hann SR, Dixit M, Sears RC and Sealy L. (1994) The alternatively initiated c-Myc proteins differentially regulate transcription through a non-canonical DNA-binding site. *Genes Dev.* 8(20):2441-52.

Harris VK, Coticchia CM, List H-J, Wellstien A and Reigel AT. (2000) Mitogen-induced expression of the fibroblast growth factor-binding protein is transcriptionally repressed through a non-canonical E-box element. *J. Biol. Chem.* 275(37), 28539-28548.

Heath VL, Murphy EE, Crain C, Tomlinson MG and O'Garra A. (2000) TGFβ1 down-regulates Th2 development and results in decreased IL-4 induced STAT6 activation and GATA-3 expression. *E. J. Immunol.* 30, 2639-2649

Henson PM, Bratton DL and Fadok VA. (2001) Apoptotic cell removal. *Current Biol.* 11, R795-R805

Herold S, Wanzel M, Beuger V, Frohme C, Beul D, Hilukkala, T, Syvaoja J, Saluz H-P, Haenel F and Eilers M. (2002) Negative regulation of the mammalian UV response by Myc through association with Miz-1. *Molecular Cell.* 10, 509-521.

Iwai K, Drake SK, Wehr NB, Weismann AM, Lavaute T, Minato N, Klausner RD, Levine RL and Rouault TA. (1998) Iron-dependent oxidation, ubiquitination and degradation of iron-regulatory protein 2. Implications for degradation of oxidised proteins. *Proc. Natl. Acad. Sci. USA.* 95, 4929-4928

Jabado N, Kankowski A, Dougaparsad S, Picard V, Grinstein S and Gros P. (2000). Natural resistance to intracellular infections: Nramp1 functions as a pH-dependent manganese transporter at the phagosomal membrane. *J.Exp.Med.*192, 1237-1247.

Jackson SH, Gallin JI and Holland SM. (1995) The $p47^{phox-/-}$ mouse knock-out model of chronic granulomatous disease. *J. Exp. Med.* 182, 751-758.

Javahery R, Khachi A, Lo K, Zenzie-Gregory B and Smale S. (1994) DNA sequence requirements for transcriptional initiator activity in mammalian cells. *Mol. Cell. Biol.* 14(1) 116-127

Johnson SC and Zwilling BS. (1985). Continuous expression of I-A antigen by peritoneal macrophages from mice resistant to Mycobacterium bovis (strain BCG). *J.Leuk.Biol.* 38, 635-647

Kadonaga JT, Carner KR, Masiarz FR and Tjian R. (1987). Isolation of cDNA encoding transcription factor Sp1 and functional analysis of the DNA binding domain. *Cell.* 51, 1079-1090.

Kaye PM, Patel NK and Blackwell JM. (1988). Acquisition of cell-mediated immunity to Leishmania. II. LSH gene regulation of accessory cell function. mmunol. 65,17-22

Kim DW, Cheriyath V, Roy AL and Cochran BH. (1998). TFII-I enhances activation of the c-*fos* promoter through interactions with upstream elements. *Mol. Cell. Biol.* 18, 3310–3320.

Kim DW and Cochran BH. (2001) JAK2 Activates TFII-I and Regulates Its Interaction with Extracellular Signal-Regulated Kinase. *Mol. Cell. Biol.* 21(10), 3387–3397

Kime L and Wright SC. (2002) *Mad4* is regulated by a transcriptional repressor complex that contains Miz-1 and c-Myc. *Biochem. J. In press.*

Kishi F, Yoshida T and Aiso S. (1996) Location of NRAMP1 molecule on the plasma membrane and its association with microtubules. *Mol. Immunol.* 33(16), 1241-1246

Kita E, Emoto M, Oku D, Nishikawa F, Hamuro A, Kamikaidou N and Kashiba S. (1992). Contribution of interferon gamma and membrane-associated interleukin 1 to the resistance to murine typhoid of Ityr mice. *J.Leuk.Biol.* 51, 244-250

Kojima Y, Kinouchi Y, Takahashi S, Negoro K, Hiwatashi N and Shimosegawa T. (2001) Inflammatory bowel disease is associated with a novel promoter polymorphism of natural resistance-associated macrophage protein 1 (NRAMP1) gene. *Tissue Antigens.* 58, 379-384

Kondo H, Saito K, Grasso JP and Aisen P. (1988) Iron metabolism in the erythrophagocytosing Kupffer cells. *Hepatol.* 8, 32-38.

Kotze MJ, de Villiers JNP, Rooney RN, Grobbelaar JJ, Mansvelt EPG, Bouwens CSH, Carr J, Stander I and du Plessis L. (2001) Analysis of the NRAMP1 gene implicated in iron transport: association with multiple sclerosis and age effects. *Blood Cells Mol and Diseases.* 27(1), 44-53

Kovarova H, Radzioch D, Hajduch M, Sirova M, Blaha V, Macela A, Stulik J, and Hernychova L. (1998). Natural resistance to intracellular parasites: a study by two-dimensional gel electrophoresis coupled with multivariate analysis. *Electrophoresis* 19,1325-1331

Kramnik I, Radzioch D and Skamene E. (1994). T-helper 1-like subset selection in Mycobacterium bovis bacillus Calmette-Guerin-infected resistant and susceptible mice. *Immunol.* 81, 618-625

Kuhn DE, Baker BD, Lafuse WP, and Zwilling BS. (1999). Differential iron transport into phagosomes isolated from the RAW 264.7 macrophage cell lines transfected with $Nramp1^{G169}$ or $Nramp1^{D169}$. *J.Leuk.Biol.* 66, 113-119.

Kuhn DE, Lafuse WP and Zwilling BS. (2001) Iron transport into mycobacterium avium-containing phagosomes from an Nramp1(Gly169)-transfected RAW264.7 macrophage cell line. *J Leukoc Biol.* 69(1), 43-9.

Lafuse WP, Alvarez GR and Zwilling BS. (2000) Regulation of Nramp1 mRNA stability by oxidants and protein kinase C in RAW 264.7 macrophages expressing *Nramp1^{G169}*. *Biochem. J.* 351, 687-696

Lafuse WP, Alvarez GR and Zwilling BS. (2002) Role of MAP kinase activation in Nramp1 mRNA stability in RAW264.7 macrophages expressing *Nramp1^{G169}*. *Cell. Immunol.* 215, 195-206.

Lang T, Prina E, Sibthorpe D, and Blackwell JM. (1997). Nramp1 transfection transfers Ity/Lsh/Bcg-related pleiotropic effects on macrophage activation: influence on antigen processing and presentation. *Infect. Immun.* 65, 380-386

Larsson LG, Ivhed I, Gidlund M, Petterson U, Vennstrom B and Nilsson. (1988) Phorbol ester-induced terminal differentiation is inhibited in human U973 cells expressing v-Myc oncogene. *Proc. Natl. Acad. Sci. USA.* 85, 2638-2642

Lau JF and Horvath CM. (2002) Mechanisms of Type I Interferon Cell Signaling and STAT-Mediated Transcriptional Responses. *The Mount Sinai J. Med.* 69(3), 156-168.

Li L-H, Nerlov C, Prendergast G, MacGregor D and Ziff EB. (1994) c-Myc represses transcription in vivo by a novel mechanism dependent on the initiator element and Myc box II. *EMBO J.* 13(17), 4070-4079

Lieu PT, Heiskala M, Peterson PA and Yang Y. (2001) The roles of iron in health and disease. *Mol. Aspects of Med.* 22, 1-87

Lissner CR, Swanson RN and O'Brien AD. (1983) Genetic control of the innate resistance of mice to *Salmonella typhimurium*: expression of the *Ity* gene in peritoneal and splenic macrophages isolated *in vitro*. *J. Immunol.* 131, 3006-3013.

Littlewood TD, Amati B, Land H, and Evan GI. (1992) Max and c-Myc/Max DNA-binding activities in cell extracts. *Oncogene.* 7, 1783-1792.

Liu J, Fujiwara TM, Buu NT *et al.* (1995) Identification of polymorphisms and sequence variants in human homologue of mouse natural resistance associated macrophage protein gene. *Am. J. Hum. Genet.* 56, 845-853

Malo D, Vogan K, Vidal S, Hu J, Cellier M, Schurr E, Fuks A, Bumstead N, Morgan K, and Gros P. (1994). Haplotype mapping and sequence analysis of the mouse Nramp gene predict susceptibility to infection with intracellular parasites. *Genomics* 23, 51-61.

Man Chan H and Thangue NBL. (2001) p300/CBP proteins: HATs for transcriptional bridges and scaffolds. *J. Cell Sci.* 114, 2363-2373

Manthey CL, Brandes ME, Perera PY and Vogel SN. (1992) Taxol increases steady-state levels of lipopolysaccharide-inducible genes and protein tyrosine phosphorylation in murine macrophages. *J. Immunol.* 149, 2459-

Mateyak MK, Obaya AJ, Adachi S, and Sedivy JM. (1997) Phenotypes of c-Myc-deficient rat fibroblasts isolated by targeted homologous recombination. *Cell Growth Differ.* 8, 1039-1048

Mc Evoy I, Williamson P and Schlegel RA. (1986) Membrane phospholipid asymmetry as a determinant for erythrocyte recognition by macrophages. *Proc. Natl. Acad. Sci. USA.* 83, 3311-3315.

McMahon SB, Van Buskirk HA, Dugan KA, Copeland TD, Cole MD. (1998) The novel ATM-related protein TRRAP is an essential cofactor for the c-Myc and E2F oncoproteins. *Cell.* 94(3):363-74.

McMahon SB, Wood MA, Cole MD. (2000) The essential cofactor TRRAP recruits the histone acetyltransferase hGCN5 to c-Myc. *Mol Cell Biol.* 20(2):556-62.

Merika M, Williams AJ, Chen G, Collins T and Thanos D. (1998) Recruitment of CBP/p300 by the INFβ enhanceosome is required for synergistic activation of transcription. *Mol. Cell.* 1, 277-287

Morse D and Choi AMK. (2002) Heme Oxygenase-1-The "emerging molecule" has arrived. *Am. J. Respir. Cell. Mol. Biol.* 27, 8-16.

Mulero V, Searle S, Blackwell JM and Brock JH (2002). *Slc11a1* (formerly *Nramp1*) regulates metabolism and release of iron acquired by phagocytic, but not transferrin receptor mediated iron uptake. *Biochem. J.* 363, 89-94.

Nasi S, Ciarapica R, Jucker R, Rosati J and Soucek L. (2001) Making decisions through Myc. *FEBS Letters.* 490, 153-162

North RJ and Medina E. (1998) How important is *Nramp1* in tuberculosis? *Trends Microbiol.* 6(11), 441-443.

Oldenborg PA, Zheleznyak A, Fang YF, Lagenaur CF, Gresham HD and Lindberg FP. (2000) Role of CD47 as a marker of self on red blood cells. *Science.* 288, 2051-2054.

Olivier M, Cook P, Desanctis J, Hel Z, WojciechowskiW, Reiner NE, Skamene E and Radzioch D. (1998) Phenotypic difference between Bcgr and Bcgs macrophages is related to differences in protein-kinase-C-dependent signaling. *Eur. J. Biochem.* 251, 734-743

Orgad S, Nelson H, Segal D and Nelson N. (1998) Metal ions suppress the abnormal taste behaviour of Drosophila mutant malvolio. *J. Exp. Med.* 201, 115-120.

Orkin SH. (1995) Transcription factors and hematopoietic development. *J. Biol. Chem.* 270(10), 4955-4958

Oster SK, Marhin WW, Asker C, Facchini LM, Dion PA, Funa K, Post M, Sedivy JM and Penn LZ. (2000) Myc is an essential negative regulator of platelet-derived growth factor beta-receptor expression. *Mol. Cell. Biol.* 20(18), 6768-6778

Peukert K, Staller P, Schneider A, Carmichael G, Hanel F and Eilers M. (1997) An alternative pathway for gene regulation by Myc. *EMBO J.* 16(18), 5672-86.

Pinner E, Gruenheid S, Raymond M and Gros P. (1997) Functional complementation of the yeast divalent cation transporter family *SMF* by *NRAMP2*, a member of the mammalian natural resistance-associated macrophage protein family. *J. Biol. Chem.* 272(46), 28933-28938

Plant J and Glynn AA (1974a). Natural resistance to *Salmonella* infection, delayed hypersensitivity and Ir genes in different strains of mice. *Nature.* 248, 345-347

Plant J and Glynn AA (1974b). Dr Plant and Professor Glynn Reply. *Nature.* 250, 354.

Plant J and Glynn AA (1976). Genetics of resistance to infection with *Salmonella typhimurium* in mice. *J. Infect. Dis.* 133, 72-78.

Plant JE, Blackwell JM, O'Brien AD, Bradley DJ, Glynn AA. (1982) Are the Lsh and Ity disease resistance genes at one locus on mouse chromosome 1? *Nature.* 297(5866):510-11

Poss KD and Tonegawa S. (1997) Heme oxygenase 1 is required for mammalian iron reutilization. *Proc. Natl. Acad. Sci. USA.* 94(20), 10919-24.

Radledge C and Dover LG. (2000) Iron metabloism in pathogenic bacteria. *Annu. Rev. Microbiol.* 54, 881-941

Raschke WC, Baird S, Ralph P and Nakoinz I. (1978) Functional macrophage cell lines transformed by abelson leukemia virus. *Cell.* 15, 261-267

Righi M, Mori L, De Libero G, Sironi M, Biondi A, Mantovani A, Donin SD and Ricciardi-Castagnoli P. (1989) Monokine production by microglial cell clones. *Eur. J. Immunol.* 19(8), 1443-1448.

Roach TI, Chatterjee D and Blackwell JM. (1994). Induction of early-response genes KC and JE by mycobacterial lipoarabinomannans: regulation of KC expression in murine macrophages by Lsh/Ity/Bcg (candidate Nramp). *Infect. Immun.* 62, 1176-1184

Rodrigues V, Cheah PY, Ray K and Chia W. (1995) *EMBO J.* 14, 3007-3020

Roig EA, Richer E, Cannone-Hergaux F, Gros P and Cellier MFM. (2002) Regulation of NRAMP1 gene expression by 1α, 25-dihydroxy-vitamin D_3 in HL-60 phagocytes. *J. Leuk. Biol.* 71, 890-904.

Roy AL, Carruthers C, Gutjahr T and Roeder RG. (1993) Direct role for Myc in transcription initiation mediated by interactions with TFII-I. *Nature.* 365, 359-361.

Saffer JD, Jackson SP, Annarella MB. (1991) Developmental expression of Sp1 in the mouse. *Mol Cell Biol.* 11, 2189

Schneider A, Peukert K, Eilers M and Hanel F. (1997) Association of Myc with the zinc-finger protein Miz-1 defines a novel pathway for gene regulation by Myc. *Curr. Top. Microbiol. Immunol.* 224, 137-46.

Schurr E, Skamene E, Forget A, Gros P. (1989) Linkage analysis of the Bcg gene on mouse chromosome 1. Identification of a tightly linked marker. *J. Immunol.* 142(12):4507-13

Schurr E, Malo D, Radzioch D, Buschman E, Morgan K, Gros P and Skamene E. (1991) Genetic control of innate resistance to mycobacterial infections. *Immunol. Today.* 12(3), A42-A45

Searle S, Bright NA, Roach TIA, Atkinson PG, Barton CH, Meloen RH, and Blackwell JM, (1998). Localisation of Nramp1 in macrophages: modulation with activation and infection. *J.Cell.Sci.* 111, 2855-2866.

Searle S and Blackwell JM. (1999). Evidence for a functional repeat polymorphism in the promoter of the human NRAMP1 gene that correlates with autoimmune versus infectious disease susceptibility. *J.Med.Genet.* 36, 295-299.

Seoane J, Pouponnot C, Staller P, Schader M, Eilers M and Massague J. (2001) TGFbeta influences Myc, Miz-1 and Smad to control the CDK inhibitor p15INK4b. *Nat. Cell. Biol.* 3(4), 400-8.

Seoane J, Le H-V and Massague J. (2002) Myc suppression of the *$p21^{cip1}$* cdk inhibitor influences the outcome of the p53 response to DNA damage. *Nature.* 419, 729-734.

Shaw MA, Clayton D, Atkinson SE, Williams H, Miller N, Sibthorpe D and Blackwell JM. (1996) Linkage of rheumatoid arthritis to the candidate gene NRAMP1 on 2q35. *J. Med. Genet.* 33, 672-677

Skameme E, Gros P, Forget A, Kongshavn PAL, St. Charles C and Taylor B. (1982) Genetic regulation of resistance to intracellular pathogens. *Nature.* 297, 506-509.

Smale ST. (1997) Transcription initiation from TATA-less promoters within eukaryotic protein-coding genes. *Biochem. Biophys. Acta.* 1351, 73-88

Soo SS, Villarreal-Ramos B, Anjam Khan CM, Hormaeche CE and Blackwell JM. (1998). Genetic control of immune response to recombinant antigens carried by an attenuated Salmonella typhimurium vaccine strain: Nramp1 influences T-helper subset responses and protection against leishmanial challenge. *Infect. Immun.* 66, 1910-1917

Soucek L, Helmer-Citterich M, Sacco A, Jucker R, Cesareni G, Nasi S. (1998) Design and properties of a Myc derivative that efficiently homodimerizes. *Oncogene.* 17(19):2463-72.

Spotts GD, Patel SV, Xiao Q, Hann SR. (1997) Identification of downstream-initiated c-Myc proteins which are dominant-negative inhibitors of transactivation by full-length c-Myc proteins. *Mol Cell Biol.* 17(3):1459-68.

Staller P, Peukert K, Kiermaier A, Seoane J, Lukas J, Karsunky H, Moroy T, Bartek J, Massague J, Hanel F and Eilers M. (2001) Repression of p15INK4b expression by Myc through association with Miz-1. *Nat. Cell. Biol.* 3(4), 392-9.

Sturgill-Koszycki S, Shiable UE and Russell DG. (1996) Mycobacterium-containing phagosomes are accessible to early endosomes and reflect a transitional state in normal phagosome biogenesis. *EMBO J.* 15, 6960-6968.

Supeck F, Supekova L, Nelson H and Nelson N. (1996) A yeast manganese transporter related to the macrophage protein involved in conferring resistance to mycobacteria. *Proc. Natl. Acad. Sci. USA.* 93, 5105-5110.

Tenen DG, Hromas R, Licht JD and Zhang DE. (1997) Transcription factors, normal myeloid development and leukaemia. *Blood.* 90(2), 489-519.

Tokuraku K, Nakagawa H, Kishi F and Kotani S. (1998) Human natural resistance-associated macrophage protein is a new type of microtubule-associated protein. *FEBS Letters.* 428, 63-67

Veenstra TD, Windebank AJ and Kumar R. (1997) 1,25-Dihydroxyvitamin D3 Regulates the Expression of N-myc, c-myc, Protein Kinase C, and Transforming Growth Factor-β2 in Neuroblastoma Cells. *Biochem. Biophys. Res. Commun.* 235, 15–18.

Vidal SM, Epstein D, Malo D, Weith A, Vekemans M and Gros P. (1992) Identification and mapping of six microdissected genomic DNA probes to the proximal region of mouse chromosome 1. *Genomics.* 14, 1-6

Vidal SM, Malo D, Vogan D, Skamene E and Gros, P. (1993). Natural resistance to infection with intracellular parasites: isolation of a candidate for Bcg. *Cell.* 73, 469-485

Vidal S, Tremblay ML, Govoni G, Gauthier S, Sebastiani G, Malo D, Skamene E, Olivier M, Jothy S, and Gros P. (1995). The *Ity/Lsh/Bcg* locus: natural resistance to infection with intracellular parasites is abrogated by disruption of the Nramp1 gene. *J.Exp.Med.* 182, 655-666.

Vo N and Goodman RH. (2001) CREB-binding protein and p300 in transcriptional regulation. *J. Biol. Chem.* 276(17), 13505-13508

Walker EM Jr and Walker SM. (2000) Effects of iron overload on the immune system. *Ann. Clin. Lab. Sci.i* 30(4), 354-365.

Wojciechowski W, DeSanctis J, Skamene E and Radzioch D. (1999). Attenuation of MHC class II expression in macrophages infected with Mycobacterium bovis bacillus Calmette-Guerin involves class II transactivator and depends on the Nramp1 gene. *J.Immunol.* 163,2688-2696

Wu KJ, Polack A, and Dalla-Favera V. (1999). Co-ordinated regulation of iron controlling genes, H-ferritin and IRP2 by c-Myc. *Science* 283, 676-679.

Yang X, Letterio JJ, Lechleider RJ, Chen L, Hayman R, Gu H, Roberts AB and Deng C. (1999) Targeted disruption of SMAD3 results in impaired mucosal immunity and diminished T cell responsiveness to TGFβ. *EMBO J.* 18, 1280-1291

Yang X-P, Freeman LA, Knapper CL, Amar MJA, Remaley A, Brewer BB and Santamarina-Fojo S. (2002) The E-box motif in the proximal ABCA1 promoter mediates transcriptional repression of the ABCA1 gene. *J. Lipid Res.* 43, 279-306.

Zhang DE, Hetherington CJ, Tan S, Dziennis SE, Gonzalez DA, Chen HM and Tenen. (1994) Sp1 is a critical factor for the monocyte specific expression of human CD14. *J. Biol. Chem.* 269, 11425-11434.

Ziegelbauer J, Shan B, Yager D, Larabell C, Hoffmann B and Tjian R. (2001) Transcription factor MIZ-1 is regulated via microtubule association. *Mol. Cell.* 8(2), 339-49.

Zwilling BS, Vespa L and Massie M. (1987). Regulation of I-A expression by murine peritoneal macrophages: differences linked to the Bcg gene. *J.Immunol.* 138, 1372-1376

Zwilling BS, Lafuse W and Brown DH. (1996) *J. Leuk. Biol.* (suppl. Meeting abstract no. 93) p28

Zwilling BS, Kuhn DE, Wikoff L, Brown D and Lafuse W. (1999) Role of iron in NRAMP1-mediated inhibition of mycobacterial growth. *Infect. and Immunol.* 67, 1386-1392

APPENDIX 1: Sequence of the pS3 *Slc11a1* Promoter Region. Sequence of pS3, relevant restriction endonuclease recognition sites are highlighted in bold with name of enzyme, position relative to transcriptional start site, and the start site for pHB *Slc11a1* promoter constructs indicated above. Transcribed sequences are underlined, and the translational initiation start codon highlighted in bold. In constructs pHB4, pHB5, pHB6 and pHB8 a synthetic BamHI site has been introduced at the ATG codon.

SalI(-6197bp, pHB1 & pHB5)

GTCGACAATGACAACAACAACCAGGGTTAGACTCTCGAAAAAGACTAGGTGGGCGGCTAGAATCCGGAGACTGGGC
CTGGCTGGGGCTGCGGCTTCAGTGGGAGATAAGCAGGGTCCTTTCCCAGTTCTACTCTGTCAGAAGGGACTGCATT
TGGCCAGCTCTTCTTGTCAAAAAAGGGAAGCTTTATTTTCGTTTACCCAGCAAGTTTCATGTTTTCTTCCTAGAGT
CTATTTTCATAGTTATGGCCATTTCAGAGAAAATAAAATTAAGGCCTGTGGCCAGGTGTGTTGGCTCAACATCTAT
AATCTCAGCCCTCAGGGTCCTGACTGAGCCAGGGGAACTACTGTGAGTTCAAGGCCAGCCAAGGCTACACAACAAA
GCCCTCTCTCAAAGATCAAATTAAAAATTAAGAAAAAGAAGGGAAAAGAAGAGGAGGAGAGGGCTGGTGAGATGGC
TCAGCGGGTAAGGGCACTGACTGCCCTTCCAAAGGTCCTAAGTTCAAATCCCAGCAACCACATGGTGGCTCACAAC
CACCCATAATGAGATCTGACACACTCTTCTGGTGTGTCTGAAGTCAGCTACAGTAAATTTATGTATAATAATAAAT
CTTTAAAAAAAAAAAGAAAAAAAAGAGGAGGAGGAGGATAAGAGGGAACCACTTAGGCCCACGCCACCCATAATCCC
AACACTTAGGAAACAGGTGAGTTTCCGGGTTCATCTTTGGTTCCCCTCCGTGAGCTTGGGTCCTGCCTGGGCTACA
TAAAATCCTGCAGGTGGGAGAGCAGGATTTGAACCTGGAGTTGGACATGAGAAGCCTGCAGTGGTGCCATGGATCT
AAACATAATTACTACTACCACCTAGAAACGAATGCATAGAAAGTGCAGGCGGTGTATAAGGAGGGACACAGGACAT
CCCTAGCCCTCACTCAGCTTCTTTGTGCTTCAGGTTCTCCTTGCCCCATCAATACACACACACATACACACACACA
CACACACACACACACGACTCCCCAGACTGTGCAAGGGCCCCCCAGCCACCCAGTAAGAAGGAAAGAGAAGCAGGAA
CCCATCACTGCCTCCAGCTTCCTCACTCACCAGCAGTTCTGGACGGTGGCTTGTCTGCCTGACGCTGGCTTTAGAA
CCTGTTGGGGGTTGGTAGTTAGGGTGCAGGCACCACACCTCCATTAACATCTCTGGCCATCAGCCCTGCTGCTTTG
AAATGAGAGACTCCGGAGGAACTCCAAGGTGTAGTGGAGAGTTCCAGTCTTGGCTACAGAGCTGAGGAATGTAAGG
GAGGGTAGTCTGTCTGTCTTCCAGAAATCACTTCAGAAGGCTTCAGACAGGGCTGCCACTTGAGCCTTGCAAAGTG
TTTTATGTCATGTCCCCCCTCCTTAAAAACAGAACAAAACATTCACAAGCTGGGTGGTGGTGGCACAAGCCTTAAT
CCCAACTCTCAGGACGCAGAGGCCAGGCTGGTCTATAGAGCAAGTTCAAGGACAACCAGAGCTACACAGAGAGATC
TTGTCTCGGCAAACACACACCACACACACACACACACACACACACACACACACACACACACACACACAACCAAACCAAAC
CAACCAACCAAAGACCCCCAAAATCAAAAGACATTCACAACCAAGAAAAATGAAATAAAACCACCACAACAAAATT
ATCTTAGTTTCTCTGTCCCAGGGCCTCACACACTCTCCCAGAGGCTTCACCCAGTCCCTGCCAAGCATTTTCTTGA
AATAGATCTTTATAATTCCAATGTATTCTCAAAATGAAATCATACCAGTAATATATGCTTGTTAGTTGGTAATTGG
ATACTTAATTATATATTATAATTTATATACATTATATATAGTGAAGCTGAAGTCGCCCTAGGTCCATTGTATTTTG
AAACACTATTTCATGTGTTGGCTTTCTGGGGCTGGGGGGGCGGGGGGTTGGGGGAATGGCTCATGTGTAAAAGTGT
TAGCTGTGCAAACCTGAGGACCCCAGTTCCACCAGTGGAACCCACATAAAAATCTGGATGTGACCCAGCATGGTGG
CCTGGGCTGAAATCCCGGCACTCAAAGGCAGAGGTGGGTGGATCTCTGAGTTCAAGGCCAGCTTCATGGCTAGCTA
CATGGTGAATTCCAGAGCAGTCAGGGTTGCACAGTGAATTCCTATCTCAAAAACAAACGACAGAAGCAGGATGCAG
TGGCATGAAGCTGTGATCCTAGCACCTCTATGGCAAGACTGGAGACAGAGAGACCGGAGAAGCACTTTGAAACTTT
TGGACTCTCTAGCCTAGAGTACACATCTGCAGCAGTAGAAACAGGCCCTGCCTCAACGAGGTAAAAGGTGGACTGG
AGCGTACCCTAGGCTGTAGGCCCCTGGACACATCGCCTTCCGTGTTCTCACACACCCCAAGACTGACTTTGCTCAT
CCATCAGTGCCCTTGGCTTTGTTATTGATCTTTCTTTGCTCTCTGGACAGTCTCATCATGAATTCTATGCTAGCTT
CAGCCTCGCAAGTGTTGAGATCACAGGTGGATACCACCATCACCAAACGACCAGTGTGTTTAGAACACACTTGTCA
TATCATTACAGCCCTCTATCTTCATGCCTCTGTATGCTGGTACAGTATGCTGGTAGGGATTTAACCCAGAGCTTCA

Appendix 1: Sequence of the pS3 Slc11a1 Promoter Region.

TGCATACTAAACACATACAAGGGAGGCACAAACTCCATTCTCTTGGTTGTCCTTTAGCCACCCCCACTTTTGGGGG
TGGGGGGAGTTGTTTGTTTTTAAAACTTTATTACATAGTTTTATTATATGTTTCTAAGATAAGGAATATGAAATTC
AAGGAAATTAGGGTTTTGATTTGTTTTGTTGCTTTTGGTTTTGGTTTTTTGGGTTTTTGTTGTTGGTGGGGTTTTT
TTTGTGTGTGTTTTGTTTTGTTTTTTTGAGATAGGGTTTCTCTGTGTAACCCTGGCTGTCCTGGAAGTTACTCTGT
AGACCAGGCTGGCCTCGAACTCAGAAATCCACCTGCCTCTGCCTCCCATGTGCTGGGATTAAAGGCGGTACACTGA
TGAAAGGGTCTTGCTGACCGAGTGAGGCAGCCATGACTTTTAGAAGACAATCCTCCAGGGCTGAAGAGTTGGCTCA
GTGGTTAGGAGTACTGTTCTCCTGAGGGACCCAGTCTGATTCCCTGCACCCACTTGCCACTTACTCAGGCACCAGG
CGTGCGTAGGTGTGGTGCACAGACATCCATGCAGGAAAAGCATTCAATCTAAAAAAAAAAAAAAAAAAAAAGTGT
AAAAAGAAAATACCCGAAGCCGAGTGTGGCGGCTCACACTGAGATGCCAATATTTGGGAGGCTAAGGAAGGAGAAT
CTTCAGTTCAAGGTCAGCATGGAGGTGAACGGACAGAAAGCTTCTCTCGTGTGTGTGTGTGTGTGTGTGTGTGT
GTGTGTACATATGCACGCACAAGTGTGGGCACTGCCGAGCACCCAGAAGAGGATGTCAAATCCCCTGCAGCTGGAG
TGGCCTGACATGGATATTGGGAACTGAATCAGCTCCTCTGCCAAAGCTGTGCCTGCTGTAACTGCCCACCCATTTC
TCCAGCCCAGTTCTGCACACTTGTTTGCTTGCTTGGGTTTTTGTTTGTTGGTTTATTTGTTTGTTGTTTTTGTTTT
TTGTTTNTTGCAGGAAGAAGAGGTTCAGACGGGGACTCAGGAAGCATAGGCTAGCCACCTTGCCGGTATCTCTTAG
CTTCCGGTGTGAGCTACATACCCTGTTTATGCTGGTGATGGAACCCACTAGGCAGACACTACCAAGTGAGCTCCAT
CCCCAGCCAGCCCCTCAAATCTCACCTGTGAGAGTAGGAAGCCTTGTGACCTCAAAGCACCCCCAAGGGTTCCACC
TCTTAATATGATTCATCACTTTGGTGCATAAATGTTGTGGGGTTACACCATTCAAACCATAATGGTGGGCAAACCT
GAAAGCCACTGTACGCATCATTACATGTTATACGTGTAACACTTGAGCTCCAAAGAACTGATGGCAGCCACAAATG
AAGTCCCATTTGGTCTTAATTTCACTTTGTAGACCAGGTGACCCTGAACGTATGGCAAACCTCCTGTCTCACCTTC
CCAAAGTGCCAGGANTGNAGNCAGGGCATGGGCCTNCCANACCCAATTCCAGCNCGATTGTTNATAAGGGGTTTNT
ANATTNCCTCATGCATCAGAATTCCATGATGTTTTAATCCCAAAGTGACATTCCGNGGCATGTCTANACTATATTG
TATTTANCCCCCCATGTGTTGACAAGATATGTGGNTGGTTTCCCATGCCTTGGCTAATGTGAATAATTGCTAGGAA
CGGGTCTTCCAATGTCTGTTTGCATTTCTACTTTTACTATAGTTGGAATACTCACATTGATCCAACGTCATGGATC
ATTATGTAATGTCCTCACTTCCTCACAGATGCACTATCTGTGGAAGGGTGCACGGACACATGGGTATATTAAGTCC
TGTTCAGTCGGTTCCCATGTGGTTTCCTTACTTACCACATCCTTACTTACCACATCTCAACAGCACAGGGCTCCTC
CAAGTCACATTTATAACCACATCCATCACCTATCTACCTGACCTATCCCTAGCCTGGGGTAACCACAAATCTGATC

XbaI (-1555bp pHB4)

TTTGCT**TCTAGA**ATGTTGCCATTGCAAAAGTACTATTTAGGGCTGGAGAAACAGCTCAGCCGTTTCTTAAGAGCAC
TGACTGCTTTTCCAGAGGTCCTGAGTTCAATTCCCAGCAACCACATGGTGGCTCACAACCATCTGTAACCAGATCT
GATGGCTTCTTCTGGTATGTCTGAAGACAGCTACAGCACAGTGTACTCATATATATAAAATAAATCTTTAAAAATA
AGTTTGTTTAAATGGAACAACAAGCTGGAGAGATGGCTCAGTGCATCCGAGCATTTGCTTTGCAAGGATGAGGAAC
AGAGGTCTAATCCTTAGCACCGTATATAAACAGGCACCACACACTCACATGCATAGAGCACATGGACCCACACACC
CATCATCCCCAGGACTCACAGTGCTCATGCACGCGCACGCACACAGCACACACACACACACACACACACACACA
CACACACACACACACACACACGGCAGGTATGACATGTATCTATAATCTCTGCATTCAGGTGCAGAGTCAGGAGGAC
TGAGAGTCTGAGCCAGCCTGGGCTACATAAAGCCTGTCTTGAAAAATCAAGAGCTGAAACTACAGGTCAATGGTAG
AGCACTTGCCTGGTATGTGCAAGGCTCACCCGGAACACACAATTCTCCTGCCGTAGACTCTGGCTACCAATTTGAA

HindIII (-868bp pHB6)

ATAATACAT**AAGCTT**TTAAAAGTGACTTAAAAAAAAACAACAACAAAACAAACCTGAGCACACATCATTCGCCCAC
TAAACGACGTCCTTACGACTGGTTTTACTTTGCAGGGTTTCACTAAGTTGTTTAGACTTAAACTCAGCCTGCAGCC
CAGGCAGATGATGAACTTCTCATTCACTATGATTTCCTGAAGATTTCTCTGTCCGTCATATGTATCCACTTACCTG
TTGATGGACAGCTCAGATAATTCCAGCTTCTGATTATTGCAAAAAACATTGCTGTAAACATCATGTGGAGGTTTTT
GTTTGGACATATGTTTAATTTCTCTGGGGTAAATACCCAGGAGTTCGTGCTTTGATATGCACACCACATTCACCCA
TGCTATCTGAGTGAGACCCTCACAGGTCCACAGGCAGAAGGAATTTTCACCTCCCTCCCATCTTCCCATTAGGTCA

Appendix 1: Sequence of the pS3 Slc11a1 Promoter Region.

ACAATGCCCCTTGAACTCCAGACTGAGATGAAAGACCTGACAAGGTCTGTGTATGTGTGTGTGTGTGTGTGTGT
GTGTGTGTGTGTGTGTGTGTGTGTGTGTGCGTGTGTAGCTGCCATGAGATATTAAACATTAATACCCAAATGGC
AGGAAGGACCAGAAATCGGAGGTAATTTTGAAAGCAAAGAATCTGGAGTGTCTGGAATGGGGCCAGACTTATTATG
GAACATAGGGTATCCAGGAGAGGAACGAAGGTCAAAACTGTGGGTTACCACCCCCTTCCGCCACAACTGGTCACTT

SphI (-71bp pHB8/20)

CTGCCTTTGGTGAGTGTTTCGAAACGCCAAGTGTGTGAAATTGTGA**GCATGC**CCTCAGTGATGTGGAGATGAGGTC
TGGAGGGGATGGGAAGGGCGTGGGTTCCCACTCTTACTCACTCGGACCAGCACCCACAGAAGGGGACAGATTGAGG

ATG Start Codon (+99bp)

AGCTAGTTGCCAGGCGATGGTGTGACCACACACAGTGTATCCTGCAGCGTGCGTCCTC**ATG**ATTAGTGAGTGGGGC
TGCGGGTCCNAGCANCCCTAATGGGATTCCAGTGGGGGTGACTTGAGGGGGCAAGAAAGATTTAGGGTCTCTGTGG
GGGCTCAGTTCTGCCAGAGGCACTTCAGTCAGGCACTTCTGTGGATTAAACCTGGTGGAGGAGACAGAGCATGGGG
GTCAAGCAGCTGAGCGAGGGGCCTCCTGTCTCACAAATCTCCTGACTCAGGGGATTTGGATCGGAGAAGTTCTGTG
CTCACTGGGAGGGAAGTGATTCTTGGAAACCTCTGCTTGGCACATAGGTGGACCTGCCAGTTGCGGGGAGCGGAGG
TCGAGGTCGTGGGAGGAGGCAGGTGGCTTGAATCCCAGGCTCTTGAAAGAAGCACACACCCACCTAGCATCCTGGG
GTCCCTGACAGGTGACAAGAGCCCCCCGAGGCTGAGCAGGCCCAGTTATGGCTCCATTTCCAGCCTGCCTGGCCCA
GCACCTCAGCCAGCGCCTTGCCGGGAGACCTACCTGAGTGAGAAGATCCCCATTCCCAGCGCAGACCAGGTAGGGA
TGGTAGGAATGTCCTCAGTGCTTCCCAGGTCCTCCGGATCCTCCACGACCTTAAAGGCTGGGGAGGGGGGCACCAT
CTGTGACCTTGACAGTGATTAAAGGAGGTGCTCTGTACTTATTTGGGAAAAACAAATCAAATGGTTCTCAAGAAGA
CCTTAGCTTTTCCACAGGGTAAAGAGCCTAGATACTATGTTGATGCTAAAAGAAGCGATCACTTAGGGACTTGTGC
AGGGATAAAGGCGAGCATCAGCCTGGTTCTGGCATGCTGCCATCCAGCTTTGCCACAATGTTTCTTTTTATAATGG
ATCACATTTATTTATTTAGTTACTTCTGTTTATTTGCCCGTATTTGCGAGTGCATGTGTAGCTGTGTCCATTATAG
AGCATGCGCGTGGAGGTCAGAGGACAACTTGTGAGAGTCAGCTCACTTCTACTACGTGGGTTCCAAGTTTGGTGGC
CTTAGCCTTGAGCCCCTTCTCGGTCCCCATTGCCACACTCTAAGCAGATTCCTAGGCTGTCGGGCCAAACCCTGAA
ATAGAGTTGAGTGACTGAGACCTCAGTGGTCCCCAGAGAGAAGAGCCTGAAGTATGAGAAGGGTCTGGGGAGGGAA
GAGCTGTAACAGGGAGGTTTAATTACAACAAGGTCCCCCTCTTGGGACTCTTGAGAAGCCTTGAAAGAGGCCAGAC
AGGTCATGTGCTGGCCAGCTGCAGAGGCTGCTGCTGAACAGGACCAACCCAGAAAGCAGAGCCATAGTGACTCAGC
AAATGGCCCTGGTCCCTCGGGGGACGGGCAGCGGTGGCATTGGGTGGGTGATGGAGGACAGGGCTGGCCAGCCTGA
CTGAAGAAGATACCTGCTGAGTTTTTAGCTGAGGGGATGGTCAAGGCCAGCTGCATCCATCCAGGAGCTAACATGA
CCCGATCTGCTTGCACCCCCAGGGTACATTCAGCCTGAGGAAGCTGTGGGCGTTCACGGGGCCTGGTTTCCTCATG
AGCATCGCTTTCCTTGACCCGGGAAACATTGAGTCCGACCTTCAAGCTGGCGCTGTGGCTGGGTTCAAAGTACTGA
GTCTGGGCCGCCATGCTTGCTTTGTGGGGAGCACGTGCCTTAGCTAGGACAGGGGAGACCCCAGTTTTCCAGAGCC
GGCTGCATGGGTGGTTTTTCTGAGGATAAGCTCCTATCGGGGAGGAAAAGGACCTTGGAGAAACCCCTGGAGAAAG
GATGCTGTAGGGTGTTAGTCTTCCCGCCCAATCCCCATCAGAGAGGCTGCTCTGGCTGAGCATCTCCTCTGTTTCC
TCACAGCTCCTCTGGGTGCTGCTCTGGGCGACTGTGCTAGGTTTGCTGTGCCAGCGGCTGGCTGCCCGGCTGGGCG
TGGTGACAGGCAAGGACTTGGGTGAAGTCTGCCATCTCTACTACCCCAAGGTGAGCTGGGAACCGGCAGAGGGGGT
CATGGACAGAAAGAACCCACAGCTCTCAAACCCTGAGCAGTTGTTGATAGCTTCCATAATAAAATAAATACAGCAG
GAGCTCCCAGGCTCAATTCATAGCACACGGACAAAGCCCCATATCCTAGGGCTAAGCACTGCTCCCTCAAGACCAC
CCAGACCACACCATGGTATATTTCAAAGAGATTTTAAAAAAAGATTTATTTAGGGCTGGTGAGATGGCTCAGTGGG
TAAGAGCACCTGACTGCTCTTCCGAAGGTCCGGAGTTCAAATCCCAGCAACCACATGGTGGCTCACAACCATCTGT

SalI (+2408bp)

AACAAGATCGA**GTCGAC**

APPENDIX 2 Alignment of the S3 *Slc11a1* Promoter Sequence with the Corresponding Sequence Published by the Mouse Genome Sequencing Project. 6296 nt of the S3 sequence (labelled pS3) were aligned against 6100 nt of the published sequence from the mouse genome sequencing project (labelled Genome). The scoring matrix revealed gap penalties: -12/-2, 96.2% identity and a global alignment score of 23617.

```
                10        20        30        40        50        60
pS3     TCGACAATGACAACAACAACCAGGGTTAGACTCTCGAAAAAGACTAGGTGGGCGGCTAGA
        :
Genome  T-----------------------------------------------------------

                70        80        90       100       110       120
pS3     ATCCGGAGACTGGGCCTGGCTGGGGCTGCGGCTTCAGTGGGAGATAAGCAGGGTCCTTTC

Genome  -----------------------------------------------------------

               130       140       150       160       170       180
pS3     CCAGTTCTACTCTGTCAGAAGGGACTGCATTTGGCCAGCTCTTCTTGTCAAAAAAGGGAA

Genome  -----------------------------------------------------------

               190       200       210       220       230       240
pS3     GCTTTATTTTCGTTTACCCAGCAAGTTTCATGTTTTCTTCCTAGAGTCTATTTTCATAGT
             :::::::::::::::::::::::::::::::::::::::::::::::::::::::
Genome  -----ATTTTCGTTTACCCAGCAAGTTTCATGTTTTCTTCCTAGAGTCTATTTTCATAGT
                     10        20        30        40        50

               250       260       270       280       290       300
pS3     TATGGCCATTTCAGAGAAAATAAAATTAAGGCCTGTGGCCAGGTGTGTTGGCTCAACATC
        ::::::::::::::::::::::::::::::::::::::::::::::::::::::::::::
Genome  TATGGCCATTTCAGAGAAAATAAAATTAAGGCCTGTGGCCAGGTGTGTTGGCTCAACATC
          60        70        80        90       100       110

               310       320       330       340       350       360
pS3     TATAATCTCAGCCCTCAGGGTCCTGACTGAGCCAGGGGAACTACTGTGAGTTCAAGGCCA
        ::::::::::::::::::::::::::::::::::::::::::::::::::::::::::::
Genome  TATAATCTCAGCCCTCAGGGTCCTGACTGAGCCAGGGGAACTACTGTGAGTTCAAGGCCA
         120       130       140       150       160       170

               370       380       390       400       410       420
pS3     GCCAAGGCTACACAACAAAGCCCTCTCTCAAAGATCAAATTAAAAATTAAGAAAAAGAAG
        ::::::::::::::::::::::::::::::::::::::::::::::::::::::::::::
Genome  GCCAAGGCTACACAACAAAGCCCTCTCTCAAAGATCAAATTAAAAATTAAGAAAAAGAAG
         180       190       200       210       220       230

               430       440       450       460       470       480
pS3     GGAAAAGAAGAGGAGGAGAGGGCTGGTGAGATGGCTCAGCGGGTAAGGGCACTGACTGCC
        ::::::::::::::::::::::::::::::::::::::::::::::::::::::::::::
Genome  GGAAAAGAAGAGGAGGAGAGGGCTGGTGAGATGGCTCAGCGGGTAAGGGCACTGACTGCC
         240       250       260       270       280       290

               490       500       510       520       530       540
pS3     CTTCCAAAGGTCCTAAGTTCAAATCCCAGCAACCACATGGTGGCTCACAACCACCCATAA
        ::::::::::::::::::::::::::::::::::::::::::::::::::::::::::::
```

```
Genome CTTCCAAAGGTCCTAAGTTCAAATCCCAGCAACCACATGGTGGCTCACAACCACCCATAA
        300       310       320       330       340       350

              550       560       570       580       590       600
pS3    TGAGATCTGACACACTCTTCTGGTGTGTCTGAAGTCAGCTACAGTAAATTTATGTATAAT
       ::::::::::::::::::::::::::::::::::::::::::::::::::::::::::::
Genome TGAGATCTGACACACTCTTCTGGTGTGTCTGAAGTCAGCTACAGTAAATTTATGTATAAT
        360       370       380       390       400       410

              610       620       630       640       650       660
pS3    AATAAATCTTTAAAAAAAAAAGAAAAAAAAGAGGAGGAGGAGGATAAGAGGGAACCACTT
       ::::::::::::::::::::::: :: : :::::::::::::: : ::::::::::::
Genome AATAAATCTTTAAAAAAAAAAGAAGAAGAGGAGGAGGAGGAGGAGAGGAGGGAACCACT-
        420       430       440       450       460       470

              670       680       690       700       710       720
pS3    AGGCCCACGCCACCCATAATCCCAACACTTAGGAAACAGGTGAGTTTCCGGGTTCATCTT
       :::::::::::::::::::::::::::::::::::::::::::::: :::::: ::::::
Genome AGGCCCACGCCACCCATAATCCCAACACTTAGGAAACAGGTGAGTT-CCGGGT-CATCTT
         480       490       500       510       520         530

              730       740       750       760       770       780
pS3    TGGTTCCCCTCCGTGAGCTTGGGTCCTGCCTGGGCTACATAAAATCCTGCAGGTGGGAGA
       ::::::::::::::::::::::::::::::::::::::::::::::::::::::::::::
Genome TGGTTCCCCTCCGTGAGCTTGGGTCCTGCCTGGGCTACATAAAATCCTGCAGGTGGGAGA
           540       550       560       570       580       590

              790       800       810       820       830       840
pS3    GCAGGATTTGAACCTGGAGTTGGACATGAGAAGCCTGCAGTGGTGCCATGGATCTAAACA
       ::::::::::::::::::::::::::::::::::::::::::::::::::::::::::::
Genome GCAGGATTTGAACCTGGAGTTGGACATGAGAAGCCTGCAGTGGTGCCATGGATCTAAACA
           600       610       620       630       640       650

              850       860       870       880       890       900
pS3    TAATTACTACTACCACCTAGAAACGAATGCATAGAAAGTGCAGGCGGTGTATAAGGAGGG
       ::::::::::::::::::::::::::::::::::::::::::::::::::::::::::::
Genome TAATTACTACTACCACCTAGAAACGAATGCATAGAAAGTGCAGGCGGTGTATAAGGAGGG
           660       670       680       690       700       710

              910       920       930       940       950       960
pS3    ACACAGGACATCCCTAGCCCTCACTCAGCTTCTTTGTGCTTCAGGTTCTCCTTGCCCCAT
       ::::::::::::::::::::::::::::::::::::::::::::::::::::::::::::
Genome ACACAGGACATCCCTAGCCCTCACTCAGCTTCTTTGTGCTTCAGGTTCTCCTTGCCCCAT
           720       730       740       750       760       770

              970       980       990      1000      1010      1020
pS3    CAATACACACACACATACACACACACACACACACACACACACGACTCCCCAGACTGTGCA
       ::::::::::::::::::::::::::::::::::::::::::::::::::::::::::::
Genome CAATACACACACACATACACACACACACACACACACACACACGACTCCCCAGACTGTGCA
           780       790       800       810       820       830

             1030      1040      1050      1060      1070      1080
pS3    AGGGCCCCCCAGCCACCCAGTAAGAAGGAAAGAGAAGCAGGAACCCATCACTGCCTCCAG
       ::::::::::::::::::::::::::::::::::::::::::::::::::::::::::::
Genome AGGGCCCCCCAGCCACCCAGTAAGAAGGAAAGAGAAGCAGGAACCCATCACTGCCTCCAG
           840       850       860       870       880       890

             1090      1100      1110      1120      1130      1140
pS3    CTTCCTCACTCACCAGCAGTTCTGGACGGTGGCTTGTCTGCCTGACGCTGGCTTTAGAAC
       ::::::::::::::::::::::::::::::::::::::::::::::::::::::::::::
Genome CTTCCTCACTCACCAGCAGTTCTGGACGGTGGCTTGTCTGCCTGACGCTGGCTTTAGAAC
```

```
            900        910        920        930        940        950

             1150       1160       1170       1180       1190       1200
pS3     CTGTTGGGGGTTGGTAGTTAGGGTGCAGGCACCACACCTCCATTAACATCTCTGGCCATC
        ::::::::::::::::::::::::::::::::::::::::::::::::::::::::::::
Genome  CTGTTGGGGGTTGGTAGTTAGGGTGCAGGCACCACACCTCCATTAACATCTCTGGCCATC
            960        970        980        990       1000       1010

             1210       1220       1230       1240       1250       1260
pS3     AGCCCTGCTGCTTTGAAATGAGAGACTCCGGAGGAACTCCAAGGTGTAGTGGAGAGTTCC
        ::::::::::::::::::::::::::::::::::::::::::::::::::::::::::::
Genome  AGCCCTGCTGCTTTGAAATGAGAGACTCCGGAGGAACTCCAAGGTGTAGTGGAGAGTTCC
           1020       1030       1040       1050       1060       1070

             1270       1280       1290       1300       1310       1320
pS3     AGTCTTGGCTACAGAGCTGAGGAATGTAAGGGAGGGTAGTCTGTCTGTCTTCCAGAAATC
        ::::::::::::::::::::::::::::::::::::::::::::::::::::::::::::
Genome  AGTCTTGGCTACAGAGCTGAGGAATGTAAGGGAGGGTAGTCTGTCTGTCTTCCAGAAATC
           1080       1090       1100       1110       1120       1130

             1330       1340       1350       1360       1370       1380
pS3     ACTTCAGAAGGCTTCAGACAGGGCTGCCACTTGAGCCTTGCAAAGTGTTTTATGTCATGT
        ::::::::::::::::::::::::::::::::::::::::::::::::::::::::::::
Genome  ACTTCAGAAGGCTTCAGACAGGGCTGCCACTTGAGCCTTGCAAAGTGTTTTATGTCATGT
           1140       1150       1160       1170       1180       1190

             1390       1400       1410       1420       1430       1440
pS3     CCCCCCTCCTTAAAAACAGAACAAAACATTCACAAGCTGGGTGGTGGTGGCACAAGCCTT
        ::::::::::::::::::::::::::::::::::::::::::::::::::::::::::::
Genome  CCCCCCTCCTTAAAAACAGAACAAAACATTCACAAGCTGGGTGGTGGTGGCACAAGCCTT
           1200       1210       1220       1230       1240       1250

             1450       1460       1470       1480       1490       1500
pS3     AATCCCAACTCTCAGGACGCAGAGGCCAGGCTGGTCTATAGAGCAAGTTCAAGGACAACC
        ::::::::::::::::::::::::::::::::::::::::::::::::::::::::::::
Genome  AATCCCAACTCTCAGGACGCAGAGGCCAGGCTGGTCTATAGAGCAAGTTCAAGGACAACC
           1260       1270       1280       1290       1300       1310

             1510       1520       1530       1540       1550       1560
pS3     AGAGCTACACAGAGAGATCTTGTCTCGGCAAACACACACCACACACACACACACACACAC
        ::::::::::::::::::::::::::::::::::::::::::::::::::::::::::::
Genome  AGAGCTACACAGAGAGATCTTGTCTCGGCAAACACACACCACACACACACACACACACAC
           1320       1330       1340       1350       1360       1370

             1570       1580       1590       1600       1610       1620
pS3     ACACACACACACACACACACACACAACCAAACCAAACCAACCAACCAAAGACCCCCAAAATC
        ::::::::::::::::::::::::::::::::::::::::::::::::::::::::::::
Genome  ACACACACACACACACACACACACAACCAAACCAAACCAACCAACCAAAGACCCCCAAAATC
           1380       1390       1400       1410       1420       1430

             1630       1640       1650       1660       1670       1680
pS3     AAAAGACATTCACAACCAAGAAAAATGAAATAAAACCACCACAACAAAATTATCTTAGTT
        ::::::::::::::::::::::::::::::::::::::::::::::::::::::::::::
Genome  AAAAGACATTCACAACCAAGAAAAATGAAATAAAACCACCACAACAAAATTATCTTAGTT
           1440       1450       1460       1470       1480       1490

             1690       1700       1710       1720       1730       1740
pS3     TCTCTGTCCCAGGGCCTCACACACTCTCCCAGAGGCTTCACCCAGTCCCTGCCAAGCATT
        ::::::::::::::::::::::::::::::::::::::::::::::::::::::::::::
Genome  TCTCTGTCCCAGGGCCTCACACACTCTCCCAGAGGCTTCACCCAGTCCCTGCCAAGCATT
           1500       1510       1520       1530       1540       1550
```

```
            1750       1760       1770       1780       1790       1800
pS3     TTCTTGAAATAGATCTTTATAATTCCAATGTATTCTCAAAATGAAATCATACCAGTAATA
        ::::::::::::::::::::::::::::::::::::::::::::::::::::::::::::
Genome TTCTTGAAATAGATCTTTATAATTCCAATGTATTCTCAAAATGAAATCATACCAGTAATA
          1560       1570       1580       1590       1600       1610

            1810       1820       1830       1840       1850       1860
pS3     TATGCTTGTTAGTTGGTAATTGGATACTTAATTATATATTATAATTTATATACATTATAT
        ::::::::::::::::::::::::::::::::::::::::::::::::::::::::::::
Genome TATGCTTGTTAGTTGGTAATTGGATACTTAATTATATATTATAATTTATATACATTATAT
          1620       1630       1640       1650       1660       1670

            1870       1880       1890       1900       1910       1920
pS3     ATAGTGAAGCTGAAGTCGCCCTAGGTCCATTGTATTTTGAAACACTATTTCATGTGTTGG
        ::::::::::::::::::::::::::::::::::::::::::::::::::::::::::::
Genome ATAGTGAAGCTGAAGTCGCCCTAGGTCCATTGTATTTTGAAACACTATTTCATGTGTTGG
          1680       1690       1700       1710       1720       1730

            1930       1940       1950       1960       1970       1980
pS3     CTTTCTGGGGCTGGGGGGGCGGGGGGTTGGGGGAATGGCTCATGTGTAAAAGTGTTAGCT
        ::::::::::::::::::::::::::::::::::::::::::::::::::::::::::::
Genome CTTTCTGGGGCTGGGGGGGCGGGGGGTTGGGGGAATGGCTCATGTGTAAAAGTGTTAGCT
          1740       1750       1760       1770       1780       1790

            1990       2000       2010       2020       2030       2040
pS3     GTGCAAACCTGAGGACCCCAGTTCCACCAGTGGAACCCACATAAAAATCTGGATGTGACC
        ::::::::::::::::::::::::::::::::::::::::::::::::::::::::::::
Genome GTGCAAACCTGAGGACCCCAGTTCCACCAGTGGAACCCACATAAAAATCTGGATGTGACC
          1800       1810       1820       1830       1840       1850

              2050       2060       2070       2080       2090
pS3     CAGCATGGTGGCCTGGGC-TGAAATCCCGGCACTCAAAGGCAGAGGTGGGTGGATCTCTG
        ::::::::::::::::: ::::::::::::::::::::::::::::::::::::::::::
Genome CAGCATGGTGGCCTGGGCCTGAAATCCCGGCACTCAAAGGCAGAGGTGGGTGGATCTCTG
          1860       1870       1880       1890       1900       1910

    2100       2110       2120       2130       2140       2150
pS3     AGTTCAAGGCCAGCTTCATGGCTAGCTACATGGTGAATTCCAGAGCAGTCAGGGTTGCAC
        ::::::::::::::::::::::::::::::::::::::::::::::::::::::::::::
Genome AGTTCAAGGCCAGCTTCATGGCTAGCTACATGGTGAATTCCAGAGCAGTCAGGGTTGCAC
          1920       1930       1940       1950       1960       1970

    2160       2170       2180       2190       2200       2210
pS3     AGTGAATTCCTATCTCAAAAACAAACGACAGAAGCAGGATGCAGTGGCATGAAGCTGTGA
        ::::::::::::::::::::::::::::::::::::::::::::::::::::::::::::
Genome AGTGAATTCCTATCTCAAAAACAAACGACAGAAGCAGGATGCAGTGGCATGAAGCTGTGA
          1980       1990       2000       2010       2020       2030

    2220       2230       2240       2250       2260       2270
pS3     TCCTAGCACCTCTATGGCAAGACTGGAGACAGAGAGACCGGAGAAGCACTTTGAAACTTT
        ::::::::::::::::::::::::::::::::::::::::::::::::::::::::::::
Genome TCCTAGCACCTCTATGGCAAGACTGGAGACAGAGAGACCGGAGAAGCACTTTGAAACTTT
          2040       2050       2060       2070       2080       2090

    2280       2290       2300       2310       2320       2330
pS3     TGGACTCTCTAGCCTAGAGTACACATCTGCAGCAGTAGAAACAGGCCCTGCCTCAACGAG
        ::::::::::::::::::::::::::::::::::::::::::::::::::::::::::::
Genome TGGACTCTCTAGCCTAGAGTACACATCTGCAGCAGTAGAAACAGGCCCTGCCTCAACGAG
          2100       2110       2120       2130       2140       2150
```

```
    2340       2350       2360       2370       2380       2390
pS3     GTAAAAGGTGGACTGGAGCGTACCCTAGGCTGTAGGCCCCTGGACACATCGCCTTCCGTG
        ::::::::::::::::::::::::::::::::::::::::::::::::::::::::::::
Genome GTAAAAGGTGGACTGGAGCGTACCCTAGGCTGTAGGCCCCTGGACACATCGCCTTCCGTG
          2160       2170       2180       2190       2200       2210

    2400       2410       2420       2430       2440       2450
pS3     TTCTCACACACCCCAAGACTGACTTTGCTCATCCATCAGTGCCCTTGGCTTTGTTATTGA
        ::::::::::::::::::::::::::::::::::::::::::::::::::::::::::::
Genome TTCTCACACACCCCAAGACTGACTTTGCTCATCCATCAGTGCCCTTGGCTTTGTTATTGA
          2220       2230       2240       2250       2260       2270

    2460       2470       2480       2490       2500       2510
pS3     TCTTTCTTTGCTCTCTGGACAGTCTCATCATGAATTCTATGCTAGCTTCAGCCTCGCAAG
        ::::::::::::::::::::::::::::::::::::::::::::::::::::::::::::
Genome TCTTTCTTTGCTCTCTGGACAGTCTCATCATGAATTCTATGCTAGCTTCAGCCTCGCAAG
          2280       2290       2300       2310       2320       2330

    2520       2530       2540       2550       2560       2570
pS3     TGTTGAGATCACAGGTGGATACCACCATCACCAAACGACCAGTGTGTTTAGAACACACTT
        ::::::::::::::::::::::::::::::::::::::::::::::::::::::::::::
Genome TGTTGAGATCACAGGTGGATACCACCATCACCAAACGACCAGTGTGTTTAGAACACACTT
          2340       2350       2360       2370       2380       2390

    2580       2590       2600       2610       2620       2630
pS3     GTCATATCATTACAGCCCTCTATCTTCATGCCTCTGTATGCTGGTACAGTATGCTGGTAG
        :::::::::::::::::::::::::::: :::::::::::::::::::::::::::::
Genome GTCATATCATTACAGCCCTCTATCTTCATGTCTCTGTATGCTGGTACAGTATGCTGGTAG
          2400       2410       2420       2430       2440       2450

    2640       2650       2660       2670       2680       2690
pS3     GGATTTAACCCAGAGCTTCATGCATACTAAACACATACAAGGGAGGCACAAACTCCATTC
        ::::::::::::::::::::::::::::::::::::::::::::::::::::::::::::
Genome GGATTTAACCCAGAGCTTCATGCATACTAAACACATACAAGGGAGGCACAAACTCCATTC
          2460       2470       2480       2490       2500       2510

    2700       2710       2720       2730       2740       2750
pS3     TCTTGGTTGTCCTTTAGCCACCCCCACTTTTGGGGGTGGGGGGAGTTGTTTGTTTTTAAA
        ::::::::::::::::::::::::::::::::::::::::::::::::::::::::::::
Genome TCTTGGTTGTCCTTTAGCCACCCCCACTTTTGGGGGTGGGGGGAGTTGTTTGTTTTTAAA
          2520       2530       2540       2550       2560       2570

    2760       2770       2780       2790       2800       2810
pS3     ACTTTATTACATAGTTTTATTATATGTTTCTAAGATAAGGAATATGAAATTCAAGGAAAT
        ::::::::::::::::::::::::::::::::::::::::::::::::::::::::::::
Genome ACTTTATTACATAGTTTTATTATATGTTTCTAAGATAAGGAATATGAAATTCAAGGAAAT
          2580       2590       2600       2610       2620       2630

    2820       2830       2840       2850       2860       2870
pS3     TAGGGTTTTGATTTGTTTTGTTGCTTTTGGTTTTGGTTTTTTGGGTTTTTGTTGTTGGTG
        ::::::::::::::::::::::::::::::::::::::::::::::::::::::::::::
Genome TAGGGTTTTGATTTGTTTTGTTGCTTTTGGTTTTGGTTTTTTGGGTTTTTGTTGTTGGTG
          2640       2650       2660       2670       2680       2690

    2880       2890       2900       2910       2920       2930
pS3     GGGTTTTTTTTGTGTGTGTTTTGTTTTGTTTTTTTGAGATAGGGTTTCTCTGTGTAACCC
        ::::::::::::::::::::::::::::::::::::::::::::::::::::::::::::
Genome GGGTTTTTTTTGTGTGTGTTTTGTTTTGTTTTTTTGAGATAGGGTTTCTCTGTGTAACCC
          2700       2710       2720       2730       2740       2750

    2940       2950       2960       2970       2980       2990
```

```
pS3     TGGCTGTCCTGGAAGTTACTCTGTAGACCAGGCTGGCCTCGAACTCAGAAATCCACCTGC
        ::::::::::::::::::::::::::::::::::::::::::::::::::::::::::::
Genome TGGCTGTCCTGGAAGTTACTCTGTAGACCAGGCTGGCCTCGAACTCAGAAATCCACCTGC
          2760      2770      2780      2790      2800      2810

    3000      3010      3020      3030      3040      3050
pS3     CTCTGCCTCCCATGTGCTGGGATTAAAGGCGGTACACTGATGAAAGGGTCTTGCTGACCG
        :::::::::::::::::::::::::::::::: ::::::::::::::::::::::::::
Genome CTCTGCCTCCCATGTGCTGGGATTAAAGGCG-TACACTGATGAAAGGGTCTTGCTGACCG
          2820      2830      2840       2850      2860      2870

    3060      3070      3080      3090      3100      3110
pS3     AGTGAGGCAGCCATGACTTTTAGAAGACAATCCTCCAGGGCTGAAGAGTTGGCTCAGTGG
        ::::::::::::::::::::::::::::::::::::::::::::::::::::::::::::
Genome AGTGAGGCAGCCATGACTTTTAGAAGACAATCCTCCAGGGCTGAAGAGTTGGCTCAGTGG
          2880      2890      2900      2910      2920      2930

    3120      3130      3140      3150      3160      3170
pS3     TTAGGAGTACTGTTCTCCTGAGGGACCCAGTCTGATTCCCTGCACCCACTTGCCACTTAC
        ::::::::::::::::::::::::::::::::::::::::::::::::::::::::::::
Genome TTAGGAGTACTGTTCTCCTGAGGGACCCAGTCTGATTCCCTGCACCCACTTGCCACTTAC
          2940      2950      2960      2970      2980      2990

    3180      3190      3200      3210      3220      3230
pS3     TCAGGCACCAGGCGTGCGTAGGTGTGGTGCACAGACATCCATGCAGGAAAAGCATTCAAT
        ::::::::::::::::::::::::::::::::::::::::::::::::::::::::::::
Genome TCAGGCACCAGGCGTGCGTAGGTGTGGTGCACAGACATCCATGCAGGAAAAGCATTCAAT
          3000      3010      3020      3030      3040      3050

    3240      3250      3260      3270      3280      3290
pS3     CTAAAAAAAAAAAAAAAAAAAAAAGTGTAAAAAGAAAATACCCGAAGCCGAGTGTGGCGG
        ::::::::::::::::::::::::::::::::::::::::::::::::::::::::::::
Genome CTAAAAAAAAAAAAAAAAAAAAAAGTGTAAAAAGAAAATACCCGAAGCCGAGTGTGGCGG
          3060      3070      3080      3090      3100      3110

    3300      3310      3320      3330      3340      3350
pS3     CTCACACTGAGATGCCAATATTTGGGAGGCTAAGGAAGGAGAATCTTCAGTTCAAGGTCA
        ::::::::::::::::::::::::::::::::::::::::::::::::::::::::::::
Genome CTCACACTGAGATGCCAATATTTGGGAGGCTAAGGAAGGAGAATCTTCAGTTCAAGGTCA
          3120      3130      3140      3150      3160      3170

    3360      3370      3380      3390      3400      3410
pS3     GCATGGAGGTGAACGGACAGAAAGCTTCTCTCGTGTGTGTGTGTGTGTGTGTGTGTGTGT
        ::::::::::::::::::::::::::::::::::::::::::::::::::::::::::::
Genome GCATGGAGGTGAACGGACAGAAAGCTTCTCTCGTGTGTGTGTGTGTGTGTGTGTGTGT
          3180      3190      3200      3210      3220      3230

    3420      3430      3440      3450      3460      3470
pS3     GTGTGTACATATGCACGCACAAGTGTGGGCACTGCCGAGCACCCAGAAGAGGATGTCAAA
        ::::::::::::::::::::::::::::::::::::::::::::::::::::::::::::
Genome GTGTGTACATATGCACGCACAAGTGTGGGCACTGCCGAGCACCCAGAAGAGGATGTCAAA
          3240      3250      3260      3270      3280      3290

    3480      3490      3500      3510      3520      3530
pS3     TCCCCTGCAGCTGGAGTGGCCTGACATGGATATTGGGAACTGAATCAGCTCCTCTGCCAA
        ::::::::::::::::::::::::::::::::::::::::::::::::::::::::::::
Genome TCCCCTGCAGCTGGAGTGGCCTGACATGGATATTGGGAACTGAATCAGCTCCTCTGCCAA
          3300      3310      3320      3330      3340      3350

    3540      3550      3560      3570      3580      3590
pS3     AGCTGTGCCTGCTGTAACTGCCCACCCATTTCTCCAGCCCAGTTCTGCACACTTGTTTGC
```

```
          :::::::::::::::::::::::::::::::::::::::::::::::::::::::::::::::::::::
Genome AGCTGTGCCTGCTGTAACTGCCCACCCATTTCTCCAGCCCAGTTCTGCACACTTGTTTGC
            3360       3370       3380       3390       3400       3410

     3600       3610       3620       3630       3640       3650
pS3     TTGCTTGGGTTTTTGTTTGTTGGTTTATTTGTTTGTTGTTTTTGTTTTTTGTTTNTTGCA
          ::::::::::::::::::::::::::::::::::::::::::::::::::::::::::::::::::::.:::::
Genome TTGCTTGGGTTTTTGTTTGTTGGTTTATTTGTTTGTTGTTTTTGTTTTTTGTTTTTTGCA
            3420       3430       3440       3450       3460       3470

     3660       3670       3680       3690       3700       3710
pS3     GGAAGAAGAGGTTCAGACGGGGACTCAGGAAGCATAGGCTAGCCACCTTGCCGGTATCTC
          ::::::::::::::::::::::::::::::::::::::::::::::::::::::::::::::::::::::::
Genome GGAAGAAGAGGTTCAGACGGGGACTCAGGAAGCATAGGCTAGCCACCTTGCCGGTATCTC
            3480       3490       3500       3510       3520       3530

     3720       3730       3740       3750       3760       3770
pS3     TTAGCTTCCGGTGTGAGCTACATACCCTGTTTATGCTGGTGATGGAACCCACTAGGCAGA
          ::::::::::::::::::::::::::::::::::::::::::::::::::::::::::::::::::::::::
Genome TTAGCTTCCGGTGTGAGCTACATACCCTGTTTATGCTGGTGATGGAACCCACTAGGCAGA
            3540       3550       3560       3570       3580       3590

     3780       3790       3800       3810       3820       3830
pS3     CACTACCAAGTGAGCTCCATCCCCAGCCAGCCCCTCAAATCTCACCTGTGAGAGTAGGAA
          ::::::::::::::::::::::::::::::::::::::::::::::::::::::::::::::::::::::::
Genome CACTACCAAGTGAGCTCCATCCCCAGCCAGCCCCTCAAATCTCACCTGTGAGAGTAGGAA
            3600       3610       3620       3630       3640       3650

     3840       3850       3860       3870       3880       3890
pS3     GCCTTGTGACCTCAAAGCACCCCCAAGGGTTCCACCTCTTAATATGATTCATCACTTTGG
          ::::::::::::::::::::::::::::::::::::::::::::::::::::::::::::::::::::::::
Genome GCCTTGTGACCTCAAAGCACCCCCAAGGGTTCCACCTCTTAATATGATTCATCACTTTGG
            3660       3670       3680       3690       3700       3710

     3900       3910       3920       3930       3940       3950
pS3     TGCATAAATGTTGTGGGGTTACACCATTCAAACCATAATGGTGGGCAAACCTGAAAGCCA
          ::::::::::::::::::::::::::::::::::::::::::::::::::::::::::::::::::::::::
Genome TGCATAAATGTTGTGGGGTTACACCATTCAAACCATAATGGTGGGCAAACCTGAAAGCCA
            3720       3730       3740       3750       3760       3770

     3960       3970       3980       3990       4000       4010
pS3     CTGTACGCATCATTACATGTTATACGTGTAACACTTGAGCTCCAAAGAACTGATGGCAGC
          ::::::::::::::::::::::::::::::::::::::::::::::::::::::::::::::::::::::::
Genome CTGTACGCATCATTACATGTTATACGTGTAACACTTGAGCTCCAAAGAACTGATGGCAGC
            3780       3790       3800       3810       3820       3830

     4020       4030       4040       4050       4060       4070
pS3     CACAAATGAAGTCCCATTTGGTCTTAATTTCACTTTGTAGACCAGGTGACCCTGAACGTA
          ::::::::::::::::::::::::::::::::::::::::::::::::::::::::::::::::::::::::
Genome CACAAATGAAGTCCCATTTGGTCTTAATTTCACTTTGTAGACCAGGTGACCCTGAACGTA
            3840       3850       3860       3870       3880       3890

     4080       4090       4100       4110       4120       4130
pS3     TGGCAAACCTCCTGTCTCACCTTCCCAAAGTGCCAGGANTGNAGNCAGGGCATGGGCCTN
          :::::::::::::::::::::::::::: ::::::::::.::.::.:::: ::::::: :.
Genome TGGCAAACCTCCTGTCTCACCTTCCCAA-GTGCCAGGACTGCAGGCAGG-CATGGGC-TA
            3900       3910       3920       3930       3940

    4140       4150       4160       4170       4180       4190
pS3     CCANACCCAATTCCAGCNCGATTGTTNATAAGGGGTTTNTANATTNCCTCATGCATCAGA
          :::.:::::::: :::::.:::: :::.:::::::::::.::.:::.:::::::::::::::
```

```
Genome CCATACCCAAT-CCAGCACGAT-GTTTATAAGGGGTTTCTATATTACCTCATGCATCAGA
    3950       3960       3970       3980       3990       4000

    4200       4210       4220       4230       4240       4250
pS3    ATTCCATGATGTTTTAATCCCAAAGTGACATTCCGNGGCATGTCTANACTATATTGTATT
       :::::::::::::::::::::: ::::::::::.:::::::::.:::::::::::::
Genome ATTCCATGATGTTTTAATCCCAA-GTGACATTCCGTGGCATGTCTATACTATATTGTATT
      4010       4020       4030       4040       4050       4060

    4260       4270       4280       4290       4300       4310
pS3    TANCCCCCCATGTGTTGACAAGATATGTGGNTGGTTTCCCATGCCTTGGCTAATGTGAAT
       ::.::    :::::::::: :::::::::.:::::::: :::::::::::::::::::
Genome TATCC----ATGTGTTGACA-GATATGTGGCTGGTTTCC-ATGCCTTGGCTAATGTGAAT
       4070          4080       4090       4100       4110       4120

    4320       4330       4340       4350       4360       4370
pS3    AATTGCTAGGAACGGGTCTTCCAATGTCTGTTTGCATTTCTACTTTTACTATAGTTGGAA
       ::::::::::::::::::::::::::::::::::::::::::::::::::::::::::::
Genome AATTGCTAGGAACGGGTCTTCCAATGTCTGTTTGCATTTCTACTTTTACTATAGTTGGAA
            4130       4140       4150       4160       4170       4180

    4380       4390       4400       4410       4420       4430
pS3    TACTCACATTGATCCAACGTCATGGATCATTATGTAATGTCCTCACTTCCTCACAGATGC
       ::::::::::::::::::::::::::::::::::::::::::::::::::::::::::::
Genome TACTCACATTGATCCAACGTCATGGATCATTATGTAATGTCCTCACTTCCTCACAGATGC
            4190       4200       4210       4220       4230       4240

    4440       4450       4460       4470       4480       4490
pS3    ACTATCTGTGGAAGGGTGCACGGACACATGGGTATATTAAGTCCTGTTCAGTCGGTTCCC
       ::::::::::::::::::::::::::::::::::::::::::::::::::::::::::::
Genome ACTATCTGTGGAAGGGTGCACGGACACATGGGTATATTAAGTCCTGTTCAGTCGGTTCCC
            4250       4260       4270       4280       4290       4300

    4500       4510       4520       4530       4540       4550
pS3    ATGTGGTTTCCTTACTTACCACATCCTTACTTACCACATCTCAACAGCACAGGGCTCCTC
       ::::::::::::::::::::::::::::::::::::::::::::::::::::::::::::
Genome ATGTGGTTTCCTTACTTACCACATCCTTACTTACCACATCTCAACAGCACAGGGCTCCTC
            4310       4320       4330       4340       4350       4360

    4560       4570       4580       4590       4600       4610
pS3    CAAGTCACATTTATAACCACATCCATCACCTATCTACCTGACCTATCCCTAGCCTGGGGT
       ::::::::::::::::::::::::::::::::::::::::::::::::::::::::::::
Genome CAAGTCACATTTATAACCACATCCATCACCTATCTACCTGACCTATCCCTAGCCTGGGGT
            4370       4380       4390       4400       4410       4420

    4620       4630       4640       4650       4660       4670
pS3    AACCACAAATCTGATCTTTGCTTCTAGAATGTTGCCATTGCAAAAGTACTATTTAGGGCT
       ::::::::::::::::::::::::::::::::::::::::::::::::::::::::::::
Genome AACCACAAATCTGATCTTTGCTTCTAGAATGTTGCCATTGCAAAAGTACTATTTAGGGCT
            4430       4440       4450       4460       4470       4480

    4680       4690       4700       4710       4720       4730
pS3    GGAGAAACAGCTCAGCCGTTTCTTAAGAGCACTGACTGCTTTTCCAGAGGTCCTGAGTTC
       ::::::::::::::::::::::::::::::::::::::::::::::::::::::::::::
Genome GGAGAAACAGCTCAGCCGTTTCTTAAGAGCACTGACTGCTTTTCCAGAGGTCCTGAGTTC
            4490       4500       4510       4520       4530       4540

    4740       4750       4760       4770       4780       4790
pS3    AATTCCCAGCAACCACATGGTGGCTCACAACCATCTGTAACCAGATCTGATGGCTTCTTC
       ::::::::::::::::::::::::::::::::::::::::::::::::::::::::::::
Genome AATTCCCAGCAACCACATGGTGGCTCACAACCATCTGTAACCAGATCTGATGGCTTCTTC
```

```
              4550       4560       4570       4580       4590       4600

     4800       4810       4820       4830       4840       4850
pS3     TGGTATGTCTGAAGACAGCTACAGCACAGTGTACTCATATATATAAAATAAATCTTTAAA
        ::::::::::::::::::::::::::::::::::::::::::::::::::::::::::::
Genome TGGTATGTCTGAAGACAGCTACAGCACAGTGTACTCATATATATAAAATAAATCTTTAAA
              4610       4620       4630       4640       4650       4660

     4860       4870       4880       4890       4900       4910
pS3     AATAAGTTTGTTTAAATGGAACAACAAGCTGGAGAGATGGCTCAGTGCATCCGAGCATTT
        ::::::::::::::::::::::::::::::::::::::::::::::::::::::::::::
Genome AATAAGTTTGTTTAAATGGAACAACAAGCTGGAGAGATGGCTCAGTGCATCCGAGCATTT
              4670       4680       4690       4700       4710       4720

     4920       4930       4940       4950       4960       4970
pS3     GCTTTGCAAGGATGAGGAACAGAGGTCTAATCCTTAGCACCGTATATAAACAGGCACCAC
        ::::::::::::::::::::::::::::::::::::::::::::::::::::::::::::
Genome GCTTTGCAAGGATGAGGAACAGAGGTCTAATCCTTAGCACCGTATATAAACAGGCACCAC
              4730       4740       4750       4760       4770       4780

     4980       4990       5000       5010       5020       5030
pS3     ACACTCACATGCATAGAGCACATGGACCCACACACCCATCATCCCCAGGACTCACAGTGC
        ::::::::::::::::::::::::::::::::::::::::::::::::::::::::::::
Genome ACACTCACATGCATAGAGCACATGGACCCACACACCCATCATCCCCAGGACTCACAGTGC
              4790       4800       4810       4820       4830       4840

     5040       5050       5060       5070       5080       5090
pS3     TCATGCACGCGCACGCACACAGCACACACACACACACACACACACACACACACACACA
        ::::::::::::::::::::::::::::::::::::::::::::::::::::::::::::
Genome TCATGCACGCGCACGCACACAGCACACACACACACACACACACACACACACACACACA
              4850       4860       4870       4880       4890       4900

     5100       5110       5120       5130       5140       5150
pS3     CACACACACACACGGCAGGTATGACATGTATCTATAATCTCTGCATTCAGGTGCAGAGTC
        ::::::::::::::::::::::::::::::::::::::::::::::::::::::::::::
Genome CACACACACACACGGCAGGTATGACATGTATCTATAATCTCTGCATTCAGGTGCAGAGTC
              4910       4920       4930       4940       4950       4960

     5160       5170       5180       5190       5200       5210
pS3     AGGAGGACTGAGAGTCTGAGCCAGCCTGGGCTACATAAAGCCTGTCTTGAAAAATCAAGA
        ::::::::::::::::::::::::::::::::::::::::::::::::::::::::::::
Genome AGGAGGACTGAGAGTCTGAGCCAGCCTGGGCTACATAAAGCCTGTCTTGAAAAATCAAGA
              4970       4980       4990       5000       5010       5020

     5220       5230       5240       5250       5260       5270
pS3     GCTGAAACTACAGGTCAATGGTAGAGCACTTGCCTGGTATGTGCAAGGCTCACCCGGAAC
        ::::::::::::::::::::::::::::::::::::::::::::::::::::::::::::
Genome GCTGAAACTACAGGTCAATGGTAGAGCACTTGCCTGGTATGTGCAAGGCTCACCCGGAAC
              5030       5040       5050       5060       5070       5080

     5280       5290       5300       5310       5320       5330
pS3     ACACAATTCTCCTGCCGTAGACTCTGGCTACCAATTTGAAATAATACATAAGCTTTTAAA
        ::::::::::::::::::::::::::::::::::::::::::::::::::::::::::::
Genome ACACAATTCTCCTGCCGTAGACTCTGGCTACCAATTTGAAATAATACATAAGCTTTTAAA
              5090       5100       5110       5120       5130       5140

     5340       5350       5360       5370       5380       5390
pS3     AGTGACTTAAAAAAAAACAACAACAAAACAAACCTGAGCACACATCATTCGCCCACTAAA
        ::::::::::::::::::::::::::::::::::::::::::::::::::::::::::::
Genome AGTGACTTAAAAAAAAACAACAACAAAACAAACCTGAGCACACATCATTCGCCCACTAAA
              5150       5160       5170       5180       5190       5200
```

```
    5400       5410       5420       5430       5440       5450
pS3     CGACGTCCTTACGACTGGTTTTACTTTGCAGGGTTTCACTAAGTTGTTTAGACTTAAACT
        ::::::::::::::::::::::::::::::::::::::::::::::::::::::::::::
Genome CGACGTCCTTACGACTGGTTTTACTTTGCAGGGTTTCACTAAGTTGTTTAGACTTAAACT
             5210       5220       5230       5240       5250       5260

    5460       5470       5480       5490       5500       5510
pS3     CAGCCTGCAGCCCAGGCAGATGATGAACTTCTCATTCACTATGATTTCCTGAAGATTTCT
        ::::::::::::::::::::::::::::::::::::::::::::::::::::::::::::
Genome CAGCCTGCAGCCCAGGCAGATGATGAACTTCTCATTCACTATGATTTCCTGAAGATTTCT
             5270       5280       5290       5300       5310       5320

    5520       5530       5540       5550       5560       5570
pS3     CTGTCCGTCATATGTATCCACTTACCTGTTGATGGACAGCTCAGATAATTCCAGCTTCTG
        ::::::::::::::::::::::::::::::::::::::::::::::::::::::::::::
Genome CTGTCCGTCATATGTATCCACTTACCTGTTGATGGACAGCTCAGATAATTCCAGCTTCTG
             5330       5340       5350       5360       5370       5380

    5580       5590       5600       5610       5620       5630
pS3     ATTATTGCAAAAAACATTGCTGTAAACATCATGTGGAGGTTTTTGTTTGGACATATGTTT
        ::::::::::::::::::::::::::::::::::::::::::::::::::::::::::::
Genome ATTATTGCAAAAAACATTGCTGTAAACATCATGTGGAGGTTTTTGTTTGGACATATGTTT
             5390       5400       5410       5420       5430       5440

    5640       5650       5660       5670       5680       5690
pS3     AATTTCTCTGGGGTAAATACCCAGGAGTTCGTGCTTTGATATGCACACCACATTCACCCA
        ::::::::::::::::::::::::::::::::::::::::::::::::::::::::::::
Genome AATTTCTCTGGGGTAAATACCCAGGAGTTCGTGCTTTGATATGCACACCACATTCACCCA
             5450       5460       5470       5480       5490       5500

    5700       5710       5720       5730       5740       5750
pS3     TGCTATCTGAGTGAGACCCTCACAGGTCCACAGGCAGAAGGAATTTTCACCTCCCTCCCA
        ::::::::::::::::::::::::::::::::::::::::::::::::::::::::::::
Genome TGCTATCTGAGTGAGACCCTCACAGGTCCACAGGCAGAAGGAATTTTCACCTCCCTCCCA
             5510       5520       5530       5540       5550       5560

    5760       5770       5780       5790       5800       5810
pS3     TCTTCCCATTAGGTCAACAATGCCCCTTGAACTCCAGACTGAGATGAAAGACCTGACAAG
        ::::::::::::::::::::::::::::::::::::::::::::::::::::::::::: :
Genome TCTTCCCATTAGGTCAACAATGCCCCTTGAACTCCAGACTGAGATGAAAGACCTGACA-G
             5570       5580       5590       5600       5610

    5820       5830       5840       5850       5860       5870
pS3     GTCTGTGTATGTGTGTGTGTGTGTGTGTGTGTGTGTGTGTGTGTGTGTGTGTGTGTGT
        ::::::::::::::::::::::::::::::::::::::::::::::::::::::::::::
Genome GTCTGTGTATGTGTGTGTGTGTGTGTGTGTGTGTGTGTGTGTGTGTGTGTGTGTGTGT
    5620       5630       5640       5650       5660       5670

    5880       5890       5900       5910       5920       5930
pS3     GTGCGTGTGTAGCTGCCATGAGATATTAAACATTAATACCCAAATGGCAGGAAGGACCAG
        ::::::::::::::::::::::::::::::::::::::::::::::::::::::::::::
Genome GTGCGTGTGTAGCTGCCATGAGATATTAAACATTAATACCCAAATGGCAGGAAGGACCAG
    5680       5690       5700       5710       5720       5730

    5940       5950       5960       5970       5980       5990
pS3     AAATCGGAGGTAATTTTGAAAGCAAAGAATCTGGAGTGTCTGGAATGGGGCCAGACTTAT
        :::::::::::::::: ::::::::::::::::::::::::::::::::::::::::::
Genome AAATCGGAGGTAATTTTGGAAGCAAAGAATCTGGAGTGTCTGGAATGGGGCCAGACTTAT
    5740       5750       5760       5770       5780       5790
```

```
    6000       6010       6020       6030       6040       6050
pS3    TATGGAACATAGGGTATCCAGGAGAGGAACGAAGGTCAAAACTGTGGGTTACCACCCCCT
       ::::::::::::::::::::::::::::::::::::::::::::::::::::::::::::
Genome TATGGAACATAGGGTATCCAGGAGAGGAACGAAGGTCAAAACTGTGGGTTACCACCCCCT
    5800       5810       5820       5830       5840       5850

    6060       6070       6080       6090       6100       6110
pS3    TCCGCCACAACTGGTCACTTCTGCCTTTGGTGAGTGTTTCGAAACGCCAAGTGTGTGAAA
       ::::::::::::::::::::::::::::::::::::::::::::::::::::::::::::
Genome TCCGCCACAACTGGTCACTTCTGCCTTTGGTGAGTGTTTCGAAACGCCAAGTGTGTGAAA
    5860       5870       5880       5890       5900       5910

    6120       6130       6140       6150       6160       6170
pS3    TTGTGAGCATGCCCTCAGTGATGTGGAGATGAGGTCTGGAGGGGATGGGAAGGGCGTGGG
       ::::::::::::::::::::::::::::::::::::::::::::::::::::::::::::
Genome TTGTGAGCATGCCCTCAGTGATGTGGAGATGAGGTCTGGAGGGGATGGGAAGGGCGTGGG
    5920       5930       5940       5950       5960       5970

    6180       6190       6200       6210       6220       6230
pS3    TTCCCACTCTTACTCACTCGGACCAGCACCCACAGAAGGGGACAGATTGAGGAGCTAGTT
       ::::::::::::::::::::::::::::::::::::::::::::::::::::::::::::
Genome TTCCCACTCTTACTCACTCGGACCAGCACCCACAGAAGGGGACAGATTGAGGAGCTAGTT
    5980       5990       6000       6010       6020       6030

    6240       6250       6260       6270       6280       6290
pS3    GCCAGGCGATGGTGTGACCACACACAGTGTATCCTGCAGCGTGCGTCCTCATGATTA---
       :::::::  :::::  :::::::::::: ::::::::: :: ::::::::::::::::
Genome GCCAGGCC-TGGTG--ACCACACACAGAGTATCCTGCCGCCTGCGTCCTCATGATTAGTG
    6040       6050       6060       6070       6080       6090
```